Title

The What in Within Prevents the Breach from Without: The Make-up of the Plasma Membrane is Integral in the Pathways of Lipotoxic Cell Death

Author

Morris, Siti Nur Sarah

Publication Date

2021

Peer reviewed|Thesis/dissertation

The What in Within Prevents the Breach from Without: The Make-up of the Plasma Membrane is Integral in the Pathways of Lipotoxic Cell Death

By

Siti Nur Sarah Morris

A dissertation submitted in partial satisfaction of the

requirements for the degree of

Doctor of Philosophy

in

Comparative Biochemistry

in the

Graduate Division

of the

University of California, Berkeley

Committee in charge:

Professor James Olzmann, Chair
Professor David Schaffer
Professor Barry Shane

Summer 2021

Abstract

The What in Within Prevents the Breach from Without: The Make-up of the Plasma Membrane is Integral in the Pathways of Lipotoxic Cell Death

by

Siti Nur Sarah Morris

Doctor of Philosophy in Comparative Biochemistry

University of California, Berkeley

Professor James Olzmann, Chair

The plasma membrane (PM) experiences a dynamic interplay of lipids and proteins to fulfil its functions of barrier and regulated transport. The dual leaflets of this bilayer face vastly different environments that require the balancing of forces alongside their own interleaflet pressures. Thus, the composition of the membrane not only defines the lateral lipid environment but also influences the opposing layer. We examine how the lipotoxic stressors of exogenous ceramides and ferroptosis affect this microcosm to ultimately decide cell survival or death.

Ceramides are a class of bioactive sphingolipids involved in crucial cellular processes that range from proliferation to death. This crux point makes ceramide regulation pivotal in determining cellular fate and endogenous ceramide concentrations are kept compartmentalised to avoid triggering an apoptotic cascade. However, not all ceramide species are alike and we explore the nuances of chain-length and the see-saw balance of life or death. Exogenous short-chain ceramides (C6-Cer) can trigger cell death and we utilised a CRISPR-Cas9 knockout (KO) screen to identify novel targets of C6-Cer toxicity. Our findings implicated transmembrane protein 30A (TMEM30A), a crucial component in functional P_4-ATPases, and ADP ribosylation factor like GTPase 5A (ARL5A), a possible recruiter for tethering complexes in endosome to Golgi retrograde transport.

Through the combination of genetic, biochemical and mass spectrometry approaches, we formulate possible mechanisms for these genes in relation to exogenous ceramide toxicity. Our results indicate that KO of TMEM30A creates an exoplasmic surface high in phosphatidylserine (PS). Literature shows that high concentrations of PS incorporates and stabilises cholesterol within its layer. This suggests that the PS phenotype of KOTMEM30A may draw cholesterol to the PM outer leaflet to create conditions that favour C24-Ceramide production. The high amounts of C24-Ceramide could offer protection against the death cascades of C6-Cer. KO of ARL5A possibly interferes with sterol regulation to cause the accumulation of cholesterol in the PM's cytoplasmic leaflet. Cholesterol alters membrane fluidity through increased membrane packing; this rigidity may increase levels of C16-Ceramide, the endogenous species responsible for cell death. Addition of exogenous C6-Cer jumpstarts these respective pathways, allowing KOTMEM30A to resist C6-Cer death whilst death in KOARL5A cells is accelerated.

Turning to another form of lipid-mediated death, ferroptosis is a form of regulated cell death that is dependent on iron and the accumulation of lipid peroxides. These lipid radicals are readily formed upon abstraction of a hydrogen from the easily accessible tails of poly-unsaturated fatty acids (PUFAs). Accumulation of peroxidated PUFA-containing phospholipids on the PM will cause membrane rupture and lead to cell death.

Acyl-CoA synthetase long-chain 4 (ACSL4) converts free long-chain fatty acids into the substrates required from PUFA synthesis. The ACSL4 gene can produce two isoenzymes that differ in length and final protein localisation. The long-form associates with lipid droplets (LDs) whilst the short-form concentrates on the PM. We propose that this differential localisation will lead to altered subcellular localisation of PUFA-containing phospholipids and protection of PUFA translocation to the PM with alter the cell's response to ferroptotic insults.

This body of work explores the intricate dance of specific gene expression and its effect upon PM composition. It is the make-up of the membrane that determines if a cell is able to survive acute lipotoxic stressors. In essence, we explore the philosophical ponderings that cell death by C6-Cer or ferroptosis is a merit of the underlying structure of the PM.

For the curiosity of Hypatia

For the ferocity of Boadicea

For justice for Rosalind Franklin

Table of Contents

List of Figures & Tables

List of Symbols

AA	arachidonic acid
ABC	ammonium bicarbonate
ACSL4	acyl-CoA synthetase long-chain 4
ACSL4-L	acyl-CoA synthetase long-chain 4, long isoform
ACSL4-S	acyl-CoA synthetase long-chain 4, short isoform
APOE	apolipoprotein E
ARF	ADP ribosylation factor
ARL5A	ARF-like 5A
BAX	BCL-2 Associated X protein
C18ORF8	chromosome 18 open reading frame 8
C-1-P	ceramide-1-phosphate
C6-Cer	C6-Ceramide
Cas9	CRISPR associated protein 9
casTLE	cas9 high-throughput maximum Likelihood Estimator
CCR4-Not	Carbon Catabolite Repression—Negative On TATA-less
CDase	ceramidase
CerS	ceramide synthase
CERT	ceramide transfer protein
CHD8	chromodomain-helicase-DNA-binding protein 8
CNOT1	CCR4-Not transcription complex subunit 1
CRISPR	clustered regularly interspaced short palindromic repeats
CRP	ceramide-rich platform
Des	desipramine HCl
DISC	death-inducing signalling complex
EC_{50}	half-maximal effective concentration
ELOVL1	elongation of very long chain fatty acids protein 1

ER	endoplasmic reticulum
FA	fatty acid
FDR	false-discovery rate
GBA	glucocerebrosidase
Glu-Cer	glucosylceramide
GOI	gene of interest
GSH	glutathione
KO	knockout
LD	lipid droplet
LLR	log-likelihood ratio
MOMP	mitochondrial outer membrane permeabilization
MRPL11	mitochondrial ribosomal protein L11
NBD	nitrobenzoxadiazole
NHS	N-hydroxysulfosuccinimide
OMM	outer mitochondrial membrane
PC	phosphatidylcholine
PE	phosphatidylethanolamine
PI	phosphatidylinositol
PS	phosphatidylserine
PUFA	polyunsaturated fatty acids
RCD	regulated cell death
S-1-P	sphingosine-1-phosphate
SCC	surface-connected compartments
SE	sterol esters
SGMS1	sphingomyelin synthase 1
sgRNA	single-guide RNA
SM	sphingomyelin

SMase	sphingomyelinase
SphK	sphingosine kinase
SPT	serine palmitoyl-transferase
TAG	triacylglycerols
TGN	*trans*-Golgi network
TMEM30A	transmembrane protein 30A
TNF	tumour necrosis factor
TNFR	tumour necrosis factor receptor
TNFRSF1A/TNFR1	tumour necrosis factor receptor superfamily member 1A
TRAIL	TNF-related apoptosis-inducing ligand
UGCG	ceramide glucosyltransferase
VKORC1	vitamin K oxidoreductase 1
VKORC1L1	vitamin K oxidoreductase-like 1
WT	wildtype

Acknowledgements

Much like Oscar speeches, I shall strive to keep this short yet thorough lest the orchestra strikes up to drown out words. In the professional sphere, a hearty thank you to my dissertation committee members for slogging through these pages: Drs. James Olzmann, David Schaffer and Barry Shane.

My graduate career can be summed up in one phrase, "Whelp, that didn't go as planned." And to that, I give further thanks to David and Barry for being on my qualifying committee and helping me fight the good fight. Especial gratitude to Barry for taking my concerns seriously and preventing further loss into the sunken-cost fallacy. Thank you to Dr. Aki Minoda; it was just 3 months, but you gave me a goal to strive for. A deep, deep thank you to James for taking in a 3rd year and giving her a place, a noun used in all its aspects.

To the team that kept me functional: Steven Bretow, DC, for keeping me physically able and relatively pain-free (I will be the first to volunteer for a bionic body); Ellen Case, MFT, and Joni Metolius, MFT, for the compassion and wisdom to mend my shattered past for sure-footed steps into the future; Susan Braun and Orion, for giving me strength of purpose and the nuances of calf muscles.

My friends, all who personify the idiom, "Blood of the covenant is thicker than the water of the womb," for, in my experience, is there anything so perfidious as family? To Andra & Todd: whom else would I converse about the mechanics of cigar-flavoured Starbucks coffee? To Elim & Steph: Let us continue to lose our flashlights and dive computers in crazy adventures, though I insist we return with our lives and all our limbs. To Jason: when I feel the days darkening, the thought that you deem me worthwhile keeps me chugging on. To Butch & Kelli: where fast connections can mean deep friendships, and of course, in a fight between a grizzly bear & Kelli, a $100 on Kelli as the winner.

Focusing on my little homestead, I give thanks to my feline devils. Puck, you are a cat through and through. Bas, my little darling, I'm not sure why, but I'm so glad you chose me. Though if you both could please refrain from yakking on the carpet, I'd be ever more grateful. I give my deep abiding love and my deep abiding thanks to my beloved, Johannes. Words fail (English words, at least, I'm sure auf Deutsch could conjugate some) to convey the complexity and ferocity of my emotion, but you have shaped me into the person that I am and of all the world, you have my trust. So, I say onto you, I See you and it is meaningful to me.

Finally, I acknowledge my journey. Should I look back on this thesis, I want to remember the deserved pride in my achievements despite (in spite?) the stacked decks set against me. To the little girl I was, I thank you. You chose defiance over despair and this strength has carried me through. We have survived much and by wit and grit, we clawed towards the ever-moving goal line. Each step forward shored my spine and these, in turn, have given an almost prophetic-weight to the words, "I can," for I know then, I will.

Let the band play. *[Exit, pursued by a bear]*[l].

[l] An apropos stage direction from Shakespeare's 'The Winter's Tale.'

Chapter 1: Ceramide, a lipid like none other

1-1: In structure lies function

Ceramides are a class of bioactive sphingolipids involved in crucial cellular processes that range from proliferation to death[1,2]. This pivotal role has implicated ceramide dysregulation as the main perpetuator in many disorders such as cancer or epileptic encephalopathy[3–5]. Yet how can a simple sphingolipid be at the crux of such a fatal choice—life or death? Moreover, how does the same molecule direct such divergent paths? The key is in its structure: a sphingoid base of 18 carbons with a 4,5-*trans* double bond, covalently bound to a fatty acyl chain via an amide bond (Figure 1-1). These acyl chains vary in length and subsequently, modify ceramide's function. The acyl chains of endogenous ceramides range from long (C16-C20), very long (C22-24) to ultra-long (≥C26), with varying degrees of saturation within each category[6,7]. Furthermore, C1 of ceramides (Figure 1-1, circled) can react with different chemical moieties to convert ceramide into more complex sphingolipids[8]. Thus, the base form of ceramide lends itself to numerous modalities where this sphingolipid can serve as a small but potent signal effector or as the building block for large and complex lipid structures[1,6].

The trigger-quick nature of ceramide signalling cascades requires healthy cells to keep tight control of ceramide levels. Fortunately, endogenous ceramides are extremely hydrophobic and as such, extremely reticent to join the polar environment of the cytosol[6,9]. Ceramides are sequestered in the cell's more hydrophobic-friendly subcellular compartments and trafficking relies on vesicular mechanisms or the use of ceramide transport proteins (CERTs)[10]. Of course, nothing in biology is simple and ceramide regulation proves no exception: the metabolism of ceramide nor its mechanism of action is confined to one location. Thus, the movement of ceramide and its derivatives is a highly choreographed ballet where one misstep can result in unregulated growth or unwanted death.

1-2: Ceramide is the alpha and omega of its synthesis

The *de novo* synthesis of ceramide begins in the endoplasmic reticulum (ER) through the condensation of serine and palmitoyl-CoA via the enzyme, serine palmitoyl transferase (SPT) to form 3-keto-dihydrosphingosine[1]. This product is then reduced to dihydrosphingosine, followed by acylation via ceramide synthases (CerS)[1,11]. These synthases have preferences for specific acyl-CoAs and are thus responsible for the different ceramide chain lengths discussed earlier. There are 6 mammalian isoforms of CERS, differentiated by cell type specificity and acyl chain lengths[11]. Dihydroceramide—the product of the CerS reaction—is then desaturated to add the characteristic 4,5-*trans* double bond of ceramide (Figure 1-1). The *de novo* pathway mainly occurs in the ER; further metabolism requires transport of ceramide to the Golgi apparatus by CERT[1,10].

Outside of the ER, ceramide can be conjoined to a phosphate group through the action of ceramide kinases to form ceramide-1-phosphate, a molecule implicated in inflammation pathways and also known for its strong mitogenic effect[12]. More complex sphingolipids are created within the confines of the Golgi. There, ceramides can be glycosidically bound to glucose via ceramide glucosyltransferase (UGCG) to create glucosylceramide (Glu-Cer), the precursor for

evermore complex versions of glycosphingolipids. Ceramides can also be modified with phosphocholine to form sphingomyelins (SM), a crucial structural molecule for many cell membranes[9,13] (Figure 1-2).

These complex sphingolipids are not the terminal product of ceramide synthesis; point in fact, cells undergo a constant state of ceramide flux as these sphingolipids are built and broken according to the cell's needs. SM can be hydrolysed by sphingomyelinases (SMases) to regenerate the pool of ceramide. These SMases are distinguished by the pH environment they operate within, namely, neutral SMases and acidic SMases. The former operates on the plasma membrane (PM) whilst the latter is found in lysosomes and late endosomes. The acidic environment of the lysosome is the hallmark site of ceramide's salvage pathway. Here, complex sphingolipids are hydrolysed into ceramides and then further catabolized by ceramidase (CDase) to form sphingosine and free fatty acids. These products—unlike ceramide—can leave the lysosome and contribute to other portions of the sphingolipid pathway (Figure 1-2). The salvage pathway is responsible for the majority of sphingolipid turnover; interestingly, CerSs can acylate both dihydrosphingosine and sphingosine; however, while dihydrosphingosine can arise from multiple pathways (though most occur from ceramide *de novo* synthesis), free sphingosines are derived exclusively from the recycling feature of the salvage pathway[2,13].

1-3: Order within the chaos

While complex sphingolipids are integral to functional membranes, ceramide itself causes considerable changes in the lipid layer in which it resides[6,7]. The long acyl chains of endogenous ceramides form an extensive networks of hydrogen bonds with vicinal lipids. This increases membrane rigidity and encourages lateral domain segregation that will lead to the formation of ceramide rafts[7,14–16]. Contributing towards this phenomenon is ceramide's intrinsic ability to rapidly flip-flop between membrane leaflets, which hastens this accumulation of membrane-bound ceramides[17–19]. These individual rafts can then coalesce into large platforms named, appropriately, ceramide-rich platforms (CRPs) that cause an invagination in the membrane. The negative curvature imparted by these CRPs will cause a spatial reorganization that clusters receptors and stabilizes large signalling complexes within a relatively small area[18,20]. This condensation counteracts entropic forces of free movement to potentiate effective signalling cascades.

1-4: The butterfly effect

Ceramide's death signal cascades involve a myriad of pathways and its particular role is less a linear route but rather a stitch pattern in the tapestry of programmed cell death. However, for the sake of simplicity, ceramide death signals can be generalized into two main categories: extrinsic or intrinsic[1,2]. The former relies on death signals that come from outside the cell and is initiated when a pro-apoptotic ligand—usually from the tumour necrosis factor (TNF) superfamily—binds to and activates a TNF receptor (TNFR). This begins the recruitment of the death-inducing signalling complex (DISC) whose stability is heavily reliant on the CRP's microenvironment[21,22]. The DISC will ultimately cause the cleavage of caspases 3 and 7, which

then cause caspase 9 activation and further caspase events that will inevitably result in apoptosis[4,23,24].

The intrinsic pathway is mediated by the mitochondria in response to intracellular stress factors. PM invaginations can fuse with the outer mitochondrial membrane (OMM) and transfer ceramides from the PM to the OMM. These immigrant ceramides cause structural changes that induce mitochondrial outer membrane permeabilization (MOMP) and disrupt OMM integrity[25,26]. There is current debate whether the action of ceramides alone or ceramides in conjunction with BCL-2 Associated X protein (BAX) causes MOMP[27]; however, by itself or with help, ceramides destabilize the OMM to release mitochondrial inter-membrane space proteins that will initiate pro-apoptotic caspase cascades[28].

1-5: When nature needs a helping hand

Ceramide's central role in life-or-death determination makes it a prime candidate for cancer cell subversion[24,29]. Cancer cells are focused on rapid ceramide turnover, especially into mitogenic forms such as C-1-P or sphingosine-1-phospate (S-1-P)[12,30] (Figure 1-2). Unfortunately, natural forms of ceramide cannot be administrated as chemotherapies as their long acyl chains makes it impossible to disperse in a hydrophilic medium. Thus, to overcome this structural limitation, exogeneous short-chain ceramides were manufactured to be water-soluble and PM permeable versions of endogenous ceramides[7,9]. C6-Ceramide's (C6-Cer) reduction in acyl-chain length (Figure 1-3, structure) disables the lateral phase separation found in its natural counterparts; however, because C6-Cer maintains its headgroup conformation, it can still initiate normal ceramide death signals[31–33]. Furthermore, C6-Cer—unlike other version of short-chain ceramides—can undergo deacylation by CDase to form sphingosines[34]. These sphingosines can then be phosphorylated—via sphingosine kinase (SphK)—or reacylated—via CerS—as the cell's salvage pathway dictates[29] (Figure 1-2).

1-6: Knockout screens: the magnet to find the needle in the haystack

Current targets of exogenous ceramide death rely on known apoptotic networks as exploration beyond these pathways can be an exhausting exercise in futility. Fortunately, the rise and fine-tuning of Clustered Regularly Interspaced Short Palindromic Repeats (CRISPR) genome technologies provides a mechanism for comprehensive screening of novel hits[35]. This technology appropriates the prokaryotic immune system, wherein CRISPR nucleases cleave phage DNA from the host genome. These nucleases, e.g. CRISPR associated protein 9 (Cas9), are guided to the target by short, single-stranded RNA that is complementary to the foreign DNA sequence. Once recognized, Cas9 creates a double-strand break that can be repaired by non-homologous end joining. This mending process introduces a frame shift mutation that results in gene loss-of-function, thus ablating phage function in CRISPR-Cas9's native state[36,37]. In a synthetic system, the prokaryotic RNA components are replaced with truncated (17-18bp) guides targeting the researcher's gene of interest (GOI)[38]. Combining multiple guides for multiple GOIs creates a knockout (KO) library capable of assessing crucial gene hits of a particular phenotype in a relatively quick, large-scale format.

We utilized the Bassik human CRISPR KO library to find new candidate regulators in ceramide-induced death[38–40]. This library contains a comprehensive array of single-guide RNAs (sgRNAs) that cover the known protein coding genome. Additionally, the library was designed with 10 individual sgRNAs to span each gene as an insurance of robust coverage and sufficient gene KO. Adding to the strength and utility of the Bassik library are their internal controls of sgSAFE and sgNONE. The former is a group of guides that target locations with no annotated function while the latter contains guides with no complementary binding site within the genome. These controls serve as excellent guide points to assess if the pooled population of cells contain adequate coverage as well as to account for false positives due to off-target Cas9 activity[38,40].

Our screen used K562, an immortalised human myelogenous leukaemia cell line, for ease in methodology and its robust response to C6-Cer[24,41] (Figure 1-3). In brief, the experimental setup is as follows:

1) K562-Cas9 expressing cell lines are infected with the Bassik library.

2) This pool of cells is equally separated to form the control group and the ceramide group.

3) The control and ceramide pools are treated with ethanol (vehicle) or C6-Cer, respectively.

4) After treatment, cells are allowed to recover and then once again undergo drug exposure.

5) This cycle occurs for a total of 4 rounds to insure enrichment or disenrichment of the KO pools.

These pools are then collected, genome DNA extracted and undergo next-generation sequencing to determine the relative sgRNA abundances between control and ceramide groups (Figure 1-4). Further details, including candidate selection, will be discussed in Chapter 2.

Chapter 1 Figures

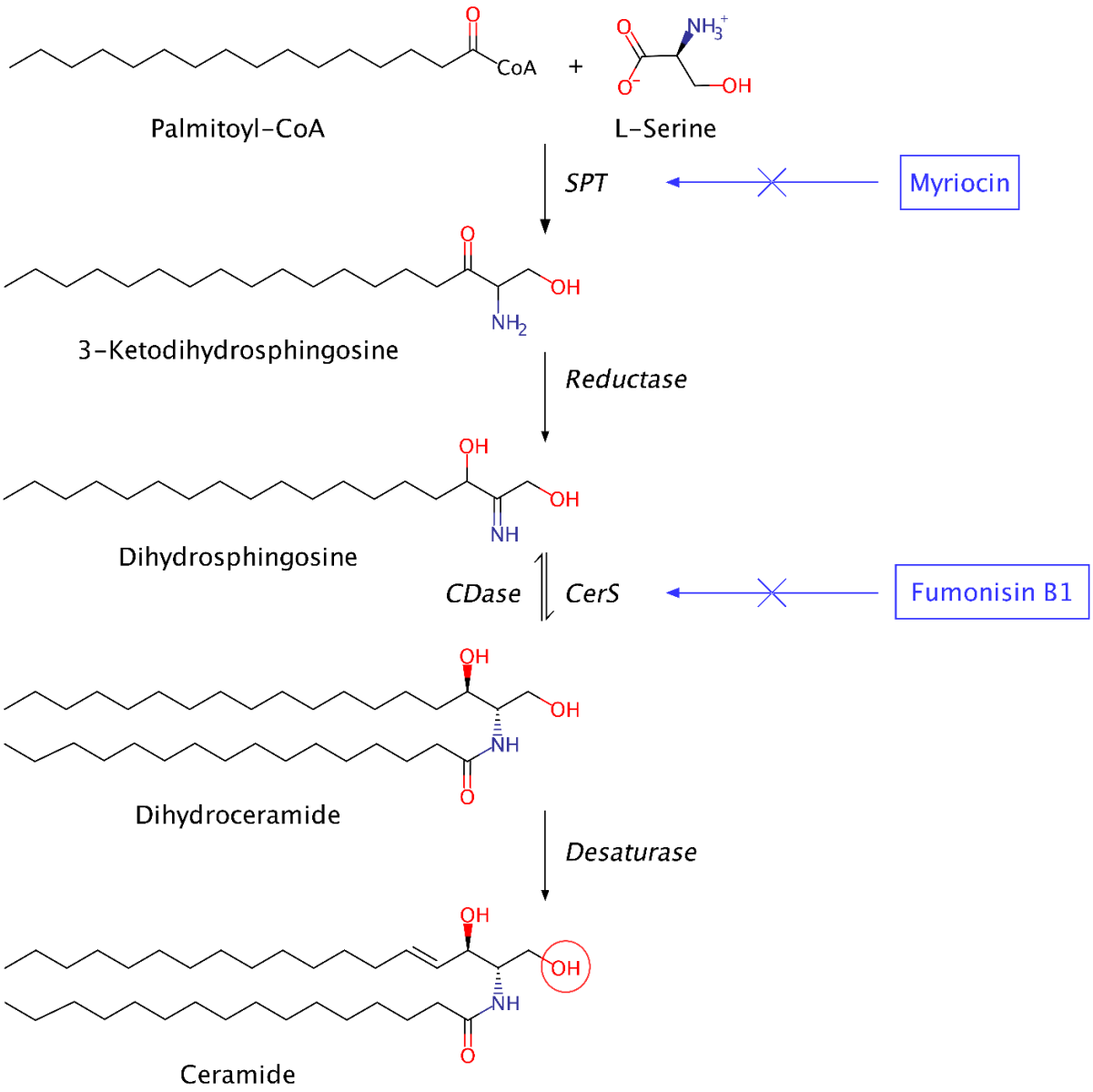

Figure 1-1: De novo synthesis of endogenous ceramides

New synthesis of ceramide begins in the ER with the condensation of palmitoyl-CoA and serine into 3-ketosphingosine. This is catalysed by SPT and it represents the rate limiting step of this process. Myriocin, a fungal derived antibiotic, is a potent inhibitor of SPT. 3-ketosphingosine is reduced into dihydrospingosine, which is then acylated by CerS into dihydroceramide (the fully saturated version of ceramide). There are 6 isoforms of CerS with differing specificity for their fatty acid-CoA substrates and it is this selectivity that gives rise to variety of endogenous ceramides. Fumonisin B1, another fungal derivative, is a pan-CerS inhibitor. Dihydroceramide undergoes a desaturation step to form ceramide; in this example, a C-16 ceramide is formed. The circled hydroxyl group denotes the site where ceramide may undergo further reactions to form the complex sphingolipids discussed in text. As part of ceramide regulation, dihydroceramide can be deacylated to reduce overall cellular levels of ceramide.

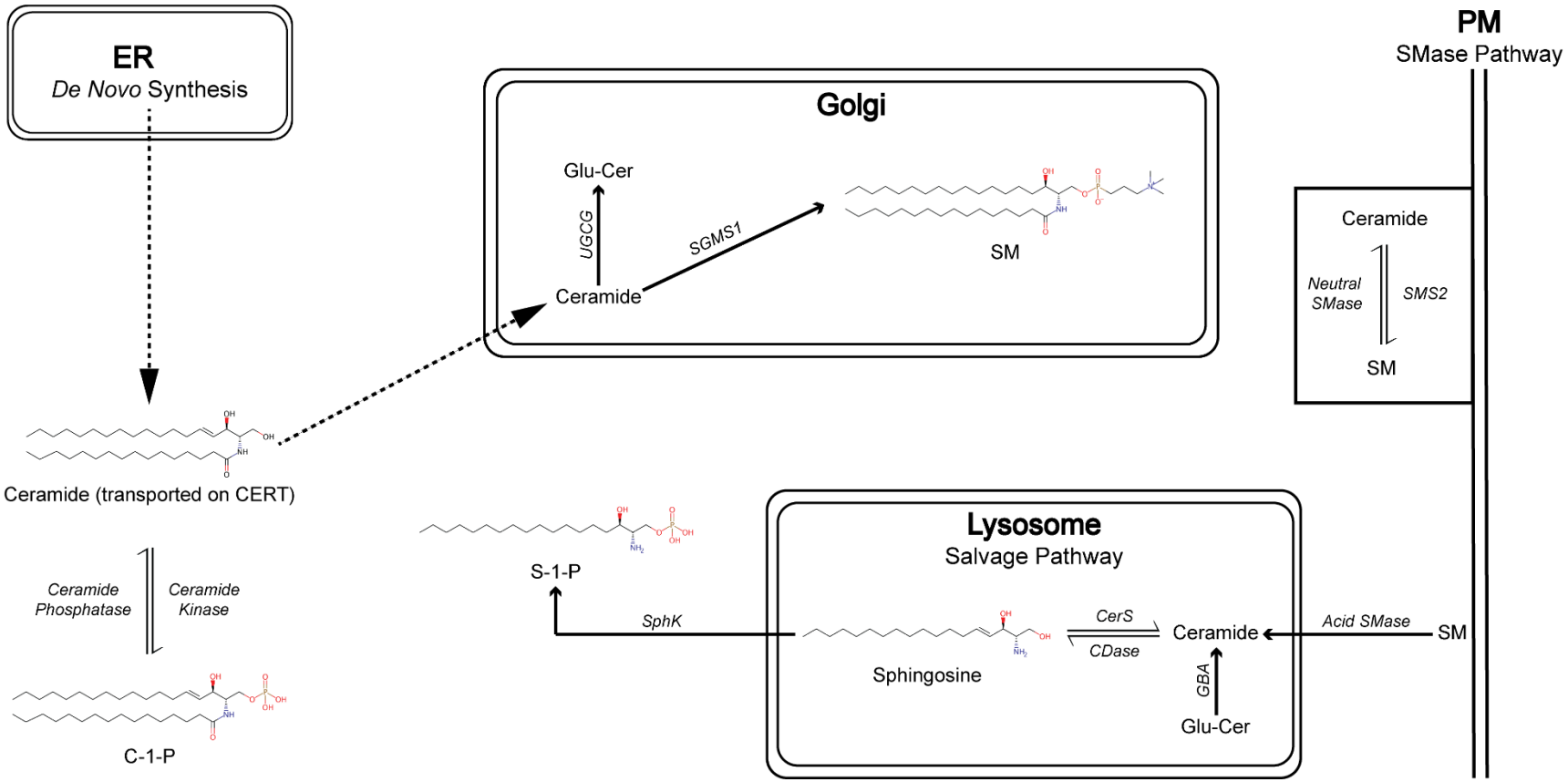

Figure 1-2: Ceramide metabolism

De novo synthesis is but one pathway to the generation of cellular ceramide. The three main routes are *de novo* (discussed in Figure 1-1), SMase catabolism of complex sphingolipids and the salvage pathway. Due to the hydrophobic nature of ceramide, these pathways are compartmentalised in the ER, PM and lysosome, respectively. Free ceramides navigate the cytosol via CERT; they can be phosphorylated in C-1-P, or they can travel to the Golgi for further modifications. The complex, structural sphingolipids are manufactured in the Golgi. In the Golgi, UGCG can add a sugar moiety to form Glu-Cer, or SGMS1 can combine ceramide and phosphocholine to form SM. These SM can be hydrolysed back into ceramide via SMases, with the neutral isoform operating on the PM and the acidic isoform functioning in lysosomes/late endosomes. These salvaged ceramides—derived from a multitude of complex sphingolipids—can undergo further catabolism via CDase to form sphingosines. These sphingosines, in turn, can be reacylated by CerS isoforms to recreate ceramide. This trio of pathways regulate overall levels of ceramide and provide nuanced control of the ceramide species within the cell. Exogenous ceramides, specifically C6-Cer can readily enter cell to be broken down by CDases into sphingosine, whereupon these sphingosines then are able to merge with the cell's native ceramide cycle.

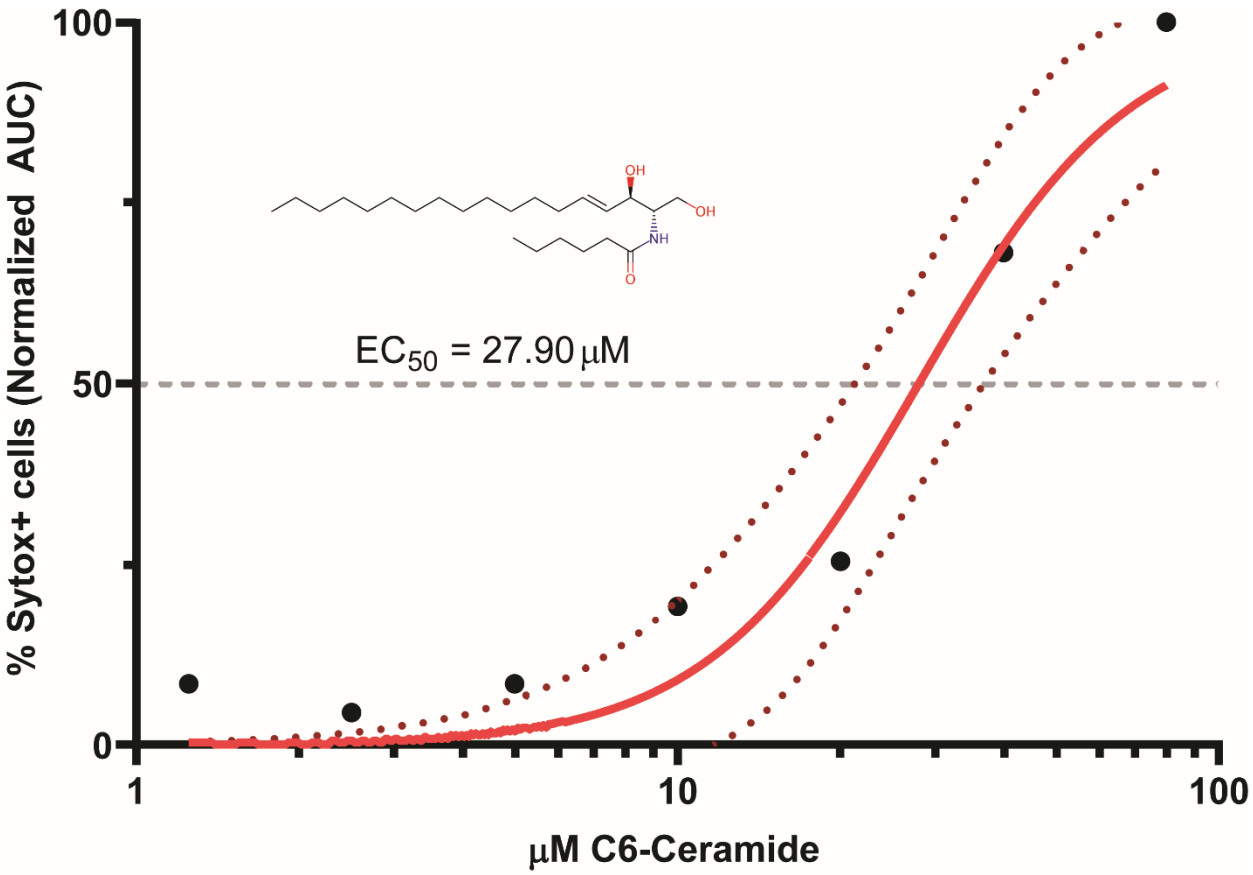

Figure 1-3: K562 response to exogenous ceramide

C6-Cer (structure shown), unlike endogenous forms of ceramide, is water-soluble and able to initiate normal ceramide death signals. Furthermore, its ability to be metabolised into the cell's native ceramide pathways makes it an ideal substitute for the less mobile long-chain ceramides. K562 cells were treated with differing concentrations of C6-Cer and measured for percent death. A sigmoidal death curve was derived (red line, red dots represent 95% confidence interval) and the EC50 was calculated.

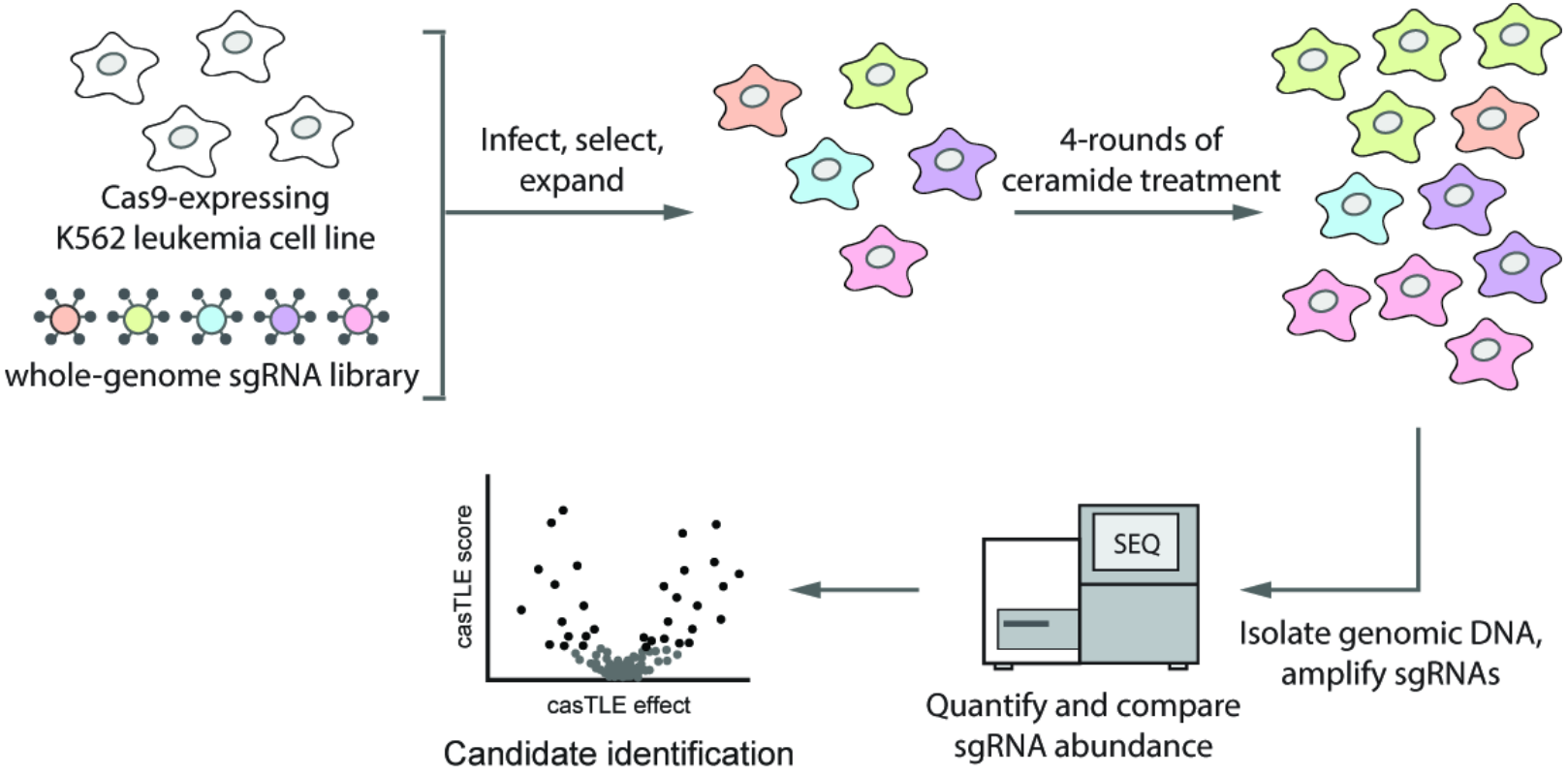

Figure 1-4: CRISPR KO screen schematic

K562-Cas9 cells are infected with the lentiviral CRISPR library and selected for sgRNA insertion. Cell numbers are grown to numbers that statistically provide comprehensive coverage. This population is subsequently split into two equal pools of control and ceramide groups. The control group is treated with vehicle and the ceramide group is treated with C6-Cer at the EC_{50} concentration. Each round of treatment involves drug exposure for 24 hours, followed by a recovery period of 48 hours. After 4 rounds, the remaining pools are enriched or depleted of particular sgRNAs. In the figure example, green represents a KO that is resistant to C6-Cer death whereas blue is a KO that sensitises the cell to ceramide. The pools are collected and genome DNA extracted; sgRNA sequences are PCR amplified and the resulting concoction is deep sequenced to identify the abundances of each sgRNA. These abundances are compared between control and treated groups and results are visualised through a volcano plot, with the x-axis representing relative fold-change to control (casTLE effect) and the y-axis representing the calculated trend of the target gene's sgRNAs (casTLE score). Namely, should all 10 sgRNAs follow the same casTLE effect, it will result in a high casTLE score. The volcano plot provides a visual aid to determine worthwhile candidates.

Chapter 2: Needles abound, needles found. Hits from a CRISPR knockout screen

2-1: Causa latet, vis est notissima[II]

We first characterised K562's response to C6-Cer by calculating the cell line's half-maximal effective concentration (EC_{50}) of 27.90 µM (Figure 1-3). This was used as the treatment dosage for our screen as lower concentrations would 'muffle' resistant responses whilst higher would result in loss of nuanced sensitisers. We created our pooled library screen by stably infecting the sgRNA library into K562-Cas9 expressing cells. Following selection and recovery of the lentiviral procedure, the resultant pool of cells was equally split into untreated (vehicle) or treated (C6-Cer) populations. After the 4 rounds of dis/enrichment—as described in Chapter 1—the PCR-amplified genome is deep sequenced to establish the absolute counts of sgRNAs (Figure 1-4).

Statistical analysis of the screen utilized the cas9 high-throughput maximum Likelihood Estimator (casTLE) programme to output an effect size estimator (casTLE effect) of each target gene alongside its associated log-likelihood ratio (LLR) (casTLE score) and appropriate p-value[38,40,42]. Essentially, casTLE effect reflects the treated gene's enrichment in comparison to the untreated version, with casTLE score providing a confidence metric of said estimation. The screen procedure was done in duplicate and the data of both sets were combined into a singular volcano plot depicting the collective casTLE scores versus casTLE effects (Figure 2-1). Volcano plots are practical graphs to visualise the vast data of whole genome screens as outliers from the main body of points can indicate potential hits. Additionally, we calculated the 1% false-discovery rate (FDR)[43] to further minimise Type I statistical errors and to highlight true discoveries (Appendix A).

2-1-1: The particulars of death

Figure 2-1A labels targets involved in sphingolipid pathways that made the FDR 1% cut-off. The high confidence scores of these known ceramide-associated genes indicates that screen was successful at identifying targets specific to ceramide toxicity rather than a general enrichment of death-involved genes (e.g., caspase 8 is within the FDR 10% but caspase 9 is outside the discovery criteria) (Appendix A).

Interestingly, the enrichment values of Figure 2-1A targets are reversed from canonical expectations of ceramide-induced cell death. As discussed in Chapter 1, cells evade this death pathway by minimising endogenous levels of ceramide. However, KO of CerS2, elongation of very long chain fatty acids protein 1 (ELOVL1) and GBA2—genes that normally *increase* endogenous ceramide concentration, and thus a KO is expected to decrease ceramide—results in *sensitivity* to C6-Cer death. Fitting this flipped pattern are UGCG, the SphKs and SGMS1, where KOs should raise ceramide levels, but instead provides resistance to C6-Cer toxicity. The exception to this trend is tumour necrosis factor receptor superfamily member 1A (TNFRSF1A), where KO of this pro-apoptotic receptor predictably confers resistance to death.

A viable explanation for this paradoxical pattern may be due to the more nuanced nature of C16 ceramides (C16-cer) versus C24 ceramides (C24-cer). Long chain ceramides are less likely

[II] Ovid's *Metamorphoses*, Book IV line 287, 'The cause is hidden; the effect is visible to all.'

than their very-long chain cousins to interdigit with the neighbouring molecules. This makes C16-cer relatively resistant to protein inserts within the ceramide microenvironment. This structural quirk, however, gives C16-cer the ability to create stable pore formations that can efficiently permeabilise membranes to fast-track apoptosis[44]. CerS6 is mainly responsible for the synthesis of C16-cer whilst CerS2 is the only CerS capable of creating C24-cer[45,46]. ELOVL1 creates C20-C22 fatty acids (FAs). These FAs are the precursors for C24 FAs, which are the required substrates of CerS2[47,48]. Thus, KO of either CerS2 or ELOVL1 will lower total levels of C24-cer that will inevitability imbalance the ratio of C16 to C24 species and increase the cell's susceptibility to apoptosis[49].

S1P is known as a survival factor; however, it also inhibits CerS2[50]. This may be the reason why KO of SphK1/2 (enzymes responsible for the phosphorylation of sphingosine to S1P) confers death resistance; the loss of SphKs results in less cellular S1P to inhibit CerS2 and the golden ratio is maintained. UGCG upregulates CerS6 whilst over-expression of UGCG hinders CerS2 activity and this mechanism may explain how the KO of UGCG protects the C16 to C24 equilibrium[51,52]. Additionally, TNFRSF1A activation causes the accumulation of C16-C20 ceramides[53]. As such, KO-TNFRSF1A has the dual effect of preventing apoptotic signalling as well as keeping the ceramide species in balance. The roles of GBA2 and SGMS1 in this theorized pathway is less clear. As GBA2 catalyses the breakdown of Glu-Cer to glucose and ceramide, the loss of GBA2 could mean a decrease in the salvage pathway's ability to synthesise C24-cer (ceramides in the salvage pathway are broken down to sphingosine, which can then be reacylated to different ceramide species) that could neutralise any imbalances. Conversely, since SGMS1 creates SM from ceramide, the KO of SGMS1 prevents this ceramide (and proportionally, sphingosine) depletion.

The screen data suggests that C6-Cer exposure likely results in a perturbation of the homeostatic ration between C16-cer and C24-cer. This continual deviation (be it from mechanisms changing the individual concentrations or inhibiting rescue pathways) can theoretically overwhelm the cell and ultimately result in death.

2-2: HC SVNT DRACONES[III]

Stepping outside the comfortable pathways of sphingolipid metabolism, we venture into the unexplored territories of exogenous ceramide death. The hits within this region would likely contain true discoveries of targets heretofore unconnected with ceramide death. We surveyed the Gene Ontology (GO) of the FDR 1% to better grasp the underlying processes of the group. We utilised g:Profiler to analyse for commonalities in location and function. g:Profiler relies on the Ensembl database for GO annotations in 'cellular component' and 'biological process' categories[54–56]. The programme also expands its over-representation analyses by utilising the databanks within Kyoto Encyclopedia of Genes and Genomes (KEGG)[57], Reactome[58] and WikiPathways[59]. The results depict high significance in terminology involving sphingolipid metabolism and mechanisms of intracellular transport (Figure 2-2). The former adds further confirmation that our screen reflects the process of ceramide death versus a listing of non-specific growth factors or apoptotic markers. Likewise, we cross-checked with the Human

[III] Transcribed on the Hunt-Lenox Globe, i.e., *hic sunt dracones*, 'here be dragons.'

Protein Atlas[60] to map the most prevalent subcellular locations of the FDR 1% hits to possibly identify spatial niches of C6-Cer toxicity (Figure 2-3).

Based on these findings and the calculated casTLE scores, we narrowed our focus to a handful of targets for further testing (Figure 2-1B):

- Vitamin K oxidoreductase-like 1 (VKORC1L1) is a paralog of VKORC1, the protein mainly responsible for reducing vitamin K epoxide into vitamin K, the cofactor required for γ-carboxylation of proteins. In the absence of VKORC1, VKORC1L1 can maintain normal γ-carboxylation levels, though its pervasive cytosolic localisations suggest that VKORC1L1 has other main functions besides VKORC1 rescue. Vitamin K can activate SPT, therefore, an example of an alternate prime directive may be to produce vitamin K for *de novo* ceramide biogenesis[61,62]. Adding weight to this credence is VKORC1's notable absence in any of the FDR gene sets.

- ADP ribosylation factor-like 5A (ARL5A) is part of the Ras superfamily of GTP-binding proteins[63,64]. The ARL branch are major regulators of vesicle trafficking with the ARL5's specifically associated with ER to Golgi retrograde trafficking[65–67].

- Transmembrane protein 30A (TMEM30A) encodes the protein that becomes the β-subunit of the P4 subfamily of P-type ATPases (P4-ATPases)[68–70]. These ATPases are lipid flippases that translocate phospholipids between the leaflets of a bilayer membrane. The TMEM30A subunit is required for the proper folding and correct localisation of the P4-ATPases[71,72].

- Chromodomain-helicase-DNA-binding protein 8 (CHD8) regulates gene expression through the selective tightening of chromatin structure. This remodelling suppresses the transcript activation of multiple genes, notably p53 and Wnt, though studies indicate its crucial time period is during foetal development[73].

- CCR4-NOT transcription complex subunit 1 (CNOT1) is a component of the Carbon Catabolic Repression-Negative On TATA-less (CCR4-NOT) complex[74]. This multiprotein unit is involved in post-transcriptional regulation through mRNA deadenylation. This 3' to 5' exonuclease shortens the poly(A) tail and thus, earmarks the strand for degradation. CNOT1 is the scaffold substrate of CCR4-NOT and does not carry out its catalytic function[74,75].

- Much remains to discover about chromosome 18 open reading frame 8 (C18ORF8/RMC1), though it is implicated in autophagic flux as part of the CCZ1-MON1-Rab7 module[76,77].

- Mitochondrial ribosomal protein 11 (MRPL11) encodes for the 39S subunit of the mitochondrial ribosome. It is an important structural element for mitochondrial genome-encoded protein synthesis[78].

2-3: Доверяй, но проверяй[IV]

Whole genome KO screens are powerful tools to identify hits, but despite extensive technical controls and strict statistical analyses, screens—by their very nature—create a heavily artificial environment that may mask accurate biological function. Therefore, we externally validated our chosen hits via an orthogonal secondary screen, namely, a competitive growth assay. Essentially, KO cell lines positive for mCherry signal are combined in an equal ratio with a control line that is negative in mCherry emission. This population is subjected to 24hours of C6-Cer and then measured via flow cytometry to calculate the number of mCherry positive cells to mCherry negative cells (Figure 2-4A). KO cell lines resistant to C6-Cer death will be proportionally higher in number than their equivalent control, while KO lines sensitive to C6-Cer will be less abundant than wildtype (WT). We created individual KO cell lines of our target list as well as for CerS2, UGCG and GBA. These three would confirm if the screen's output of these sphingolipid pathway hits held true; GBA was chosen over GBA2 as both exhibited the same trend in enrichment but GBA would reveal if target effects of the FDR 10% were also reproducible.

The competitive growth assay generally upheld screen results (apart from CNOT1 and C18ORF8) (Figure 2-4B). Moreover, the KOs of CerS2, UGCG and GBA replicated screen trends, suggests that the patterns discussed in section 2-1-1 are real biological effects and not off-targets of the artificial screen environment. Meanwhile, CHD8 and TMEM30A both showed strong resistance to C6-Cer toxicity, with only a small increase in fold-change for MRPL11. Of the remaining purported sensitisers, VKORC1L1 did not display the robust disenrichment of the KO screen whilst ARL5A matched the casTLE effect.

2-3-1: Audacibus annue coeptis[V]

We chose ARL5A and TMEM30A for future mechanistic studies as these had the highest casTLE scores of the validated gene list and are also not of a known sphingolipid pathway (Figure 2-5A). Moreover, the functional enrichment analysis outputted many terms regarding intracellular transport, and both ARL5A and TMEM30A have prior literature supporting their involvement in trafficking. This correlation is especially critical as these two genes represent entirely novel targets in exogenous ceramide death, thus we required a viable foundation to begin our initial forays into mechanism. This criterion ruled out MRPL11, whilst the differing results in our competitive growth assay ruled out CNOT1 and C18ORF8. Furthermore, ARL5A and TMEM30A exhibited consolidated effects for their respective sgRNAs. This 'pooling' may limit the issue of isoform expression being the root cause of the observed phenotype and thereby prevent further complications towards mechanistic discoveries (Figure 2-5B&C). We shall delve into mechanistic interplay in Chapter 3.

[IV] Russian proverb, 'Trust, but verify.'

[V] Virgil's *Georgics* Book I line 40, 'Look with favour upon a bold beginning.'

2-4: Chapter 2 Materials & Methods

2-4-1: Cell lines and culture conditions

HEK293T was obtained from UC Berkeley's cell culture facility. K562 and K562-Cas9-BFP cells were a generous donation from R. Kopito (Stanford University). HEK293T was maintained in DMEM containing 4.5 g/l glucose and L-glutamine (Corning, 10-017). K562 cells and their derivatives were maintained in RPMI-1640 with L-glutamine (Corning, 10-040-CM). All media was supplemented with 10% foetal bovine serum (Gemini Bio Products) and penicillin (10,000 I.U mL^{-1}). Cell lines were maintained at 37°C with 5% CO_2 with regular screening for mycoplasma contamination.

2-4-2: EC_{50} Death Assay

Cell death was assayed via the Essen IncuCyte Live-Cell imaging system (Sartorius). Ten thousand K562 cells per well were seeded in black 96-well plates (Corning, 3904). Media containing a final concentration of 15nM SYTOX-Green Dead Cell Stain (Invitrogen, S34860) and C6-Ceramide (d18:1/6:0) (Enzo, BML-SL110) at various concentrations was added to produce a final cell density of 500,000 cells/mL. Plates were carefully transferred to the IncuCyte system (kept at 37°C with 5% CO_2) and imaged for 24hours (24hr). Three images per well were captured in the green and brightfield channels every hour for the treatment period. The Sartorius image analysis software outputs the number of green objects (SYTOX-Green positive, i.e., dead cells) as well as the total number of objects (brightfield segmentation). For each C6-Cer concentration, the ratio of dead objects over total objects was plotted over the 24hr imaging cycle. From this, Prism (Graphpad) was used to calculate the area under the curve (AUC), plotted as function of C6-Cer dosage and mathematically determine the EC_{50}.

2-4-3: CRISPR-Cas9 synthetic lethal screen

The screen was performed as previously described[40]. The Bassik Human CRISPR Knockout Library (Addgene, 101926-101934) is separated into 9 sublibraries comprising a total of 225,171 elements and targeting approximately 20,500 genes (10 sgRNAs per target). To generate the lentiviral library pool, each sublibrary pool was co-transfected with third-generation lentiviral packaging plasmids (pVSV-G/MD2.G [Addgene, 12259], pRSV-Rev [Addgene, 12253] and pMDLg [Addgene, 12251]) into low-passage HEK293T cells. Lentiviral-containing media was collected at 48hr and at 72hr post-transfection. These media pools were then combined and filtered via 0.45-micron cartridge. The resultant lentiviral media was used to infect approximately 2.0×10^8 K562-Cas9 cells for 72hr. After this infection period, the cells were spun down at 500 × g for 5min and viral-laden media was removed. These cells then underwent 5µg/mL Puromycin Dihydrochloride (Gibco, A1113803) selection until the population was over 97% mCherry positive. Cells then recovered in puromycin-free media until a total of 2.5×10^8 (~1,000-fold total library elements). This pool was then split and treated with either ethanol (EtOH) or 30µM C6-Cer for 24hr. The treatment period was followed by a 48hr recovery and subsequently, the treatment cycle was repeated thrice more. Each subsequent cycle required a slight uptick in C6-Cer concentration as

the pools experienced rapid resistance to death and thus the drug concentration was raised to achieve ~50% death. The dosage for cycle 2 and upwards is as follows: 32.5µM, 35µM and finally, 40µM. Throughout the screen, K562 cells are maintained at 500,000 cells/mL.

After the last bout of treatment, cells were twice-washed with PBS, pelleted into numbers approximating 250-fold of total library elements and stored at -80°C. Genomic DNA was extracted using the QIAmp DNA Blood Maxi Kit (Qiagen) according to the manufacturer's directions. This genomic DNA underwent two rounds of PCR to first amplify sgRNA sequences and then index them using Illumina TruSeq LT adaptor sequences.

PCR amplicons from each sample were pooled into a 1:1 ratio (EtOH:C6-Cer) based on concentrations determined by Qubit Fluorometric Quantification (Invitrogen). Deep sequencing was done on an Illumina NextSeq instrument at the Oklahoma Medical Research Foundation. Sequence reads were trimmed, then aligned using Bowtie with zero mismatches tolerated. Enrichment, confidence scores and p-values were calculated using the casTLE Python code as previously described[38].

2-4-5: Generation of CRISPR-Cas9 genome-edited cell lines

KO cell lines were generated the same way as the lentiviral portion of the CRISPR-Cas9 screen. Cas9 cutting functionality was validated via infecting K562-Cas9 with a self-cutting mCherry plasmid (a kind gift from M. Bassik, Stanford University) that expresses mCherry as well as a sgRNA sequence targeting said gene.

sgRNA sequences selected from the CRISPR KO screen were used to create the individual transfection plasmids. All guide sequences were inserted into pMCB320 between the BstXI and BlpI sites as previously described[79].

Plasmid	Sequence (5' to 3')
sgARL5A (sg93.3)	GTACATACATCTCCTACAAT
sgC18ORF8	GTTGACTTAGGCGCAGC
sgCERS2	GCGTGATATAGAGATCTG
sgCHD8	GCTACGGGAATATCAGT
sgCNOT1	GTAAGAACGCAGAAGATC
sgGBA	GCGGCTGAAGGTACCAA
sgMRPL11	GTGATCCGGGCGATCGTGC
sgSAFE	GAGCAGAGACCTCCTGAACC
sgTMEM30A (sg0.2)	GACAAACCAATTGCTCCTTG
sgUGCG	GAAGAGGACGAACCCGAAGA
sgVKORC1L1	GACTAGTTTACTTGAACG

2-4-6: Competitive Growth Assay

WT cells (self-cut mCherry, no mCherry emission) and KO cells (mCherry positive) were seeded in a 1:1 ratio with a final density of 500,000 cells/mL into a 96-well round-bottom plate. Wells were treated with either vehicle (EtOH, untreated) or C6-Ceramide for 24hr. Cells were

then spun down, media aspirated and then replenished with media containing 15nM SYTOX-Green. The plate was assayed via flow cytometry on a BD LSRFortessa in the UC Berkeley Flow Cytometry Facility; dead cells were gated out (positive SYTOX-Green) and live cells were analysed to discover the percentages of mCherry +/- cells. Two-way ANOVA was calculated on Prism.

Chapter 2 Figures

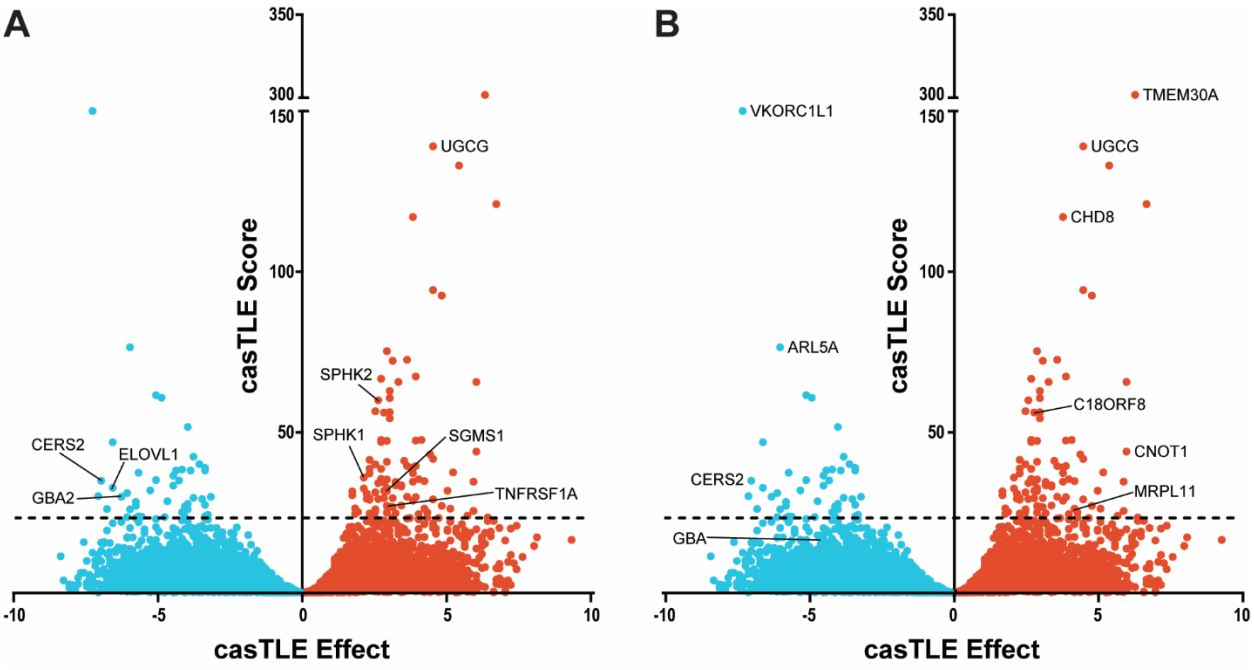

Figure 2-1: Volcano plots of screen hits

Combined screen data with effect and confidence score calculated by casTLE utilizing an empirical Bayesian approach. X-axis uses sgRNA frequencies to find an adjusted log2 enrichment (casTLE effect) and y-axis is the LLR (casTLE score). Dashed line represents the approximate FDR 1% cut-off. (A) Known genes of the sphingolipid pathway that meet the FDR 1% requirement. (B) Chosen target genes for further experimental validation.

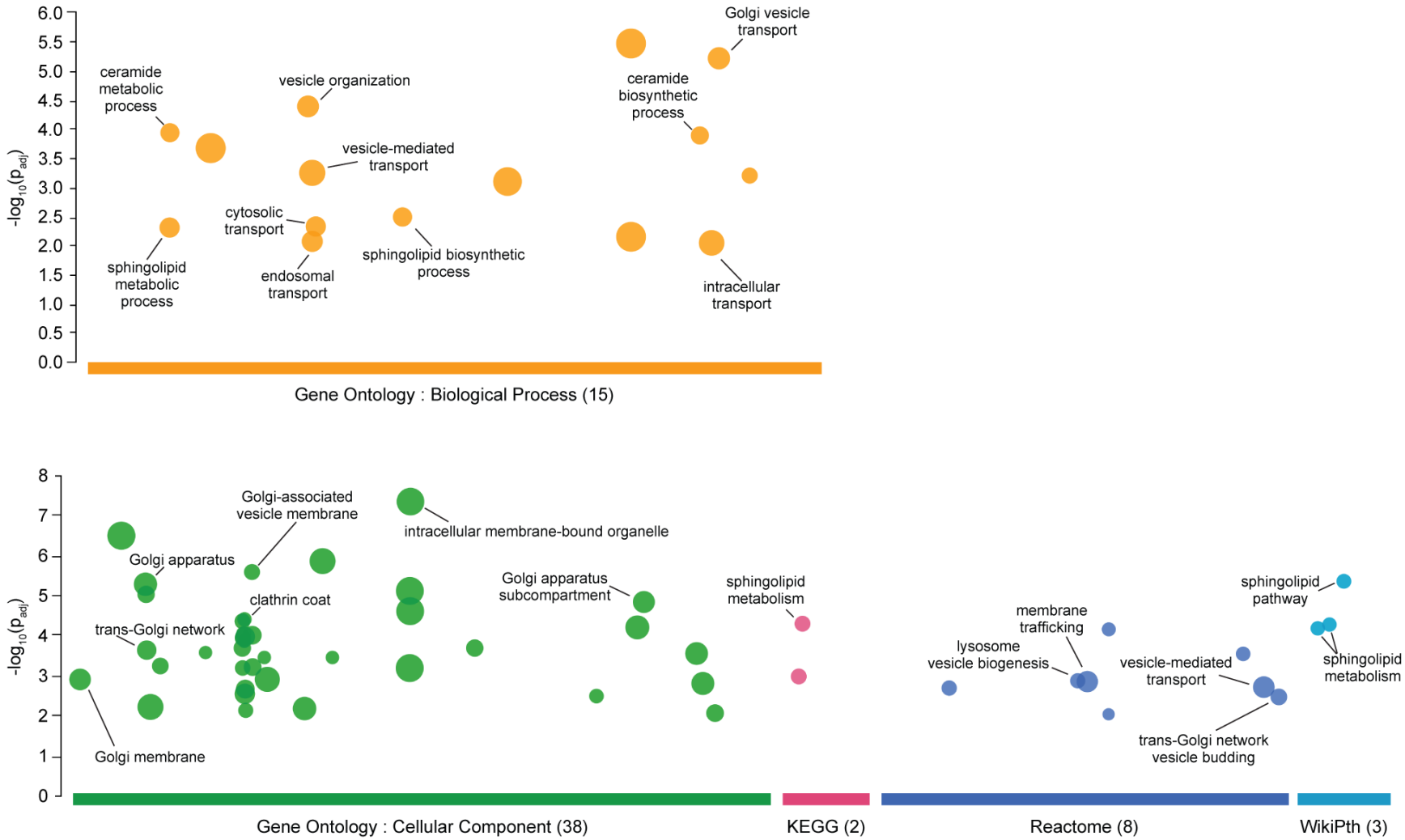

Figure 2-2: Functional enrichment analysis of FDR 1% discoveries

The FDR 1% genes were analysed via g:Profiler for similar biological categories between terms. The x-axis categorises the functional identifiers of the data source and the y-axis notes the corresponding p-value calculated by g:(Set Counts and Sizes)[54]. Individual circles represent a single functional identifier and the sized accordingly to the number of annotated genes within the identifier. Top hits within each database are focused

on ceramide pathways or cellular transport. See Appendix B for a full listing of functional identifiers as well as the screen hits that correspond to that grouping.

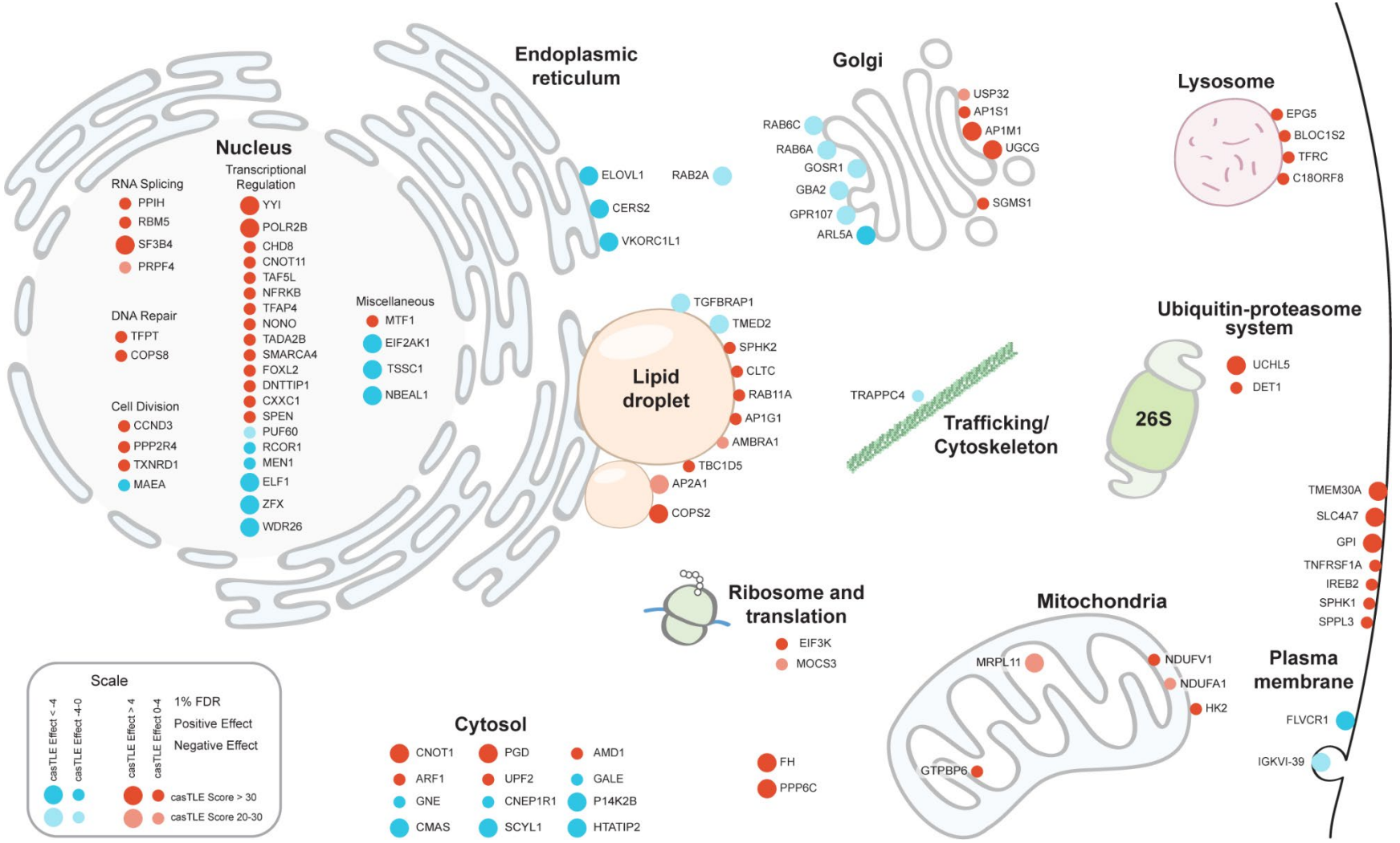

Figure 2-3: Cellular localisation of the FDR 1% discoveries

Protein localisation of the FDR 1% genes. Locations are based on a compilation of current literature as well as Cell Atlas[60] data. Hits from the combined CRISPR KO screen show a diverse spread in intracellular compartments, though this could reflect C6-Cer's propensity for disrupting trafficking patterns.

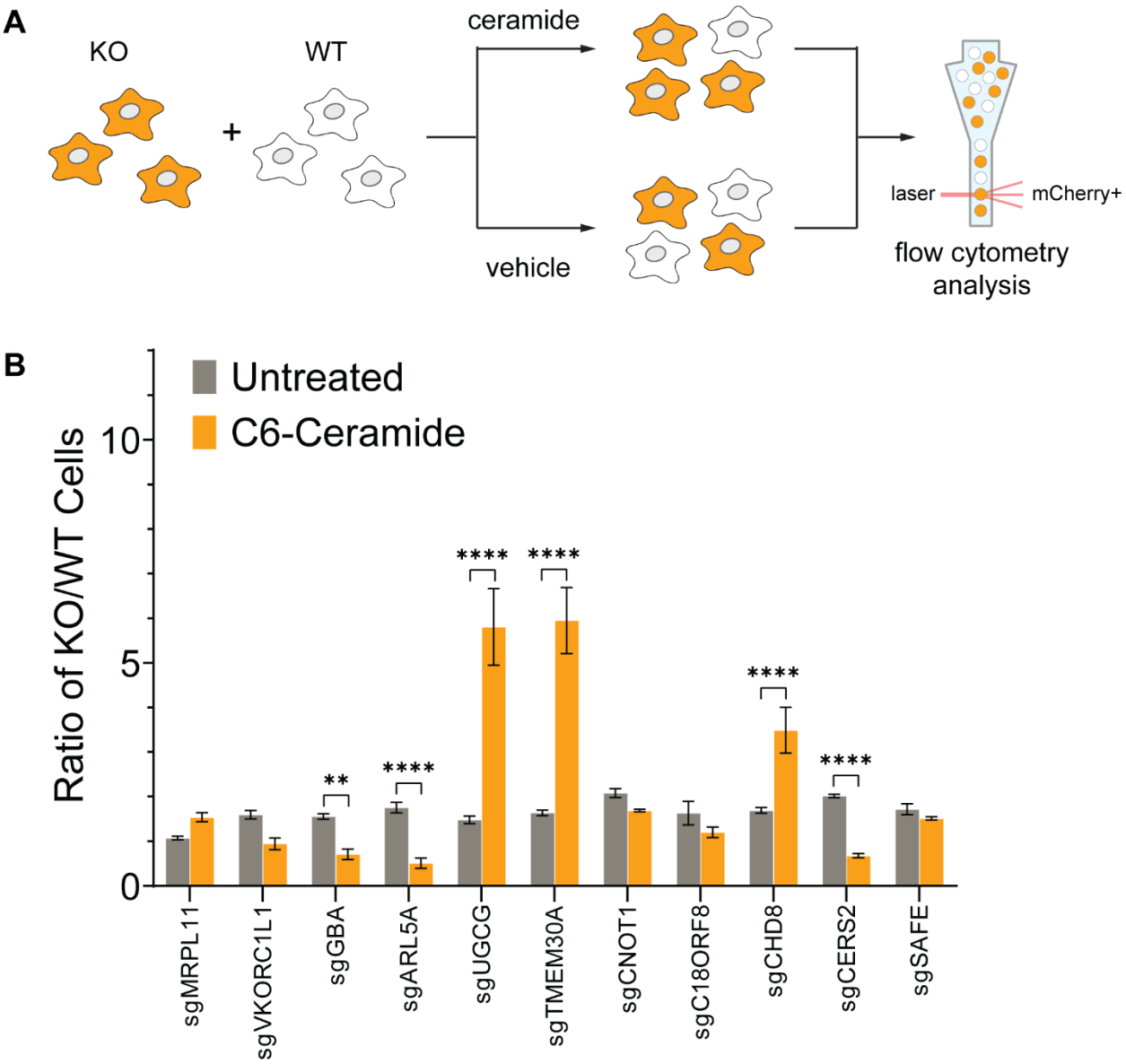

Figure 2-4: Validation of screen hits via competitive growth assay

(A) Schematic of competitive growth assay. To minimise experimental variability, WT cells express a self-cutting mCherry plasmid but are functionally mCherry negative. Cells are exposed for 24hours to either 40µM C6-Cer or equivalent vehicle control and then assessed via flow cytometry to measure the percentage of mCherry positive cells in the population. (B) Experiment done in triplicate. Bars represent the percentage of mCherry+ cells over the percentage of mCherry- cells for vehicle treated (grey) and C6-Cer treated (orange) populations. sgSAFE represents the control cell line to account for Cas9 cutting effects. Statistical significance determined by two-way ANOVA (p-value 0.0332 [*], 0.0021 [**], 0.0002 [***], <0.0001 [****]).

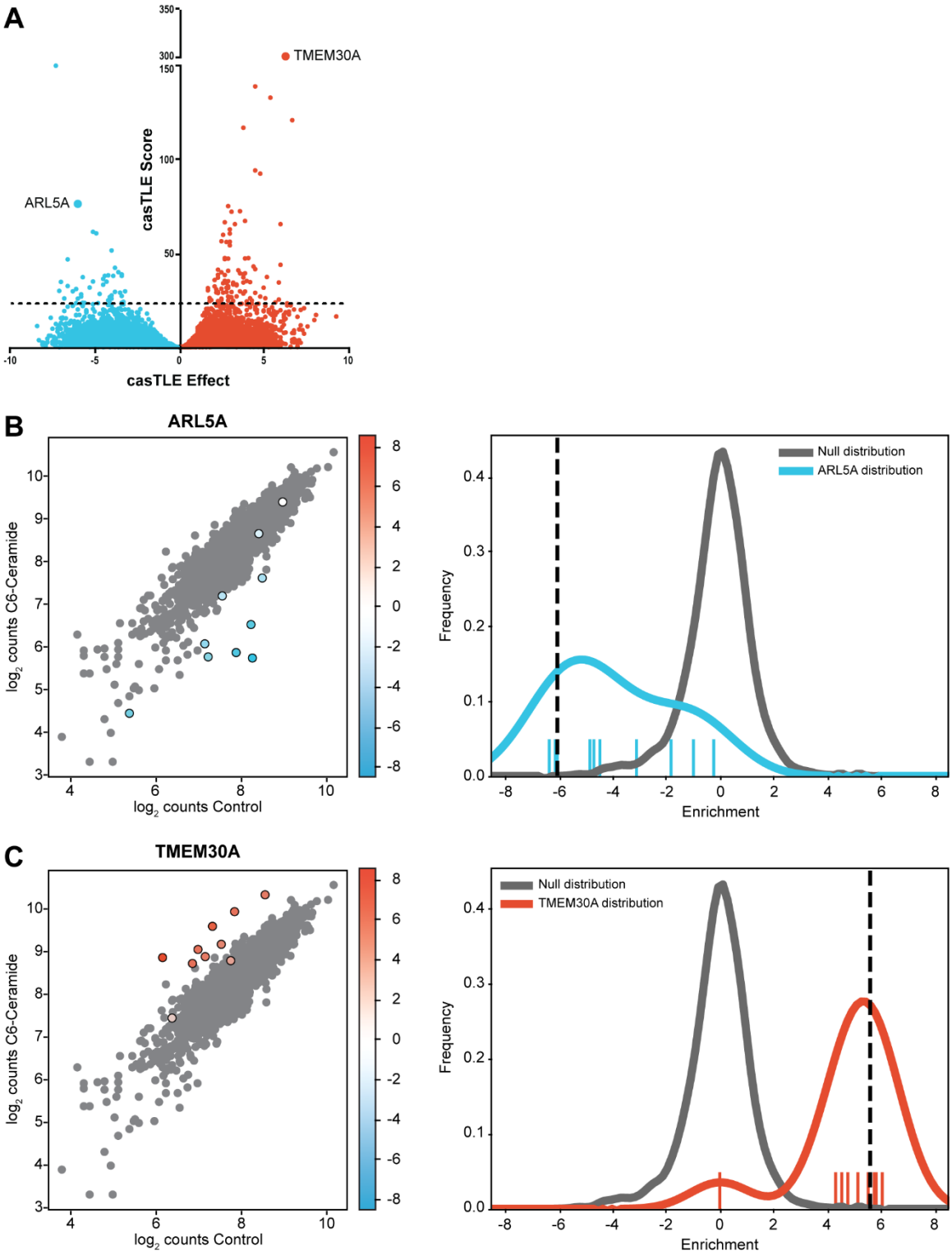

Figure 2-5: Specificity of ARL5A and TMEM30A sgRNAs

(A) Volcano plot of ARL5A and TMEM30A. (B) Histogram plot depicting density of ARL5A sgRNA elements (blue) and negative controls (grey). Shade of blue indicates the calculated casTLE effect of the specific sgRNA. ARL5A elements are enriched in the control population. This can also be seen in the frequency plot, with the grey line representing the smoothed distribution of sgNONE controls. The short vertical

lines depict the individual guides with the blue line showing the smoothed distribution of ARL5A. The vertical dotted line visualises the calculated casTLE effect. (C) Histogram and frequency plot of TMEM30A, with heavy enrichment in the C6-Cer population.

Chapter 3: Wherein death is only the beginning

3-1: The Cast of Characters

3-1-1: TMEM30A, the lynchpin of flippases

Descriptions of TMEM30A's physiological importance requires a brief introduction into flippases, which in turn, requires us to begin with membrane asymmetry. In particular, the leaflets in the eukaryotic PM are not mirror images in their lipid arrangement; this distinction is critically important as the layers 'face' extremely different environments and therefore, require different components to maintain their respective physiological roles[80,81]. In normal conditions, the exoplasmic leaflet is enriched in phosphatidylcholine (PC), SM and other large glycolipids[82,83]. The latter two molecules, in conjunction with sterols, creates the tight packing environment that maintains the PM's barrier to the extracellular ecosystem. Conversely, the cytoplasmic leaflet is 'freer' to allow higher lateral mobility of signalling networks. This layer is high in phosphatidylserine (PS), phosphatidylethanolamine (PE) and phosphatidylinositol (PI)[84–86].

Ensuring the balanced growth of the bilayer is a challenge as most phospholipids are synthesised in the ER and transported to the cytosolic layer[87]. Therefore, to prevent PM perturbations, half of these newly made phospholipids must flip into the outer leaflet. This action is unlikely to happen spontaneously as transferring the polar headgroups through the hydrophobic interior is extremely thermodynamically unfavourable[88]. Thus, the cell relies on 3 families of proteins to facilitate the movement of phospholipids across the bilayer. (1) Scramblases span the height of the bilayer to create a favourable corridor for phospholipids to travel. They are energy-independent structures that allow bi-directional travel of membrane components. (2) ATP-binding cassette transporters, as the name suggests, require ATP to move specific lipids from the cytoplasmic to the exoplasmic layer. They are also known as floppases. (3) P_4-ATPases are a subsection of the P-type ATPases; however, P_4s are unique as they flip phospholipids across membranes whilst the other P-types focus on ion transport[89]. P_4-ATPases are called flippases and are mainly responsible for flipping phospholipids from extracellular leaflet to the inner layer[83]. We shall focus on this last class as its fate is intrinsically tied to TMEM30A's function.

When localised to the PM, a functional P_4-ATPase sits like a metaphorical iceberg since very little of its α-subunit structure juts into the extracellular environment. The α-subunit consists of 4 domains: the nucleotide-binding (N) section that binds the necessary ATP, the phosphorylation (P) section that contains the aspartic acid residue to undergo transient phosphorylation, the actuator (A) domain that dephosphorylates the intermediate species to continue the reaction and finally, the membrane (M) domain to serve as the physical pathway for lipid substrates. The M-domain usually contains 10 transmembrane sections with M1-M6 serving as the main site for phospholipid flipping and M7-M10 serving as support (Figure 3-1)[71,83,90,91]. Though the α-subunit contains both the localisation sequence and the catalytic domains, it remains non-functional without its accessory β-subunit[92,93].

In mammalian systems, this accessory unit is from the TMEM30 family, of which, there are 3 members: TMEM30A, TMEM30B and TMEM30C. TMEM30s are required for stability,

proper folding of the heteromeric complex and exit of the Pα-ATPase from the ER to its intended destination. The TMEM30 glycoprotein is comprised of two transmembrane units that are joined by the long linker located in the extracellular phase. This linker is N-linked to oligosaccharide chains that stabilise the TMEM30; furthermore, there are 4 conserved cysteine residues that maintain the tertiary structure through the formation of disulphide bonds (Figure 3-1)[94]. Most mammalian cells use TMEM30A as the primary β-subunit, though many α-subunits can utilise all members of the TMEM30 family (Table 3-1)[83,95]. Assemblage of the two subunits permits the P4-ATPase to exit the ER, whereupon it may establish phospholipid asymmetry in the PM or in other intracellular membranes that require active flippases.

3-1-2: ARL5A, the mystery within trafficking

Vesicle trafficking in the *trans*-Golgi network (TGN) uses tethering complexes to establish long range contact between carriers and subcellular organelles. One such tethering complex is the Golgi-associated retrograde protein (GARP) from the Complex Associated with Tethering Containing Helical Rods (CATCHR) family. GARP is involved with the endosome-derived retrograde transport carriers of the TGN[96–98]. Recruitment of GARP to the TGN falls under the governance of small G proteins of the Arf family[99]. These G proteins cycle between their GDP-bound inactive state (localised in the cytosol) to the active GTP-bound form (associated in membranes). A sub-family of Arfs, called Arf-like (ARL), have similar genomic sequences to the Arfs, though they lack the Arf ability to activate phospholipase D[100,101].

The ARL family have diverse roles in cellular organisation, ranging from microtubule assembly to lysosomal motility; however, the function of the ARL5 class is relatively undiscovered. Studies show that the ARL5A and ARL5B are located on the Golgi and ablation of ARL5B in tissue culture cells partially delocalises GARP from the Golgi; this in turn, disrupts the retrograde trafficking from endosome to Golgi. Knock-down of ARL5A produced less significant effects, though it is surmised to have similar functionality to ARL5B[100].

3-2: Act I—Two knockouts, both alike in dignity, / In fair cell, where we lay our scene[VI,VII]

We created additional KO lines (using different sgRNAs) of our individual targets and tested these cell lines via the competitive growth assay to ensure that thus far described phenotypes were not the auspicious fate of just one sgRNA. In all cases, trends held firm (Figure 3-2). Unfortunately, commercially available antibodies to our KOs proved unreliable, therefore, we verified our lines through Tracking of Indels by Decomposition (TIDE)[102]. Successful Cas9 cutting introduces indels at the genome site that is complementary to the sgRNA sequence. TIDE analysis compares this genomic region of the KO versus the equivalent region in WT and determines the percentage of success. Thus, while we are unable to ascertain the relative protein quantification of the KO cell lines, the combination of a consistent phenotype and successful TIDE

[VI] Section and subsection headings adapted from the prologue of Shakespeare's 'Romeo & Juliet.'
[VII] Two households, both alike in dignity, / In fair Verona, where we lay our scene,

percentages (KOTMEM30A and KOARL5A lines are ≥ 90%) provides sufficient evidence that these are true protein-modified cell lines.

3-2-1: From Cas9 cut give rise to new lipid asymmetry, / Where ceramide in cytosol may be unseen[VIII]

ARL5A's TGN implications and TMEM30A's flippase association teased the possibility of a warped PM phospholipid distribution. We ascertained the relative amount of PS in the outer leaflet via a flow cytometric assay using Annexin V conjugated to FITC. Annexins bind to negatively-charged phospholipids, such as PS, in the presence of Ca^{2+} ions; thus, a high FITC signal is correlated to a large portion of bound Annexin V-FITC, which in turn, is indicative of the amount of PS on the exoplasmic surface. Dead cells were gated out via the presence of a SYTOX-live/dead cell dye. KOARL5A lines exhibit a modest increase in PS concentration within a small percentage of the population. This translates to an approximate 1.8-fold increase from control in the Annexin V-FITC geometric mean (Figure 3-3, blue). KOTMEM30A lines showed a drastic increase with more than 90% of the population holding a narrow range beyond control parameters. This is numerically seen as an approximate 6-fold increase from control in PS concentrations (Figure 3-3, red).

This dramatic change in KOTMEM30A lines is likely related to TMEM30A's accessory function as KO of the β-subunit should prevent the function of all its associated P_4-ATPase α-subunits. To measure flippase activity, we incubated cells with fluorescently-tagged PS, either TopFluor (dipyrromethene boron difluoride) PS or nitrobenzoxadiazole (NBD) PS, then quenched—in the case of TopFluor PS—or BSA-stripped—in the case of NBD PS—the outer PM leaflet. We subsequently assayed the fluorescent readout via flow cytometry. As our method abrogated any exterior fluorescence, the remaining signal represents PS moieties that were flipped into the cytoplasmic layer. As expected KOTMEM cell lines are significantly impaired in PS flipping with minimal effect in KOARL5A lines (Figure 3-4A). Based on this data, KOTMEM30A's PS distribution is likely due to the cell's inhibited flippase activity. Conversely, our flippase experiments do not support the theory of dysfunctional flippases being the root cause of KOARL5A's small PS increase.

The distinctive lipid environments of the KO cells could affect the cell's C6-Cer intake; should this be the case then KOTMEM30A's resistance would simply be the results of the lessened cytosolic exposure to the toxin and KOARL5A's sensitisation a matter of more C6-Cer uptake. To check for this phenomenon, we first established if C6-Cer encountered the same flippase deficiencies as with PS. Using fluorescently tagged short-chain ceramides (BODIPY FL (TopFluor fluorophore equivalent) C5-Ceramide and NBD C6-Ceramide) in the previously described flippase assay, we see that ceramide intralayer transport is not hindered in either KOTMEM30A or KOARL5A. Point in fact, flippase activity with regards to either ceramide is unchanged from WT (Figure 3-4B). Therefore, we then expanded our temporal scope to see if fluorescent signal changed over a further range via incubating cells with the dyes for 5min, 30min and 60min. After the proscribed interval, we removed the unabsorbed dyes and measure the

[VIII] From ancient grudge break to new mutiny, / Where civil blood makes civil hands unclean.

fluorescent signal by flow cytometry. In this case, emission detected is equivalent to intracellular levels of exogenous ceramide. A discrepancy between KOARL5A KO lines at the 5min time span, with the clonal KO-ARL5A showing higher uptake but the pooled KOARL5A-94.4 showing less (Figure 3-5, top). In KOTMEM30A, there is a slight but significant increase in dye uptake for the 5min mark (Figure 3-5, bottom). However, in all conditions, uptake is stabilised by the hour timepoint and as our screen reflects a 24hr period, it is unlikely that differential uptake in the first half-hour of exposure is the culprit behind the phenotypes. Image microscopy over an 18hr timespan with hourly scans correlate our uptake observations: uptake is unaffected in the KOs nor are there observable differences in subcellular localisation (data not shown).

3-2-2: From forth the altered genes does new death predispose / Or is synthesis where answers lie rife[IX]

As ceramide and cell death are intertwined (see Chapter 1), we wondered if these individual KOs also sensitised or resisted specific forms of cell death. If these differences in KO genes did occur, then the main players of that death pathway may provide mechanistic clues of the deeper interplay between TMEM30A/ARL5A and death. We performed an extensive array of competitive growth studies using known cell death inducers:

- Apoptosis
  - TNF-related apoptosis-inducing ligand (TRAIL)
  - FasL
  - Apoptosis Activator 2
  - Etoposide
  - TNF-α
  - Z-VAD-FMK (pan-caspase inhibitor)
- Ferroptosis
  - RSL3
  - Erastin2
  - ML162
  - Ferrostatin-1 (ferroptosis inhibitor)
- Other
  - H_2O_2 (reactive oxidation species)
  - Sorafenib (growth inhibition)
  - Obinutuzumab/anti-CD20 (cytotoxic)

In all aforementioned experiments, no significant trends emerged; thus, our KOs are not genes that pre-destines the cell to death or immortality but are intrinsically linked to ceramide, specifically, ceramide's ability to determine cell fate (data not shown). Following that logic path, we abrogated specific paths of ceramide metabolism to assess its effect in the KO lines. Myriocin, a fungal compound isolated from *Mycelia sterilia*, is a potent inhibitor of SPT, the rate-limiting step of *de novo* synthesis. Fumonisin B1, also of fungal origin but more specifically, within the genus *Fusarium*, is a competitive inhibitor of CERSs (Figure 1-1). Usage of either inhibitor did not

[IX] From forth the fatal loins of these two foes / A pair of star-cross'd lovers take their life;

provide significant results (data not shown) and as such, the *de novo* pathway is an unlikely source for answers.

Deflated but not defeated, we continued on to other routes of ceramide synthesis by harnessing chemical inhibitors of acidic SMase, desipramine HCl (Des), and neutral SMase, GW4869; to stimulate the reader's recall: acidic SMase converges in lysosomes and endosomes whilst neutral SMase are concentrated on the PM's inner leaflet (Figure 1-2). Here we see that inhibiting acidic SMase partially rescues KOTMEM30A's C6-Cer resistance as there is a significant difference between cells treated with C6-Cer and cells dual-treated with C6-Cer and Des. By itself, Des does not alter the population of cells from untreated, therefore the observed increase in Des + C6-Cer is unattributable to any innate ability of Des to confer C6-Cer resistance. KOARL5A poses an interesting conundrum as the trend suggests a full rescue of KOARL5A's C6-Cer sensitisation; however, this change is considered statistically insignificant (Figure 3-6A). Turning to neutral SMase, again we see that GW4869 treated cells are unchanged from untreated in either KO cell lines; however, co-incubation of C6-Cer + GW4869 shows full rescue of the KO phenotypes of both KOTMEM30A and KOARL5A (Figure 3-6B). The effects of Des and GW4869 indicate that functional SMases are partially—or mayhap fully—responsible for the functional effects of the KOs. As SMase catalyse the breakdown of SM into ceramide, this additionally suggests that C6-Cer's stimulation of the cell's non *de novo* production of endogenous ceramides is a driving force of the cell's fate.

3-2-3: Whole mechanisms in the cellular tableaux / By SMase may we explain C6-Cer's strife[X]

While the lack of positive targets in our forays of specific cell death are frustrating, it nonetheless provides valuable validation of our screen hits. As discussed in prior chapters, a legitimate critique of death-based screens is the real possibility that identified genes are general death markers (e.g., caspase-9 for apoptosis, FSP1 for ferroptosis) rather than compound specific hits. The unchanging effects of the assays in Chapter 3-2-2 provide conclusive proof that KOTME30A and KOARL5A are specific agents in C6-Cer's route of cellular toxicity.

In terms of mechanism of action, the differential rescue abilities of the SMase inhibitors strongly suggests that while catabolism of SM into ceramide is a factor, full rescue is ultimately determined by the location of the SMase (Figure 3-6). Acidic SMases operate in low pH environs such as lysosome and later-stage endosomes. This is also the site of the salvage pathway, from which acidic SMases offers 3 ceramide fates: one, to remain as ceramide; two, to catabolise further into sphingosine and then reform as a new ceramide species; three, to breakdown into sphingosine but under phosphorylation into S-1-P (Figure 1-2). This last path represents a deduction in global endogenous ceramide; thus, if our KO phenotypes rely on endogenous pools, then the S-1-P possibility could explain why inhibition of acidic SMase creates a partial—not full—ablation of the KO's phenotype. This 'continuous pool' theory may also explain neutral SMase's full rescue effect. These enzymes populate the inner leaflet of the PM and are dedicated to the production of ceramides. Moreover, PM localisation means the cell's first (and likely quickest)

[X] Whole misadventured piteous overthrows / Do with their death bury their parents' strife.

way to produce these endogenous ceramides is via the neutral SMase since this enzyme subclass is not reliant of the added transport time of journeying to a specialised subcellular compartment (i.e., acidic SMase and SM must be transported to a lysosome).

C6-Cer's mass movement could explain the fluctuations seen in the uptake assays (Figure 3-5). Addition or subtraction of the PM operates in a 'tit for tat' function; as one leaflet changes in size, the other must quickly accommodate in like mode or risk the protective barrier of the PM[85,103,104]. Therefore, C6-Cer exoplasmic exposure creates a biophysical challenge where the solution is a minimisation of C6-Cer concentration by either preventing the compound from outer leaflet insertion or equalising the interfaces; since C6-Cer does invade, the cell must undergo the latter. Exogenous additions of ceramide in multilammelar vesicles increases the surface pressure of the outer monolayer; conversely, ceramide formation from SM creates an initial pressure decrease in the outer layer and could quickly stabilise the pressure increase from the invading C6-Cer. This effect may explain why a 60min interval was required to stabilise C6-Cer uptake and moreover, why neutral SMase had such a startling effect: the individual actions of each SMase took time to equilibrate and a continuous pool of endogenous ceramides on the cytoplasmic PM leaflet is a necessity to balance out the physical forces of C6-Cer. However, the actions of neutral SMase do not account for KOTMEM30A's resistance nor KOARL5A's sensitivity as the GW4869 + C6-Cer condition mimicked their respective untreated cell ratios (Figure 3-6). What, therefore, is the missing link?

In answer, we turn to our flippase data and its implications in lipid asymmetry. We see that PS-flipping in KOTMEM30A is vastly decreased, with KOARL5A's PS-flipping relatively unperturbed (Figure 3-4A, red and blue, respectively). KOTMEM30A results in an extremely large concentration of PS in its exoplasmic leaflet (Figure 3-3, red). As an aside, our experiments also show that C6-Cer intake is independent of flippase activity, or more specifically, TMEM30A-associated P_4-ATPase activity. These short-chain ceramides have numerous possibilities of cellular entry (e.g., scramblases); additionally, C16-cers—and to a lesser ability, C6-Cer—can induce trans-layer lipid movement and thereby provide another thermodynamically route of intake[105]. Referring back to the point of lipid asymmetry, WT cells concentrate PC and SM on the exoplasmic surface. Ceramide does not intermix well with these phospholipids and in such a lipid environment, CRPs readily form[103,106,107]. By contrast, high PS in the exoplasmic layer creates a more fluid membrane, hence why cell-surface receptors undergo more lateral movement in KOTMEM30A cells[68,69,108,109]. Therefore, it is possible that there are less CRPs in the PS environment and this in turn, could change the compounds that are exposed on the individual KOs. In essence, the surface may contain key mechanistic differences that identifies the interplay of TMEM30A, ARL5A and C6-Cer.

3-3: Act II—Now is the experiment to find proteins absent / And see how the knockouts do fork; / The queries and questions we shall not grouse / As answers lend a visage non-harried[XI,XII]

Understanding the deviations of the cell surface required isolation of the PM proteins from the total cell proteome. We achieved this required separation by conjugating the surface expressed peptides to biotin through use of a *N*-hydroxysulfosuccinimide (NHS) ester disulphide bound to biotin (NHS-SS-Biotin). The NHS ester reacts with primary amines, like that of the N-terminus of a polypeptide or the side chain of lysine, to form a stable amide bond through the release of NHS as the leaving group. As the sulfonate group of NHS-SS-Biotin cannot permeate the cell membrane, this reagent can only crosslink with primary amines exposed to the extracellular medium (Figure 3-1, K-label). After biotinylation, cells are lysed then the total protein extract is incubated with NeutrAvidin resin. The biotin binds to the resin and the efflux is removed through subsequent wash steps; the disulphide bond of the now protein-SS-Biotin-NeutrAvidin complex is reduced to free the bound protein from the biotin-resin matrix. Removal of the resin leaves a pool of surface proteins that can be analysed by protein mass spectrometry to identify the resultant polypeptides.

3-3-1: Now our minds alight from data the mass spec bequeaths; / As proteins are no mere ornaments; / The peptides we analyse in further proceedings, / To see the difference in knockout features[XIII]

The UpSet plots of figure 3-7 are visualisations of the number of individual surface proteins identified per cell line, the intersections between cell lines and the aggregates of said intersections. Control lines are represented by sgSAFE and self-cut mCherry; sgSAFE served as our control mCherry+ line in our competitive growth assays with self-cut mCherry serving as our WT mCherry-. The combination of these two lines minimises targets that are only unique to their individual backgrounds in order to provide a true WT comparison. KO3-TMEM30A and KO5-TMEM30A are clonal lines of sgTMEM30A-0.2 with KOTMEM30A-7.9 a KO pool of sgTMEM30A-7.9. KO2-ARL5A and KO5-ARL5A are clonal lines of sgARL5A-93.3 whilst KOARL5A-91.1 and KOARL5A-94.4 are polyclonal pools of sgARL5A-91.1 and sgARL5A-94.4, respectively. Appendix C provides the protein abundances of each line.

Figure 3-7 shows the overlap of the same proteins detected in the indicated cell lines; but much like dark matter, we can infer much from what is not seen. To that end, we calculated the fold change and p-values of the protein abundances of the individual KO lines to the pooled control; from these datasets, we mined out hits with p-values < 0.012. Figure 3-8 represents the number of significant hits and their overlap between the respective KOs. The aggregate middle

[XI] Section and subsection headings adapted from Shakespeare's 'Richard III.'

[XII] Now is the winter of our discontent / Made glorious summer by this sun of York; / And all the clouds that lour'd upon our house / In the deep bosom of the ocean buried.

[XIII] Now are our brows bound with victorious wreaths; / Our bruised arms hung up for monuments; / Our stern alarums changed to merry meetings, / Our dreadful marches to delightful measures.

of the Venn diagrams shows the number of proteins that are significant in all the lines of the specific KO gene. This gives us 191 targets that are important in all KOTMEM30A lines. This combinatorial approach essentially creates an isogenic background from which we can conclude that KO of TMEM30A, regardless of which sgRNA, results in altered expression of these 191 hits when compared to control (Appendix D). In KOARL5A, there are 185 hits that fit the aforementioned criteria (Appendix E). Within these datasets, 104 targets are specific for KOTMEM30A, 98 for KOARL5A and an overlap of 87 proteins between the two KO sets (Figure 3-9, Venn diagram). The mean $\log_{10}$(fold change) of the proteins was calculated and arranged by increasing standard deviation of the mean (Figure 3-9, charts). TMEM30A arose as the top protein hit for the KOTMEM30A-only hits (107 pool) and provides proof positive that KOTMEM30A cell lines are, indeed, KOs of TMEM30A. Additionally, within the top 25 of this set, ATP11B emerged as a target. ATP11B is a P_4-ATPase α-subunit that complexes with TMEM30A to form a flippase unit with preferential affinity for PS (Table 3-1). As we have previously shown that KOTMEM30A cells exhibit high PS in the outer leaflet, perhaps this subunit is the main culprit behind KOTMEM30A's PS phenotype.

Trace analysis of the detected ATP11B peptide fragments confirm the calculated negative $\log_{10}$(fold change) of KOTMEM30A versus control (Figure 3-10A; Appendix F: MS2 of ATP11B peptides). Interestingly, while the N-terminal fragments are absent in the KOTMEM30A traces, C-terminal peptides do appear (Figure 3-10A, red and green lines). The mammalian system contains 3 forms of TMEM30 and each can bind to ATP11B. Perhaps the lack of functional TMEM30A results in a compensatory pathway of ATP11B associating with the other paralogs. As the TMEM30 paralogs all contain two transmembrane helices and a heavily glycosylated exoplasmic domain, this structural similarity may be enough to remove the complexed P_4-ATPase from the ER and translocate to the PM[110,111] (recall that the α-subunit contains the localisation sequence of the heterodimer). However, while the different isoform is enough to entail transport, enough folding mismatches can occur that the ATP11B complex is too impaired for a full membrane insertion. Since the β-subunit is required for full P4-ATPase stability, the substitution of a non-TMEM30A unit may only stabilise the closest ATP11B helices, namely, those at the C-terminal end of the polypeptide.

We assessed the basal levels of ATP11B in the KOTMEM30A cell lines where, once again, we run afoul of commercial antibodies and thus, western blots of ATP11B are not possible. Thus, we checked ATP11B mRNA expression via RT-qPCR and found that transcript levels are equal between control and KOTMEM30A (Figure 3-10B). Assuming that translation is not hindered, this means that protein expression of ATP11B is equal in both KO and control. Thus, the differences we observed from trace analysis are entirely due to post-translational interplay of the missing TMEM30A and the lonesome ATP11B.

To test our hypothesis of ATP11B's role in the KOTMEM30A mechanism, we initiated a siRNA knock down of the gene in the control cells. After confirming the successful knockdown by RT-qPCR (Figure 3-10C), we assayed the cells to determine their competitive growth and PS exoplasmic concentration. Annexin V results depict the siATP11B population's increase in PS levels versus control conditions (cells treated with non-targeting siRNAs). This population increase translates to approximately a 2-fold increase from control. (Figure 3-11A,B).

Furthermore, the competitive growth assay definitively shows that knockdown of ATP11B resists C6-Cer death (Figure 3-11C). The results from both experiments track the same trends as KOTMEM30A.

3-3-2: Pensive brow hath dogged our hunt; / And now, surface hits thus proceeds / Thoughts, plots and pathway commentaries, / The PS, the enzymes, the ports of ceramide harbour, / Converging all to just one route[XIV]

Knockdown of ATP11B follows KO of TMEM30A as the common causalities in both is resistance to C6-Cer death and a higher concentrate of PS in the extracellular PM leaflet. True, the phenotypes in ATP11B knockdown are less abrupt, but that could relate to the fact that our ATP11B studies are reflections of partial protein expressions in a knockdown rather than the complete nullification of a KO. TMEM30A is tied to other P_4-ATPases that populate all membrane-bound organelles, thus its higher fold changes could be the additive effect of downregulating multiple flippases. However, it must be noted that of the known P_4-ATPases, ATP11B appeared as a significant hit in both the CRISPR-KO screen (Table 3-1, p-value is within 10% FDR) and the surface protein mass spectrometry, whereas all other α-subunits remained amongst the weeds. Therefore, the compilation of my data implicates ATP11B in the TMEM30A and as ATP11B's main function is to flip PS, we propose that KOTMEM30A's resistance to C6-Cer is due to extremely high levels of PS in the exoplasmic leaflet.

Perhaps the high concentration of this phospholipid means a concurrent loss of PC and SM in said environment. Our microscopy data did not indicate a size difference amongst the KO and control lines; thus, the cell must accommodate the increased PS by displacing other lipids to the inner leaflet[112,113]. The location of SM, especially, might explain the importance of neutral SMase in our KO phenotypes. The direct impact of PS upon neutral SMase is unclear as literature disagrees on whether the phospholipid inhibits or stimulates the enzyme's activity[114,115]. In either case, our SMase inhibition experiments strongly suggests that the catalytic function of SMase, particularly the neutral SMase, is critical in C6-Cer death (Figure 3-5).

The nuanced answer of why neutral SMase can rescue both a resistor and sensitiser lie in its production of particular types of endogenous ceramides. The chain length of ceramide is a result of the hydrolysed SM (e.g., a C16-SM will produce a C16-cer)[116]. Increased concentration of a particular type of ceramide species could alter the ratio of C16:C24 ceramides and thus, effect cell fate. Section 2-1-1 outlines how K562 survival is determined by KOs that increase C24-cer while paths that produce C16-cer lead towards C6-Cer death. Perhaps this trend also applies to KOTMEM30A and KOARL5A. KO of TMEM30A could drive C24-SM hydrolysis and thus, towards life, while KO of ARL5A pushes C16-SM hydrolysis, and thus, towards death. This possibility would account for why negation of neutral SMase (the enzyme that drives both stated reactions) equalises the KO phenotypes to that of control.

[XIV] Grim-visaged war hath smooth'd his wrinkled front; / And now, instead of mounting barded steeds / To fright the souls of fearful adversaries, / He capers nimbly in a lady's chamber / To the lascivious pleasing of a lute.

This ceramide species interplay is, mayhap, where we find the reasoning behind KOTMEM30A's and ATP11B-knockdown's connection of PS and C6-Cer resistance; however, we must first explain the involvement of the thus far shadow player, cholesterol. Cholesterol's hydrophobic structure associates tightly with its neighbouring lipids, moreover, its small headgroup gives it relatively easier ability to flip-flop between membrane bilayers[117]. PS is able to induce phase separation in cholesterol-bound lipid bilayers to draw cholesterol to the phospholipid's layer whereupon PS is essential for retaining the cholesterol within its leaflet[82,118,119]. Furthermore, cholesterol-PS nanodomains reflects an enrichment of C24-SM in the opposing layer[120–124]. Therefore, high concentration of PS in the exoplasmic leaflet similarly retains a high amount of cholesterol in the outer layer. This in turn increases the amount of C24-SM in the cytoplasmic layer which is then hydrolysed by neutral SMase to C24-cer. This uptick in C24-cer shifts the ratio of C16:C24 endogenous ceramide pools to favour cell survival (Figure 3-12A).

The cholesterol driver in the theory of C16:C24 is further tantalised when we look at the individual hits of KOARL5A (Figure 3-9). Of the hits specific to KOARL5A lines, apolipoprotein E (APOE) arises to the top. APOE is released from its storage compartments when cells are prevented from successful phagocytotic functions; APOE can then localise to the PM invaginations of surface-connected compartments (SCC)[125–129]. These SCCs are rife with cholesterol crystals where APOE is required to facilitate cholesterol solubilisation[126,130–134]. The appearance of APOE in KOARL5A strongly suggests that these cells suffer from an overabundance of cytosolic cholesterol and thus, APOE is needed to transition cholesterol to the outer leaflet (this could also account for the slight increase in KOARL5A's PS exposure in Figure 3-3). Sterols have a marked preference for C16-SM[105,121,123] and the conjunction of cholesterol and C16-SM create expansive, rigid lipid domains that cement the SCC structure[124,135–137]. The secretion of APOE is likely an attempt to 'release' the cholesterol:C16-SM of the SCC via solubilising cholesterol. To combat the other arm of the duo, neutral SMase can convert C16-SM into C16-cer. Adding to the runaway chain of C16-cer production is ARL5A's rather unexplored role in the TGN. Cholesterol can also associate with C16-cer and research shows that late endosomes and the TGN are heavily populated by cholesterol:C16-cer domains[133,138–140]. As ARL5A is implicated in the TGN, specifically that of retrograde transport from endosome to Golgi, perhaps the KO of ARL5A halts the continuing processing of these cholesterol:C16-cer compartments[122,128,141,142]. Thus, through the hydrolysis of C16-SM and the shuttered activity of the TGN, C16-cer concentration grows and drives the cell towards death (Figure 3-12B).

Therefore, the addition of C6-Cer exacerbates the conditions pre-formed by the respective KOs. Prolonged exogenous exposure of C6-Cer (like that of our screen conditions) requires cells to undergo a requisite uptick in endogenous ceramide production via neutral SMase (to stabilise the biophysical pressures between leaflets). Per our proposed mechanism, the cytosolic leaflet of KOTMEM30A is high in C24-SMs, thus the uptick in SMase activity is production of pro-survival C24-cer. For the KOARL5A, C6-Cer's increase in SMase activity is the tipping point that overwhelms the cell's ability to process the ever-increasing amounts of C16-cer and thus, the cell succumbs to death.

The results in this body of work support the proposed mechanism, albeit through a piece meal fashion. Truly delving the depths of this theory requires a readout of the lipid species within each KO. Lipidomics of the steady-state of KOs and upon perturbation of C6-Cer would provide a comprehensive readout of the rise and/or fall of the lipids discussed herein. Furthermore, imaging and quantifying cholesterol subcellular localisations would map the movements that drive the changing lipidome; perhaps, too, this could highlight the SCCs that are hinted by KOARL5A's APOE.

3-4: Chapter 3 Materials & Methods

3-4-1: Cell lines and culture conditions

Same conditions as described in Chapter 2-4-1. Additionally, U-2 OS Tet-On cells were purchased from Clontech (630919). U2OS HEK293T was obtained from UC Berkeley's cell culture facility. U-2 OS Tet-On and MDA-MB-453 lines stably expressing Cas9 were generated by infection with lentiCas9-Blast, a gift from F. Zhang (Addgene, 52962). U-2 OS Tet-On cell lines were maintained in DMEM containing 4.5 g/l glucose and L-glutamine (Corning, 10-017-CV) supplemented with 10% foetal bovine serum (Gemini Bio Products) and penicillin (10,000 I.U mL^{-1}). Cell lines were maintained at 37°C with 5% CO_2 with regular screening for mycoplasma contamination.

3-4-2: Generation of additional CRISPR-Cas9 generated cell lines

Methods as described in Chapter 2-4-5. Single clones were isolated from the sgTMEM30A-0.2 line and the sgARL5A-93.3 line via serial dilution. The sgRNA sequences for the additional KO lines are as follows:

Plasmid	Sequence (5' to 3')
sgARL5A-91.1	GGACAGTACAGACAGAGAG
sgARL5A-94.4	GTTAGTATAGTAAGTGTTCC
sgTMEM30A-3.5	GTGCCAGCCGTAAGGAT
sgTMEM30A-7.9	GGCAACGTGTTTATGTATTA

3-4-3: Competitive Growth & Caspase 3/7 Assays

Competitive growth assays are as described in Chapter 2-4-6. Caspase assays follow the same experimental setup and the use of the Cell Event Caspase 3/7 Green Flow Cytometry Assay kit (Invitrogen, C10740). List of the compounds used is as follows:

Apoptosis Activator 2	Cayman, 10004176
Desipramine HCl	Sigma, D3800
Erastin2	Cayman, 27087
FasL	Abcam, AB186673
Ferrostatin-1	Cayman, 17729
Fumonisin B1	Enzo, BML-SL220-0001

GW4869	MedChemExpress, HY-19363
H_2O_2	Thermo, H325-100
ML162	Cayman, 20455
Myriocin	Sigma, M1177
Obinutuzumab	GenScript, A01945-40
RSL3	Cayman, 19288
Sorafenib	Cayman, 10009644
TNF-α	FisherSci, MAB2101
TRAIL	Abcam, AB9960
Z-VAD-FMK	Cayman, 27421

3-4-4: Annexin V Assay

Assay was adapted from manufacturer directions of the FITC Annexin V Apoptosis Detection Kit (BD Pharmingen, 556547). K562 cells were collected from cultures that were 98% live (determined by Trypan Blue staining). Samples were incubated with SYTOX-Deep Red Live/Dead Fluorescent Dye (Invitrogen, S11380) for 15min at 37°C, then washed twice with DPBS (Gibco, 14190-144) before proceeding with Annexin V-FITC incubation. Samples were analysed by flow cytometry; dead cells (i.e., SYTOX-Deep Red positive) were gated out and the FITC spectra measured of the remaining population.

3-4-5: Flippase Assay

NBD C6-Ceramide (Cayman, 62527), TopFluor PS (Avanti, 810283C) and NBD PS (Avanti, 810194C) were prepared as previously described[119]. In brief, compounds were dried under N_2 and resuspend in methanol. BODIPY FL C5-Ceramide (Invitrogen, D3521) was resuspended as per manufacturer directions.

Incorporation of lipids is modified from methods described[86,143]. Compounds are pre-incubated in 4mg/mL BSA (Sigma, A8806) in H_2O under constant rotation at 300rpm for 30min at 37°C. K562 cells were collected via centrifugation, washed and equilibrated at 15°C for 30min in Hank's balanced salt solution (HBSS) containing 1g/L glucose (Gibco, 14025-092) at a concentration of 500,000 cells/mL. After cell equilibration, the incubated compounds were added to the cell suspension to the required lipid concentration. This mixture was incubated at 15°C for 20min with constant rotational speed of 300rpm. At the end of the timepoint, NBD conjugated compounds were mixed with equal volume of ice-cold 5mg/mL BSA in HBSS to extract the lipids incorporated into the exoplasmic PM leaflet. TopFluor and BODIPY FL compounds were quenched with Trypan Blue (Corning, 25-900-CL) to a final concentration of 0.2% Trypan Blue. Cells were then analysed by flow cytometry to find the geometric mean of FITC emission. Replicates were averaged and normalised to control values.

3-4-6: Uptake Assay

Uptake assay is adapted from the flippase method. Samples were plated in a 96-well round bottom plate to a final concentration of 500,000 cells/mL with lipid incorporation occurring in regular media. Samples were incubated at 37°C at 5% CO_2 for the designated timepoints. At the end of each timepoint, cells were washed thrice with DPBS and assayed by flow cytometry. Replicates were averaged and normalised to control values.

3-4-7: Surface Biotinylation Assay

All buffers were filter sterilised prior to use. Each sample required 24 million cells that were pelted and washed with PBS, twice. 10mM of freshly prepared EZ-Link™ Sulfo-NHS-SS-Biotin (Thermo, A39258) in PBS and added to the cell mixture at 80µL of 10mM NHS-SS-Biotin per mL of sample volume. Samples were incubated by rocking at room temperature for 30min. After incubation, cells were pelleted at 300 g-force for 3 min, excess biotin discarded and then washed twice with ice-cold TBS.

Proteins were collected from cells via lysing with dissolved Pierce™ Protease Inhibitor Mini Tablets, EDTA-free (Thermo, A32955) in RIPA buffer (Thermo, 89901). Samples were sonicated for 15sec at 15% amplitude, followed by vortexing for 10sec every 10min for 30min. This was followed by a 5min centrifugation at 15,000 g-force and supernatant.

Enrichment of biotinylated proteins proceeded by overnight incubation at 4°C on NeutrAvidin resin (Thermo, 53150) at a ratio of 10µL of beads per 100µg protein. After incubation, samples were centrifuged at 700 g-force for 2min at 4°C. Pellets then underwent a series of wash steps: twice with lysis buffer, thrice with ultrapure H_2O and finally, twice with 50mM ammonium bicarbonate (ABC), pH 8.0. A portion of clarified proteins were assessed for biotinylation efficiency via western-blotting with a streptavidin secondary antibody (Li-Cor, 32230). Biotinylated proteins were eluted from resin using 10mM dithiothreitol (Thermo, R0861) dissolved in 50mM ABC by end-over-end rotation at room temperature for 30min. Sample was centrifuged at 700 g-force for 2min and supernatant collected.

Sample preparation for mass spectrometry required the addition of 25µL of freshly-prepared 55mM iodoacetamide (dissolved in 50mM ABC) with a requisite 30min incubation at room temperature in the dark. After the time interval, we added ice-cold acetone to mix overnight at -20°C. Samples were then centrifuged at 15,000 g-force for 10min, then decanted for 30min at room temperature to precipitate proteins.

Precipitated proteins were resuspended in 25mM ammonium bicarbonate, digested overnight using 1µg of trypsin (Promega, V5113) at 37°C. Samples were acidified with 10% v/v of trifluoroacetic acid, desalted using C18 stage tips, and dried. For MS analysis, peptides were resuspended in 1% formic acid and separated on an Easy nLC 1000 UHPLC equipped with a 15cm nanoLC column. Using a flow rate of 300 nL/min, the linear gradient was 5% to 35% over B for 90 min, 35% to 95% over B for 5 min, and 95% hold over B for 15 min (solvent A: 0.1% formic acid (FA) in water, solvent B: 0.1% FA in ACN). The table indicates ley mass spectrometer parameters.

Method parameter	**Value**
Polarity	Positive
Full MS	
Microscans	1
Resolution	120,000
Automatic gain control (AGC) target	1×10^6 ion counts
Maximum injection time	50 ms
Scan range	350-2000 *m/z*
dd-MS²	
Microscans	1
AGC target	1×10^4 ion counts
Maximum injection time	50 ms
Isolation window	2 *m/z*
Normalized collision energy	27
dd settings	
Ion trap scan rate	Rapid
Desired minimum points across the peak	6
Charge inclusion	1-7
Exclude isotopes	on
Dynamic exclusion	15 s
Mass tolerance	10 ppm

Peptide identities and relative abundances were determined using Proteome Discoverer 2.4. Ion chromatograms were extracted using Xcalibur Qual Browser for each peptide of interest with a mass tolerance of 0.5 Da. We thank Dr. Steve Eyles (UMass Amherst, RRID: SCR_019063) for assistance with high-resolution MS acquired on an Orbitrap Fusion mass spectrometer (NIH grant: 1S10OD010645-01A1).

3-4-8: Analysis of Protein Abundances

UpSet plot analysis used the Appyter set comparison notebook[144]. To remove the effect of any off-target targets, sample protein abundances were subtracted with the respective protein abundances of the PBS-control. PBS-control underwent the sample preparation described in Chapter 3-4-7, save the lack of NHS-SS-Biotin during the PBS incubation. From this, we zeroed out any negative amounts. High-throughput data analysis proceeded via the Appyter bulk analysis pipeline comparing the combined control lines to the individual KO line[144]. We utilised Z normalisation, without filtering out low expression hits using the limma differential expression method. This outputted datasets of fold change between controls versus KO with the associated p-value. Proteins that met the threshold of p-value < 0.012 were isolated and target lists compared between the appropriate KO lines.

3-4-9: siRNA Knockdown of ATP11B

sgSAFE cells were transfected with either siATP11B (Horizon, L-023660-00-0005) or siNon-targeting control (Horizon, D-001810-10-05) using Lipofectamine RNAiMax transfection reagent (Thermo, 13778) according to manufacturer directions. Incubation proceeded for 48hr, whereupon samples were washed and divvied into 3 populations: two for subsequent competitive growth assays and Annexin V studies, with the last assessed for knockdown efficiency via RT-qPCR. K562 self-cutting mCherry cells were also transfected with siNon-targeting control to serve as the mCherry- population in our competitive growth assay.

3-4-10: RT-qPCR

Total RNA of cell samples was extracted using the Monarch Total RNA kit (NEB, T2010S) and then reverse transcribed with iScript cDNA Synthesis kit (Biorad, 1708890). cDNA was measured using a CFX96 Touch Deep Well Real-Time PCR system (Biorad) with the probe-based PrimeTime Gene Expression Master Mix (IDT, 1055770). Fold changes in cDNA were determined using the $\Delta\Delta C_t$ method[145] normalised to PPIA cDNA. Primer pairs were purchased from IDT's predesigned PrimeTime Standard qPCR assay; sequences are as follows:

Gene	Primer	Sequence (5' to 3')
	Probe	/56-FAM/AACACAATA/ZEN/CCAATCCTTGCAGCAGC/31ABkFQ/
ATP11B Exon 14-16	Primer 1	ATCGCAGTTGGAGTACTATGC
	Primer 2	CCGTTCCAGTTTTCCAAGAGT
	Probe	/56-FAM/ACCAACGAC/ZEN/AGGAGCATCTTGACTC/31ABkFQ/
ATP11B Exon 29-30	Primer 1	GTAGTCCAACCCACATCAGC
	Primer 2	CCCTTTAACAAGTAGATGAGTCCA
	Probe	/56-FAM/AATTCACGC/ZEN/AGAAGGAACCAGACAGT/31ABkFQ/
PPIA Exon 5-5	Primer 1	GTGGCGGATTTGATCATTTGG
	Primer 2	CAAGACTGAGATGCACAAGTG

3-4-11: Cell counts, Statistical Analysis and Reproducibility

Unless otherwise indicated, cell amount/concentrations were derived from live cell counts (determined by Trypan Blue staining). Experimental populations were collected from growing pools that exhibited ≥ 97% live. Additionally, unless otherwise indicated, experiments were done in triplicate with statistical significance calculated in Prism.

Chapter 3 Figures & Tables

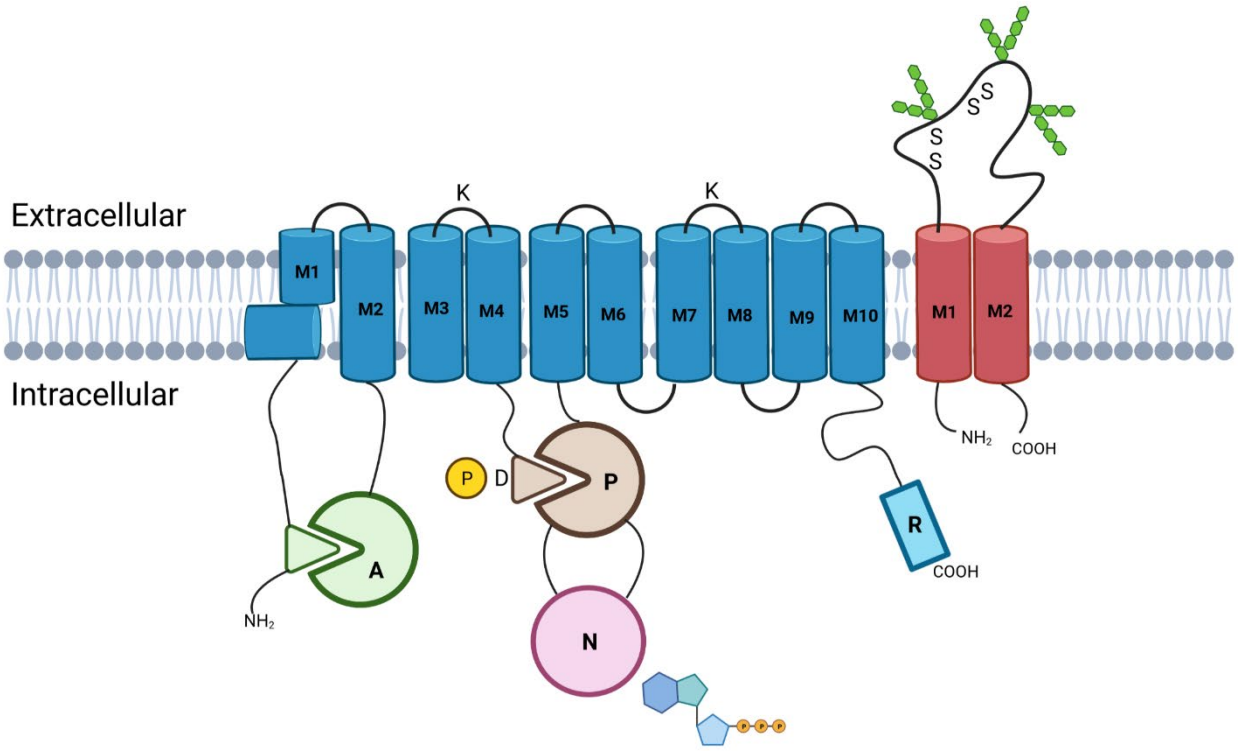

Figure 3-1: Structure of P_4-ATPase flippase embedded in the PM[xv]

P4-ATPases overcome the thermodynamically unfavourable transport of their preferred lipid substrates from the outer to inner leaflet. The α-subunit is the catalytic section of this heteromer and contains 4 domains. The ATPase portion consists of N-domain (pink) to bind ATP (molecule), P-domain (brown) to be transiently phosphorylated on its aspartic acid (D) and A-domain (green) to aid the dephosphorylation of P-domain and reset the ATPase reaction. The blue cylinders are the transmembrane helices of the M-domain and are the site of lipid transport. The β-subunit, TMEM30, is represented with two red transmembrane domains with a substantial presence in the extracellular environment. The exoplasmic linker is heavily glycosylated and further stabilised by disulphide (SS) bonds. The α- and β-subunits must properly assemble in order for the P_4-ATPase to leave the ER. Lysine (K) residues depict potential sites for NHS-Biotin tagging and subsequent pulldown.

[xv] Figure created with Biorender.com.

Class	P_4-ATPase α	Ensembl Gene ID	Substrate	casTLE Effect	casTLE Score	casTLE p-value
Class 1a	ATP8A1	ENSG00000124406	PS > PE	0	0	0.874
	ATP8A2	ENSG00000132932	PS > PE	-0.6	0.622	0.550
Class 1b	ATP8B1	ENSG00000081923	PC, possibly PS	-1.7	3	0.126
	ATP8B2	ENSG00000143515	PC	2.6	12.6	0.00169
	ATP8B3*	ENSG00000130270	Possibly PS	-2.3	0.593	0.560
	ATP8B4	ENSG00000104043	Unknown	2.4	4.24	0.0944
Class 5	ATP10A	ENSG00000206190	PC	0	0	0.867
	ATP10B	ENSG00000118322	Unknown	-2.9	2.31	0.185
	ATP10D	ENSG00000145246	Unknown	-1.7	1.19	0.356
Class 6	ATP11A	ENSG00000068650	PS > PE	0.4	0.335	0.656
	ATP11B	ENSG00000058063	PS > PE	2.9	14.5	0.00618
	ATP11C	ENSG00000101974	PS > PE	-2.2	6.59	0.0367

*Unknown β-subunit

Table 3-1: Mammalian P_4-ATPases with TMEM30A as the β-subunit
List of known α-subunits that use TMEM30A as their preferred accessory unit. Classes are categorised by similarities in genomic sequence and protein structure. casTLE effect, score and p-value are calculated from the combined CRISPR-KO screens.

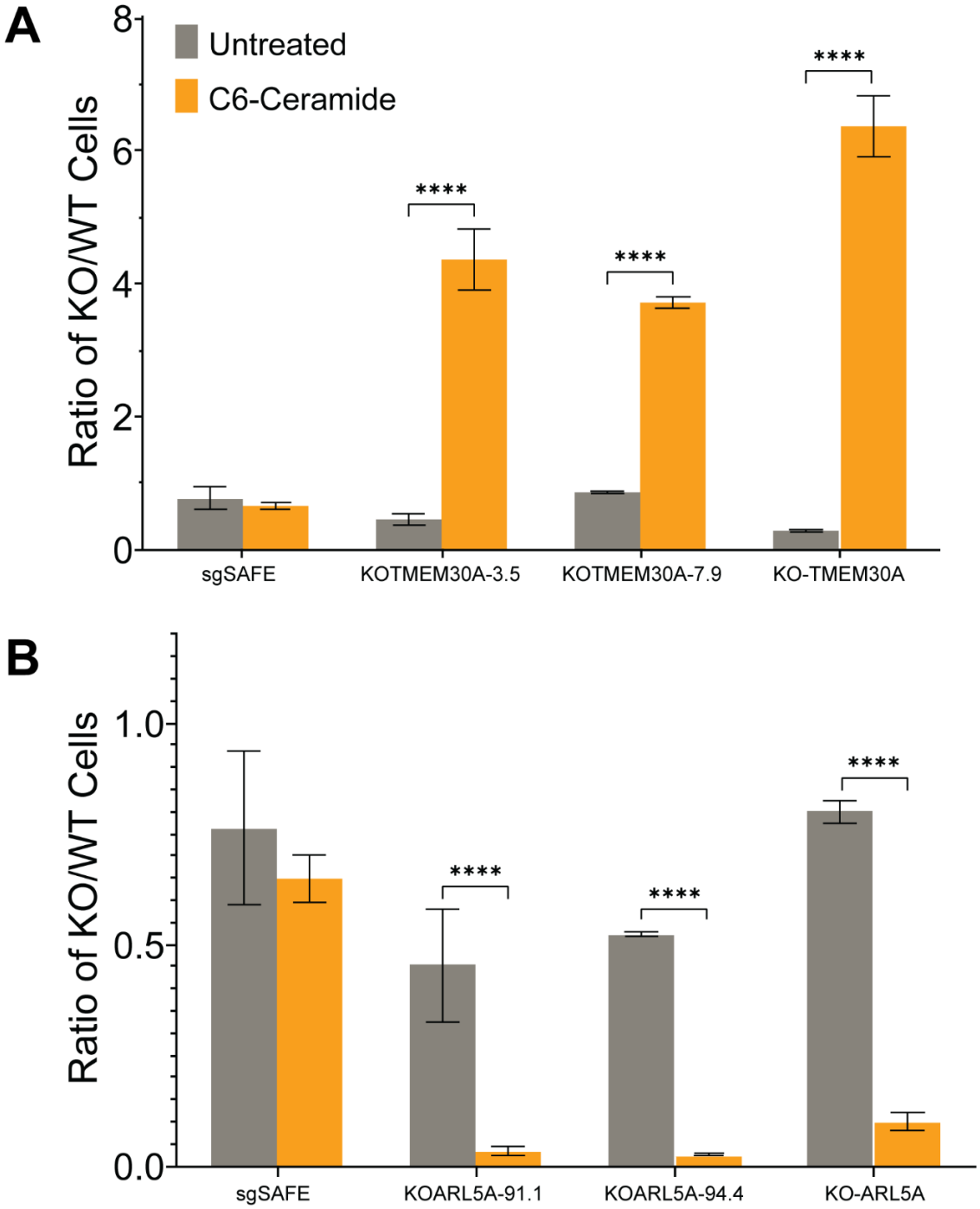

Figure 3-2: Competitive growth assays of multiple sgRNAs

Experiment done in quadruplicate. Bars represent the percentage of mCherry+ cells over the percentage of mCherry- cells for vehicle treated (grey) and 40µM C6-Cer treated (orange) populations. sgSAFE represents the control cell line to account for Cas9 cutting effects. Statistical significance determined by two-way ANOVA (p-value 0.0332 [*], 0.0021 [**], 0.0002 [***], <0.0001 [****]). (A) KOTMEM30A-3.5 and KOTMEM30A-7.9 are KO pools of their respective sgRNAs. KO-TMEM30A is a clonal line derived from sgTMEM30A-0.2. KO of TMEM30A results in resistance to C6-Cer death. (B) KOARL5A-91.1 and KOARL5A-94.4 are KO pools of their respective sgRNAs. KO-ARL5A is a clonal line derived from sgARL5A-93.3. KO of ARL5A sensitises cells to C6-Cer toxicity.

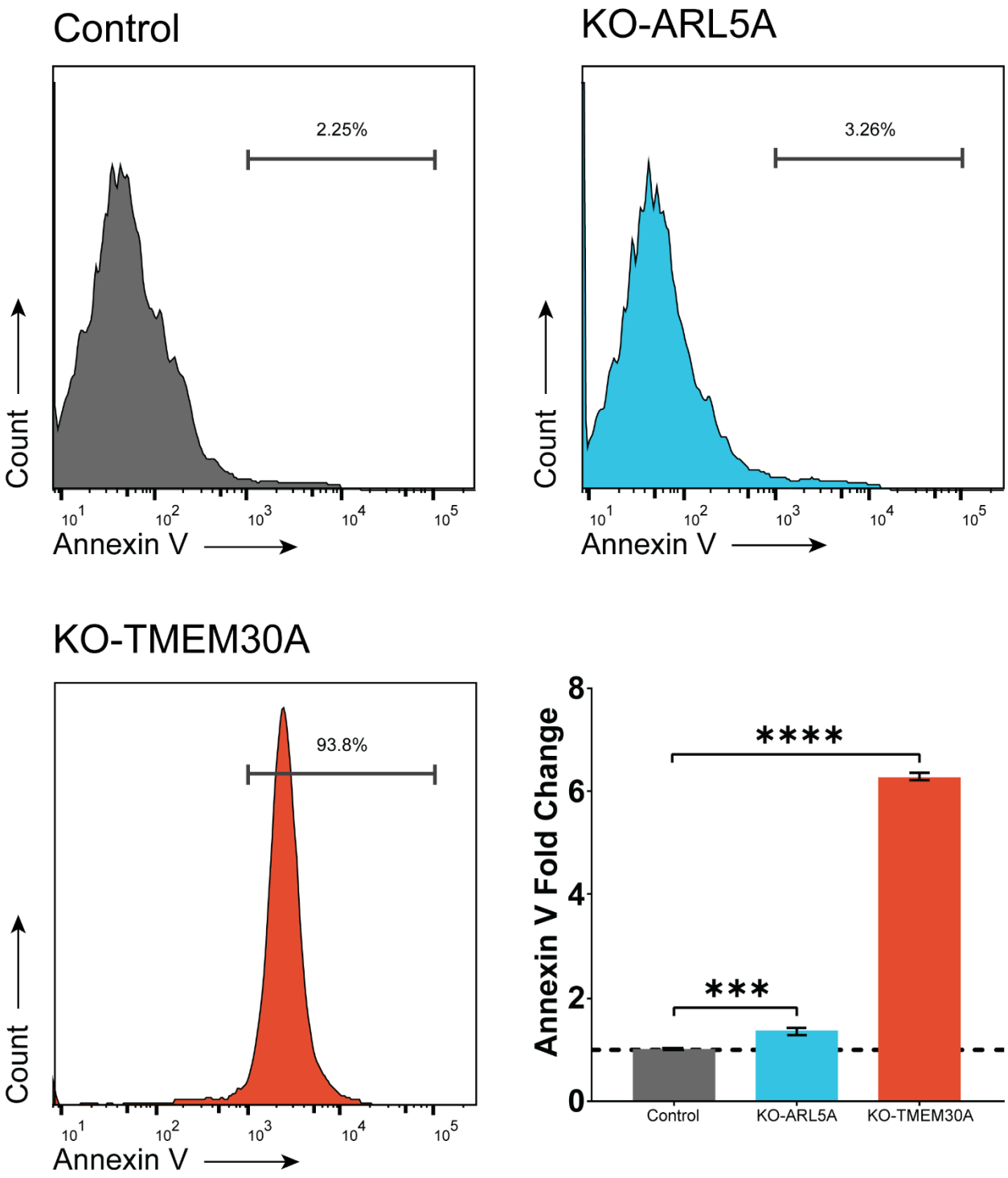

Figure 3-3: Annexin V correlates to PS exposure on the exoplasmic surface

Representative histograms of Annexin V signalling of live cells (i.e., SYTOX-Deep Red negative). PS and Annexin V have high binding affinity and Annexin V conjugated to FITC cannot transverse the PM. Therefore, Annexin V-FITC signal is directly correlated to PS concentration on the extracellular leaflet. The capped line shows the percentage of the population within the indicated range. The FITC geometric mean of each sample was calculated and normalised to the average of control. Statistical significance was determined by two-way ANOVA (p-value 0.0332 [*], 0.0021 [**], 0.0002 [***], <0.0001 [****]).

KOTMEM30A's exoplasmic leaflet is highly enriched with PS, with a much smaller—albeit still significant—increase for KOARL5A.

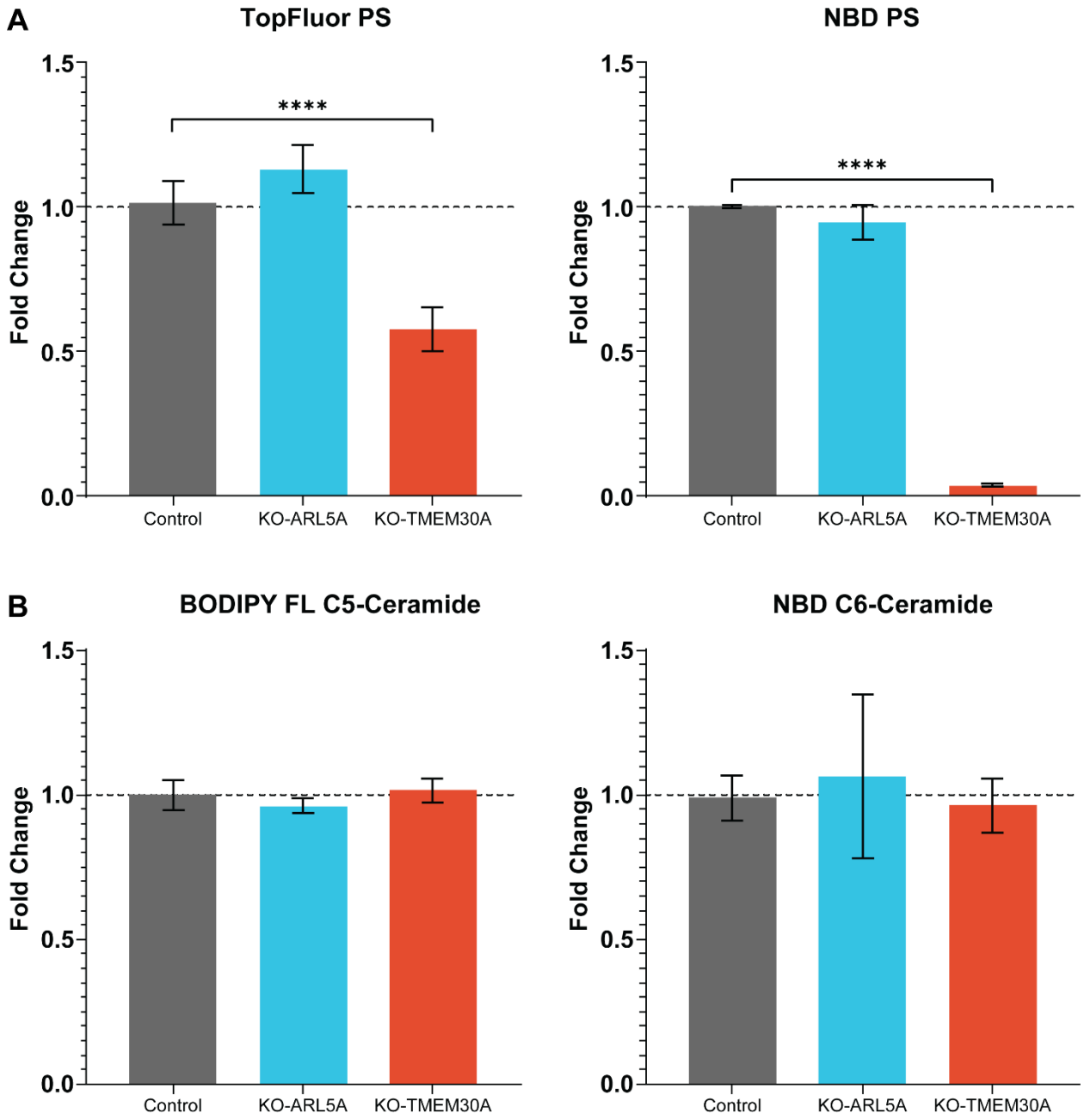

Figure 3-4: Flippase activity of PS is hindered in KOTMEM30A cell lines

Experiments done in quadruplicate with samples normalised to the average of control. Statistical significance was determined by two-way ANOVA (p-value 0.0332 [*], 0.0021 [**], 0.0002 [***], <0.0001 [****]). (A) Cells were treated with either 1µM of TopFluor PS or 2µM NBD PS followed by quenching of TopFluor PS signal or BSA-stripping of NBD PS. KOTMEM30A consistently exhibits impaired PS flipping. This is consistent with the results seen in Figure 3-3. KOARL5A does not show an impaired flippases function, therefore, its slight increase in PS is caused by other means. (B) Cells were incubated with either 0.5µM BODIPY FL C5-Ceramide or 2µM NBD C6-Ceramide. Flow cytometry readout occurred after quenching of BODIBPY FL C5-Ceramide or BSA-stripping of NBD C6-Ceramide. No discernible changes are seen between KO versus control, thus if any impairment in the uptake of short-chain ceramides exists, it is unlikely caused by a dysfunctional flippase.

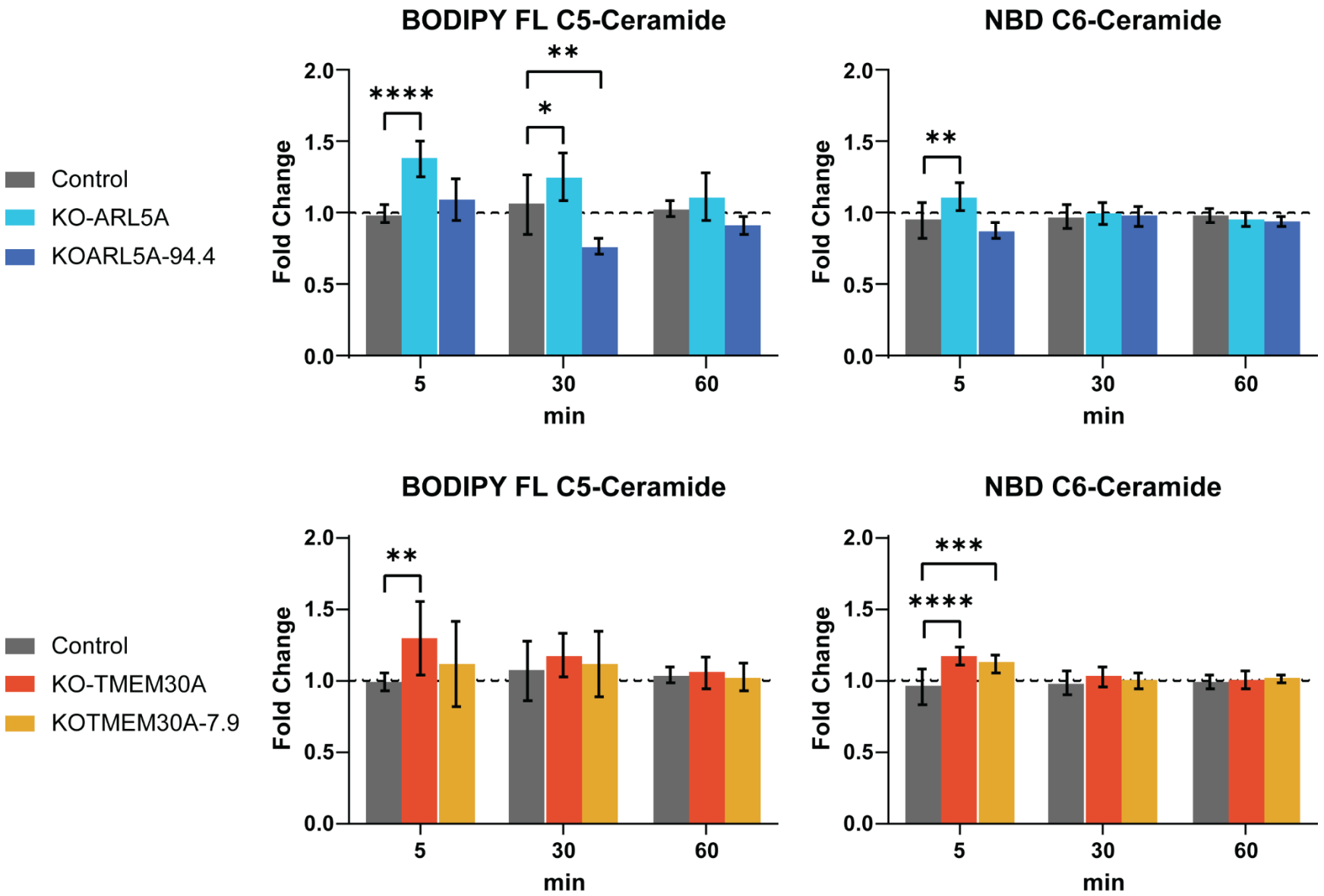

Figure 3-5: Sensitisation or resistance to C6-Cer is not due to differential uptake of exogenous ceramide

Experiments done in quadruplicate with statistical significance determined by two-way ANOVA (p-value 0.0332 [*], 0.0021 [**], 0.0002 [***], <0.0001 [****]). Uptake was evaluated from fluorescent emission at the indicated timepoints, with values normalised to the control average. Cells were treated with either 1µM BODIPY FL C5-Ceramide or 5µM NBD C6-Ceramide. Fluctuations in early timepoints are stabilised by 60min in all KO conditions. Since our screen represents a 24hr exposure, it is unlikely the KO phenotypes are from differential uptake. (A) KO-ARL5A (light blue) is a clonal line from sgARL5A-93.3. KOARL5A-94.4 (dark blue) is a KO pool of sgARL5A-94.4. (B) KO-TMEM30A (red) is a clonal line from sgTMEM30A-0.2 whereas KOTMEM30A-7.9 (orange) is a KO pool of sgTMEM30A-7.9.

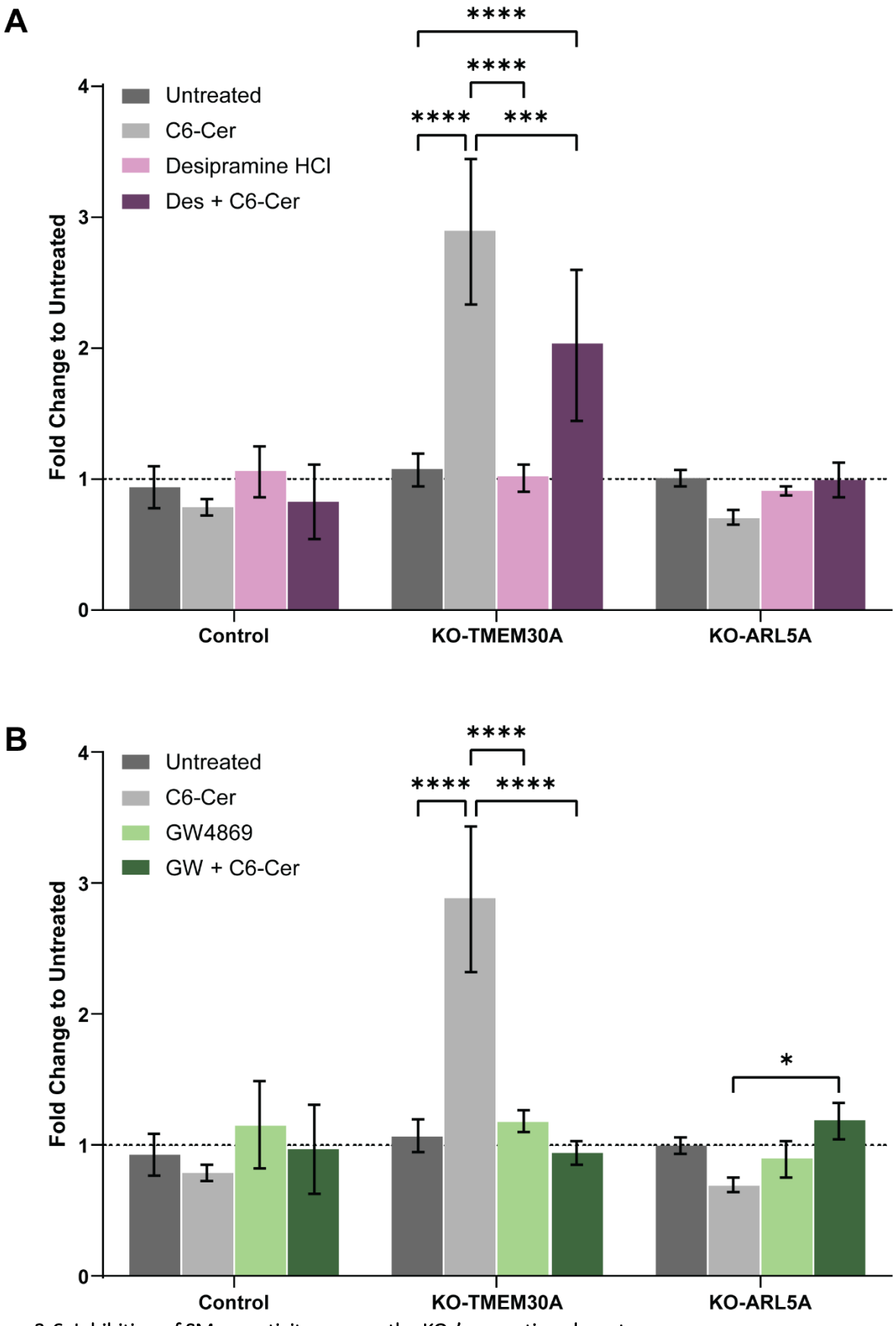

Figure 3-6: Inhibition of SMase activity rescues the KOs' respective phenotypes

Competitive growth assay with coincubation of 40µM C6-Cer and 10µM SMase inhibitors. Sample values are the ratio of mCherry+ to mCherry- cells, normalised to the mean of the untreated population. Statistical significance is determined by two-way ANOVA (p-value 0.0332 [*], 0.0021 [**], 0.0002 [***], <0.0001 [****]). Inhibitors alone did not alter population ratios from that of untreated. (A) Desipramine HCl (Des) is an inhibitor of acidic SMase that causes partial rescue of KOTMEM30A C6-Cer resistance. Unpaired t-test of KOARL5a untreated versus C6-Cer yields a p-value of 0.0016. (B) GW4869 (GW) inhibits neutral SMase activity. Co-incubation of C6-Cer and GW shows full rescue in both KOTMEM30A and KOARL5A when compared to just C6-Cer treatment. Unpaired t-test of KOARL5a untreated versus C6-Cer yields a p-value of 0.0016.

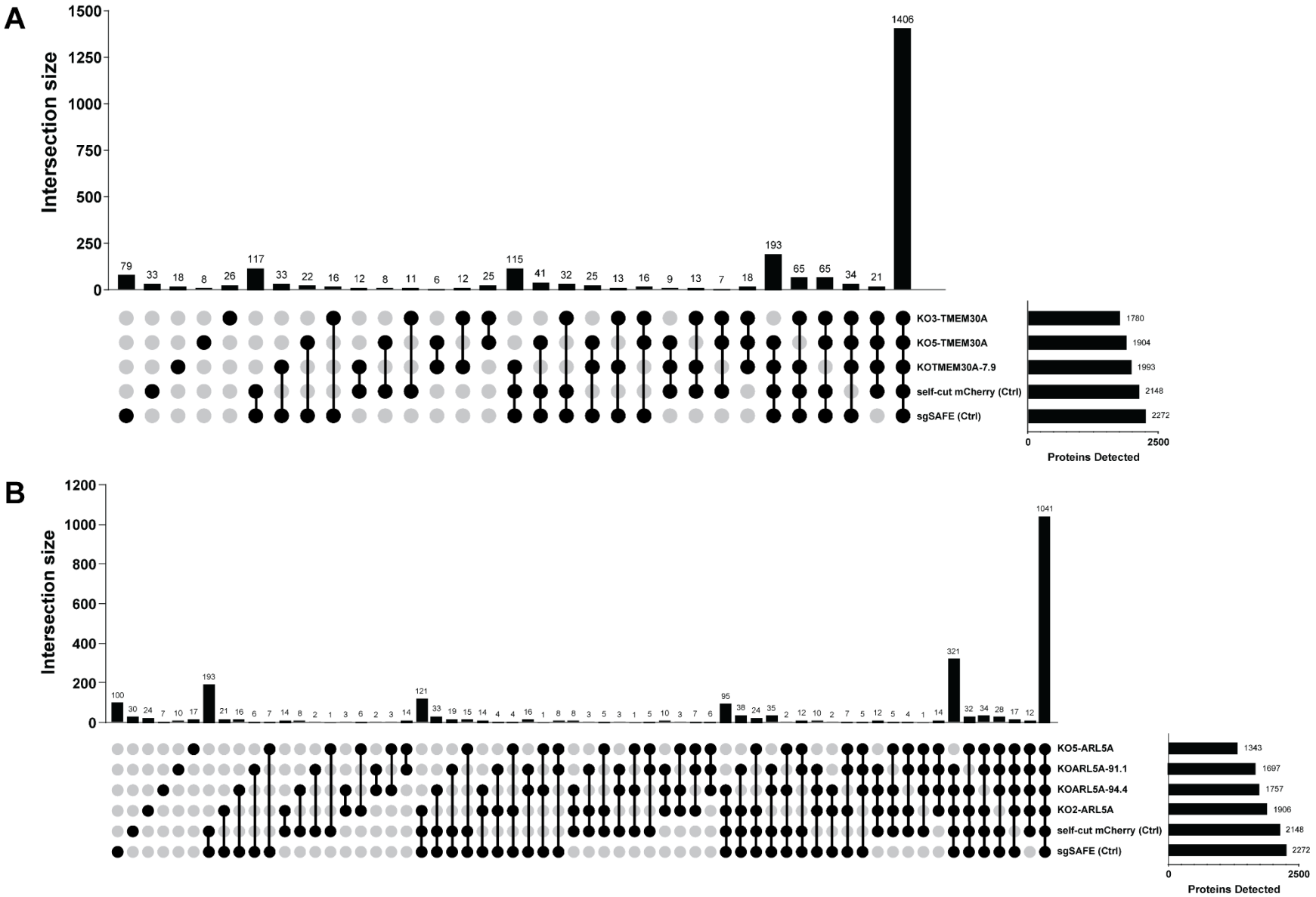

Figure 3-7: UpSet Plot—detected protein aggregations between KO lines and controls

The number of identified proteins in the surface biotinylation experiments are visualised on the horizontal bar graph to the right of each plot. Unlike Venn Diagrams, UpSet plots relies on a matrix (represented by the circles) where each row corresponds to a cell line and each column corresponds to a matched segment (rather like the overlap in the circles of a Venn diagram). Light-grey is a null state, black-filled is a participant. Lines between black circles are simple visual guides. The bar graphed over a column of circles indicates the number of matched values in the intersection. Plots were recreated from analyses done on the Appyter notebook. Both (A) KOTMEM30A and (B) KOARL5A show the vast majority of detected proteins are shared between KOs and controls.

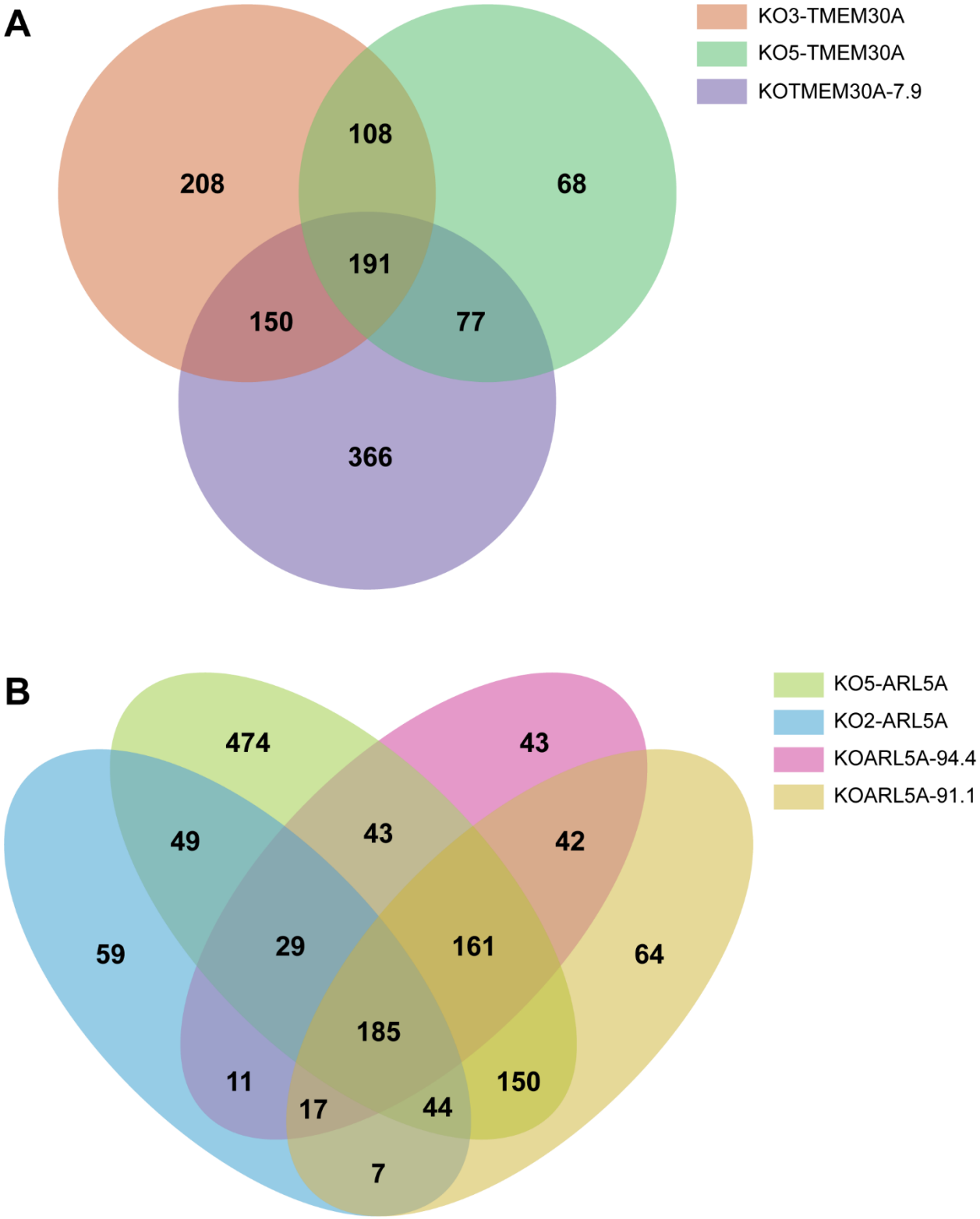

Figure 3-8: Venn Diagrams of the shared significant hits within KO lines

Protein targets are considered significant when the fold change of protein abundance between individual KO versus controls holds a p-value < 0.012. The significant hits are herein visualised to display the matched

targets of the KO. (A) 191 proteins appeared as significant in all KOTMEM30A lines. (B) 185 proteins are deemed significant in all KOARL5A lines.

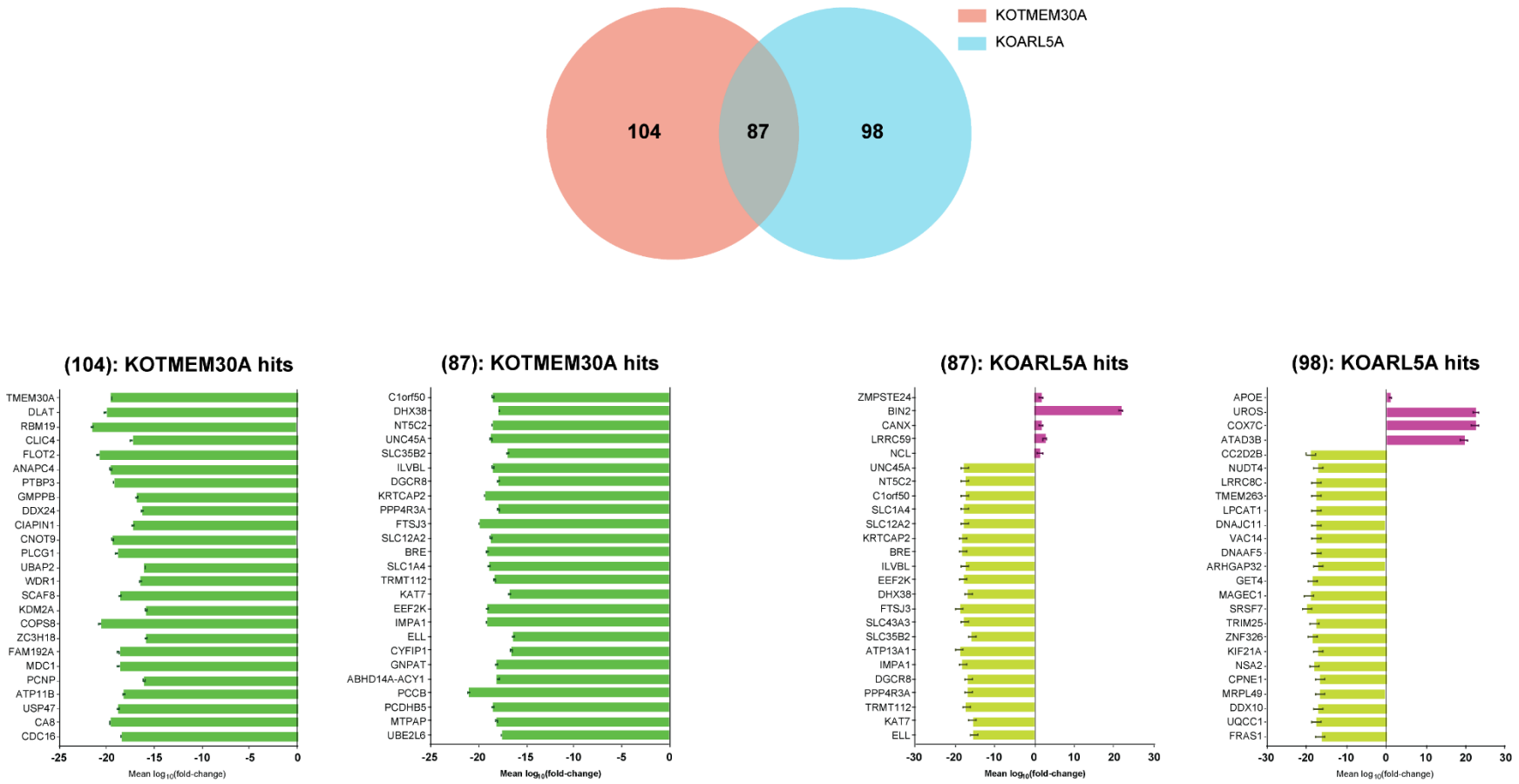

Figure 3-9: Significant hits specific to either KOTMEM30A or KOARL5A offer insights into C6-Cer mechanisms

From the matched values determined in Figure 3-8 (KOTMEM30A-191 hits, KOARL5A-185 hits), we further isolated the proteins that are specific to either KOTMEM30A (red, 104 hits) or KOARL5A (blue, 98 hits). We calculated the mean $\log_{10}$(Fold-change) (x-axis) of the proteins (y-axis) and sorted by ascending standard deviation (top to bottom). The top 25 targets of each dataset are shown. Of the hits specific to KOTMEM30A, '(104): KOTMEM30A hits', TMEM30 emerged as massively reduced (dark green) and serves as a validation of our methodology in both experimental preparation and statistical analyses. ATP11B, a P_4-ATPase, also appears in this listing and it too, is massively reduced in KOTMEM30A lines. In the hits specific to KOARL5A, '(98): KOARL5A hits', APOE represents the top hit and this protein appears over-expressed (purple) in the KOARL5A lines. Top hits of KOTMEM30A and KOARL5A in the overlapped section are also shown ('(87): KOTMEM30A hits' and '(87): KOARL5A hits', respectively)—the mean $\log_{10}$ (Fold-change) and standard deviation of each listing is calculated strictly from their respective KO lines.

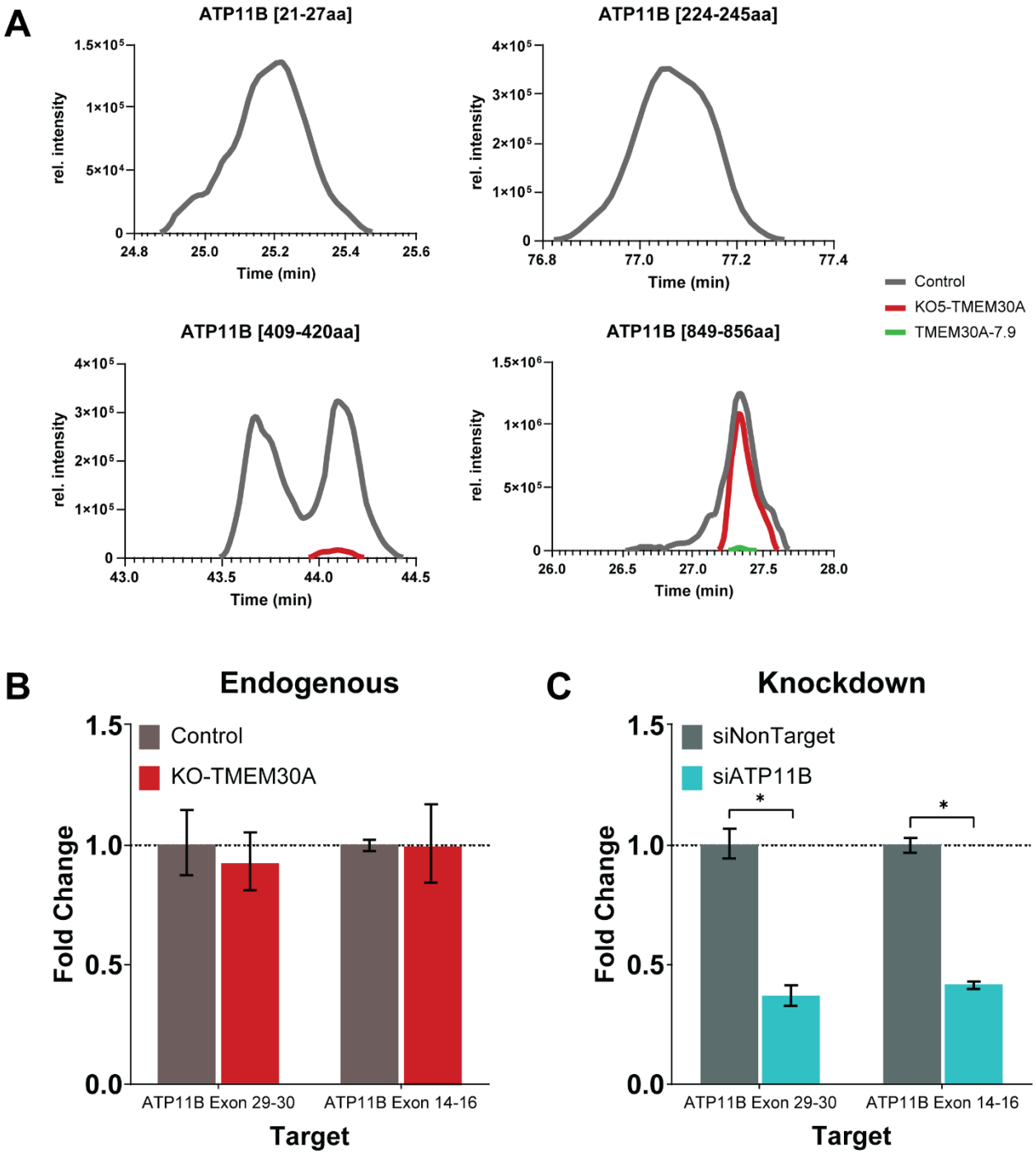

Figure 3-10: Exploring the role of ATP11B in C6-Cer toxicity

(A) Trace analysis of the peptides detected and assigned to ATP11B. Peptides in the N-terminal portion are only found in control (grey). Peptides towards the C-terminus portion are seen in KOTMEM30A (red: clonal KOTMEM30A, green: pooled line) though still in lesser intensity than control. Trace analysis confirms that ATP11B is lowered in the PM of KOTMEM30A. (B) RT-qPCR on the endogenous expression of ATP11B the negligible difference between control and KO-TMEM30A. Assuming that this trend is reflected in correct protein translation, this means that the decrease seen in our surface biotinylation screen arises from post-translational effects—likely, the lack of TMEM30A to properly fold the heteromeric complex for translocation to the PM. (C) RT-qPCR confirmation on the transfection efficiency

of the ATP11B siRNA. These pools of cells are used in the experiments of Figure 3-11. Statistical significance determined by unpaired t-test of siNonTarget versus siATP11B (p-value 0.0332 [*], 0.0021 [**], 0.0002 [***], <0.0001 [****]).

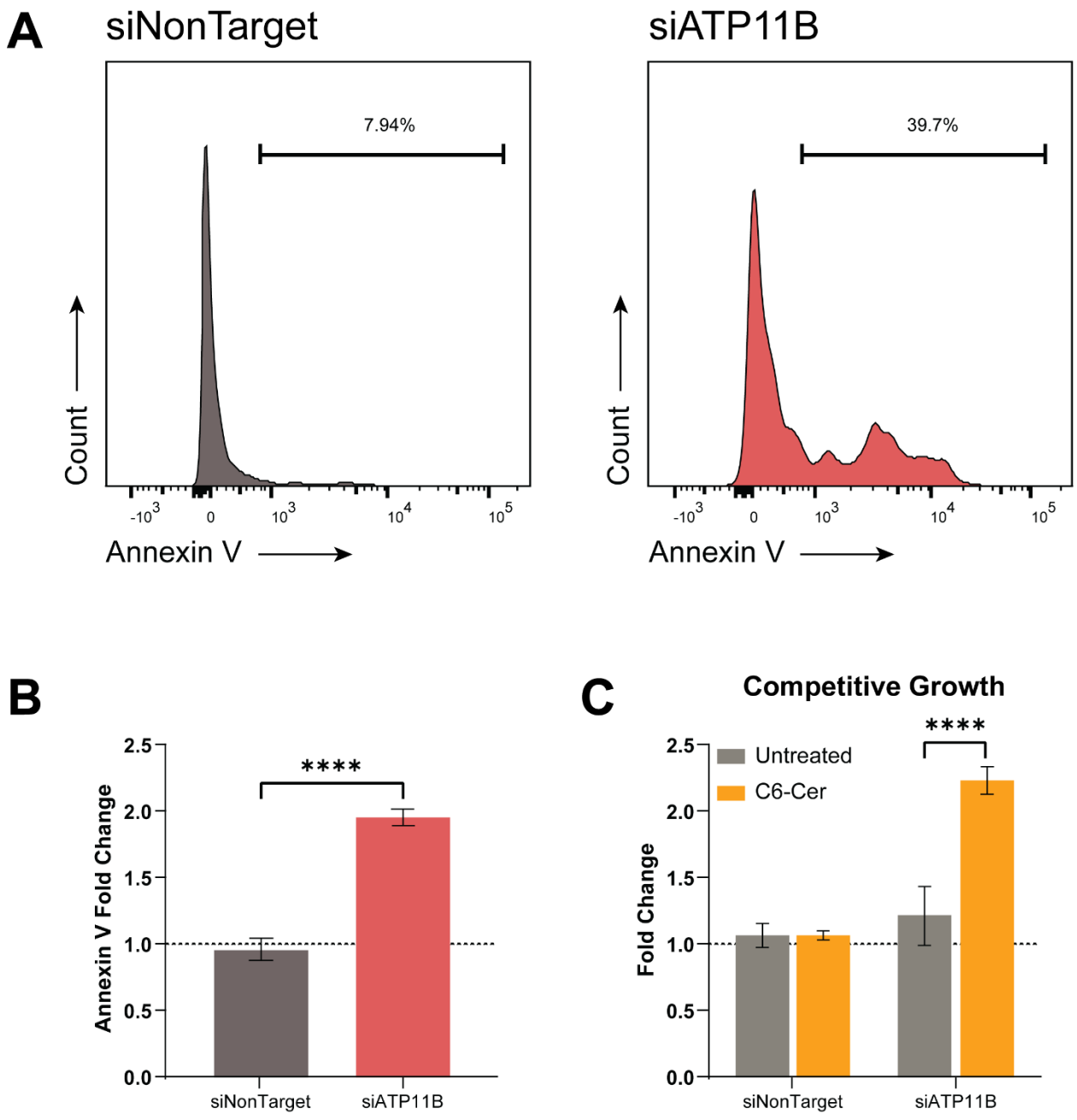

Figure 3-11: Knockdown of ATP11B phenocopies KO of TMEM30A

(A) Representative histograms of our siRNA pools. As seen in the KOTMEM30A results of Figure 3-3, siATP11B (red) has a significant population of live cells with higher PS exoplasmic exposure. (B) Comparison of the geometric mean shows that siATP11B (red) PS concentration is approximately 2-fold higher than siNonTarget (grey). The FITC geometric mean of each sample was calculated and normalised to the average of siNonTarget. (C) Competitive growth assay shows a relatively higher population of mCherry+ cells in siATP11B; this reflects the same resistant phenotype of KOTMEM30A. The mCherry- population in this experiment is derived from self-cutting mCherry cells transfected with siNonTarget. Growth ratios are calculated from the percentage of mCherry+ over mCherry- and then normalised to the untreated set. Statistical significance in (B) and (C) was determined by two-way ANOVA (p-value 0.0332 [*], 0.0021 [**], 0.0002 [***], <0.0001 [****]).

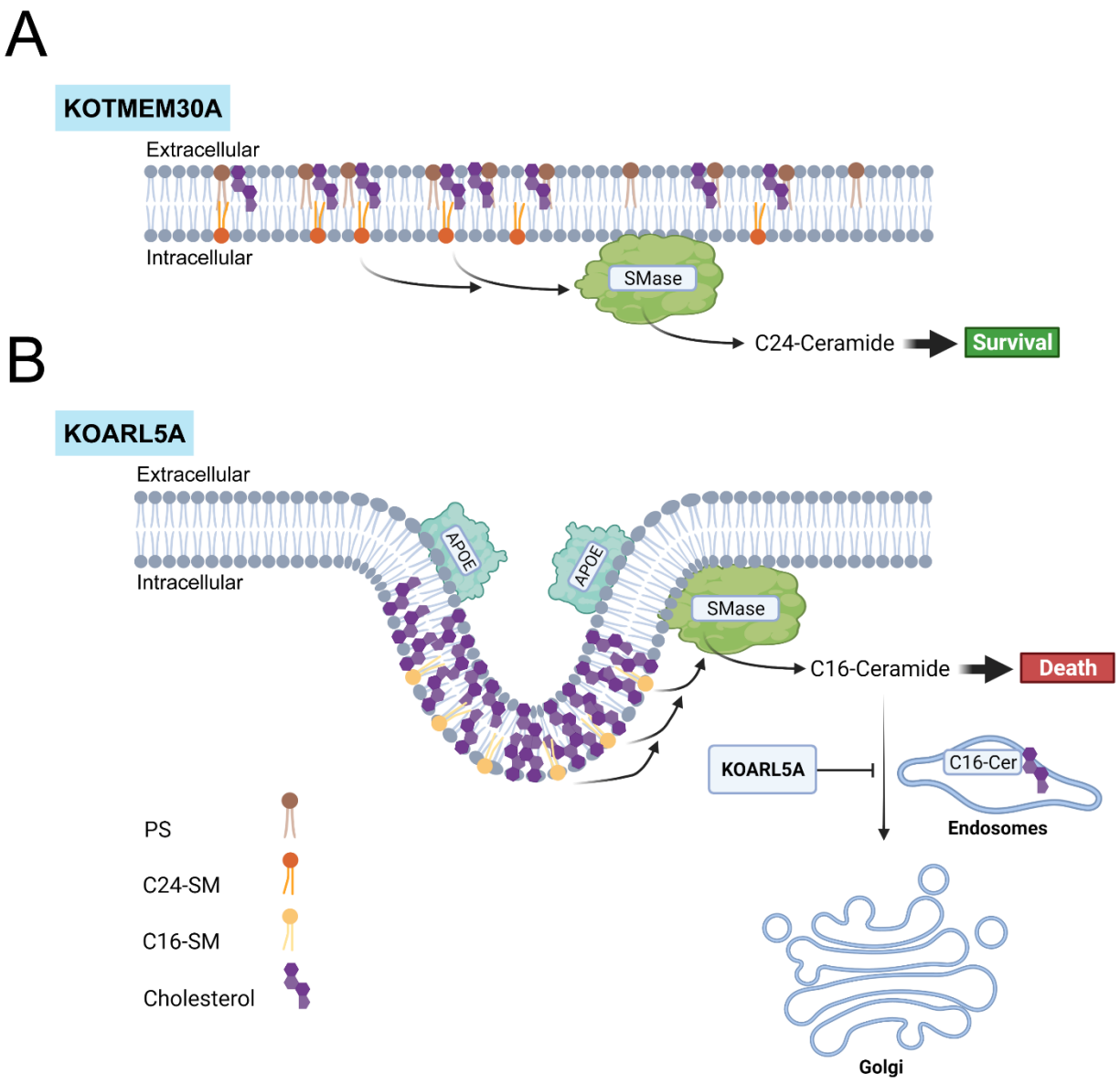

Figure 3-12: Cholesterol enters the field—Proposed mechanism of C6-Cer toxicity in KOTMEM30A and KOARL5A[XVI]

KOTMEM30A resistance and KOARL5A sensitisation to C6-Cer death is a result of the KOs' proclivity for engineering certain endogenous ceramides species. The KOs create unique 'resting' states that either favour production of C24-cer (in the case of KOTMEM30A) or C16-cer (in the case of KOARL5A). Addition of C6-Cer perturbs the cell's equilibrium of C16-cer to C24-cer to favour survival when C24-cer production is increased, or death when C16-cer is increased. Cholesterol plays a critical role in each of the proposed mechanisms. (A) The inhibited flippase activity of KOTMEM30A causes high PS exposure in the exoplasmic leaflet. PS attracts, and then stabilises cholesterol in the extracellular leaflet. Cholesterol does not associate well with C24-SM and the balancing of interleaflet forces means a higher-than-normal concentration of C24-SM in the intracellular leaflet. This localisation and concentration of C24-SM

[XVI] Figure created with Biorender.com.

increases the likelihood that neutral SMase will hydrolyse C24-SM into C24-cer. This increase pushes the ratio of C16:C24-Ceramide in favour of survival. (B) APOE on the extracellular surface indicates the increased abundance of cholesterol in the cell—likely driven by KOARL5A's perturbation of the endosome-to-Golgi transport in the TGN. Cholesterol crystals can stabilise the formation and preservation of the SCCs that produce deep invaginations in the PM. Cholesterol readily associates with C16-SM to form rigid lipid microdomains. The KOARL5A cell may use APOE to solubilise the cholesterol and neutral SMase to hydrolyse the C16-SM, both in an effort to 'release' the SCCs. The C16-cer formed from hydrolysis of C16-SM can also associate with cholesterol and, in a normal cell, are taken through the TGN for processing. However, KOARL5A cells cannot accommodate these compartments and thus, C16-cer concentrations are increased. Moreover, the state of KOARL5A means that C6-Cer exposure makes it a high likelihood that neutral SMase will act on C16-SM, adding strain to the already overloaded mechanisms and thus, driving the cell towards death.

Chapter 4: When lipids force a cell to *ferro incumbere*[XVII]

[XVII] *Latin,* fall on one's sword

4-1: The power of lipids

Lipids play crucial roles in the structure and function of cells; therefore, the health of the cell is critically tied to maintaining correct lipid composition and preventing damage to membrane lipids. Ferroptosis is a recently characterized form of regulated cell death that is reliant on the iron-dependent generation of reactive oxygen species[146,147]. These radicals abstract a hydrogen from the easily accessible tails of poly-unsaturated fatty acids (PUFAs), leading to the creation of toxic lipid peroxides (lipid-OOH)[148,149]. The subsequent accumulation of these toxic molecules in membranes abrogates cellular integrity and ultimately leads to cell death[150] (Figure 4-1, red). The best-characterized protective mechanism against this fatal build-up of lipid radicals relies on a glutathione peroxidase, GPX4. This enzyme converts lipid peroxides into non-toxic lipid alcohols and is reliant on functional glutathione synthesis[151] (Figure 4-1, green). Thus, inhibition of either the cysteine-glutamate exchanger SLC7A11 or GPX4 are common methods to induce ferroptosis[149].

Ferroptosis has been implicated in multiple degenerative conditions, most notably in neurodegenerative disorders, where chemical inhibition of ferroptosis results in reduction of neuropathologies[152–154]. Conversely, induction of ferroptosis has gained substantial traction as a novel strategy for cancer treatment as ferroptosis is capable of killing even drug-resistant forms of cancer in *in vivo* models[155,156]. The possibilities of ferroptosis in health and disease remain vast; however, our understanding of the mechanisms of this iron-dependent death remains limited.

To that end, we propose a possible regulatory pathway of ferroptosis via the acyl-CoA synthetase long-chain 4 (ACSL4) enzyme that converts free long-chain fatty acids into activated fatty acyl-CoA thioesters[157,158]. The ACSL4 gene can produce two isoenzymes via alternative splicing; these isoforms differ in length and in localisation, where the long form co-localises to lipid droplets (LDs) (Figure 4-1, dashed green line) and the short form co-localises to the plasma membrane[159–161] (Figure 4-1, dashed red line). We hypothesise that this differential localisation determines ferroptotic sensitivity by controlling PUFA channelling into distinct lipids.

4-1-1: The biochemical basis of ferroptosis

Ferroptosis is newly discovered form of regulated cell death (RCD) that is distinct from other forms of RCD such as apoptosis, necroptosis and autophagic cell death[146,162,163]. This unique form of RCD is driven by reactive oxygen species (ROS) generated from the iron-dependent Fenton's reaction (e.g. hydroxide anions and hydroxyl radicals)[164] (Figure 4-1). These ROS abstract a hydrogen from PUFAs in phospholipids and give rise to lipid radicals that initiate a positive feed forward chain reaction that culminates in catastrophic amounts of lipid peroxides[148,165] (Figure 4-1, red pathway). This accumulation of lipid peroxidation products in the plasma membrane compromises cellular integrity, and thus, ultimately results in cell death[149,150].

Ferroptosis is considered a default pathway that is triggered upon the impairment of lipid peroxidation repair pathways[148,163]. Cells contain a protective pathway in which the glutathione-dependent enzyme, GPX4, detoxifies these lipid radicals through the conversion of dangerous

lipid peroxides into relatively harmless lipid alcohols[149,151,162] (Figure 4-1, green pathway). Glutathione (GSH) levels are inherently dependent on cysteine, which in turn, is reliant on system x_c^- —an amino acid transporter that exchanges intracellular glutamate with extracellular cystine. This cystine is rapidly reduced to cysteine, which is then used to generate GSH[153,166]. Inactivation of GPX4 through GSH depletion via the chemical inhibitor, Erastin2, or through a direct GPX4 inhibitor, RSL3, will subsequently lead to cell death through the overwhelming accumulation of lipid peroxides[167].

Lipid metabolism is intimately involved with ferroptosis, as this iron-dependent RCD prefers long-chain PUFAs[146,168,169]. This selectivity is likely due to the PUFAs easily accessible bis-allylic hydrogen atoms that are necessary for the ferroptotic mechanism. Thus, the abundance and localisation of PUFAs is highly correlated to the cell's susceptibility to ferroptosis[170] (Figure 4-2). Therefore, the biosynthesis of PUFA-containing phospholipids serves as an additional point of ferroptotic regulation; to that end, long-chain acyl-CoA synthetase 4—and no other ACSL family member—has been shown to promote ferroptotic sensitivity[157]. ACSL4 converts free long-chain fatty acids into fatty acyl-CoA esters; this formation activates the esterified FA for further FA oxidation or lipid biosynthesis. ACSL4 preferentially utilizes arachidonate as a substrate[171], and as such, increased amounts of arachidonic acid (AA) increases ferroptotic sensitivity (Figure 4-2B). Interestingly, ACSL4 has two in-frame AUG-translational initiators that produce isoforms of different lengths. The longer isoform is expressed in neurons while the shorter splice is more ubiquitously expressed in all other cell types. Additionally, the shorter variant localises to the plasma membrane and cytosol whereas the longer version is associated with the lipid droplet [160,161,172] (Figure 4-1, dashed lines). LDs are complex organelles responsible for the storage of neutral lipids; they consist of an organic core of neutral lipids—mainly triacylglycerols (TAGs) and sterol esters (SE)—bounded by a monolayer of charged phospholipids[173,174]. How this non-plasma membrane localisation of ACSL4 affects ferroptosis is unknown; therefore, the main focus of this project is to understand and characterise the ferroptotic mechanism of each ACSL4 isoenzymes.

4-1-2: Relevance to human health

Ferroptosis has been connected with a variety of degenerative diseases ranging from age-related diseases (such as Alzheimer's, Parkinson's and Huntington's) to traumatic brain injury[152,153]. Although the pathophysiologies of these diseases/injuries vary, the main cause of these dysfunctions is propagated through some form of neuronal death. Inhibition of ferroptosis through iron chelators can significantly reduce neurotoxicity and in some cases, restore the number of healthy neurons[154,158,175]. Moreover, the deletion of GPX4 (the main biochemical protection against ferroptosis) causes hippocampal neurodegeneration and kidney failure, suggesting that it is this specific form of iron-dependent RCD that is the underlying reason behind massive cell death and thus, tissue malfunction[153,176,177]. Taken together, these findings suggest that understanding the regulation of ferroptosis in neuronal cells may provide new opportunities for the treatment of a myriad of neurological disorders.

Conversely, the discovery of ferroptosis has gained considerable excitement as a potential target for killing cancer cells[156,178]. Chemical inductions of ferroptosis that either deplete GSH or

inactivate GPX4 are lethal to RAS mutant cancer cells, whilst drugs that inhibit system x_c^- halt tumorigenesis[166,179]. These findings underscore the high potential for ferroptotic drugs as form of chemotherapeutics. However, as with most anti-cancer drugs, it is critical that new therapeutics do minimal harm to normal cells by specifically targeting mutated populations. Therefore, elucidating the nexus point between sensitivity and protection is crucial in the development of safe and effective techniques. We hypothesise that the ACSL4 isoforms will dictate ferroptotic susceptibility and thus, provide novel pathways of ferroptotic regulation.

4-2: Testing the waters

A crucial criterion of our experimental design is ensuring that our cell line of choice follows current paradigms of ferroptosis. CRISPR/Cas9 genome editing was used in U-2 OS to create a ferroptotic sensitive line through ablation of a novel protective ferroptotic mechanism[180] (Figure 4-2A, green line). Ferroptosis suppressor protein 1 (FSP1) catalyses the regeneration of CoQ_{10} using NAD(P)H and KO of FSP1 protects against iron-mediated RCD. An additional line was created with KO of endogenous ACSL4 in this sensitised line (Figure 4-2A, red line). These lines were treated with varying doses of RSL3—a ferroptosis inducer—and assayed for cell death using SYTOX staining in the Essen IncuCyte fluorescence microscopy system to determine their respective EC_{50}s. KO of ACSL4 resulted in a 2-fold increase in EC_{50} when compared to control (Figure 4-2A, red line versus black line) and a near 40-fold increase when compared to sensitised cells (Figure 4-2A, red line versus green line). These data confirm the reported ferroptosis sensitising role for ACSL4 in cancer cells.

Ferroptosis is also determined by PUFA concentration as pre-exposure to AA sensitises control cell lines to this iron-dependent RCD (Figure 4-2B), wherein the addition of 5µM AA leads to a 3.5-fold decrease in EC_{50}. The incorporation of AAs also induces LD biogenesis (Figure 4-2C), raising the possibility that fatty acid flux into LDs could affect ferroptosis.

KO-ACSL4 Hek293 cells were transfected with S-tagged ACSL4 isoforms. Western blotting of KO-ACSL4 confirmed the complete loss of endogenous ACSL4 whilst exogenous ACSL4 exhibited equal amounts of protein expression between the isoforms (data not shown). These cell lines were subjected to RSL3 treatment and assayed for 48 hours in the IncuCyte as previously described. Hek293 control cells maintained a healthy population until the extreme dosages of RSL3 whilst KO-ACSL4 cells remained relatively unperturbed to ferroptotic insults (Figure 4-3A-B, respectively). The expression of ACSL4-Long in the KO-ACSL4 line sensitises the previously resistant cells to levels concurrent with control; however, the incorporation of ACSL4-Short greatly exacerbates RCD with even small amounts of RSL3 (Figure 4-3C-D, respectively). Calculation of EC_{50}s show that ACSL4-Long has a 2-fold decrease compared to KO-ACSL4 whilst ACSL4-Short is ten times more sensitive than KO-ACSL4 (Figure 4-4A). The reason for this extreme difference in ferroptotic susceptibility may be due to the localisation of the different isoforms. The transfection of U-2 OS with these S-tagged isoforms reveals ACSL4-Short's strong PM incorporation versus ACSL4-Long's LD incorporation (Figure 4-4B).

4-3: Chronos brings the Delphian oracle

Time and circumstance prevented a full flushing of this fledging project. But what follows are a series of thought-out proposals to elucidate this tantalising mechanism of ACSL4 genetics, post-translation location and RCD.

4-3-1: Confirming the theory

To investigate the function of specific ACSL4 isoforms without interference of the endogenous enzyme, stable cell lines will be created that lack endogenous ACSL4 (ACSL4-KO). ACSL4 mediates the activation of PUFAs and is required for PUFA incorporation into phospholipids[146,169]. These activated PUFAs are necessary for death via ferroptosis[147,181]; as evidence of this, our KO of ACSL4 results in significant resistance to ferroptosis (Figure 4-2A, red line). Furthermore, our preliminary data shows that cells expressing the long form of ACSL4 in Hek293 cells are less sensitive than its ACSL4-short form counterpart (Figure 4-4A). We propose to use the human osteosarcoma line, U-2 OS, to assess the impact of ACSL4 isoforms on cancer cell ferroptotic sensitivity. This experiment would confirm if the different ACSL4 isoforms in cancer cells bestow different sensitivity to ferroptotic insults.

Endogenous ACSL4 gene locus will be deleted via ciCas9_pcDNA5 (a chemically inducible Cas9)[182] loaded with a short guide RNA sequence specific to ACSL4. ACSL4 will be deleted in U-2 OS Flp-In[183] stable cell lines, which harbour a FRT site for facile knock-in of the different ACSL4 isoforms. Successful KO will be verified by Western blotting for expression of ACLS4 protein. Only cells that show complete reduction of ACSL4 expression will be considered for further analysis. ACSL4-KO lines will then be transfected with the CMV-68_HNF44A2 expression plasmid that contains a cytomegalovirus (CMV) promoter for constitutive expression of either the long or the short ACSL4 isoforms to create stable ACSL4-Short (ACSL4-S) and ACSL4-Long (ACLS4-L) cell lines via Flp mediated site directed integration. This will insure that the isoforms are not randomly inserting into the genome, reducing the possibility of off-target phenotypes. Additionally, these constructs carry a C-terminal S-tag to facilitate expression verification and subcellular localisation studies. Stably transfected lines with either construct will be established via antibiotic selection and ACSL4 expression will be verified by Western blotting.

To verify that the tagged ACSL4-S and ACSL4-L constructs are functional, at least five independently derived lines for each constructs will be tested for ACSL4 enzymatic activity as described in published articles[184,185]. In short, cytosolic cellular extracts will be incubated with Acetyl-CoA and the 3H or 14C labelled ACSL4 substrate arachidonic acid. The resulting Ac-CoA ester will be extracted using hexane and radioactivity counts will be determined using a scintillation counter. Only lines that show similar ACSL4 activity to the original wild type lines will be considered for further experiments. If necessary, untagged versions of ACSL4 isoforms could be employed.

The different ACSL4 isoforms are expected to have different subcellular localisations, with the short isoform localised to the plasma membrane and the long version to lipid droplets and the ER (Figure 4-4B). Cell lines expressing ACSL4-S and ACSL4-L will be analysed by

immunofluorescence to confirm the subcellular localisation of the different enzyme isoforms. Cells will be grown on gelatine-coated coverslips until 90% confluent and fixed using paraformaldehyde. Cells will then be incubated with anti-S-tag primary antibodies and fluorescently labelled secondary antibodies, followed by visualization using confocal microscopy. Only lines that show the correct localisation will be used for further experiments.

In order to determine whether the various ACSL4 isoforms sensitise or desensitise cells to ferroptotic stimuli, cells expressing functional ACSL4 isoforms will be incubated with various concentrations of RSL3 to induce ferroptosis. RSL3 activates ferroptosis through binding of GPX4 and ablating the cell's protective mechanisms against iron mediate lipid peroxidation. Moreover, to increase the dynamic range of sensitivity, these stable lines will be assayed in the presence and absence of additional exogenous AA. Cell death will be measured in an Essen IncuCyte fluorescence microscope for a period of 48hrs. We will generate timecourse results of STYOX-positive (dead cells) to create highly confident EC_{50}s of the isoforms' sensitivity to RSL3, plus/minus the addition of AA.

Cells expressing the short isoform are expected to have higher susceptibility to RSL3 treatment than ACSL4-L because of ACSL4-S' potential increased incorporation of PUFAs into plasma membrane phospholipids. We believe this concentration of PUFAs creates increased targets for the run-away lipid peroxidation damage that characterizes ferroptosis. The experiments will provide the concentrations of RSL3 that will ensure that stable lines are exposed to amounts of RSL3 well within their dynamic ranges. We hypothesize that the populations incubated with AA will be further sensitised to RSL3. Moreover, we expect that KO-ACSL4 cells will be extremely resistant to ferroptotic insults and thus, will define the maximum dosage for RSL3 treatment—higher concentrations of the drug would only increase opportunities of off-target effects. Cell lines with exogenous ACSL4 isoforms that mimic WT levels of enzymatic activity whilst exhibiting differences in ferroptotic responses.

4-3-2: Location, location, location

The current paradigm suggests that the only difference in isoform enzyme activity is their respective localisations; however, it is unknown if this differential localisation is enough to cause a difference in ferroptotic sensitivity. To precisely define the site of action for ferroptosis, we propose to target ACSL4-S to different cellular compartments—namely, the plasma membrane (PM), the endoplasmic reticulum (ER), the mitochondria and finally, lipid droplets (LDs)—and assay them to ferroptotic insults.

Cell lines will be created that carry unique exogenous ACLS4-S S-tag constructs in the context of an ACSL4KO background (as described in the previous section). In these ACSL4-S constructs, the wild type targeting sequences will be addended at the C-terminus with sequences that target the enzyme to different subcellular compartments. Lines will be created that target ACSL4-S to the:

- PM^{186}: via Lyn-11, a short peptide sequence from the tyrosine-protein kinase Lyn protein shown to preferentially target the plasma membrane (ACSL4-PM)

- ER[187]: via the charged C-terminal sequence (CTS) of cytochrome b5 (ACSL4-ER)
- Outer mitochondrial membrane[188]: through the inclusion of Tom20's transmembrane domain (ACSL4-Mito)
- LDs[189]: via inclusion of the perilipin 2 (PLIN2) sequence (ACSL4-LD)

The short isoform was chosen for these experiments to minimise complications from intramolecular deletions of the intrinsic localisation domain. Enzyme expression and activity levels will be measured to ensure correct translation and folding of ACSL4 production and folding, despite changes to the localisation sequence. Finally, the sensitivity to ferroptosis of the differentially targeted ACLS4-S lines assayed by exposing cells to RSL3 and measuring cell viability using SYTOX-staining and IncuCyte experiments.

We predict that ferroptosis susceptibility may be due to PM bound ACSL4 and thus, differential targeting of ACLS4-S may be sufficient to dampen the ferroptotic response. This may in part be due to the sequestration of PUFAs away from the PM; therefore, ACSL4-LD may mimic the ACSL4-L phenotype or, as PLIN2 is strongly associated with LDs, ACSL4-LD could be protective to ferroptosis since ACSL4-L may still have off-target PM effects. Additionally, the mitochondria in ferroptotic cells have been described as hyper-condensed masses that contribute to cell death. Thus, we suspect that the mitochondria-bound ACSL4 will likely produce RSL3 sensitive cells, albeit less so than PM-bound ACSL4. Subcellular localisations of exogenous ACSL4 will modulate ferroptotic response; thereby concluding that ACSL4 localisation is a key component in ferroptotic regulation. Furthermore, the differential localisation will highlight which subcellular compartments sensitise or protect against ferroptosis.

4-3-3: The flux of fatty acids in ferroptosis

LDs are critical organelles for lipid metabolism and are known to protect against various cellular lipotoxic insults across many organisms[173,178,190]. Indeed, our lab previously showed that LD sequestration of fatty acids during autophagy protects against mitochondrial damage[191], supporting a role for LDs as a key lipid buffer. As ferroptosis proceeds through a positive feedback loop of lipid peroxidation, one can consider ferroptosis a version of lipotoxic death. Thus, we postulate that LDs can protect against ferroptosis through sequestration of PUFAs that would otherwise be susceptible to damage in the cell's PM. Prior research shows that KO of ACSL3—the acyl-CoA synthetase that promotes lipid droplet biogenesis—does NOT create ferroptotic resistant cells[157,159,161]. However, the ACSL4-L isoform and its proscribed localisation to LDs indicate a possible connection between LDs, ACSL4 isoforms and ferroptosis. Thus, our next set of methodologies will focus on how the possible sequestration of PUFAs in the LDs impacts ferroptosis and cellular energetics.

We shall reduce cellular LDs via chemical inhibition of the acyl-coA diacylglycerol acyltransferases (DGAT1 and DGAT2)[191–193]. These enzymes catalyse the final step in TAG synthesis through esterification of diacylgycerol to TAGs[194–196]. As LDs are mainly composed of TAGs and SEs, the lack of TAGs shall prevent the formation of new LDs[191,197]. The transgenic lines

in section 4-3-1 will be pre-incubated for 48 hours with the LD inhibitors to decrease endogenous LDs and then assayed for ferroptotic sensitivity via the methods previously described.

Next, we shall employ Raman spectroscopy in order to characterise the lipid environment of LDs during ferroptosis[198–200]. Raman spectroscopy is a non-destructive method that relies on Raman scattering to probe the vibrational signature of molecules[200]. Data from Raman spectroscopy will yield information on the molecule classes inside a cell compartment, specifically the PM and LD. This methodology delves into the dynamic processes inside living cells without causing potential off-target effects of synthetic fatty acids.

In order to distinguish the PUFAs of interest from the rest of the cellular environment, we will first incubate the lines developed with a stable isotope of AA, followed by the appropriate dosage of RSL3. Cells will be subjected to monochromatic laser excitations to determine the vibrational signatures of the samples. This step utilises coherent anti-stokes Raman scattering on a custom scaffold to provide a spectral analysis of the lipid environment[199,201]. These data will undergo a custom Python programming script to interpret the spectral data to learn the spatial distribution of PUFA abundance in the different isoenzyme lines. This step is an important characteristic to map out PUFA sequestration of ACSL4. Data from this experiment will provide visual confirmation that the differential localisation of ACSL4 isoforms is correlated to PUFA localisation.

Numerous publications describe the metabolomes of cells that have underwent general ferroptotic stresses; however, it is unknown if the different ACSL4 isoforms create differing cell lipid compositions. Elucidating these lipid landscapes will highlight intermediates or end products that would contribute to ferroptosis via the different isoform pathways. Furthermore, the isotopic tracing will determine if the ACSL4 variants metabolize PUFAs differently and thereby, possibly changing the incorporation of PUFAs into different lipid species of the cell. These samples will undergo a high-throughput, non-targeted, top-down strategy to created datasets of their respective metabolites. Univariant and multivariant data analyses methods will be applied to these datasets to ascertain the general structure of the metabolome and how these molecules are related to the individual phenotype of the biological samples.

We hypothesise that LDs act as storage centres for dangerous lipid radicals. These lipid radicals would otherwise be found in the PM, causing disruptions in cell integrity and ultimately, death. Thus, a decrease in LDs via the DGAT inhibitors will sensitise cells to ferroptosis. Furthermore, as ACSL4-L targets the LD, we believe that a decrease in LDs will “rescue” the isoform’s protection against ferroptosis. Our Raman microscopy will strengthen the correlation between ACSL4 localisation and localised PUFA sequestration, where isotopic tracing reveals high amounts of AA in the LD or PM for ACSL4-L or ACSL4-S, respectively. The metabolomic data generated will reveal whether isotopically labelled AA is channelled into specific lipids (e.g., phospholipids versus triacylglycerol). Metabolomics is also a discovery tool for otherwise unknown effects of ACSL4 isoforms and will provide potential targets for future projects. Raman spectroscopy and metabolomics provide complimentary metrics of the FA flux caused by ferroptosis. LD depletion increases the cell’s sensitivity to ferroptotic insults, as proven through microscopic confirmation of PUFA flux and metabolomics. These data would discover a novel role for lipid droplets in regulating ferroptosis via the sequestration of PUFAs in triacylglycerol.

Successful completion of these proposed steps would elucidate the mechanisms of how ACSL4 isoforms and LD storage capacity regulates ferroptosis.

4-4: Chapter 4 Materials & Methods

4-4-1: Cell lines, culture conditions, plasmids and transfection conditions

U-2 OS cell lines were generated as previously described and generation of KO-ACSL4 lines in HEK293T are as cited[180]. U-2 OS and HEK293T were maintained in DMEM containing 4.5 g/l glucose and L-glutamine (Corning, 10-017). All media was supplemented with 10% foetal bovine serum (Gemini Bio Products) and penicillin (10,000 I.U mL^{-1}). Cell lines were maintained at 37°C with 5% CO_2 with regular screening for mycoplasma contamination.

ACSL4-long (NM_001318509.1) and ACSL4-short (NM_004458.3) were cloned into pcDNA3.1(-) with a GSGS linker between the c-terminus of the ACSL4 gene and the start of the S-tag. Transfections of the ACSL4 isoforms used X-tremeGENE transfection reagent (Roche, 6365779001) per manufacturer's directions.

4-4-2: EC_{50} Death Assay

Cell death was assayed via the Essen IncuCyte Live-Cell imaging system (Sartorius) in black, clear bottom 96-well plates (Corning, 3904). Cells were plated at a density of 5,000 cells per well and left to grow overnight. Fresh media containing a final concentration of 15nM SYTOX-Green Dead Cell Stain (Invitrogen, S34860) and 1S,3R-RSL3 (Cayman, 19288) at various concentrations was then added. Plates were carefully transferred to the IncuCyte system (kept at 37°C with 5% CO_2) and imaged for 48hours (48hr). Three images per well were captured in the green and brightfield channels every hour for the treatment period. The Sartorius image analysis software outputs the number of green objects (SYTOX-Green positive, i.e., dead cells) as well as the total number of objects (brightfield segmentation). For each RSL3, the ratio of dead objects over total objects was plotted over the 24hr imaging cycle. From this, Prism (Graphpad) was used to calculate the area under the curve (AUC), plotted as function of RSL3 dosage and mathematically derive the EC_{50}. Confidence intervals were calculated in Prism.

4-4-3: Fluorescence microscopy

Cells for S-tag fluorescence microscopy were washed thrice with PBS, fixed for 20min in 4% (w/v) paraformaldehyde and then thrice more washed in PBS. Cells were permeabilised for 2 min in 0.2% Triton X-100, washed with PBS and incubated in blocking solution (1% BSA, 0.3M glycine in PBS) for 30 min. Cells were incubated with anti-S-tag antibody for 2hr at room temperature. These were then washed and incubated in anti-rabbit secondary antibody conjugated to Alexa Fluor 488 (1:250 dilution). After more washes, coverslips were mounted on glass slides using Permount mounting medium (FisherSci, SP15). Images were acquired as previously described[191].

BODIPY imaging proceeded as previously described[191]. In brief, 5×10^4 cells were seeded on Nunc LabTek II chambered coverglass. LDs were stained with 1µg BODIPY 493/503 and Hoescht for nuclei staining. Cells were incubated at 37°C with 5% CO_2 in a humidified chamber and images were taken using a Deltavision Elite widefield epifluoresence deconvolution microscope with a 60× oil immersion objective.

Chapter 4 Figures

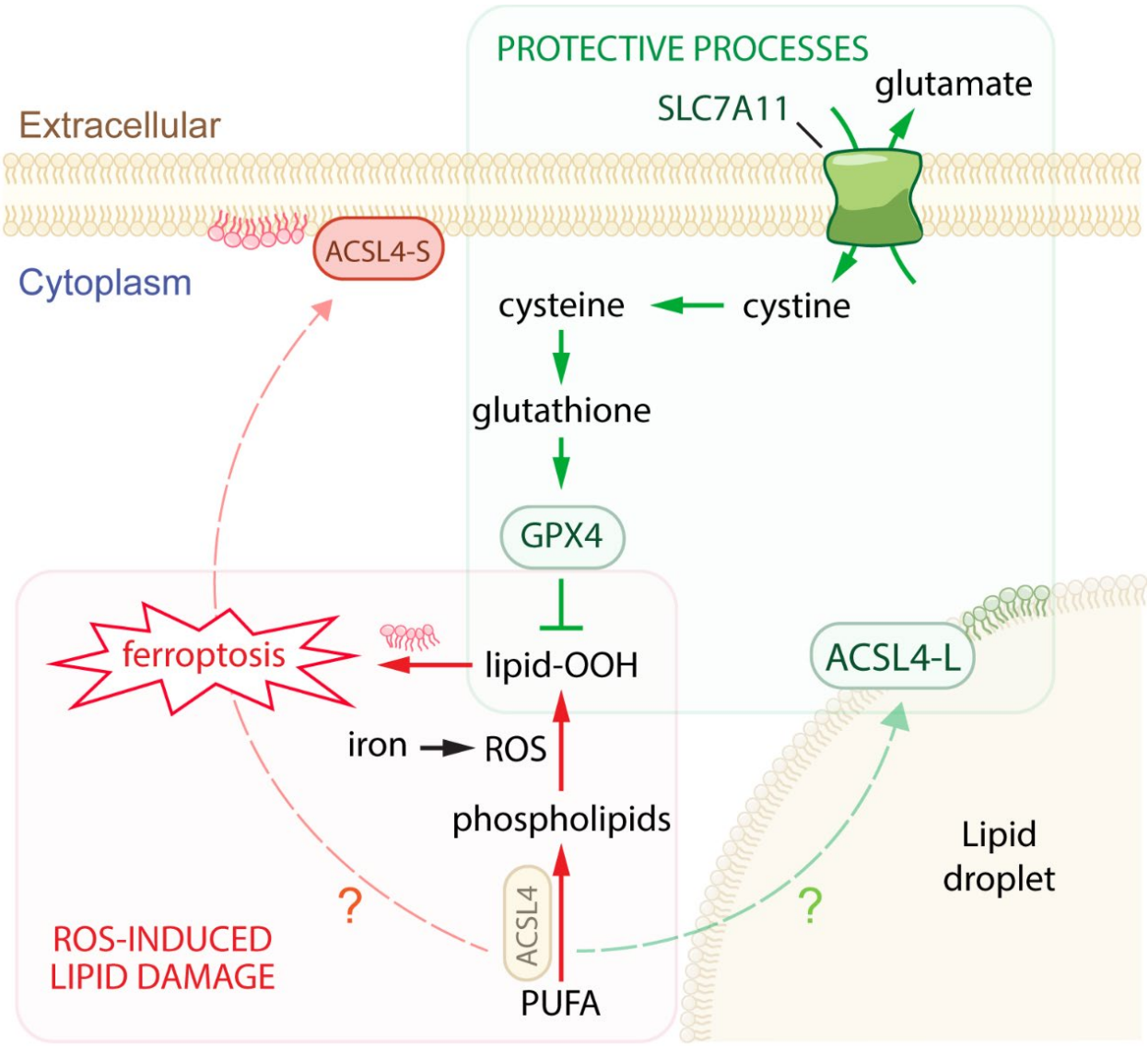

Figure 4-1: Pathways in ferroptosis

Death by ferroptosis is a peroxidation-driven RCD. These lipids peroxides are derived from phospholipids that originate from ACSL4-activated PUFAs. ACSL4 has two known isoenzymes that localise to different subcellular compartments—ACSL4-long travels to LDs whilst ACSL4-short is found at the PM. We hypothesise that this differential localisation leads to a difference in ferroptotic sensitivity.

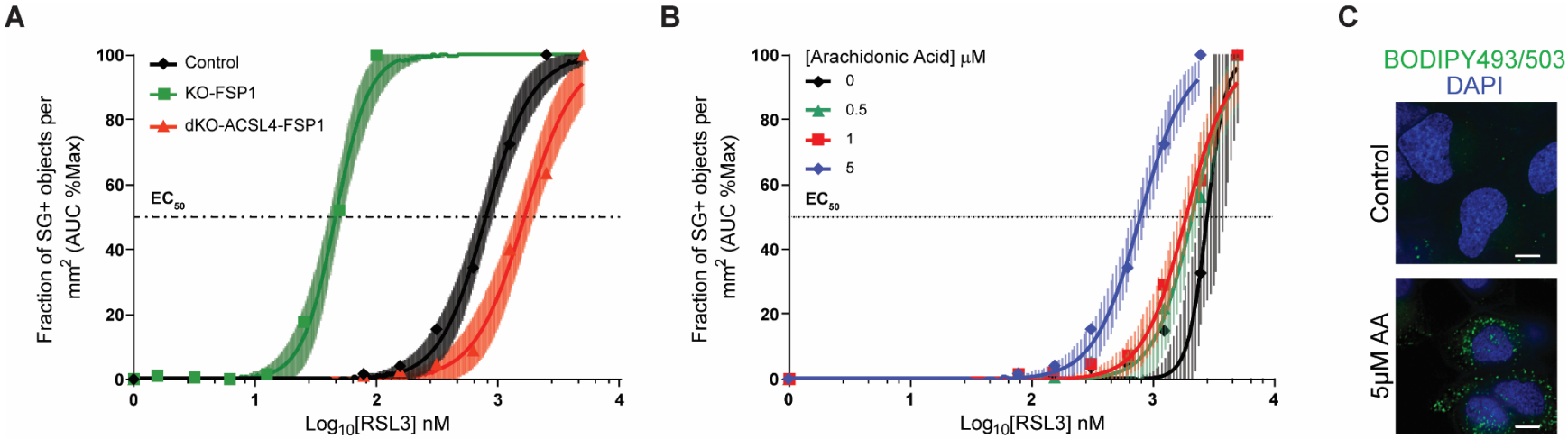

Figure 4-2: ACSL4 and ACSL4 activity is directly correlated to ferroptotic sensitivity

Shading represents 95% confidence interval of calculated non-regression line. (A) KO-FSP1 is ferroptotic protective pathway and it results in ferroptotic sensitive cells (green line). Double KO (dKO) of ACSL4 and FSP1 prevents RCD by ferroptosis (red line). (B) AA cellular concentration correlates to ferroptotic sensitivity (graph). (C) Incorporation of AA results in higher amounts of LDs (green, BODIPY 493/503 stained). Nucleus is blue, DAPI-stained. Scale bar = 10μm.

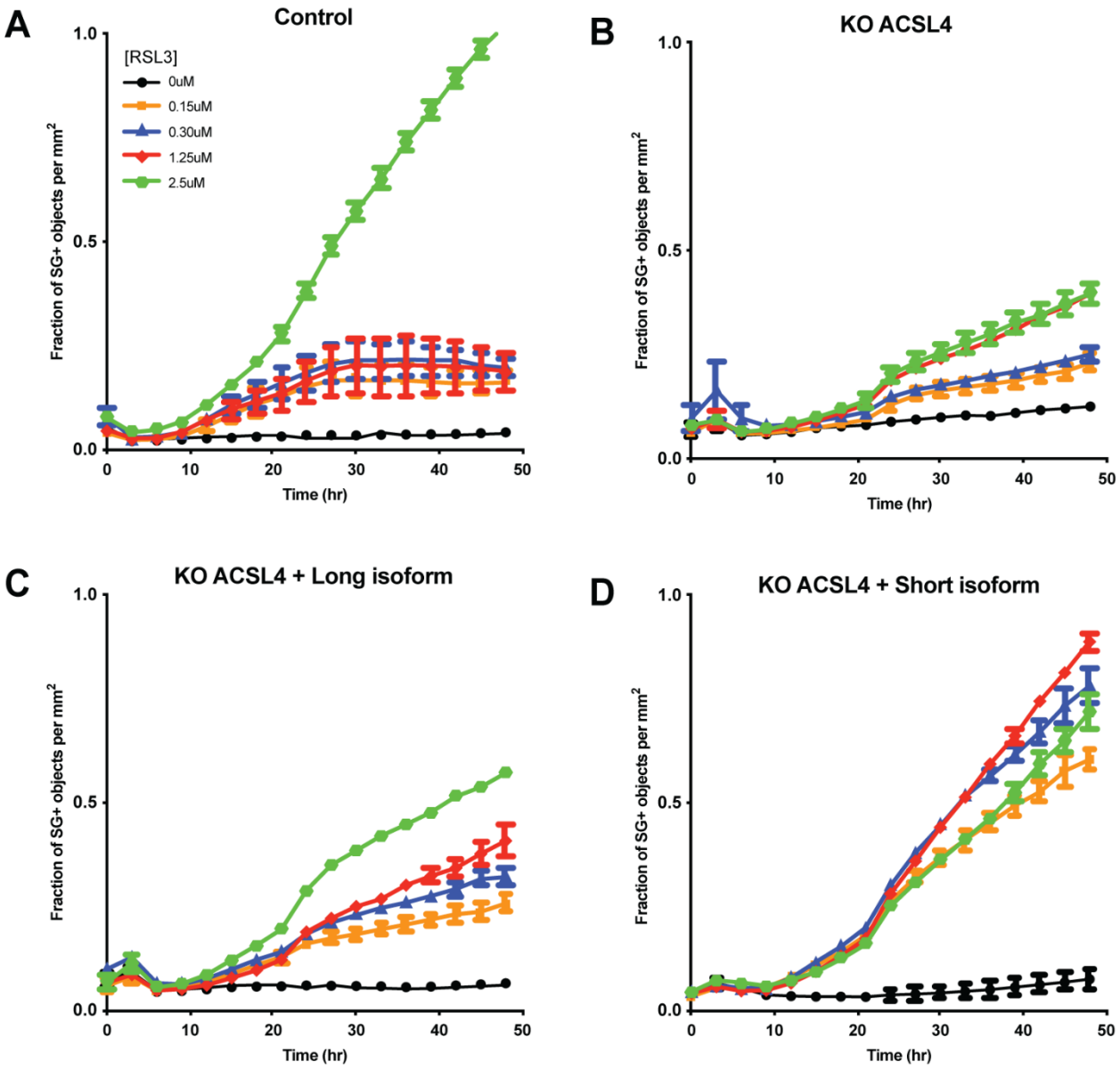

Figure 4-3: Correlation in ACSL4 isoforms and ferroptotic sensitivity

(A-D) Timecourse of different HEK293 cell lines to RSL3 insult. Each data point represents the mean and SEM of experimental quadruplicates of the ratio of SYTOX positive to total number of cells. KO ACSL4-short is far more sensitive than control to RSL3, whereas the long form of ACSL4 is phenotypically closer to KO ACSL4.

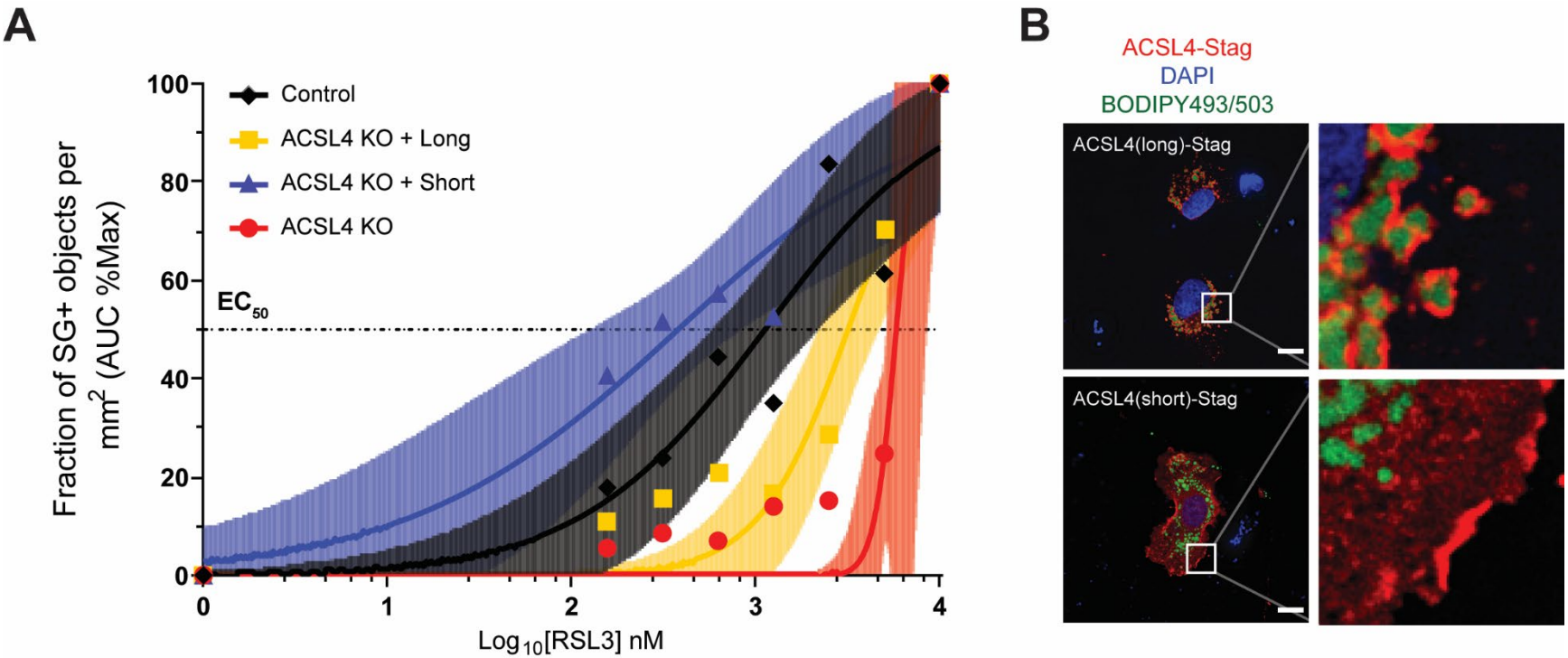

Figure 4-4: The localisation of the ACSL4 isoforms determines resistance to ferroptotic insult

(A) EC_{50} analysis derived from timecourse data of Figure 4-3. Shading represents 90% confidence interval of calculated non-regression line. (B) ACSL4 long and short isoforms conjugated to S-tag (red) were expressed in U-2 OS. Cells were treated with oleate to induce LD biogenesis (green). Nuclei are stained blue. Scale bar = 10µM. ACSL4-long (top) concentrates at LDs; ACSL4-short (bottom) embeds in the PM. PUFAs in the PM perturb the barrier function of the cell and creates the positive feedback loop of ferroptotic death.

Chapter 5: As you, from crimes would pardoned be, / Let your indulgence set me free[XVIII]

[XVIII] 'The Tempest' by William Shakespeare. The last line of The Bard's last full,published play.

5-1: A dutiful summation

As with many lengthy prose, death is the theme, and more specifically to this thesis, the tie-in of cell death and the PM make-up. Simplistic models oft show the PM as a static player: the mirror-like bilayers a mere clothesline to hang the protein landscape. True, the PM is a barrier against the extracellular matrix, but like in most historical clashes, the action occurs at the fortress walls. And like these human-built constructs, it is the strength of materials and type of outside bombardment that determines if a barrier prevails or falls.

5-1-1: Ceramide and cholesterol; the fall of Constantinople, 1453 AD

Chapter 1 introduced the diverse role of the sphingolipid metabolic pathway within cell survival and growth. The PM is intimately involved in ceramides and their cellular fates since ceramide structure can alter the bilayer environment and the PM is a site for ceramide biogenesis. However, not all ceramides are alike, and Chapter 2 explores the interplay of C16 and C24-cer in cell death or survival, respectively. This relationship is exacerbated by the addition of exogenous short-chain ceramides. Our goal to find novel targets within these connected relationships led us to ARL5A and TMEM30A. KO of ARL5A sensitises cells to C6-Cer whiles KO in TMEM30A imparts resistance. The experiments of Chapter 3 describe the unique plasmalemmal environment in each KO. KOTMEM30A produces an exoplasmic leaflet that may draw cholesterol to the outer surface that partials the cell toward C24-cer formation. KOARL5A, on the other hand, hints to a cytoplasmic environment that is unbending with cholesterol. These create rigid formations that favour C16-cer formation. In subsequent battering by exogenous ceramides, KOTMEM30A withstands the siege with the C24-cer reinforcements to thwart the C6-Cer toxicity. However, the same bombardment becomes artillery on the C16-cer foundations of KOARL5A and the cell succumbs to the infernal pounding.

5-1-2: Ferroptosis and PUFAs; Ephialtes at Thermopylae, 480 BC

The PM requires an unbiased front to hold off extracellular pressures. Ferroptosis uses pernicious peroxidated PUFAs to perturb the PM and drive the cell to RCD. Chapter 4 details how ACSL4—the enzyme that engineers PUFAs—isoforms can push the lipid make-up of the PM towards death or survival. The short isoform of ACSL4 localises to the PM whereupon its enzyme activity ensures a high concentration of PUFAs in the PM. ACSL4-long translocates to the LDs and funnels PUFA production to this compartment. Upon ferroptotic insult, the cascade of lipid radicals occurs in the subcellular location with the highest amount of PUFAs. Should this be the PM, the bilayer structure is attacked on multiple sides, barrier function is lost, the cytosol is exposed and the cell dies from osmotic forces. PUFAs on the LD offer both temporal and spatial respite; the cell has time for its rescue pathways to clear offending lipids before the positive feedback loop reaches the PM and performs irrecoverable damage.

5-2: The what in within prevents the breach from without

The underlying genotype of the cell predisposes a unique PM phenotype. The particular make-up of the PM of each of these genetic backgrounds is functional enough for daily traffic; but, its mettle is truly tested upon an acute stressor. The lipotoxic pathways of either exogenous ceramides or ferroptosis pushes on the PM's intrinsic foundations. If its mortar is weak, the cell crumbles, but if the materials hold true, then the barrier is maintained and the cell wins the sortie.

References

1. Morad, S. A. F. & Cabot, M. C. Ceramide-orchestrated signalling in cancer cells. *Nat. Rev. Cancer* **13,** 51–65 (2013).

2. Moro, K., Nagahashi, M., Gabriel, E., Takabe, K. & Wakai, T. Clinical application of ceramide in cancer treatment. *Breast Cancer* **26,** 407–415 (2019).

3. Park, J.-W., Park, W.-J. & Futerman, A. H. Ceramide synthases as potential targets for therapeutic intervention in human diseases. *Biochim. Biophys. Acta* **1841,** 671–681 (2014).

4. Oskouian, B. & Saba, J. D. Cancer treatment strategies targeting sphingolipid metabolism. *Adv. Exp. Med. Biol.* **688,** 185–205 (2010).

5. Sandhoff, R., Schulze, H. & Sandhoff, K. Ganglioside metabolism in health and disease. *Prog Mol Biol Transl Sci* **156,** 1–62 (2018).

6. Goñi, F. M., Sot, J. & Alonso, A. Biophysical properties of sphingosine, ceramides and other simple sphingolipids. *Biochem. Soc. Trans.* **42,** 1401–1408 (2014).

7. Goñi, F. M. & Alonso, A. Biophysics of sphingolipids I. Membrane properties of sphingosine, ceramides and other simple sphingolipids. *Biochim. Biophys. Acta* **1758,** 1902–1921 (2006).

8. Hannun, Y. A. & Obeid, L. M. Principles of bioactive lipid signalling: lessons from sphingolipids. *Nat. Rev. Mol. Cell Biol.* **9,** 139–150 (2008).

9. Castro, B. M., Prieto, M. & Silva, L. C. Ceramide: a simple sphingolipid with unique biophysical properties. *Prog. Lipid Res.* **54,** 53–67 (2014).

10. Hanada, K., Kumagai, K., Tomishige, N. & Kawano, M. CERT and intracellular trafficking of ceramide. *Biochim. Biophys. Acta* **1771,** 644–653 (2007).

11. Pewzner-Jung, Y., Ben-Dor, S. & Futerman, A. H. When do Lasses (longevity assurance genes) become CerS (ceramide synthases)?: Insights into the regulation of ceramide synthesis. *J. Biol. Chem.* **281,** 25001–25005 (2006).

12. Gómez-Muñoz, A. Ceramide 1-phosphate/ceramide, a switch between life and death. *Biochim. Biophys. Acta* **1758,** 2049–2056 (2006).

13. Kitatani, K., Idkowiak-Baldys, J. & Hannun, Y. A. The sphingolipid salvage pathway in ceramide metabolism and signaling. *Cell Signal.* **20,** 1010–1018 (2008).

14. Ruiz-Argüello, M. B., Basáñez, G., Goñi, F. M. & Alonso, A. Different effects of enzyme-generated ceramides and diacylglycerols in phospholipid membrane fusion and leakage. *J. Biol. Chem.* **271,** 26616–26621 (1996).

15. Pinto, S. N. *et al.* Changes in membrane biophysical properties induced by sphingomyelinase depend on the sphingolipid N-acyl chain. *J. Lipid Res.* **55,** 53–61 (2014).

16. Jiménez-Rojo, N., García-Arribas, A. B., Sot, J., Alonso, A. & Goñi, F. M. Lipid bilayers containing sphingomyelins and ceramides of varying N-acyl lengths: a glimpse into sphingolipid complexity. *Biochim. Biophys. Acta* **1838,** 456–464 (2014).

17. Montes, L. R., Ruiz-Argüello, M. B., Goñi, F. M. & Alonso, A. Membrane restructuring via ceramide results in enhanced solute efflux. *J. Biol. Chem.* **277,** 11788–11794 (2002).

18. López-Montero, I., Vélez, M. & Devaux, P. F. Surface tension induced by sphingomyelin to ceramide conversion in lipid membranes. *Biochim. Biophys. Acta* **1768,** 553–561 (2007).

19. Pohl, A., López-Montero, I., Rouvière, F., Giusti, F. & Devaux, P. F. Rapid transmembrane diffusion of ceramide and dihydroceramide spin-labelled analogues in the liquid ordered phase. *Mol Membr Biol* **26,** 194–204 (2009).

20. Fanani, M. L. & Maggio, B. The many faces (and phases) of ceramide and sphingomyelin I - single lipids. *Biophys. Rev.* **9,** 589–600 (2017).

21. Alonso, A. & Goñi, F. M. The physical properties of ceramides in membranes. *Annu. Rev. Biophys.* **47,** 633–654 (2018).

22. Stancevic, B. & Kolesnick, R. Ceramide-rich platforms in transmembrane signaling. *FEBS Lett.* **584,** 1728–1740 (2010).

23. Ruvolo, P. P. Intracellular signal transduction pathways activated by ceramide and its metabolites. *Pharmacol. Res.* **47,** 383–392 (2003).

24. Nica, A. F. *et al.* Ceramide promotes apoptosis in chronic myelogenous leukemia-derived K562 cells by a mechanism involving caspase-8 and JNK. *Cell Cycle* **7,** 3362–3370 (2008).

25. Babiychuk, E. B. *et al.* The targeting of plasmalemmal ceramide to mitochondria during apoptosis. *PLoS One* **6,** e23706 (2011).

26. Renault, T. T. & Chipuk, J. E. Death upon a kiss: mitochondrial outer membrane composition and organelle communication govern sensitivity to BAK/BAX-dependent apoptosis. *Chem. Biol.* **21,** 114–123 (2014).

27. von Haefen, C. *et al.* Ceramide induces mitochondrial activation and apoptosis via a Bax-dependent pathway in human carcinoma cells. *Oncogene* **21,** 4009–4019 (2002).

28. Kantari, C. & Walczak, H. Caspase-8 and bid: caught in the act between death receptors and mitochondria. *Biochim. Biophys. Acta* **1813,** 558–563 (2011).

29. Gencer, E. B., Ural, A. U., Avcu, F. & Baran, Y. A novel mechanism of dasatinib-induced apoptosis in chronic myeloid leukemia; ceramide synthase and ceramide clearance genes. *Ann. Hematol.* **90,** 1265–1275 (2011).

30. Yagci, Z. B., Esvap, E., Ozkara, H. A., Ulgen, K. O. & Olmez, E. O. Inflammatory response and its relation to sphingolipid metabolism proteins: Chaperones as potential indirect anti-inflammatory agents. *Adv. Protein Chem. Struct. Biol.* **114,** 153–219 (2019).

31. Fillet, M. *et al.* Mechanisms involved in exogenous C2- and C6-ceramide-induced cancer cell toxicity. *Biochem. Pharmacol.* **65,** 1633–1642 (2003).

32. Voelkel-Johnson, C., Hannun, Y. A. & El-Zawahry, A. Resistance to TRAIL is associated with defects in ceramide signaling that can be overcome by exogenous C6-ceramide without requiring down-regulation of cellular FLICE inhibitory protein. *Mol. Cancer Ther.* **4,** 1320–1327 (2005).

33. Ji, C. *et al.* Exogenous cell-permeable C6 ceramide sensitizes multiple cancer cell lines to Doxorubicin-induced apoptosis by promoting AMPK activation and mTORC1 inhibition. *Oncogene* **29,** 6557–6568 (2010).

34. Takeda, S., Mitsutake, S., Tsuji, K. & Igarashi, Y. Apoptosis occurs via the ceramide recycling pathway in human HaCaT keratinocytes. *J. Biochem.* **139,** 255–262 (2006).

35. Jiang, F. & Doudna, J. A. CRISPR-Cas9 Structures and Mechanisms. *Annu. Rev. Biophys.* **46,** 505–529 (2017).

36. Sanjana, N. E. Genome-scale CRISPR pooled screens. *Anal. Biochem.* **532,** 95–99 (2017).

37. Wu, K. & Malek, S. N. CRISPR/Cas9-Based Gene Dropout Screens. *Methods Mol. Biol.* **1881,** 185–200 (2019).

38. Morgens, D. W., Deans, R. M., Li, A. & Bassik, M. C. Systematic comparison of CRISPR/Cas9 and RNAi screens for essential genes. *Nat. Biotechnol.* **34,** 634–636 (2016).

39. Deans, R. M. *et al.* Parallel shRNA and CRISPR-Cas9 screens enable antiviral drug target identification. *Nat. Chem. Biol.* **12,** 361–366 (2016).

40. Morgens, D. W. *et al.* Genome-scale measurement of off-target activity using Cas9 toxicity in high-throughput screens. *Nat. Commun.* **8,** 15178 (2017).

41. Andersson, L. C., Nilsson, K. & Gahmberg, C. G. K562--a human erythroleukemic cell line. *Int. J. Cancer* **23,** 143–147 (1979).

42. Leto, D. E. *et al.* Genome-wide CRISPR Analysis Identifies Substrate-Specific Conjugation Modules in ER-Associated Degradation. *Mol. Cell* **73,** 377–389.e11 (2019).

43. Benjamini, Y., Krieger, A. M. & Yekutieli, D. Adaptive linear step-up procedures that control the false discovery rate. *Biometrika* **93,** 491–507 (2006).

44. Siskind, L. J. & Colombini, M. The lipids C2- and C16-ceramide form large stable channels. Implications for apoptosis. *J. Biol. Chem.* **275,** 38640–38644 (2000).

45. Levy, M. & Futerman, A. H. Mammalian ceramide synthases. *IUBMB Life* **62,** 347–356 (2010).

46. Laviad, E. L. *et al.* Characterization of ceramide synthase 2: tissue distribution, substrate specificity, and inhibition by sphingosine 1-phosphate. *J. Biol. Chem.* **283,** 5677–5684 (2008).

47. Ohno, Y. *et al.* ELOVL1 production of C24 acyl-CoAs is linked to C24 sphingolipid synthesis. *Proc. Natl. Acad. Sci. USA* **107,** 18439–18444 (2010).

48. Sassa, T. *et al.* Impaired epidermal permeability barrier in mice lacking elovl1, the gene responsible for very-long-chain fatty acid production. *Mol. Cell. Biol.* **33,** 2787–2796 (2013).

49. Sassa, T., Suto, S., Okayasu, Y. & Kihara, A. A shift in sphingolipid composition from C24 to C16 increases susceptibility to apoptosis in HeLa cells. *Biochim. Biophys. Acta* **1821,** 1031–1037 (2012).

50. Spiegel, S. & Milstien, S. Sphingosine-1-phosphate: an enigmatic signalling lipid. *Nat. Rev. Mol. Cell Biol.* **4,** 397–407 (2003).

51. Wegner, M.-S. *et al.* UDP-glucose ceramide glucosyltransferase activates AKT, promoted proliferation, and doxorubicin resistance in breast cancer cells. *Cell Mol. Life Sci.* **75,** 3393–3410 (2018).

52. Wegner, M.-S., Gruber, L., Mattjus, P., Geisslinger, G. & Grösch, S. The UDP-glucose ceramide glycosyltransferase (UGCG) and the link to multidrug resistance protein 1 (MDR1). *BMC Cancer* **18,** 153 (2018).

53. Osawa, Y. *et al.* Roles for C16-ceramide and sphingosine 1-phosphate in regulating hepatocyte apoptosis in response to tumor necrosis factor-alpha. *J. Biol. Chem.* **280,** 27879–27887 (2005).

54. Reimand, J., Kull, M., Peterson, H., Hansen, J. & Vilo, J. g:Profiler--a web-based toolset for functional profiling of gene lists from large-scale experiments. *Nucleic Acids Res.* **35,** W193–200 (2007).

55. Raudvere, U. *et al.* g:Profiler: a web server for functional enrichment analysis and conversions of gene lists (2019 update). *Nucleic Acids Res.* **47,** W191–W198 (2019).

56. Reimand, J. *et al.* Pathway enrichment analysis and visualization of omics data using g:Profiler, GSEA, Cytoscape and EnrichmentMap. *Nat. Protoc.* **14,** 482–517 (2019).

57. Kanehisa, M., Sato, Y., Furumichi, M., Morishima, K. & Tanabe, M. New approach for understanding genome variations in KEGG. *Nucleic Acids Res.* **47,** D590–D595 (2019).

58. Jassal, B. *et al.* The Reactome Pathway Knowledgebase. *Nucleic Acids Res.* **48,** D498–D503 (2020).

59. Slenter, D. N. *et al.* WikiPathways: a multifaceted pathway database bridging metabolomics to other omics research. *Nucleic Acids Res.* **46,** D661–D667 (2018).

60. Thul, P. J. *et al.* A subcellular map of the human proteome. *Science* **356,** (2017).

61. Lacombe, J. & Ferron, M. VKORC1L1, an enzyme mediating the effect of vitamin K in liver and extrahepatic tissues. *Nutrients* **10,** (2018).

62. Oldenburg, J., Watzka, M. & Bevans, C. G. VKORC1 and VKORC1L1: Why do Vertebrates Have Two Vitamin K 2,3-Epoxide Reductases? *Nutrients* **7,** 6250–6280 (2015).

63. Casalou, C., Ferreira, A. & Barral, D. C. The role of ARF family proteins and their regulators and effectors in cancer progression: A therapeutic perspective. *Front. Cell Dev. Biol.* **8,** 217 (2020).

64. Wang, Q. *et al.* microRNA-202-3p inhibits cell proliferation by targeting ADP-ribosylation factor-like 5A in human colorectal carcinoma. *Clin. Cancer Res.* **20,** 1146–1157 (2014).

65. Shi, M. *et al.* Amino acids stimulate the endosome-to-Golgi trafficking through Ragulator and small GTPase Arl5. *Nat. Commun.* **9,** 4987 (2018).

66. Donaldson, J. G. & Jackson, C. L. ARF family G proteins and their regulators: roles in membrane transport, development and disease. *Nat. Rev. Mol. Cell Biol.* **12,** 362–375 (2011).

67. Ishida, M. & Bonifacino, J. S. ARFRP1 functions upstream of ARL1 and ARL5 to coordinate recruitment of distinct tethering factors to the trans-Golgi network. *J. Cell Biol.* **218,** 3681–3696 (2019).

68. Yang, F. *et al.* Deletion of a flippase subunit Tmem30a in hematopoietic cells impairs mouse fetal liver erythropoiesis. *Haematologica* **104,** 1984–1994 (2019).

69. Yang, Y., Liu, W., Sun, K., Jiang, L. & Zhu, X. Tmem30a deficiency leads to retinal rod bipolar cell degeneration. *J. Neurochem.* **148,** 400–412 (2019).

70. Coleman, J. A. & Molday, R. S. Critical role of the beta-subunit CDC50A in the stable expression, assembly, subcellular localization, and lipid transport activity of the P4-ATPase ATP8A2. *J. Biol. Chem.* **286,** 17205–17216 (2011).

71. He, Y., Xu, J., Wu, X. & Li, L. Structures of a P4-ATPase lipid flippase in lipid bilayers. *Protein Cell* **11,** 458–463 (2020).

72. Palmgren, M., Østerberg, J. T., Nintemann, S. J., Poulsen, L. R. & López-Marqués, R. L. Evolution and a revised nomenclature of P4 ATPases, a eukaryotic family of lipid flippases. *Biochim. Biophys. Acta Biomembr.* **1861,** 1135–1151 (2019).

73. Nishiyama, M. *et al.* CHD8 suppresses p53-mediated apoptosis through histone H1 recruitment during early embryogenesis. *Nat. Cell Biol.* **11,** 172–182 (2009).

74. Kruszka, P. *et al.* A CCR4-NOT Transcription Complex, Subunit 1, CNOT1, Variant Associated with Holoprosencephaly. *Am. J. Hum. Genet.* **104,** 990–993 (2019).

75. Zheng, X. *et al.* Cnot1, Cnot2, and Cnot3 maintain mouse and human ESC identity and inhibit extraembryonic differentiation. *Stem Cells* **30,** 910–922 (2012).

76. Vaites, L. P., Paulo, J. A., Huttlin, E. L. & Harper, J. W. Systematic analysis of human cells lacking ATG8 proteins uncovers roles for gabaraps and the CCZ1/MON1 regulator c18orf8/rmc1 in macroautophagic and selective autophagic flux. *Mol. Cell. Biol.* **38,** (2018).

77. Tsui, C. K. *et al.* CRISPR-Cas9 screens identify regulators of antibody-drug conjugate toxicity. *Nat. Chem. Biol.* **15,** 949–958 (2019).

78. Zhang, Z. & Gerstein, M. Identification and characterization of over 100 mitochondrial ribosomal protein pseudogenes in the human genome. *Genomics* **81,** 468–480 (2003).

79. Han, K. *et al.* Synergistic drug combinations for cancer identified in a CRISPR screen for pairwise genetic interactions. *Nat. Biotechnol.* **35,** 463–474 (2017).

80. Lenoir, G., Williamson, P. & Holthuis, J. C. M. On the origin of lipid asymmetry: the flip side of ion transport. *Curr. Opin. Chem. Biol.* **11,** 654–661 (2007).

81. Uchida, Y. *et al.* Intracellular phosphatidylserine is essential for retrograde membrane traffic through endosomes. *Proc. Natl. Acad. Sci. USA* **108,** 15846–15851 (2011).

82. Cho, K.-J. *et al.* Inhibition of Acid Sphingomyelinase Depletes Cellular Phosphatidylserine and Mislocalizes K-Ras from the Plasma Membrane. *Mol. Cell. Biol.* **36,** 363–374 (2016).

83. Andersen, J. P. *et al.* P4-ATPases as Phospholipid Flippases-Structure, Function, and Enigmas. *Front. Physiol.* **7,** 275 (2016).

84. Huang, H. W., Goldberg, E. M. & Zidovetzki, R. Ceramides modulate protein kinase C activity and perturb the structure of Phosphatidylcholine/Phosphatidylserine bilayers. *Biophys. J.* **77,** 1489–1497 (1999).

85. Kobayashi, T. & Menon, A. K. Transbilayer lipid asymmetry. *Curr. Biol.* **28,** R386–R391 (2018).

86. Takatsu, H. *et al.* Phospholipid flippase ATP11C is endocytosed and downregulated following Ca2+-mediated protein kinase C activation. *Nat. Commun.* **8,** 1423 (2017).

87. Sheetz, M. P. & Singer, S. J. Biological membranes as bilayer couples. A molecular mechanism of drug-erythrocyte interactions. *Proc. Natl. Acad. Sci. USA* **71,** 4457–4461 (1974).

88. Lorent, J. H. *et al.* Plasma membranes are asymmetric in lipid unsaturation, packing and protein shape. *Nat. Chem. Biol.* **16,** 644–652 (2020).

89. Xie, Z. & Cai, T. Na+-K+--ATPase-mediated signal transduction: from protein interaction to cellular function. *Mol Interv* **3,** 157–168 (2003).

90. López-Marqués, R. L. *et al.* Structure and mechanism of ATP-dependent phospholipid transporters. *Biochim. Biophys. Acta* **1850,** 461–475 (2015).

91. Naik, J. *et al.* The P4-ATPase ATP9A is a novel determinant of exosome release. *PLoS One* **14,** e0213069 (2019).

92. Van Der Woerd, W. L., Wichers, C. G. K. & Vestergaard, A. L. Defective plasma membrane targeting of p. I661T-ATP8B1, associated with familial intrahepatic cholestasis, can be rescued in vitro by CFTR correctors. *ATP8B1 …* (2016).

93. Kato, U. *et al.* Role for phospholipid flippase complex of ATP8A1 and CDC50A proteins in cell migration. *J. Biol. Chem.* **288,** 4922–4934 (2013).

94. Folmer, D. E. *et al.* Cellular localization and biochemical analysis of mammalian CDC50A, a glycosylated β-subunit for P4 ATPases. *J. Histochem. Cytochem.* **60,** 205–218 (2012).

95. Roland, B. P., Jain, B. K. & Graham, T. R. Exofacial membrane composition and lipid metabolism regulates plasma membrane P4-ATPase substrate specificity. *BioRxiv* (2020). doi:10.1101/2020.06.24.169672

96. Rosa-Ferreira, C., Christis, C., Torres, I. L. & Munro, S. The small G protein Arl5 contributes to endosome-to-Golgi traffic by aiding the recruitment of the GARP complex to the Golgi. *Biol. Open* **4,** 474–481 (2015).

97. Whyte, J. R. C. & Munro, S. Vesicle tethering complexes in membrane traffic. *J. Cell Sci.* **115,** 2627–2637 (2002).

98. Yu, I.-M. & Hughson, F. M. Tethering factors as organizers of intracellular vesicular traffic. *Annu. Rev. Cell Dev. Biol.* **26,** 137–156 (2010).

99. D'Souza-Schorey, C. & Chavrier, P. ARF proteins: roles in membrane traffic and beyond. *Nat. Rev. Mol. Cell Biol.* **7,** 347–358 (2006).

100. Houghton, F. J. *et al.* Arl5b is a Golgi-localised small G protein involved in the regulation of retrograde transport. *Exp. Cell Res.* **318,** 464–477 (2012).

101. Pasqualato, S., Renault, L. & Cherfils, J. Arf, Arl, Arp and Sar proteins: a family of GTP-binding proteins with a structural device for "front-back" communication. *EMBO Rep.* **3,** 1035–1041 (2002).

102. Brinkman, E. K., Chen, T., Amendola, M. & van Steensel, B. Easy quantitative assessment of genome editing by sequence trace decomposition. *Nucleic Acids Res.* **42,** e168 (2014).

103. Tepper, A. D. *et al.* Sphingomyelin hydrolysis to ceramide during the execution phase of apoptosis results from phospholipid scrambling and alters cell-surface morphology. *J. Cell Biol.* **150,** 155–164 (2000).

104. Zhai, X. *et al.* Phosphatidylserine Stimulates Ceramide 1-Phosphate (C1P) Intermembrane Transfer by C1P Transfer Proteins. *J. Biol. Chem.* **292,** 2531–2541 (2017).

105. Contreras, F.-X., Basañez, G., Alonso, A., Herrmann, A. & Goñi, F. M. Asymmetric addition of ceramides but not dihydroceramides promotes transbilayer (flip-flop) lipid motion in membranes. *Biophys. J.* **88,** 348–359 (2005).

106. Chen, K. *et al.* Aminoglycerophospholipid flipping and P4-ATPases in Toxoplasma gondii. *J. Biol. Chem.* **296,** 100315 (2021).

107. Shamseddine, A. A. *et al.* P53-dependent upregulation of neutral sphingomyelinase-2: role in doxorubicin-induced growth arrest. *Cell Death Dis.* **6,** e1947 (2015).

108. Ennishi, D. *et al.* TMEM30A loss-of-function mutations drive lymphomagenesis and confer therapeutically exploitable vulnerability in B-cell lymphoma. *Nat. Med.* **26,** 577–588 (2020).

109. Coleman, J. A. *et al.* Phospholipid flippase ATP8A2 is required for normal visual and auditory function and photoreceptor and spiral ganglion cell survival. *J. Cell Sci.* **127,** 1138–1149 (2014).

110. Katoh, Y. & Katoh, M. Identification and characterization of CDC50A, CDC50B and CDC50C genes in silico. *Oncol. Rep.* (2004). doi:10.3892/or.12.4.939

111. Vestergaard, A. L. *et al.* Specific mutations in mammalian P4-ATPase ATP8A2 catalytic subunit entail differential glycosylation of the accessory CDC50A subunit. *FEBS Lett.* **589,** 3908–3914 (2015).

112. Holopainen, J. M., Brockman, H. L., Brown, R. E. & Kinnunen, P. K. Interfacial interactions of ceramide with dimyristoylphosphatidylcholine: impact of the N-acyl chain. *Biophys. J.* **80,** 765–775 (2001).

113. Carrer, D. C. & Maggio, B. Phase behavior and molecular interactions in mixtures of ceramide with dipalmitoylphosphatidylcholine. *J. Lipid Res.* **40,** 1978–1989 (1999).

114. Wu, B. X. *et al.* Identification of novel anionic phospholipid binding domains in neutral sphingomyelinase 2 with selective binding preference. *J. Biol. Chem.* **286,** 22362–22371 (2011).

115. Hassouneh, L. K. M. Effects of vitamin E on the synthesis of phospholipids and brain functions in old rats. *Neurophysiology* **50,** 166–172 (2018).

116. Loidl, A., Claus, R., Deigner, H. P. & Hermetter, A. High-precision fluorescence assay for sphingomyelinase activity of isolated enzymes and cell lysates. *J. Lipid Res.* **43,** 815–823 (2002).

117. Ikonen, E. Cellular cholesterol trafficking and compartmentalization. *Nat. Rev. Mol. Cell Biol.* **9,** 125–138 (2008).

118. Maekawa, M. & Fairn, G. D. Complementary probes reveal that phosphatidylserine is required for the proper transbilayer distribution of cholesterol. *J. Cell Sci.* **128,** 1422–1433 (2015).

119. Kay, J. G., Koivusalo, M., Ma, X., Wohland, T. & Grinstein, S. Phosphatidylserine dynamics in cellular membranes. *Mol. Biol. Cell* **23,** 2198–2212 (2012).

120. Courtney, K. C. *et al.* C24 Sphingolipids Govern the Transbilayer Asymmetry of Cholesterol and Lateral Organization of Model and Live-Cell Plasma Membranes. *Cell Rep.* **24,** 1037–1049 (2018).

121. Slotte, J. P. & Bierman, E. L. Depletion of plasma-membrane sphingomyelin rapidly alters the distribution of cholesterol between plasma membranes and intracellular cholesterol pools in cultured fibroblasts. *Biochem. J.* **250,** 653–658 (1988).

122. García-Arribas, A. B., Alonso, A. & Goñi, F. M. Cholesterol interactions with ceramide and sphingomyelin. *Chem Phys Lipids* **199,** 26–34 (2016).

123. Ten Grotenhuis, E. *et al.* Phase behavior of stratum corneum lipids in mixed Langmuir-Blodgett monolayers. *Biophys. J.* **71,** 1389–1399 (1996).

124. Ernst, A. M., Contreras, F.-X., Thiele, C., Wieland, F. & Brügger, B. Mutual recognition of sphingolipid molecular species in membranes. *Biochim. Biophys. Acta* **1818,** 2616–2622 (2012).

125. Bandaru, V. V. R. *et al.* ApoE4 disrupts sterol and sphingolipid metabolism in Alzheimer's but not normal brain. *Neurobiol. Aging* **30,** 591–599 (2009).

126. Legleiter, J., Fryer, J. D., Holtzman, D. M. & Kowalewski, A. The modulating effect of mechanical changes in lipid bilayers caused by apoE-containing lipoproteins on Aβ induced membrane disruption. *ACS Chem. Neurosci.* **2,** 588–599 (2011).

127. Zhang, W.-Y., Gaynor, P. M. & Kruth, H. S. Aggregated Low Density Lipoprotein Induces and Enters Surface-connected Compartments of Human Monocyte-Macrophages. *J. Bio. Chem.* **272,** 31700–31706 (1997).

128. Werb, Z., Takemura, R., Stenberg, P. E. & Bainton, D. F. Directed exocytosis of secretory granules containing apolipoprotein E to the adherent surface and basal vacuoles of macrophages spreading on immobile immune complexes. *Am. J. Pathol.* **134,** 661–670 (1989).

129. Kockx, M., Jessup, W. & Kritharides, L. Regulation of endogenous apolipoprotein E secretion by macrophages. *Arterioscler. Thromb. Vasc. Biol.* **28,** 1060–1067 (2008).

130. Morita, S. *et al.* Formation of ceramide-enriched domains in lipid particles enhances the binding of apolipoprotein E. *FEBS Lett.* **579,** 1759–1764 (2005).

131. Morita, S. Effects of sphingomyelin on apolipoprotein E- and lipoprotein lipase-mediated cell uptake of lipid particles. *Biochimica et Biophysica Acta (BBA) - Molecular and Cell Biology of Lipids* **1631,** 169–176 (2003).

132. Crivelli, S. M. *et al.* Ceramide analog [18F]F-HPA-12 detects sphingolipid disbalance in the brain of Alzheimer's disease transgenic mice by functioning as a metabolic probe. *Sci. Rep.* **10,** 19354 (2020).

133. Puri, V. *et al.* Cholesterol modulates membrane traffic along the endocytic pathway in sphingolipid-storage diseases. *Nat. Cell Biol.* **1,** 386–388 (1999).

134. Kruth, H. S., Skarlatos, S. I., Lilly, K., Chang, J. & Ifrim, I. Sequestration of acetylated LDL and cholesterol crystals by human monocyte-derived macrophages. *J. Cell Biol.* **129,** 133–145 (1995).

135. Goldschmidt-Arzi, M., Shimoni, E., Sabanay, H., Futerman, A. H. & Addadi, L. Intracellular localization of organized lipid domains of C16-ceramide/cholesterol. *J. Struct. Biol.* **175,** 21–30 (2011).

136. Jaikishan, S. & Slotte, J. P. Effect of hydrophobic mismatch and interdigitation on sterol/sphingomyelin interaction in ternary bilayer membranes. *Biochim. Biophys. Acta* **1808,** 1940–1945 (2011).

137. McIntosh, T. J., Simon, S. A., Needham, D. & Huang, C. H. Structure and cohesive properties of sphingomyelin/cholesterol bilayers. *Biochemistry* **31,** 2012–2020 (1992).

138. Grimmer, S., Iversen, T. G., van Deurs, B. & Sandvig, K. Endosome to Golgi transport of ricin is regulated by cholesterol. *Mol. Biol. Cell* **11,** 4205–4216 (2000).

139. Mukherjee, S. & Maxfield, F. R. Role of membrane organization and membrane domains in endocytic lipid trafficking. *Traffic* **1,** 203–211 (2000).

140. Maulik, P. R. & Shipley, G. G. N-palmitoyl sphingomyelin bilayers: structure and interactions with cholesterol and dipalmitoylphosphatidylcholine. *Biochemistry* **35,** 8025–8034 (1996).

141. Duran, J. M. *et al.* Sphingomyelin organization is required for vesicle biogenesis at the Golgi complex. *EMBO J.* **31,** 4535–4546 (2012).

142. Deng, J., Rudick, V. & Dory, L. Lysosomal degradation and sorting of apolipoprotein E in macrophages. *J. Lipid Res.* **36,** 2129–2140 (1995).

143. Jensen, M. S., Costa, S., Günther-Pomorski, T. & López-Marqués, R. L. Cell-Based Lipid Flippase Assay Employing Fluorescent Lipid Derivatives. *Methods Mol. Biol.* **1377,** 371–382 (2016).

144. Clarke, D. J. B. *et al.* Appyters: Turning Jupyter Notebooks into data-driven web apps. *Patterns (N Y)* **2,** 100213 (2021).

145. Livak, K. J. & Schmittgen, T. D. Analysis of relative gene expression data using real-time quantitative PCR and the 2(-Delta Delta C(T)) Method. *Methods* **25,** 402–408 (2001).

146. Dixon, S. J. & Stockwell, B. R. The hallmarks of ferroptosis. *Annu. Rev. Cancer Biol.* **3,** 35–54 (2019).

147. Stockwell, B. R. *et al.* Ferroptosis: A regulated cell death nexus linking metabolism, redox biology, and disease. *Cell* **171,** 273–285 (2017).

148. Cao, J. Y. & Dixon, S. J. Mechanisms of ferroptosis. *Cell Mol. Life Sci.* **73,** 2195–2209 (2016).

149. Yang, W. S. & Stockwell, B. R. Ferroptosis: death by lipid peroxidation. *Trends Cell Biol.* **26,** 165–176 (2016).

150. Conrad, M. *et al.* Regulation of lipid peroxidation and ferroptosis in diverse species. *Genes Dev.* **32,** 602–619 (2018).

151. Friedmann Angeli, J. P. *et al.* Inactivation of the ferroptosis regulator Gpx4 triggers acute renal failure in mice. *Nat. Cell Biol.* **16,** 1180–1191 (2014).

152. Weiland, A. *et al.* Ferroptosis and its role in diverse brain diseases. *Mol. Neurobiol.* **56,** 4880–4893 (2019).

153. Wu, J.-R., Tuo, Q.-Z. & Lei, P. Ferroptosis, a recent defined form of critical cell death in neurological disorders. *J. Mol. Neurosci.* **66,** 197–206 (2018).

154. Lee, H.-C. *et al.* LPIAT1 regulates arachidonic acid content in phosphatidylinositol and is required for cortical lamination in mice. *Mol. Biol. Cell* **23,** 4689–4700 (2012).

155. Yang, W. S. *et al.* Regulation of ferroptotic cancer cell death by GPX4. *Cell* **156,** 317–331 (2014).

156. Shen, Z. *et al.* Emerging strategies of cancer therapy based on ferroptosis. *Adv. Mater. Weinheim* **30,** e1704007 (2018).

157. Yuan, H., Li, X., Zhang, X., Kang, R. & Tang, D. Identification of ACSL4 as a biomarker and contributor of ferroptosis. *Biochem. Biophys. Res. Commun.* **478,** 1338–1343 (2016).

158. Zhang, Y., Chen, D. & Wang, Z. Analyses of mental dysfunction-related ACSl4 in Drosophila reveal its requirement for Dpp/BMP production and visual wiring in the brain. *Hum. Mol. Genet.* **18,** 3894–3905 (2009).

159. Radif, Y. *et al.* The endogenous subcellular localisations of the long chain fatty acid-activating enzymes ACSL3 and ACSL4 in sarcoma and breast cancer cells. *Mol. Cell. Biochem.* **448,** 275–286 (2018).

160. Küch, E.-M. *et al.* Differentially localized acyl-CoA synthetase 4 isoenzymes mediate the metabolic channeling of fatty acids towards phosphatidylinositol. *Biochim. Biophys. Acta* **1841,** 227–239 (2014).

161. Doll, S. *et al.* ACSL4 dictates ferroptosis sensitivity by shaping cellular lipid composition. *Nat. Chem. Biol.* **13,** 91–98 (2017).

162. Dixon, S. J. *et al.* Ferroptosis: an iron-dependent form of nonapoptotic cell death. *Cell* **149,** 1060–1072 (2012).

163. Xie, Y. *et al.* Ferroptosis: process and function. *Cell Death Differ.* **23,** 369–379 (2016).

164. Dixon, S. J. & Stockwell, B. R. The role of iron and reactive oxygen species in cell death. *Nat. Chem. Biol.* **10,** 9–17 (2014).

165. Gaschler, M. M. & Stockwell, B. R. Lipid peroxidation in cell death. *Biochem. Biophys. Res. Commun.* **482,** 419–425 (2017).

166. Tagde, A., Singh, H., Kang, M. H. & Reynolds, C. P. The glutathione synthesis inhibitor buthionine sulfoximine synergistically enhanced melphalan activity against preclinical models of multiple myeloma. *Blood Cancer J.* **4,** e229 (2014).

167. Shintoku, R. *et al.* Lipoxygenase-mediated generation of lipid peroxides enhances ferroptosis induced by erastin and RSL3. *Cancer Sci.* **108,** 2187–2194 (2017).

168. Agmon, E. & Stockwell, B. R. Lipid homeostasis and regulated cell death. *Curr. Opin. Chem. Biol.* **39,** 83–89 (2017).

169. Magtanong, L., Ko, P. J. & Dixon, S. J. Emerging roles for lipids in non-apoptotic cell death. *Cell Death Differ.* **23,** 1099–1109 (2016).

170. Kagan, V. E. *et al.* Oxidized arachidonic and adrenic PEs navigate cells to ferroptosis. *Nat. Chem. Biol.* **13,** 81–90 (2017).

171. Kan, C. F. K., Singh, A. B., Stafforini, D. M., Azhar, S. & Liu, J. Arachidonic acid downregulates acyl-CoA synthetase 4 expression by promoting its ubiquitination and proteasomal degradation. *J. Lipid Res.* **55,** 1657–1667 (2014).

172. Soupene, E. & Kuypers, F. A. Mammalian long-chain acyl-CoA synthetases. *Exp. Biol. Med.* **233,** 507–521 (2008).

173. Guo, Y., Cordes, K. R., Farese, R. V. & Walther, T. C. Lipid droplets at a glance. *J. Cell Sci.* **122,** 749–752 (2009).

174. Wilfling, F. *et al.* Triacylglycerol synthesis enzymes mediate lipid droplet growth by relocalizing from the ER to lipid droplets. *Dev. Cell* **24,** 384–399 (2013).

175. Skouta, R. *et al.* Ferrostatins inhibit oxidative lipid damage and cell death in diverse disease models. *J. Am. Chem. Soc.* **136,** 4551–4556 (2014).

176. Piccini, M. *et al.* FACL4, a new gene encoding long-chain acyl-CoA synthetase 4, is deleted in a family with Alport syndrome, elliptocytosis, and mental retardation. *Genomics* **47,** 350–358 (1998).

177. Ursini, F., Maiorino, M., Valente, M., Ferri, L. & Gregolin, C. Purification from pig liver of a protein which protects liposomes and biomembranes from peroxidative degradation and exhibits glutathione peroxidase activity on phosphatidylcholine hydroperoxides. *Biochim. Biophys. Acta* **710,** 197–211 (1982).

178. Shyu, P., Wong, X. F. A., Crasta, K. & Thibault, G. Dropping in on lipid droplets: insights into cellular stress and cancer. *Biosci. Rep.* **38,** (2018).

179. Apffel, C. A. & Baker, J. R. Lipid droplets in the cytoplasm of malignant cells. *Cancer* **17,** 176–184 (1964).

180. Bersuker, K. *et al.* The CoQ oxidoreductase FSP1 acts parallel to GPX4 to inhibit ferroptosis. *Nature* **575,** 688–692 (2019).

181. Yang, W. S. *et al.* Peroxidation of polyunsaturated fatty acids by lipoxygenases drives ferroptosis. *Proc. Natl. Acad. Sci. USA* **113,** E4966–75 (2016).

182. Rose, J. C. *et al.* Rapidly inducible Cas9 and DSB-ddPCR to probe editing kinetics. *Nat. Methods* **14,** 891–896 (2017).

183. Senkel, S., Waldner, C., Ryffel, G. U. & Thomas, H. Improved conditional expression systems resulting in physiological level of HNF4alpha expression confirm HNF4alpha induced apoptosis in the pancreatic beta-cell line INS-1. *BMC Res. Notes* **2,** 210 (2009).

184. Füllekrug, J. & Poppelreuther, M. Measurement of Long-Chain Fatty Acyl-CoA Synthetase Activity. *Methods Mol. Biol.* **1376,** 43–53 (2016).

185. Lageweg, W., Steen, I., Tager, J. M. & Wanders, R. J. A. A fluorimetric assay for acyl-CoA synthetase activities. *Anal. Biochem.* **197,** 384–388 (1991).

186. Inoue, T., Heo, W. D., Grimley, J. S., Wandless, T. J. & Meyer, T. An inducible translocation strategy to rapidly activate and inhibit small GTPase signaling pathways. *Nat. Methods* **2,** 415–418 (2005).

187. Henderson, M. P. A., Hwang, Y. T., Dyer, J. M., Mullen, R. T. & Andrews, D. W. The C-terminus of cytochrome b5 confers endoplasmic reticulum specificity by preventing spontaneous insertion into membranes. *Biochem. J.* **401,** 701–709 (2007).

188. Kanaji, S., Iwahashi, J., Kida, Y., Sakaguchi, M. & Mihara, K. Characterization of the signal that directs Tom20 to the mitochondrial outer membrane. *J. Cell Biol.* **151,** 277–288 (2000).

189. Itabe, H., Yamaguchi, T., Nimura, S. & Sasabe, N. Perilipins: a diversity of intracellular lipid droplet proteins. *Lipids Health Dis.* **16,** 83 (2017).

190. Plötz, T., Hartmann, M., Lenzen, S. & Elsner, M. The role of lipid droplet formation in the protection of unsaturated fatty acids against palmitic acid induced lipotoxicity to rat insulin-producing cells. *Nutr. Metab. (Lond.)* **13,** 16 (2016).

191. Nguyen, T. B. *et al.* DGAT1-Dependent Lipid Droplet Biogenesis Protects Mitochondrial Function during Starvation-Induced Autophagy. *Dev. Cell* **42,** 9–21.e5 (2017).

192. Cao, J. *et al.* Targeting Acyl-CoA:diacylglycerol acyltransferase 1 (DGAT1) with small molecule inhibitors for the treatment of metabolic diseases. *J. Biol. Chem.* **286,** 41838–41851 (2011).

193. McLaren, D. G. *et al.* DGAT2 Inhibition Alters Aspects of Triglyceride Metabolism in Rodents but Not in Non-human Primates. *Cell Metab.* **27,** 1236–1248.e6 (2018).

194. Roe, N. D., Handzlik, M. K., Li, T. & Tian, R. The role of diacylglycerol acyltransferase (DGAT) 1 and 2 in cardiac metabolism and function. *Sci. Rep.* **8,** 4983 (2018).

195. Bhatt-Wessel, B., Jordan, T. W., Miller, J. H. & Peng, L. Role of DGAT enzymes in triacylglycerol metabolism. *Arch. Biochem. Biophys.* **655,** 1–11 (2018).

196. Hung, Y.-H., Carreiro, A. L. & Buhman, K. K. Dgat1 and Dgat2 regulate enterocyte triacylglycerol distribution and alter proteins associated with cytoplasmic lipid droplets in response to dietary fat. *Biochim. Biophys. Acta Mol. Cell Biol. Lipids* **1862,** 600–614 (2017).

197. Gao, Q., Shang, Y., Huang, W. & Wang, C. Glycerol-3-phosphate Acyltransferase contributes to triacylglycerol biosynthesis, lipid droplet formation, and host invasion in Metarhizium robertsii. *Appl. Environ. Microbiol.* **79,** 7646–7653 (2013).

198. Jaeger, D. *et al.* Label-free in vivo analysis of intracellular lipid droplets in the oleaginous microalga Monoraphidium neglectum by coherent Raman scattering microscopy. *Sci. Rep.* **6,** 35340 (2016).

199. Wu, H. *et al.* In vivo lipidomics using single-cell Raman spectroscopy. *Proc. Natl. Acad. Sci. USA* **108,** 3809–3814 (2011).

200. Fu, D. *et al.* In vivo metabolic fingerprinting of neutral lipids with hyperspectral stimulated Raman scattering microscopy. *J. Am. Chem. Soc.* **136,** 8820–8828 (2014).

201. Matthäus, C. *et al.* Noninvasive imaging of intracellular lipid metabolism in macrophages by Raman microscopy in combination with stable isotopic labeling. *Anal. Chem.* **84,** 8549–8556 (2012).

Appendices

Appendix A: Combined KO screen FDR 10%

List of significant gene hits of the combined CRISPR KO screen. Organised via ascending p-value. Cut-off p-values for FDR 1%: 4.52E-05, FDR 5%: 4.3E-04 and FDR 10%: 1.57E-03.

Ensembl GeneID	Gene Symbol	casTLE Effect	castTLE Score	p-value	Min. Estimated Effect	Max. Estimated Effect
ENSG00000112697	TMEM30A	6.3	301.0	1.59E-06	5.5	7.7
ENSG00000196715	VKORC1L1	-7.3	150.0	1.59E-06	-9.3	-5.9
ENSG00000148154	UGCG	4.5	139.0	1.59E-06	3.8	6.2
ENSG00000142657	PGD	5.4	133.0	1.59E-06	4.1	6.8
ENSG00000100811	YY1	6.7	121.0	1.59E-06	4.9	8.6
ENSG00000100888	CHD8	3.8	117.0	1.59E-06	3.1	5.1
ENSG00000119414	PPP6C	4.5	94.2	1.59E-06	3.4	6.3
ENSG00000166200	COPS2	4.8	92.5	1.59E-06	3.4	7.2
ENSG00000162980	ARL5A	-6.0	76.4	1.59E-06	-7.6	-4.7
ENSG00000159399	HK2	2.9	75.2	1.59E-06	2.3	4.1
ENSG00000105619	TFPT	3.6	72.5	1.59E-06	2.7	4.7
ENSG00000170322	NFRKB	3.1	72.2	1.59E-06	2.3	4.1
ENSG00000152223	EPG5	3.9	67.3	1.59E-06	2.4	5.1
ENSG00000103769	RAB11A	2.7	66.6	1.59E-06	2.1	3.9
ENSG00000123505	AMD1	3.3	65.6	1.59E-06	2.5	4.4
ENSG00000091483	FH	6.0	65.6	1.59E-06	3.8	8.8
ENSG00000090447	TFAP4	3.0	62.8	1.59E-06	2.3	4.6
ENSG00000162769	FLVCR1	-5.1	61.5	1.59E-06	-6.7	-3.8
ENSG00000142186	SCYL1	-4.9	60.7	1.59E-06	-6.4	-3.9
ENSG00000196072	BLOC1S2	3.0	60.6	1.59E-06	2.2	4.2
ENSG00000063176	SPHK2	2.6	59.9	1.59E-06	1.9	3.7
ENSG00000140543	DET1	2.5	56.5	1.59E-06	1.9	3.7
ENSG00000147140	NONO	3.0	56.2	1.59E-06	2.2	4.2
ENSG00000141452	C18ORF8	2.8	56.1	1.59E-06	2.1	4.0
ENSG00000188786	MTF1	3.0	54.3	1.59E-06	2.1	4.1
ENSG00000133895	MEN1	-4.0	51.6	1.59E-06	-5.5	-3.1
ENSG00000127616	SMARCA4	2.7	47.5	1.59E-06	1.8	3.8
ENSG00000105220	GPI	4.1	47.5	1.59E-06	2.8	5.8
ENSG00000131374	TBC1D5	3.9	47.3	1.59E-06	2.7	6.2
ENSG00000157837	SPPL3	2.9	47.2	1.59E-06	2.1	4.7
ENSG00000141367	CLTC	2.7	46.9	1.59E-06	2.2	7.4
ENSG00000144426	NBEAL1	-6.6	46.8	1.74E-06	-8.6	-5.0
ENSG00000125107	CNOT1	6.0	43.9	1.74E-06	4.1	8.8
ENSG00000072958	AP1M1	4.4	43.0	1.74E-06	3.0	6.2
ENSG00000158435	CNOT11	3.6	39.4	1.74E-06	2.5	5.3
ENSG00000178605	GTPBP6	3.9	39.4	1.74E-06	2.6	5.6
ENSG00000178982	EIF3K	4.0	35.3	1.74E-06	2.9	6.7

ENSG00000143418	CERS2	-7.0	34.8	1.74E-06	-9.4	-4.8
ENSG00000116750	UCHL5	4.2	34.7	1.74E-06	2.9	6.2
ENSG00000106367	AP1S1	3.8	34.5	1.74E-06	1.9	9.1
ENSG00000143368	SF3B4	5.9	34.5	1.74E-06	3.7	10.6
ENSG00000198612	COPS8	3.4	33.4	1.74E-06	2.4	6.5
ENSG00000066322	ELOVL1	-6.6	32.6	3.48E-06	-9.5	-4.8
ENSG00000166747	AP1G1	2.9	32.5	3.48E-06	2.0	4.7
ENSG00000174903	RAB1B	-5.3	31.8	3.48E-06	-8.3	-3.7
ENSG00000198964	SGMS1	2.9	31.6	3.48E-06	1.8	4.2
ENSG00000032389	TSSC1	-6.1	31.0	3.48E-06	-8.1	-4.6
ENSG00000175582	RAB6A	-7.1	30.0	5.22E-06	-10.1	-4.1
ENSG00000070610	GBA2	-6.3	29.8	5.22E-06	-11.1	-4.1
ENSG00000122958	VPS26A	3.6	29.8	5.22E-06	2.3	5.4
ENSG00000136875	PRPF4	3.9	29.7	5.22E-06	2.5	6.1
ENSG00000144840	RABL3	2.3	29.4	5.22E-06	1.6	4.0
ENSG00000110497	AMBRA1	3.1	29.4	5.22E-06	1.7	5.2
ENSG00000111530	CAND1	2.6	29.1	5.22E-06	1.7	4.1
ENSG00000196961	AP2A1	4.5	29.0	5.22E-06	2.7	7.4
ENSG00000222014	RAB6C	-5.8	28.2	6.96E-06	-8.6	-3.9
ENSG00000159921	GNE	-3.8	42.3	9.52E-06	-5.0	-2.9
ENSG00000124217	MOCS3	3.4	27.1	1.04E-05	2.0	5.8
ENSG00000242371	IGKV1-39	-5.8	27.0	1.04E-05	-8.5	-4.1
ENSG00000033867	SLC4A7	4.5	41.6	1.11E-05	3.3	6.8
ENSG00000174547	MRPL11	4.2	26.1	1.22E-05	3.0	7.6
ENSG00000148358	GPR107	-6.8	26.0	1.22E-05	-10.0	-4.8
ENSG00000154832	CXXC1	2.3	41.3	1.43E-05	1.7	3.5
ENSG00000171960	PPIH	3.5	41.0	1.43E-05	2.5	5.0
ENSG00000104388	RAB2A	-6.0	25.9	1.57E-05	-8.3	-4.5
ENSG00000173011	TADA2B	2.9	40.7	1.59E-05	1.8	4.7
ENSG00000089902	RCOR1	-3.6	40.0	1.90E-05	-5.3	-2.6
ENSG00000151461	UPF2	2.5	39.9	1.90E-05	1.8	4.5
ENSG00000112576	CCND3	3.8	38.9	2.06E-05	2.5	5.7
ENSG00000090316	MAEA	-3.4	38.8	2.06E-05	-6.9	-1.9
ENSG00000065526	SPEN	2.3	38.6	2.06E-05	1.5	3.4
ENSG00000183770	FOXL2	2.7	38.5	2.06E-05	1.8	4.4
ENSG00000120690	ELF1	-4.2	38.3	2.06E-05	-6.3	-3.2
ENSG00000038210	PI4K2B	-4.4	38.0	2.06E-05	-6.7	-3.3
ENSG00000205423	CNEP1R1	-3.9	38.0	2.06E-05	-5.5	-2.7
ENSG00000117308	GALE	-3.4	38.0	2.06E-05	-4.9	-2.5
ENSG00000047315	POLR2B	5.2	37.4	2.38E-05	3.0	9.1
ENSG00000109854	HTATIP2	-5.7	37.3	2.38E-05	-8.1	-3.4

ENSG00000136381	IREB2	3.8	37.2	2.38E-05	2.8	5.9
ENSG00000198431	TXNRD1	2.3	37.1	2.38E-05	1.6	5.7
ENSG00000086232	EIF2AK1	-4.5	36.4	2.70E-05	-6.2	-3.2
ENSG00000170832	USP32	2.3	24.6	2.78E-05	1.3	4.0
ENSG00000176170	SPHK1	2.1	35.8	2.86E-05	1.4	3.3
ENSG00000101457	DNTTIP1	2.7	35.4	3.17E-05	1.9	4.1
ENSG00000143761	ARF1	2.9	35.2	3.17E-05	1.4	5.1
ENSG00000162923	WDR26	-5.1	35.0	3.33E-05	-6.9	-3.3
ENSG00000005889	ZFX	-4.3	34.9	3.33E-05	-6.3	-2.6
ENSG00000072274	TFRC	3.2	34.4	3.33E-05	2.3	5.1
ENSG00000167792	NDUFV1	2.8	34.3	3.33E-05	1.9	4.2
ENSG00000119383	PPP2R4	2.6	34.1	3.49E-05	1.8	3.9
ENSG00000135801	TAF5L	3.2	33.4	3.81E-05	2.1	4.8
ENSG00000111726	CMAS	-4.5	33.3	3.81E-05	-6.2	-2.8
ENSG00000003756	RBM5	3.4	33.0	4.13E-05	2.1	5.0
ENSG00000108587	GOSR1	-5.7	23.7	4.17E-05	-8.1	-4.2
ENSG00000086598	TMED2	-5.6	23.6	4.35E-05	-8.1	-2.7
ENSG00000067182	TNFRSF1A	2.1	32.4	4.44E-05	1.3	3.3
ENSG00000135966	TGFBRAP1	-6.1	23.5	4.52E-05	-9.1	-3.8
ENSG00000141030	COPS3	2.8	31.7	4.92E-05	1.8	4.2
ENSG00000147536	GINS4	5.0	31.7	4.92E-05	3.6	9.1
ENSG00000169714	CNBP	1.7	31.5	4.92E-05	1.2	3.0
ENSG00000124222	STX16	-5.8	23.2	5.04E-05	-9.0	-3.5
ENSG00000108733	PEX12	3.7	23.2	5.04E-05	2.3	6.3
ENSG00000077549	CAPZB	4.7	23.2	5.04E-05	2.6	8.0
ENSG00000139163	ETNK1	2.5	31.2	5.24E-05	1.9	10.0
ENSG00000125304	TM9SF2	-5.1	22.9	5.39E-05	-7.5	-3.8
ENSG00000005339	CREBBP	2.2	30.8	5.56E-05	1.3	3.3
ENSG00000059804	SLC2A3	1.7	30.3	6.19E-05	1.0	7.3
ENSG00000179950	PUF60	-3.2	29.8	6.67E-05	-5.2	-2.2
ENSG00000080603	SRCAP	-3.8	29.5	7.14E-05	-5.3	-2.6
ENSG00000125356	NDUFA1	2.8	29.4	7.14E-05	1.7	5.7
ENSG00000105583	WDR83OS	2.2	29.2	7.30E-05	1.6	4.1
ENSG00000196655	TRAPPC4	-3.5	29.1	7.30E-05	-5.3	-2.5
ENSG00000189079	ARID2	2.3	29.1	7.30E-05	1.4	3.8
ENSG00000172464	OR5AP2	-6.3	22.0	7.30E-05	-11.2	-3.3
ENSG00000136631	VPS45	-5.7	21.9	7.30E-05	-8.4	-3.8
ENSG00000081307	UBA5	3.1	21.9	7.30E-05	1.5	5.1
ENSG00000149182	ARFGAP2	-6.6	21.6	7.65E-05	-9.2	-3.8
ENSG00000106244	PDAP1	2.3	28.9	7.94E-05	1.4	4.5
ENSG00000155380	SLC16A1	3.8	28.6	8.73E-05	2.2	5.8

ENSG00000161217	PCYT1A	-4.7	28.4	8.89E-05	-7.3	-3.1
ENSG00000175826	CTDNEP1	-4.0	27.6	1.03E-04	-6.1	-2.3
ENSG00000153060	TEKT5	7.4	20.8	1.10E-04	4.5	14.7
ENSG00000168724	DNAJC21	2.9	20.7	1.11E-04	1.5	5.1
ENSG00000130150	MOSPD2	3.3	20.7	1.11E-04	1.5	5.1
ENSG00000135655	USP15	2.6	20.6	1.13E-04	1.3	6.6
ENSG00000067560	RHOA	-3.4	27.3	1.14E-04	-5.7	-2.3
ENSG00000211791	TRAV13-2	4.5	20.5	1.18E-04	3.0	7.7
ENSG00000126767	ELK1	2.9	27.0	1.22E-04	1.4	4.3
ENSG00000204152	TIMM23B	4.8	27.0	1.22E-04	2.1	8.9
ENSG00000083642	PDS5B	-4.1	26.8	1.22E-04	-6.0	-2.1
ENSG00000135387	CAPRIN1	3.4	20.3	1.23E-04	1.9	5.9
ENSG00000119537	KDSR	3.0	26.7	1.27E-04	1.6	4.6
ENSG00000129993	CBFA2T3	3.1	26.6	1.33E-04	1.9	5.6
ENSG00000198128	OR2L3	-6.0	20.1	1.37E-04	-10.9	-3.7
ENSG00000125912	NCLN	6.8	20.1	1.37E-04	3.2	13.5
ENSG00000181924	COA4	-3.8	20.0	1.41E-04	-6.1	-2.4
ENSG00000121680	PEX16	7.2	19.9	1.44E-04	2.9	15.0
ENSG00000100796	SMEK1	1.8	26.2	1.48E-04	1.1	3.4
ENSG00000236334	PPIAL4G	4.0	19.8	1.48E-04	2.5	8.5
ENSG00000215717	TMEM167B	-5.5	19.7	1.51E-04	-8.6	-2.9
ENSG00000134480	CCNH	5.1	26.1	1.52E-04	1.6	9.5
ENSG00000119801	YPEL5	-4.4	19.6	1.57E-04	-6.3	-2.6
ENSG00000267757	C19ORF83	5.0	19.6	1.57E-04	3.1	9.3
ENSG00000117143	UAP1	-4.0	25.9	1.63E-04	-5.9	-2.4
ENSG00000169976	SF3B5	2.5	25.9	1.63E-04	1.5	4.1
ENSG00000100280	AP1B1	2.9	19.4	1.65E-04	1.5	4.9
ENSG00000119820	YIPF4	-6.8	19.3	1.70E-04	-11.7	-4.2
ENSG00000138081	FBXO11	3.0	19.3	1.70E-04	1.5	5.7
ENSG00000172613	RAD9A	5.9	25.4	1.86E-04	3.3	11.3
ENSG00000145041	VPRBP	2.3	19.1	1.91E-04	1.3	4.3
ENSG00000162377	COA7	3.3	19.1	1.91E-04	1.5	5.7
ENSG00000110619	CARS	2.5	25.2	1.98E-04	1.5	3.9
ENSG00000267228	IER3IP1	-5.0	19.0	1.98E-04	-7.9	-3.6
ENSG00000158717	RNF166	3.3	19.0	1.98E-04	1.8	5.4
ENSG00000120616	EPC1	1.9	25.1	2.02E-04	1.1	3.0
ENSG00000092531	SNAP23	-4.2	25.0	2.14E-04	-6.2	-2.2
ENSG00000229769	TRBV10-2	-4.3	18.8	2.17E-04	-7.2	-2.4
ENSG00000103591	AAGAB	3.4	18.8	2.17E-04	2.0	6.0
ENSG00000169592	INO80E	3.5	18.8	2.17E-04	1.8	6.4
ENSG00000081154	PCNP	2.9	24.9	2.22E-04	1.7	4.6

ENSG00000196419	XRCC6	4.3	24.9	2.22E-04	3.1	7.5
ENSG00000117505	DR1	3.6	18.7	2.23E-04	2.0	6.7
ENSG00000132522	GPS2	3.2	24.7	2.43E-04	1.8	5.2
ENSG00000136942	RPL35	3.2	24.7	2.43E-04	2.0	5.6
ENSG00000262526	CTD-2545G14.7	-5.5	18.5	2.43E-04	-8.0	-3.1
ENSG00000072310	SREBF1	1.8	24.5	2.52E-04	1.1	3.2
ENSG00000164754	RAD21	4.0	24.4	2.62E-04	1.3	8.6
ENSG00000174776	WDR49	3.3	18.1	2.80E-04	1.7	6.1
ENSG00000008838	MED24	-3.3	24.2	2.84E-04	-5.2	-2.3
ENSG00000177463	NR2C2	-3.3	24.2	2.84E-04	-5.4	-1.9
ENSG00000108433	GOSR2	-4.5	17.9	3.06E-04	-7.4	-2.8
ENSG00000161981	SNRNP25	2.8	17.9	3.06E-04	1.5	5.1
ENSG00000137078	SIT1	5.7	23.9	3.22E-04	3.9	11.1
ENSG00000214325	AC025287.1	-4.7	17.8	3.22E-04	-7.7	-2.9
ENSG00000102100	SLC35A2	-3.4	23.7	3.40E-04	-5.0	-2.1
ENSG00000143771	CNIH4	-4.6	17.7	3.41E-04	-8.0	-2.8
ENSG00000106771	TMEM245	-4.1	23.6	3.60E-04	-5.9	-2.3
ENSG00000164040	PGRMC2	-4.8	23.5	3.75E-04	-7.2	-2.9
ENSG00000139718	SETD1B	2.3	23.4	3.81E-04	1.3	3.8
ENSG00000172765	TMCC1	6.4	23.4	3.81E-04	1.6	11.4
ENSG00000116560	SFPQ	3.1	23.3	3.90E-04	1.7	5.0
ENSG00000198730	CTR9	4.3	23.3	3.90E-04	2.3	8.4
ENSG00000105677	TMEM147	2.6	17.4	3.97E-04	1.2	4.6
ENSG00000023228	NDUFS1	2.5	23.2	4.08E-04	1.7	5.0
ENSG00000249008	RP11-487E13.1	4.2	17.3	4.09E-04	3.0	8.7
ENSG00000042429	MED17	-3.4	23.1	4.14E-04	-5.3	-2.1
ENSG00000136270	TBRG4	3.6	23.0	4.32E-04	1.7	5.7
ENSG00000166685	COG1	-6.1	17.2	4.37E-04	-10.4	-3.3
ENSG00000099797	TECR	-5.9	17.2	4.37E-04	-10.3	-3.3
ENSG00000182827	ACBD3	-5.9	17.2	4.37E-04	-9.1	-3.6
ENSG00000178828	RNF186	2.3	17.2	4.37E-04	1.2	3.9
ENSG00000254462	TMX2-CTNND1	8.1	17.2	4.37E-04	5.8	17.0
ENSG00000165283	STOML2	5.5	17.1	4.57E-04	2.7	9.5
ENSG00000112159	MDN1	-6.1	17.0	4.73E-04	-10.3	-3.9
ENSG00000164303	ENPP6	2.7	17.0	4.73E-04	1.7	4.9
ENSG00000101811	CSTF2	-3.3	22.8	4.78E-04	-5.5	-2.0
ENSG00000103018	CYB5B	4.0	22.8	4.78E-04	2.1	6.6
ENSG00000259063	DUX4L5	-3.3	22.7	4.95E-04	-5.4	-2.2
ENSG00000064012	CASP8	2.2	22.7	4.95E-04	1.4	11.3
ENSG00000260914	RP11-343C2.11	-4.2	16.8	5.23E-04	-8.3	-2.4
ENSG00000140157	NIPA2	-4.2	22.5	5.38E-04	-6.3	-1.8

ENSG00000116670	MAD2L2	2.8	22.5	5.38E-04	1.8	4.7
ENSG00000267261	CTD-2132N18.3	-3.6	16.6	5.67E-04	-8.9	-1.9
ENSG00000176890	TYMS	6.4	22.3	5.75E-04	4.4	13.0
ENSG00000116251	RPL22	6.6	22.3	5.75E-04	3.9	14.0
ENSG00000143543	JTB	-5.3	16.5	5.90E-04	-8.0	-3.1
ENSG00000115446	UNC50	-4.5	16.5	5.90E-04	-7.1	-2.6
ENSG00000166987	MBD6	1.9	16.5	5.90E-04	1.1	5.2
ENSG00000170385	SLC30A1	2.1	16.5	5.90E-04	1.1	3.9
ENSG00000179241	LDLRAD3	2.2	22.2	5.97E-04	1.3	3.8
ENSG00000115289	PCGF1	-5.1	16.4	6.07E-04	-8.2	-2.3
ENSG00000169340	PDILT	-4.2	16.4	6.07E-04	-6.5	-2.5
ENSG00000241128	OR14A2	9.3	16.4	6.07E-04	4.2	19.0
ENSG00000187555	USP7	-4.0	22.1	6.22E-04	-6.1	-2.8
ENSG00000127463	EMC1	-5.3	16.3	6.40E-04	-8.7	-3.3
ENSG00000099956	SMARCB1	2.8	22.0	6.43E-04	1.1	8.0
ENSG00000158864	NDUFS2	3.2	22.0	6.43E-04	2.2	5.9
ENSG00000132604	TERF2	5.1	22.0	6.43E-04	2.5	9.5
ENSG00000121022	COPS5	2.6	21.9	6.59E-04	1.5	4.4
ENSG00000167920	TMEM99	2.6	21.8	6.75E-04	1.5	4.8
ENSG00000121903	ZSCAN20	7.0	16.2	6.83E-04	4.8	14.0
ENSG00000113460	BRIX1	3.7	16.0	7.23E-04	1.6	6.7
ENSG00000198900	TOP1	2.4	21.6	7.25E-04	1.3	4.0
ENSG00000061794	MRPS35	3.0	21.6	7.25E-04	1.8	4.9
ENSG00000086475	SEPHS1	3.1	21.6	7.25E-04	2.1	5.3
ENSG00000131748	STARD3	1.9	15.9	7.43E-04	0.9	3.3
ENSG00000141985	SH3GL1	4.5	21.5	7.49E-04	2.6	7.2
ENSG00000093072	CECR1	-6.9	15.8	7.67E-04	-10.7	-2.6
ENSG00000101166	SLMO2	-4.5	15.8	7.67E-04	-7.5	-2.6
ENSG00000184140	OR4F6	-4.4	15.8	7.67E-04	-7.8	-2.6
ENSG00000268790	CTC-429P9.4	-7.6	15.7	7.88E-04	-15.0	-5.7
ENSG00000089234	BRAP	1.9	15.7	7.88E-04	0.9	3.5
ENSG00000073712	FERMT2	3.7	15.7	7.88E-04	1.8	6.8
ENSG00000183773	AIFM3	2.6	15.6	8.03E-04	1.1	4.6
ENSG00000184206	GOLGA6L4	3.5	15.6	8.03E-04	2.0	6.3
ENSG00000102967	DHODH	4.2	21.3	8.10E-04	2.5	8.5
ENSG00000162341	TPCN2	5.5	21.3	8.10E-04	1.0	10.0
ENSG00000214921	AC003102.1	-7.0	15.5	8.19E-04	-12.0	-2.8
ENSG00000144136	SLC20A1	2.5	15.5	8.19E-04	1.2	4.6
ENSG00000165895	ARHGAP42	2.7	15.5	8.19E-04	1.4	5.1
ENSG00000092931	MFSD11	2.9	15.5	8.19E-04	1.4	6.8
ENSG00000080802	CNOT4	3.1	15.5	8.19E-04	1.4	6.0

ENSG00000057608	GDI2	-6.7	15.4	8.28E-04	-9.9	-2.5
ENSG00000196236	XPNPEP3	2.7	15.4	8.28E-04	1.3	4.7
ENSG00000121314	TAS2R8	-6.9	15.3	8.42E-04	-12.3	-2.7
ENSG00000213132	AC022498.1	-3.6	15.2	8.61E-04	-6.0	-2.2
ENSG00000197775	DHRS4-AS1	6.3	15.2	8.61E-04	3.6	13.0
ENSG00000270617	URGCP-MRPS24	4.7	15.1	8.71E-04	2.1	9.6
ENSG00000111684	LPCAT3	2.8	14.9	9.03E-04	1.4	5.5
ENSG00000129559	NEDD8	3.5	14.9	9.03E-04	1.6	7.3
ENSG00000221938	OR2A14	-5.1	14.8	9.18E-04	-8.3	-2.3
ENSG00000065268	WDR18	3.4	14.8	9.18E-04	1.6	7.2
ENSG00000266953	RP11-618P17.4	3.7	14.8	9.18E-04	1.7	8.2
ENSG00000128891	C15ORF57	2.5	20.9	9.35E-04	1.4	4.1
ENSG00000138069	RAB1A	-5.7	14.7	9.37E-04	-8.5	-3.6
ENSG00000168538	TRAPPC11	-4.2	14.7	9.37E-04	-9.3	-2.3
ENSG00000171953	ATPAF2	3.2	14.7	9.37E-04	1.6	6.0
ENSG00000162959	MEMO1	-3.6	14.6	9.57E-04	-5.7	-1.9
ENSG00000123091	RNF11	2.2	14.6	9.57E-04	1.1	4.8
ENSG00000160209	PDXK	-3.5	20.8	9.78E-04	-5.6	-2.0
ENSG00000181495	AC026703.1	-4.6	14.5	9.83E-04	-8.0	-2.6
ENSG00000167699	GLOD4	-3.3	14.5	9.83E-04	-7.9	-1.6
ENSG00000171680	PLEKHG5	8.0	14.5	9.83E-04	2.5	17.0
ENSG00000253729	PRKDC	1.9	20.7	1.00E-03	1.1	3.3
ENSG00000145736	GTF2H2	3.3	20.7	1.00E-03	2.0	5.9
ENSG00000204574	ABCF1	-5.1	14.4	1.01E-03	-9.9	-3.0
ENSG00000127780	OR1E2	-5.0	14.4	1.01E-03	-8.1	-2.7
ENSG00000126581	BECN1	3.1	14.4	1.01E-03	1.1	5.9
ENSG00000211650	IGLV5-45	-4.5	14.3	1.04E-03	-8.3	-2.7
ENSG00000169813	HNRNPF	2.3	14.3	1.04E-03	1.2	4.3
ENSG00000183735	TBK1	-3.6	20.5	1.05E-03	-5.9	-2.2
ENSG00000152520	PAN3	1.7	20.5	1.05E-03	1.0	3.0
ENSG00000038274	MAT2B	-4.5	14.2	1.07E-03	-6.9	-1.8
ENSG00000211647	IGLV5-48	-4.4	14.2	1.07E-03	-7.6	-2.1
ENSG00000228537	AL353608.1	-4.4	14.2	1.07E-03	-7.1	-2.3
ENSG00000113558	SKP1	-5.1	20.4	1.08E-03	-8.5	-2.2
ENSG00000125656	CLPP	1.6	20.4	1.08E-03	0.9	2.8
ENSG00000134255	CEPT1	-6.4	14.1	1.10E-03	-9.7	-2.2
ENSG00000058272	PPP1R12A	-3.9	20.3	1.11E-03	-6.0	-2.1
ENSG00000099381	SETD1A	-2.3	20.3	1.11E-03	-3.7	-1.4
ENSG00000106261	ZKSCAN1	-4.2	14.0	1.13E-03	-7.1	-2.2
ENSG00000113396	SLC27A6	-4.2	14.0	1.13E-03	-6.4	-1.9
ENSG00000143207	RFWD2	2.8	14.0	1.13E-03	1.1	4.9

ENSG00000033800	PIAS1	3.8	14.0	1.13E-03	1.3	7.2
ENSG00000129933	MAU2	1.8	20.2	1.15E-03	1.1	3.5
ENSG00000212997	AC023632.1	-6.2	13.9	1.15E-03	-8.7	-2.4
ENSG00000159346	ADIPOR1	-4.0	13.9	1.15E-03	-7.4	-2.4
ENSG00000157911	PEX10	1.6	13.9	1.15E-03	0.8	3.1
ENSG00000174957	OR5J2	2.5	13.9	1.15E-03	1.0	4.5
ENSG00000111341	MGP	3.7	13.9	1.15E-03	1.6	6.5
ENSG00000141858	SAMD1	-3.0	13.8	1.18E-03	-6.0	-1.5
ENSG00000137094	DNAJB5	2.0	13.8	1.18E-03	0.9	3.5
ENSG00000048649	RSF1	-4.5	20.1	1.21E-03	-6.7	-2.1
ENSG00000136938	ANP32B	-3.2	20.1	1.21E-03	-4.7	-1.8
ENSG00000131149	GSE1	-3.0	20.1	1.21E-03	-4.8	-1.8
ENSG00000104827	CGB	2.9	20.1	1.21E-03	1.3	4.6
ENSG00000089685	BIRC5	4.5	20.1	1.21E-03	2.7	9.0
ENSG00000175334	BANF1	-4.5	13.7	1.22E-03	-9.5	-2.4
ENSG00000130311	DDA1	1.8	13.7	1.22E-03	0.8	3.2
ENSG00000035681	NSMAF	1.8	13.7	1.22E-03	0.8	3.3
ENSG00000128510	CPA4	2.0	13.7	1.22E-03	1.1	5.7
ENSG00000167118	URM1	2.6	13.7	1.22E-03	1.1	5.3
ENSG00000183579	ZNRF3	6.0	13.7	1.22E-03	2.2	11.4
ENSG00000102786	INTS6	-6.0	13.6	1.25E-03	-9.1	-3.6
ENSG00000101464	PIGU	2.6	13.6	1.25E-03	1.1	4.8
ENSG00000133983	COX16	3.7	13.6	1.25E-03	2.0	7.0
ENSG00000171940	ZNF217	1.7	20.0	1.26E-03	1.0	3.0
ENSG00000179918	SEPHS2	3.3	20.0	1.26E-03	1.5	5.4
ENSG00000149823	VPS51	-5.3	13.5	1.28E-03	-8.5	-2.9
ENSG00000268172	AL590452.1	-4.6	13.5	1.28E-03	-7.8	-2.8
ENSG00000105404	RABAC1	2.7	13.5	1.28E-03	1.1	4.9
ENSG00000169020	ATP5I	3.2	13.5	1.28E-03	1.4	6.2
ENSG00000156990	RPUSD3	3.5	13.5	1.28E-03	1.8	6.5
ENSG00000140876	NUDT7	3.7	13.5	1.28E-03	1.2	6.4
ENSG00000135587	SMPD2	-3.4	19.9	1.29E-03	-5.8	-2.4
ENSG00000086589	RBM22	4.6	19.9	1.29E-03	2.5	9.1
ENSG00000197965	MPZL1	5.3	19.9	1.29E-03	1.0	8.6
ENSG00000188277	C15ORF62	-5.3	13.4	1.32E-03	-8.7	-2.7
ENSG00000214978	RP11-477N12.3	-4.9	13.4	1.32E-03	-8.1	-2.8
ENSG00000174093	RP11-1407O15.2	-4.5	13.4	1.32E-03	-8.6	-2.6
ENSG00000248540	RP11-247C2.2	-3.0	13.4	1.32E-03	-6.9	-1.8
ENSG00000212710	CTAGE1	-4.1	19.8	1.34E-03	-6.7	-2.5
ENSG00000168297	PXK	2.0	19.8	1.34E-03	1.1	3.4
ENSG00000166508	MCM7	3.5	19.8	1.34E-03	2.1	6.3

ENSG00000181867	FTMT	-6.3	13.3	1.36E-03	-9.3	-2.4
ENSG00000144035	NAT8	-3.8	13.3	1.36E-03	-7.5	-2.2
ENSG00000132388	UBE2G1	2.1	13.3	1.36E-03	0.9	3.8
ENSG00000117632	STMN1	6.0	19.7	1.40E-03	2.8	13.0
ENSG00000253251	CTC-534A2.2	-5.1	13.2	1.40E-03	-7.8	-1.8
ENSG00000037637	FBXO42	4.0	13.2	1.40E-03	1.9	7.1
ENSG00000132432	SEC61G	4.8	13.2	1.40E-03	1.6	8.6
ENSG00000212952	BX088651.1	-6.5	13.1	1.44E-03	-10.7	-3.1
ENSG00000015568	RGPD5	-5.9	13.1	1.44E-03	-9.8	-3.2
ENSG00000101290	CDS2	-5.0	13.1	1.44E-03	-8.4	-2.4
ENSG00000151151	IPMK	2.8	19.5	1.48E-03	1.6	5.2
ENSG00000164180	TMEM161B	2.8	19.5	1.48E-03	1.5	5.0
ENSG00000176904	OR51H1P	-7.0	13.0	1.49E-03	-11.3	-1.8
ENSG00000197454	OR2L5	-5.0	13.0	1.49E-03	-9.1	-2.9
ENSG00000168993	CPLX1	2.4	13.0	1.49E-03	1.0	7.0
ENSG00000129354	AP1M2	2.5	13.0	1.49E-03	1.2	5.0
ENSG00000175556	LONRF3	3.0	13.0	1.49E-03	1.1	5.9
ENSG00000088247	KHSRP	3.6	13.0	1.49E-03	1.8	7.2
ENSG00000100567	PSMA3	3.4	19.4	1.52E-03	2.0	6.5
ENSG00000211649	IGLV7-46	-4.3	12.9	1.53E-03	-8.0	-2.7
ENSG00000188612	SUMO2	2.7	12.9	1.53E-03	1.1	5.4
ENSG00000145907	G3BP1	3.0	12.9	1.53E-03	1.1	6.5
ENSG00000154803	FLCN	-3.7	19.3	1.57E-03	-5.9	-2.4
ENSG00000169249	ZRSR2	3.4	19.3	1.57E-03	1.2	5.0
ENSG00000103855	CD276	5.6	19.3	1.57E-03	0.7	9.9
ENSG00000266958	AC006126.3	-6.1	12.8	1.57E-03	-11.3	-2.5
ENSG00000163625	WDFY3	4.4	12.8	1.57E-03	1.5	8.2

Appendix B: gProfiler output of FDR 1% targets with p-value ≤ 0.01 determining significance

Source: database for comparison. Term Name: description of group. Term ID: numerical identification of term name within source database. Elements in Term: number of genes within term ID. Intersections: specific screen hits (Ensembl ID form) found within term.

Full query link: https://biit.cs.ut.ee/gplink/l/PibZnQu0Rd

Source	Term Name	Term ID	Adjusted p-value	Elements in Term	Intersections
GO:BP	cellular metabolic process	GO:0044237	3.57E-06	10941	ENSG00000196715 ENSG00000148154 ENSG00000142657 ENSG00000100811 ENSG00000100888 ENSG00000119414 ENSG00000166200 ENSG00000159399 ENSG00000105619 ENSG00000170322 ENSG00000152223 ENSG00000103769 ENSG00000123505 ENSG00000091483 ENSG00000090447 ENSG00000162769 ENSG00000142186 ENSG00000196072 ENSG00000063176 ENSG00000140543 ENSG00000147140 ENSG00000141452 ENSG00000188786 ENSG00000133895 ENSG00000105220 ENSG00000127616 ENSG00000131374 ENSG00000157837 ENSG00000141367 ENSG00000125107 ENSG00000159921 ENSG00000154832 ENSG00000171960 ENSG00000173011 ENSG00000089902 ENSG00000151461 ENSG00000158435 ENSG00000112576 ENSG00000090316 ENSG00000065526 ENSG00000183770 ENSG00000120690 ENSG00000038210 ENSG00000205423 ENSG00000047315 ENSG00000109854 ENSG00000136381 ENSG00000198431 ENSG00000086232 ENSG00000176170 ENSG00000178982 ENSG00000143761 ENSG00000005889 ENSG00000143418 ENSG00000116750 ENSG00000143368 ENSG00000072274 ENSG00000167792 ENSG00000119383 ENSG00000198612 ENSG00000135801 ENSG00000111726 ENSG00000003756 ENSG00000066322 ENSG00000067182 ENSG00000174903 ENSG00000198964 ENSG00000032389 ENSG00000175582 ENSG00000070610 ENSG00000179950 ENSG00000136875 ENSG00000110497 ENSG00000125356 ENSG00000196655 ENSG00000196961 ENSG00000124217 ENSG00000242371 ENSG00000174547 ENSG00000104388 ENSG00000170832 ENSG00000086598 ENSG00000135966
GO:BP	Golgi vesicle transport	GO:0048193	6.42E-06	415	ENSG00000119414 ENSG00000142186 ENSG00000141367 ENSG00000072958 ENSG00000143761 ENSG00000106367 ENSG00000166747 ENSG00000174903 ENSG00000175582 ENSG00000196655 ENSG00000196961 ENSG00000222014 ENSG00000104388 ENSG00000108587 ENSG00000086598
GO:BP	vesicle organization	GO:0016050	4.32E-05	342	ENSG00000119414 ENSG00000103769 ENSG00000196072 ENSG00000072958 ENSG00000038210 ENSG00000176170 ENSG00000143761 ENSG00000166747 ENSG00000174903 ENSG00000196655 ENSG00000108587 ENSG00000086598 ENSG00000135966
GO:BP	ceramide metabolic process	GO:0006672	1.23E-04	104	ENSG00000148154 ENSG00000063176 ENSG00000176170 ENSG00000143418 ENSG00000066322 ENSG00000067182 ENSG00000198964 ENSG00000070610
GO:BP	ceramide biosynthetic process	GO:0046513	1.37E-04	70	ENSG00000148154 ENSG00000063176 ENSG00000176170 ENSG00000143418 ENSG00000066322 ENSG00000067182 ENSG00000198964
GO:BP	metabolic process	GO:0008152	2.25E-04	11915	ENSG00000196715 ENSG00000148154 ENSG00000142657 ENSG00000100811 ENSG00000100888 ENSG00000119414 ENSG00000166200 ENSG00000159399 ENSG00000105619 ENSG00000170322 ENSG00000152223 ENSG00000103769 ENSG00000123505 ENSG00000091483 ENSG00000090447 ENSG00000162769 ENSG00000142186 ENSG00000196072 ENSG00000063176 ENSG00000140543 ENSG00000147140 ENSG00000141452 ENSG00000188786 ENSG00000133895 ENSG00000105220 ENSG00000127616 ENSG00000131374 ENSG00000157837 ENSG00000141367 ENSG00000125107 ENSG00000159921 ENSG00000154832 ENSG00000171960 ENSG00000173011 ENSG00000089902 ENSG00000151461

					ENSG00000158435 ENSG00000112576 ENSG00000090316 ENSG00000065526 ENSG00000183770 ENSG00000120690 ENSG00000038210 ENSG00000205423 ENSG00000117308 ENSG00000047315 ENSG00000109854 ENSG00000136381 ENSG00000198431 ENSG00000086232 ENSG00000176170 ENSG00000178982 ENSG00000143761 ENSG00000005889 ENSG00000143418 ENSG00000116750 ENSG00000143368 ENSG00000072274 ENSG00000167792 ENSG00000119383 ENSG00000198612 ENSG00000135801 ENSG00000111726 ENSG00000003756 ENSG00000066322 ENSG00000067182 ENSG00000174903 ENSG00000198964 ENSG00000032389 ENSG00000175582 ENSG00000070610 ENSG00000179950 ENSG00000136875 ENSG00000110497 ENSG00000125356 ENSG00000196655 ENSG00000196961 ENSG00000124217 ENSG00000242371 ENSG00000174547 ENSG00000104388 ENSG00000170832 ENSG00000086598 ENSG00000135966
GO:BP	vesicle-mediated transport	GO:0016192	6.03E-04	2193	ENSG00000112697 ENSG00000119414 ENSG00000162980 ENSG00000152223 ENSG00000103769 ENSG00000142186 ENSG00000196072 ENSG00000063176 ENSG00000105220 ENSG00000131374 ENSG00000141367 ENSG00000072958 ENSG00000086232 ENSG00000176170 ENSG00000143761 ENSG00000106367 ENSG00000072274 ENSG00000166747 ENSG00000174903 ENSG00000032389 ENSG00000175582 ENSG00000196655 ENSG00000196961 ENSG00000222014 ENSG00000242371 ENSG00000148358 ENSG00000104388 ENSG00000108587 ENSG00000086598 ENSG00000135966
GO:BP	regulation of defense response to virus by virus	GO:0050690	6.72E-04	29	ENSG00000072958 ENSG00000143761 ENSG00000106367 ENSG00000166747 ENSG00000196961
GO:BP	cellular nitrogen compound metabolic process	GO:0034641	8.52E-04	6576	ENSG00000148154 ENSG00000100811 ENSG00000100888 ENSG00000119414 ENSG00000166200 ENSG00000159399 ENSG00000105619 ENSG00000170322 ENSG00000123505 ENSG00000091483 ENSG00000090447 ENSG00000162769 ENSG00000196072 ENSG00000063176 ENSG00000147140 ENSG00000188786 ENSG00000133895 ENSG00000105220 ENSG00000127616 ENSG00000157837 ENSG00000125107 ENSG00000159921 ENSG00000154832 ENSG00000171960 ENSG00000173011 ENSG00000089902 ENSG00000151461 ENSG00000158435 ENSG00000112576 ENSG00000065526 ENSG00000183770 ENSG00000120690 ENSG00000047315 ENSG00000109854 ENSG00000136381 ENSG00000198431 ENSG00000086232 ENSG00000176170 ENSG00000178982 ENSG00000005889 ENSG00000143418 ENSG00000116750 ENSG00000143368 ENSG00000072274 ENSG00000198612 ENSG00000135801 ENSG00000111726 ENSG00000003756 ENSG00000066322 ENSG00000067182 ENSG00000198964 ENSG00000070610 ENSG00000179950 ENSG00000136875 ENSG00000124217 ENSG00000174547 ENSG00000086598 ENSG00000135966
GO:BP	sphingolipid biosynthetic process	GO:0030148	3.47E-03	112	ENSG00000148154 ENSG00000063176 ENSG00000176170 ENSG00000143418 ENSG00000066322 ENSG00000067182 ENSG00000198964
GO:BP	cytosolic transport	GO:0016482	5.05E-03	169	ENSG00000131374 ENSG00000141367 ENSG00000166747 ENSG00000032389 ENSG00000175582 ENSG00000196961 ENSG00000222014 ENSG00000108587
GO:BP	sphingolipid metabolic process	GO:0006665	5.28E-03	170	ENSG00000148154 ENSG00000063176 ENSG00000176170 ENSG00000143418 ENSG00000066322 ENSG00000067182 ENSG00000198964 ENSG00000070610
GO:BP	primary metabolic process	GO:0044238	7.61E-03	10642	ENSG00000196715 ENSG00000148154 ENSG00000142657 ENSG00000100811 ENSG00000100888 ENSG00000119414 ENSG00000166200 ENSG00000159399 ENSG00000105619 ENSG00000170322 ENSG00000103769 ENSG00000123505 ENSG00000091483 ENSG00000090447 ENSG00000142186 ENSG00000196072 ENSG00000063176 ENSG00000140543 ENSG00000147140 ENSG00000188786 ENSG00000133895

					ENSG00000105220 ENSG00000127616 ENSG00000157837 ENSG00000141367 ENSG00000125107 ENSG00000159921 ENSG00000154832 ENSG00000171960 ENSG00000173011 ENSG00000089902 ENSG00000151461 ENSG00000158435 ENSG00000112576 ENSG00000090316 ENSG00000065526 ENSG00000183770 ENSG00000120690 ENSG00000038210 ENSG00000205423 ENSG00000117308 ENSG00000047315 ENSG00000109854 ENSG00000136381 ENSG00000198431 ENSG00000086232 ENSG00000176170 ENSG00000178982 ENSG00000143761 ENSG00000005889 ENSG00000143418 ENSG00000116750 ENSG00000143368 ENSG00000072274 ENSG00000119383 ENSG00000198612 ENSG00000135801 ENSG00000003756 ENSG00000066322 ENSG00000067182 ENSG00000174903 ENSG00000198964 ENSG00000032389 ENSG00000175582 ENSG00000070610 ENSG00000179950 ENSG00000136875 ENSG00000110497 ENSG00000196961 ENSG00000124217 ENSG00000242371 ENSG00000174547 ENSG00000104388 ENSG00000170832 ENSG00000086598 ENSG00000135966
GO:BP	endosomal transport	GO:0016197	9.14E-03	244	ENSG00000152223 ENSG00000103769 ENSG00000196072 ENSG00000131374 ENSG00000141367 ENSG00000032389 ENSG00000175582 ENSG00000222014 ENSG00000108587
GO:BP	intracellular transport	GO:0046907	9.69E-03	1723	ENSG00000112697 ENSG00000119414 ENSG00000162980 ENSG00000152223 ENSG00000103769 ENSG00000196072 ENSG00000131374 ENSG00000141367 ENSG00000072958 ENSG00000151461 ENSG00000109854 ENSG00000143761 ENSG00000106367 ENSG00000166747 ENSG00000174903 ENSG00000032389 ENSG00000175582 ENSG00000196655 ENSG00000196961 ENSG00000222014 ENSG00000104388 ENSG00000108587 ENSG00000086598 ENSG00000135966
GO:CC	intracellular membrane-bounded organelle	GO:0043231	4.55E-08	12046	ENSG00000112697 ENSG00000196715 ENSG00000148154 ENSG00000142657 ENSG00000100811 ENSG00000100888 ENSG00000119414 ENSG00000166200 ENSG00000162980 ENSG00000159399 ENSG00000105619 ENSG00000170322 ENSG00000152223 ENSG00000103769 ENSG00000091483 ENSG00000090447 ENSG00000162769 ENSG00000142186 ENSG00000196072 ENSG00000063176 ENSG00000140543 ENSG00000147140 ENSG00000141452 ENSG00000188786 ENSG00000133895 ENSG00000105220 ENSG00000127616 ENSG00000131374 ENSG00000157837 ENSG00000141367 ENSG00000125107 ENSG00000072958 ENSG00000033867 ENSG00000154832 ENSG00000171960 ENSG00000173011 ENSG00000089902 ENSG00000151461 ENSG00000158435 ENSG00000112576 ENSG00000090316 ENSG00000065526 ENSG00000183770 ENSG00000120690 ENSG00000038210 ENSG00000205423 ENSG00000047315 ENSG00000109854 ENSG00000136381 ENSG00000198431 ENSG00000176170 ENSG00000101457 ENSG00000178982 ENSG00000143761 ENSG00000162923 ENSG00000005889 ENSG00000143418 ENSG00000116750 ENSG00000106367 ENSG00000143368 ENSG00000072274 ENSG00000167792 ENSG00000119383 ENSG00000198612 ENSG00000135801 ENSG00000111726 ENSG00000003756 ENSG00000066322 ENSG00000166747 ENSG00000067182 ENSG00000174903 ENSG00000198964 ENSG00000032389 ENSG00000175582 ENSG00000070610 ENSG00000179950 ENSG00000136875 ENSG00000110497 ENSG00000125356 ENSG00000196655 ENSG00000196961 ENSG00000222014 ENSG00000174547 ENSG00000148358 ENSG00000104388 ENSG00000170832 ENSG00000108587 ENSG00000086598 ENSG00000135966
GO:CC	intracellular anatomical structure	GO:0005622	3.24E-07	14808	ENSG00000112697 ENSG00000196715 ENSG00000148154 ENSG00000142657 ENSG00000100811 ENSG00000100888 ENSG00000119414 ENSG00000166200 ENSG00000162980 ENSG00000159399 ENSG00000105619 ENSG00000170322 ENSG00000152223 ENSG00000103769 ENSG00000123505 ENSG00000091483 ENSG00000090447 ENSG00000162769

					ENSG00000142186 ENSG00000196072 ENSG00000063176 ENSG00000140543 ENSG00000147140 ENSG00000141452 ENSG00000188786 ENSG00000133895 ENSG00000105220 ENSG00000127616 ENSG00000131374 ENSG00000157837 ENSG00000141367 ENSG00000144426 ENSG00000125107 ENSG00000072958 ENSG00000159921 ENSG00000033867 ENSG00000154832 ENSG00000171960 ENSG00000173011 ENSG00000089902 ENSG00000151461 ENSG00000178605 ENSG00000158435 ENSG00000112576 ENSG00000090316 ENSG00000065526 ENSG00000183770 ENSG00000120690 ENSG00000038210 ENSG00000205423 ENSG00000117308 ENSG00000047315 ENSG00000109854 ENSG00000136381 ENSG00000198431 ENSG00000086232 ENSG00000176170 ENSG00000101457 ENSG00000178982 ENSG00000143761 ENSG00000162923 ENSG00000005889 ENSG00000143418 ENSG00000116750 ENSG00000106367 ENSG00000143368 ENSG00000072274 ENSG00000167792 ENSG00000119383 ENSG00000198612 ENSG00000135801 ENSG00000111726 ENSG00000003756 ENSG00000066322 ENSG00000166747 ENSG00000067182 ENSG00000174903 ENSG00000198964 ENSG00000032389 ENSG00000175582 ENSG00000070610 ENSG00000179950 ENSG00000136875 ENSG00000110497 ENSG00000125356 ENSG00000196655 ENSG00000196961 ENSG00000222014 ENSG00000124217 ENSG00000174547 ENSG00000148358 ENSG00000104388 ENSG00000170832 ENSG00000108587 ENSG00000086598 ENSG00000135966
GO:CC	protein-containing complex	GO:0032991	1.40E-06	5541	ENSG00000112697 ENSG00000100811 ENSG00000100888 ENSG00000166200 ENSG00000105619 ENSG00000170322 ENSG00000103769 ENSG00000091483 ENSG00000090447 ENSG00000142186 ENSG00000196072 ENSG00000063176 ENSG00000140543 ENSG00000147140 ENSG00000141452 ENSG00000133895 ENSG00000127616 ENSG00000131374 ENSG00000141367 ENSG00000125107 ENSG00000072958 ENSG00000154832 ENSG00000171960 ENSG00000173011 ENSG00000089902 ENSG00000151461 ENSG00000158435 ENSG00000112576 ENSG00000090316 ENSG00000065526 ENSG00000205423 ENSG00000047315 ENSG00000101457 ENSG00000178982 ENSG00000143761 ENSG00000162923 ENSG00000116750 ENSG00000106367 ENSG00000143368 ENSG00000072274 ENSG00000167792 ENSG00000119383 ENSG00000198612 ENSG00000135801 ENSG00000003756 ENSG00000166747 ENSG00000067182 ENSG00000032389 ENSG00000136875 ENSG00000125356 ENSG00000196655 ENSG00000196961 ENSG00000242371 ENSG00000174547 ENSG00000108587 ENSG00000135966
GO:CC	Golgi-associated vesicle membrane	GO:0030660	2.63E-06	52	ENSG00000142186 ENSG00000157837 ENSG00000141367 ENSG00000106367 ENSG00000166747 ENSG00000196961 ENSG00000086598
GO:CC	Golgi apparatus	GO:0005794	5.30E-06	1593	ENSG00000112697 ENSG00000148154 ENSG00000162980 ENSG00000103769 ENSG00000142186 ENSG00000131374 ENSG00000157837 ENSG00000141367 ENSG00000072958 ENSG00000038210 ENSG00000143761 ENSG00000106367 ENSG00000166747 ENSG00000067182 ENSG00000174903 ENSG00000198964 ENSG00000032389 ENSG00000175582 ENSG00000070610 ENSG00000196655 ENSG00000196961 ENSG00000222014 ENSG00000148358 ENSG00000104388 ENSG00000170832 ENSG00000108587 ENSG00000086598
GO:CC	membrane-bounded organelle	GO:0043227	7.79E-06	13201	ENSG00000112697 ENSG00000196715 ENSG00000148154 ENSG00000142657 ENSG00000100811 ENSG00000100888 ENSG00000119414 ENSG00000166200 ENSG00000162980 ENSG00000159399 ENSG00000105619 ENSG00000170322 ENSG00000152223 ENSG00000103769 ENSG00000091483 ENSG00000090447 ENSG00000162769 ENSG00000142186 ENSG00000196072 ENSG00000063176 ENSG00000140543 ENSG00000147140 ENSG00000141452 ENSG00000188786 ENSG00000133895 ENSG00000105220 ENSG00000127616

					ENSG00000131374 ENSG00000157837 ENSG00000141367 ENSG00000125107 ENSG00000072958 ENSG00000033867 ENSG00000154832 ENSG00000171960 ENSG00000173011 ENSG00000089902 ENSG00000151461 ENSG00000158435 ENSG00000112576 ENSG00000090316 ENSG00000065526 ENSG00000183770 ENSG00000120690 ENSG00000038210 ENSG00000205423 ENSG00000047315 ENSG00000109854 ENSG00000136381 ENSG00000198431 ENSG00000176170 ENSG00000101457 ENSG00000178982 ENSG00000143761 ENSG00000162923 ENSG00000005889 ENSG00000143418 ENSG00000116750 ENSG00000106367 ENSG00000143368 ENSG00000072274 ENSG00000167792 ENSG00000119383 ENSG00000198612 ENSG00000135801 ENSG00000111726 ENSG00000003756 ENSG00000066322 ENSG00000166747 ENSG00000067182 ENSG00000174903 ENSG00000198964 ENSG00000032389 ENSG00000175582 ENSG00000070610 ENSG00000179950 ENSG00000136875 ENSG00000110497 ENSG00000125356 ENSG00000196655 ENSG00000196961 ENSG00000222014 ENSG00000242371 ENSG00000174547 ENSG00000148358 ENSG00000104388 ENSG00000170832 ENSG00000108587 ENSG00000086598 ENSG00000135966
GO:CC	Golgi-associated vesicle	GO:0005798	9.51E-06	95	ENSG00000142186 ENSG00000157837 ENSG00000141367 ENSG00000143761 ENSG00000106367 ENSG00000166747 ENSG00000196961 ENSG00000086598
GO:CC	Golgi apparatus subcompartment	GO:0098791	1.47E-05	845	ENSG00000148154 ENSG00000162980 ENSG00000103769 ENSG00000141367 ENSG00000072958 ENSG00000038210 ENSG00000143761 ENSG00000106367 ENSG00000166747 ENSG00000067182 ENSG00000174903 ENSG00000198964 ENSG00000032389 ENSG00000175582 ENSG00000070610 ENSG00000196655 ENSG00000104388 ENSG00000108587 ENSG00000086598
GO:CC	intracellular organelle	GO:0043229	2.51E-05	13117	ENSG00000112697 ENSG00000196715 ENSG00000148154 ENSG00000142657 ENSG00000100811 ENSG00000100888 ENSG00000119414 ENSG00000166200 ENSG00000162980 ENSG00000159399 ENSG00000105619 ENSG00000170322 ENSG00000152223 ENSG00000103769 ENSG00000091483 ENSG00000090447 ENSG00000162769 ENSG00000142186 ENSG00000196072 ENSG00000063176 ENSG00000140543 ENSG00000147140 ENSG00000141452 ENSG00000188786 ENSG00000133895 ENSG00000105220 ENSG00000127616 ENSG00000131374 ENSG00000157837 ENSG00000141367 ENSG00000125107 ENSG00000072958 ENSG00000033867 ENSG00000154832 ENSG00000171960 ENSG00000173011 ENSG00000089902 ENSG00000151461 ENSG00000158435 ENSG00000112576 ENSG00000090316 ENSG00000065526 ENSG00000183770 ENSG00000120690 ENSG00000038210 ENSG00000205423 ENSG00000047315 ENSG00000109854 ENSG00000136381 ENSG00000198431 ENSG00000176170 ENSG00000101457 ENSG00000178982 ENSG00000143761 ENSG00000162923 ENSG00000005889 ENSG00000143418 ENSG00000116750 ENSG00000106367 ENSG00000143368 ENSG00000072274 ENSG00000167792 ENSG00000119383 ENSG00000198612 ENSG00000135801 ENSG00000111726 ENSG00000003756 ENSG00000066322 ENSG00000166747 ENSG00000067182 ENSG00000174903 ENSG00000198964 ENSG00000032389 ENSG00000175582 ENSG00000070610 ENSG00000179950 ENSG00000136875 ENSG00000110497 ENSG00000125356 ENSG00000196655 ENSG00000196961 ENSG00000222014 ENSG00000174547 ENSG00000148358 ENSG00000104388 ENSG00000170832 ENSG00000108587 ENSG00000086598 ENSG00000135966
GO:CC	clathrin adaptor complex	GO:0030131	4.01E-05	24	ENSG00000131374 ENSG00000072958 ENSG00000106367 ENSG00000166747 ENSG00000196961
GO:CC	clathrin coat	GO:0030118	4.48E-05	47	ENSG00000131374 ENSG00000141367 ENSG00000072958 ENSG00000106367 ENSG00000166747 ENSG00000196961

GO:CC	bounding membrane of organelle	GO:0098588	6.37E-05	2165	ENSG00000112697 ENSG00000148154 ENSG00000159399 ENSG00000103769 ENSG00000142186 ENSG00000196072 ENSG00000063176 ENSG00000141452 ENSG00000105220 ENSG00000131374 ENSG00000157837 ENSG00000141367 ENSG00000125107 ENSG00000072958 ENSG00000176170 ENSG00000143761 ENSG00000106367 ENSG00000072274 ENSG00000166747 ENSG00000067182 ENSG00000174903 ENSG00000198964 ENSG00000175582 ENSG00000070610 ENSG00000110497 ENSG00000196655 ENSG00000196961 ENSG00000104388 ENSG00000108587 ENSG00000086598
GO:CC	clathrin vesicle coat	GO:0030125	9.11E-05	28	ENSG00000131374 ENSG00000141367 ENSG00000106367 ENSG00000166747 ENSG00000196961
GO:CC	coated vesicle membrane	GO:0030662	9.99E-05	177	ENSG00000142186 ENSG00000131374 ENSG00000141367 ENSG00000072958 ENSG00000106367 ENSG00000072274 ENSG00000166747 ENSG00000196961 ENSG00000086598
GO:CC	coated vesicle	GO:0030135	1.09E-04	296	ENSG00000142186 ENSG00000131374 ENSG00000141367 ENSG00000072958 ENSG00000143761 ENSG00000106367 ENSG00000072274 ENSG00000166747 ENSG00000196961 ENSG00000148358 ENSG00000086598
GO:CC	vesicle coat	GO:0030120	1.17E-04	55	ENSG00000142186 ENSG00000131374 ENSG00000141367 ENSG00000106367 ENSG00000166747 ENSG00000196961
GO:CC	clathrin coat of trans-Golgi network vesicle	GO:0030130	1.43E-04	13	ENSG00000141367 ENSG00000106367 ENSG00000166747 ENSG00000196961
GO:CC	membrane coat	GO:0030117	2.09E-04	97	ENSG00000142186 ENSG00000131374 ENSG00000141367 ENSG00000072958 ENSG00000106367 ENSG00000166747 ENSG00000196961
GO:CC	coated membrane	GO:0048475	2.09E-04	97	ENSG00000142186 ENSG00000131374 ENSG00000141367 ENSG00000072958 ENSG00000106367 ENSG00000166747 ENSG00000196961
GO:CC	trans-Golgi network	GO:0005802	2.36E-04	255	ENSG00000162980 ENSG00000103769 ENSG00000141367 ENSG00000072958 ENSG00000038210 ENSG00000143761 ENSG00000106367 ENSG00000166747 ENSG00000032389 ENSG00000175582
GO:CC	trans-Golgi network transport vesicle membrane	GO:0012510	2.71E-04	15	ENSG00000141367 ENSG00000106367 ENSG00000166747 ENSG00000196961
GO:CC	nuclear protein-containing complex	GO:0140513	2.87E-04	1236	ENSG00000100811 ENSG00000100888 ENSG00000166200 ENSG00000105619 ENSG00000170322 ENSG00000147140 ENSG00000133895 ENSG00000127616 ENSG00000154832 ENSG00000171960 ENSG00000173011 ENSG00000089902 ENSG00000151461 ENSG00000047315 ENSG00000101457 ENSG00000116750 ENSG00000143368 ENSG00000198612 ENSG00000135801 ENSG00000003756 ENSG00000136875
GO:CC	Ino80 complex	GO:0031011	3.60E-04	16	ENSG00000100811 ENSG00000105619 ENSG00000170322 ENSG00000116750
GO:CC	DNA helicase complex	GO:0033202	3.60E-04	16	ENSG00000100811 ENSG00000105619 ENSG00000170322 ENSG00000116750
GO:CC	clathrin-coated pit	GO:0005905	5.88E-04	72	ENSG00000131374 ENSG00000141367 ENSG00000176170 ENSG00000106367 ENSG00000072274 ENSG00000196961
GO:CC	clathrin-coated vesicle membrane	GO:0030665	6.25E-04	114	ENSG00000131374 ENSG00000141367 ENSG00000072958 ENSG00000106367 ENSG00000072274 ENSG00000166747 ENSG00000196961
GO:CC	AP-type membrane coat adaptor complex	GO:0030119	6.59E-04	41	ENSG00000131374 ENSG00000072958 ENSG00000106367 ENSG00000166747 ENSG00000196961
GO:CC	organelle	GO:0043226	6.64E-04	14027	ENSG00000112697 ENSG00000196715 ENSG00000148154 ENSG00000142657 ENSG00000100811 ENSG00000100888 ENSG00000119414 ENSG00000166200 ENSG00000162980 ENSG00000159399 ENSG00000105619 ENSG00000170322 ENSG00000152223 ENSG00000103769 ENSG00000091483 ENSG00000090447 ENSG00000162769 ENSG00000142186 ENSG00000196072 ENSG00000063176 ENSG00000140543 ENSG00000147140 ENSG00000141452 ENSG00000188786 ENSG00000133895 ENSG00000105220 ENSG00000127616 ENSG00000131374 ENSG00000157837 ENSG00000141367 ENSG00000125107 ENSG00000072958 ENSG00000033867

					ENSG00000154832 ENSG00000171960 ENSG00000173011 ENSG00000089902 ENSG00000151461 ENSG00000158435 ENSG00000112576 ENSG00000090316 ENSG00000065526 ENSG00000183770 ENSG00000120690 ENSG00000038210 ENSG00000205423 ENSG00000047315 ENSG00000109854 ENSG00000136381 ENSG00000198431 ENSG00000176170 ENSG00000101457 ENSG00000178982 ENSG00000143761 ENSG00000162923 ENSG00000005889 ENSG00000143418 ENSG00000116750 ENSG00000106367 ENSG00000143368 ENSG00000072274 ENSG00000167792 ENSG00000119383 ENSG00000198612 ENSG00000135801 ENSG00000111726 ENSG00000003756 ENSG00000066322 ENSG00000166747 ENSG00000067182 ENSG00000174903 ENSG00000198964 ENSG00000032389 ENSG00000175582 ENSG00000070610 ENSG00000179950 ENSG00000136875 ENSG00000110497 ENSG00000125356 ENSG00000196655 ENSG00000196961 ENSG00000222014 ENSG00000242371 ENSG00000174547 ENSG00000148358 ENSG00000104388 ENSG00000170832 ENSG00000108587 ENSG00000086598 ENSG00000135966
GO:CC	organelle membrane	GO:0031090	1.27E-03	3644	ENSG00000112697 ENSG00000196715 ENSG00000148154 ENSG00000159399 ENSG00000103769 ENSG00000162769 ENSG00000142186 ENSG00000196072 ENSG00000063176 ENSG00000141452 ENSG00000105220 ENSG00000131374 ENSG00000157837 ENSG00000141367 ENSG00000125107 ENSG00000072958 ENSG00000205423 ENSG00000176170 ENSG00000143761 ENSG00000143418 ENSG00000106367 ENSG00000072274 ENSG00000167792 ENSG00000066322 ENSG00000166747 ENSG00000067182 ENSG00000174903 ENSG00000198964 ENSG00000175582 ENSG00000070610 ENSG00000110497 ENSG00000125356 ENSG00000196655 ENSG00000196961 ENSG00000174547 ENSG00000104388 ENSG00000108587 ENSG00000086598
GO:CC	Golgi membrane	GO:0000139	1.28E-03	725	ENSG00000148154 ENSG00000141367 ENSG00000072958 ENSG00000143761 ENSG00000106367 ENSG00000166747 ENSG00000067182 ENSG00000174903 ENSG00000198964 ENSG00000175582 ENSG00000070610 ENSG00000196655 ENSG00000104388 ENSG00000108587 ENSG00000086598
GO:CC	catalytic complex	GO:1902494	1.60E-03	1377	ENSG00000100811 ENSG00000100888 ENSG00000105619 ENSG00000170322 ENSG00000140543 ENSG00000133895 ENSG00000131374 ENSG00000154832 ENSG00000173011 ENSG00000089902 ENSG00000112576 ENSG00000090316 ENSG00000205423 ENSG00000047315 ENSG00000101457 ENSG00000162923 ENSG00000116750 ENSG00000167792 ENSG00000119383 ENSG00000135801 ENSG00000125356
GO:CC	clathrin-coated vesicle	GO:0030136	2.22E-03	194	ENSG00000131374 ENSG00000141367 ENSG00000072958 ENSG00000106367 ENSG00000072274 ENSG00000166747 ENSG00000196961 ENSG00000148358
GO:CC	transport vesicle	GO:0030133	2.93E-03	416	ENSG00000112697 ENSG00000103769 ENSG00000141367 ENSG00000106367 ENSG00000166747 ENSG00000174903 ENSG00000175582 ENSG00000196655 ENSG00000196961 ENSG00000108587 ENSG00000086598
GO:CC	INO80-type complex	GO:0097346	3.33E-03	27	ENSG00000100811 ENSG00000105619 ENSG00000170322 ENSG00000116750
GO:CC	cytosol	GO:0005829	6.22E-03	5361	ENSG00000142657 ENSG00000119414 ENSG00000166200 ENSG00000159399 ENSG00000103769 ENSG00000123505 ENSG00000091483 ENSG00000142186 ENSG00000196072 ENSG00000063176 ENSG00000133895 ENSG00000105220 ENSG00000131374 ENSG00000141367 ENSG00000144426 ENSG00000125107 ENSG00000072958 ENSG00000159921 ENSG00000154832 ENSG00000151461 ENSG00000158435 ENSG00000038210 ENSG00000205423 ENSG00000117308 ENSG00000109854 ENSG00000136381 ENSG00000198431 ENSG00000176170 ENSG00000178982 ENSG00000143761 ENSG00000162923 ENSG00000116750 ENSG00000106367 ENSG00000167792 ENSG00000198612 ENSG00000166747

					ENSG00000174903 ENSG00000175582 ENSG00000070610 ENSG00000110497 ENSG00000196655 ENSG00000196961 ENSG00000222014 ENSG00000124217 ENSG00000104388 ENSG00000170832 ENSG00000108587
GO:CC	organelle subcompartment	GO:0031984	6.82E-03	1764	ENSG00000196715 ENSG00000148154 ENSG00000162980 ENSG00000103769 ENSG00000157837 ENSG00000141367 ENSG00000072958 ENSG00000038210 ENSG00000143761 ENSG00000143418 ENSG00000106367 ENSG00000066322 ENSG00000166747 ENSG00000067182 ENSG00000174903 ENSG00000198964 ENSG00000032389 ENSG00000175582 ENSG00000070610 ENSG00000196655 ENSG00000104388 ENSG00000108587 ENSG00000086598
GO:CC	trans-Golgi network transport vesicle	GO:0030140	7.58E-03	33	ENSG00000141367 ENSG00000106367 ENSG00000166747 ENSG00000196961
GO:CC	ATPase complex	GO:1904949	8.87E-03	115	ENSG00000112697 ENSG00000100811 ENSG00000105619 ENSG00000170322 ENSG00000127616 ENSG00000116750
KEGG	Sphingolipid metabolism	KEGG:00600	5.15E-05	49	ENSG00000148154 ENSG00000063176 ENSG00000176170 ENSG00000143418 ENSG00000198964 ENSG00000070610
KEGG	Amino sugar and nucleotide sugar metabolism	KEGG:00520	1.07E-03	48	ENSG00000159399 ENSG00000105220 ENSG00000159921 ENSG00000117308 ENSG00000111726
REAC	Nef-mediates down modulation of cell surface receptors by recruiting them to clathrin adapters	REAC:R-HSA-164938	7.12E-05	20	ENSG00000072958 ENSG00000143761 ENSG00000106367 ENSG00000166747 ENSG00000196961
REAC	The role of Nef in HIV-1 replication and disease pathogenesis	REAC:R-HSA-164952	2.93E-04	26	ENSG00000072958 ENSG00000143761 ENSG00000106367 ENSG00000166747 ENSG00000196961
REAC	Lysosome Vesicle Biogenesis	REAC:R-HSA-432720	1.38E-03	35	ENSG00000141367 ENSG00000072958 ENSG00000143761 ENSG00000106367 ENSG00000166747
REAC	Membrane Trafficking	REAC:R-HSA-199991	1.44E-03	625	ENSG00000119414 ENSG00000166200 ENSG00000103769 ENSG00000141367 ENSG00000072958 ENSG00000143761 ENSG00000106367 ENSG00000072274 ENSG00000198612 ENSG00000166747 ENSG00000174903 ENSG00000175582 ENSG00000196655 ENSG00000196961 ENSG00000108587 ENSG00000086598
REAC	Vesicle-mediated transport	REAC:R-HSA-5653656	1.98E-03	719	ENSG00000119414 ENSG00000166200 ENSG00000103769 ENSG00000141367 ENSG00000072958 ENSG00000143761 ENSG00000106367 ENSG00000072274 ENSG00000198612 ENSG00000166747 ENSG00000174903 ENSG00000175582 ENSG00000196655 ENSG00000196961 ENSG00000242371 ENSG00000108587 ENSG00000086598
REAC	DNA Damage Recognition in GG-NER	REAC:R-HSA-5696394	2.09E-03	38	ENSG00000100811 ENSG00000166200 ENSG00000105619 ENSG00000170322 ENSG00000198612
REAC	trans-Golgi Network Vesicle Budding	REAC:R-HSA-199992	3.48E-03	72	ENSG00000141367 ENSG00000072958 ENSG00000143761 ENSG00000106367 ENSG00000072274 ENSG00000166747
REAC	Nef mediated downregulation of MHC class I complex cell surface expression	REAC:R-HSA-164940	9.48E-03	9	ENSG00000072958 ENSG00000106367 ENSG00000166747
WP	Sphingolipid pathway	WP:WP1422	4.48E-06	30	ENSG00000148154 ENSG00000063176 ENSG00000176170 ENSG00000143418 ENSG00000198964 ENSG00000070610
WP	Sphingolipid Metabolism (general overview)	WP:WP4725	5.41E-05	24	ENSG00000148154 ENSG00000063176 ENSG00000176170 ENSG00000143418 ENSG00000198964
WP	Sphingolipid Metabolism (integrated pathway)	WP:WP4726	6.73E-05	25	ENSG00000148154 ENSG00000063176 ENSG00000176170 ENSG00000143418 ENSG00000198964

Appendix C: Surface biotinylation mass-spectrometry protein abundances

Due to the large size of the dataset, only significant hits in the KO lines are shown. PBS is the background noise with sgSAFE and self-cut mCherry lines serving as control. KO3-TMEM30A and KO5-TMEM30A are monoclonal lines of KOTMEM30A-sg0.2 (sequence in Chapter 2 Materials & Methods). KO2-ARL5A AND KO5-ARL5A are monoclonal lines of KOARL5A-sg93.3 (sequence in Chapter 2 Materials & Methods). All other lines are polyclonal pools of their respective guides (sequences in Chapter 3 Materials & Methods). Blank entries denote protein's AUC of its associated peptides is negligible.

Accession	PBS	sgSAFE	self-cut mCherry	KO3 TMEM30A	KO5 TMEM30A	KO TMEM30A 7.9	KO2 ARL5A	KO5 ARL5A	KO ARL5A 91.1	KO ARL5A 94.4
A0A024QZ42		2.11E+06	8.30E+05	1.89E+06		1.11E+06	1.05E+06	3.08E+05		2.41E+05
A0A024RCR6	1.86E+04	2.76E+06	2.88E+06			9.78E+05	1.77E+06		2.26E+05	3.88E+05
A0A087WT20	3.51E+04	1.23E+06	2.17E+05	5.45E+05		2.51E+05	1.98E+04			
A0A087WU07	1.80E+05	4.79E+05	3.49E+05	1.16E+06	6.57E+05			1.07E+05	1.60E+05	
A0A087WUM3		8.79E+04	5.98E+04	3.92E+05		3.15E+04	3.47E+04	3.49E+05	9.87E+04	2.57E+04
A0A087WVM4		1.65E+06	1.55E+06	1.57E+05	1.92E+05	6.73E+04	1.37E+04			8.79E+04
A0A087WVQ6	1.41E+06	8.33E+07	4.80E+07	2.61E+07	8.31E+06	2.96E+07	1.97E+07	2.02E+06	5.08E+06	1.14E+07
A0A087WXM8	1.43E+04	6.21E+04	4.36E+04		8.49E+03	1.11E+04	5.09E+04		9.81E+03	1.04E+04
A0A087WY55		7.19E+05	3.33E+05	4.61E+05	3.61E+05	1.35E+06				
A0A087WZX2	5.74E+04			1.12E+05				3.26E+05	3.23E+04	
A0A087X1K9		4.76E+05	1.64E+05							
A0A087X295		4.09E+04	5.27E+04				1.69E+04			8.77E+03
A0A087X2I1	1.76E+05	9.11E+06	9.68E+06	1.31E+06	2.87E+06	2.97E+06	3.04E+06	1.40E+04	8.13E+05	1.07E+06
A0A0A0MQX8		1.81E+06	1.30E+06	8.70E+05	8.79E+05	2.35E+05	7.33E+05		3.99E+05	1.15E+06
A0A0A0MR02	7.75E+05	5.67E+07	3.97E+07	3.74E+07	2.15E+07	2.32E+07	1.95E+07	3.45E+06	8.41E+06	1.97E+07
A0A0B4J1V8	9.86E+04	1.21E+06	6.51E+05	2.46E+05	2.97E+05	4.58E+05		4.43E+04	7.41E+04	1.20E+05
A0A0C4DFL7		2.37E+05	5.11E+05	4.30E+05	8.00E+05			1.29E+05	1.30E+05	3.16E+05
A0A0C4DG76		6.45E+05	2.30E+06	6.02E+04	1.52E+05	9.65E+05	2.49E+05			5.73E+05
A0A0C4DG84		1.31E+06	6.68E+05	3.97E+05	2.96E+05			1.29E+05	1.98E+05	8.71E+04
A0A0C4DG89	5.00E+04	2.03E+06	7.26E+05	3.20E+05	2.89E+05	2.46E+05	7.00E+05			
A0A0C4DGN7		1.69E+06	7.25E+05	4.04E+05	3.97E+05	2.64E+05	3.35E+05		1.63E+05	2.99E+04
A0A0C4DGU3		1.10E+06	6.47E+05			2.82E+05	3.11E+05			

A0A0D9SF54		1.79E+06	6.46E+05	2.43E+04		2.21E+05		1.23E+04		
A0A0J9YX62		6.40E+05	5.38E+05		1.64E+05	2.49E+05	2.11E+05		6.79E+04	1.48E+05
A0A0U1RRK1		2.30E+05	1.02E+05			8.50E+04	1.13E+05			8.54E+04
A0AVT1		4.89E+06	3.39E+06	6.94E+05	1.56E+06	1.09E+06	1.60E+06		2.13E+05	7.07E+05
A0PJX0				1.55E+05				1.06E+05	6.64E+04	
A2A3N6		3.11E+04	1.08E+04			1.96E+04	8.50E+03			9.63E+03
A5YKK6		2.25E+06	8.14E+05			9.52E+05	2.39E+05	6.20E+04		
A6NDU8					5.56E+05	6.55E+05				
A6NEM2		1.23E+06	4.96E+05	2.74E+05	2.78E+05	2.34E+05	3.06E+05			4.20E+05
A6NHJ8	3.94E+04	7.62E+05	3.06E+05			1.60E+05				9.68E+04
A6NHL2		5.31E+06	4.15E+06	1.20E+06	1.49E+06	2.47E+06	1.24E+06			
A6NHR9		1.83E+06	6.12E+05		7.19E+05	4.98E+05	1.23E+05			
A8MZA4	3.59E+04	1.76E+06	1.45E+06	7.03E+05	8.43E+05	5.21E+05	3.17E+05	1.62E+05	7.72E+05	6.16E+05
B0QY34		6.10E+04	1.19E+05	4.32E+04	1.26E+04	9.74E+04	5.12E+04		2.82E+04	2.87E+04
B0QYK0	1.26E+05	1.77E+06	7.26E+05	2.73E+05	2.13E+05	1.13E+05	1.13E+06	1.99E+05	4.05E+05	1.12E+06
B0QZ18		1.96E+05	2.37E+05		3.01E+05	1.92E+05				
B1AHN4						9.77E+05	6.12E+05	1.46E+06	2.02E+05	5.80E+05
B1AJY5		6.68E+04	8.84E+05		5.79E+05		7.86E+05	2.59E+03		6.30E+05
B1APM4		1.19E+05	4.91E+04			1.33E+04				
B2R5W2	4.89E+06	3.92E+07	3.10E+07	3.93E+07	3.37E+07	1.64E+07	2.42E+07	8.29E+06	1.95E+07	2.51E+07
B3KR61		5.29E+05	6.73E+05	3.08E+05	3.02E+05	1.76E+05			3.51E+05	2.37E+05
B3KS98	9.51E+04	3.90E+06	2.26E+06	4.75E+05	1.45E+06	2.37E+06	2.08E+06	5.01E+04	1.00E+06	1.55E+06
B4DDF4	1.47E+04	1.78E+06	1.17E+06	9.64E+05	1.03E+06		3.92E+05	1.82E+05	5.20E+05	6.21E+05
B4DKY1		5.79E+06	2.40E+06	4.44E+05	1.62E+06	2.25E+06	3.49E+06		4.47E+05	1.27E+06
B4DXR9		5.68E+05	3.90E+05	1.05E+06	2.72E+05	2.68E+05	3.00E+05			
B4DXZ6	7.10E+04	1.41E+07	8.75E+06	1.82E+06	6.20E+06	5.85E+06	4.61E+06	5.70E+04	1.71E+06	6.49E+06
B4E0K5	1.25E+05	1.49E+06	1.16E+06		1.20E+06	2.52E+05				
B4E101		4.47E+05	1.33E+05			1.48E+05	1.46E+05			
B4E1N1		1.95E+06	1.09E+06	2.61E+06	1.11E+06	1.40E+06	4.78E+05	2.46E+05	9.14E+05	8.33E+05
B7Z645		9.11E+06	3.44E+06	1.80E+06	1.46E+06	2.50E+06	2.05E+06	1.30E+05	1.31E+06	1.62E+06

B7Z6Z4	5.61E+04	3.02E+06	2.36E+06	9.14E+05	1.06E+06	2.07E+06	2.12E+06	5.82E+05	1.18E+06	3.16E+06
B7Z7P8	2.35E+05	1.96E+07	1.40E+07	1.70E+07	5.03E+06	8.34E+06	1.01E+07	5.82E+05	2.79E+06	4.82E+06
B7ZKQ9		5.61E+05	3.34E+05			2.91E+05	8.00E+05			3.66E+05
B8ZZ54		5.01E+06	3.33E+06	7.71E+06	5.03E+06	2.42E+06	4.41E+06	5.46E+05	1.78E+06	1.35E+06
B8ZZT4	1.65E+04	3.66E+05	2.73E+05	2.38E+06	8.56E+05			7.81E+05	1.36E+05	4.15E+04
C9JJ19		5.70E+05	1.54E+05		4.70E+04		5.17E+05	1.46E+05	2.74E+05	3.59E+05
C9JVE2		4.00E+06	6.66E+06		2.09E+05	7.55E+05	3.87E+05			
C9JZR2		7.05E+05	5.57E+05		7.93E+04	7.12E+04	2.23E+04			6.63E+04
D6REX3	1.64E+04	4.81E+06	3.14E+06	3.37E+06	5.86E+05	2.25E+06	2.59E+06	3.69E+05	1.03E+06	1.95E+05
D6RIY6		2.03E+06	2.37E+06	4.43E+05	5.66E+05		1.73E+06	1.98E+05	8.92E+05	1.33E+06
E7ERK9	2.35E+04	1.21E+06	8.62E+05	2.51E+05	7.09E+04	4.36E+05	5.72E+05			
E7EW05	1.81E+05	2.96E+06	2.10E+06	1.31E+06	5.54E+05	7.69E+05	7.07E+05	2.29E+05	1.33E+05	8.75E+05
E9PCN2	3.03E+04	1.77E+06	1.37E+06	1.90E+05	5.11E+05	2.15E+05	2.72E+05		3.99E+05	3.64E+05
E9PCY7	1.29E+06	2.59E+07	1.79E+07	1.04E+07	1.04E+07	1.69E+07	9.83E+06	3.02E+06	6.26E+06	7.39E+06
E9PGC8		1.18E+05	1.83E+04							
E9PHY5		1.50E+06	1.14E+06	2.73E+05	7.84E+05	3.35E+05	6.19E+05	1.45E+04	4.50E+05	3.72E+05
E9PIM0	3.98E+04	5.17E+05	7.23E+05	3.44E+05	6.17E+05				2.63E+05	1.64E+06
E9PMI6	2.04E+05	1.28E+06	9.57E+05	4.99E+05	7.36E+05	4.96E+05	1.89E+06	1.70E+05	2.95E+05	5.49E+05
F2Z2J1		2.48E+05	6.33E+05	1.71E+05						
F5GZ28		3.27E+05	1.54E+05		1.72E+05	1.89E+05			9.13E+04	4.66E+05
F5H0R1		1.70E+05	3.50E+05	1.15E+06	3.54E+05	4.25E+05	6.85E+05			
F5H2X7		1.00E+06	5.05E+05			5.37E+05	2.27E+05			
F5H385		5.66E+05	8.02E+05		6.59E+05	6.98E+05	7.31E+05		1.82E+05	2.80E+05
F5H5D3		2.50E+06	1.66E+06		2.06E+05	8.88E+05	3.10E+05			
F5H5I6	3.14E+04	1.72E+06	4.42E+05	7.40E+05	6.24E+05	3.32E+05	4.24E+05		1.04E+05	4.58E+05
F5H6I7		5.13E+04	3.31E+04	3.67E+04	2.11E+04	3.23E+04	1.75E+04		7.54E+03	1.11E+04
F6RGN5		1.28E+05	1.04E+05		4.39E+04	6.60E+04	4.37E+04		2.32E+04	3.83E+04
F6T1Q0	1.79E+05	6.21E+05	3.12E+05	3.70E+05	1.62E+06	7.81E+05				
F8VVT9	7.01E+04	2.43E+06	1.12E+06	1.06E+06	7.52E+05	5.48E+05	8.72E+05		5.67E+05	
F8VWW8	8.10E+03	8.90E+04	3.64E+05							

F8VXU5		1.01E+06	7.27E+05			2.68E+05	2.69E+05		4.66E+05	1.81E+06
F8VY04										
F8VZX2										
G0XQ39		1.43E+05	1.68E+05		1.00E+05	4.84E+04	5.27E+04		3.65E+04	
G3V0I5	2.02E+04	3.41E+06	2.45E+06	3.69E+05	3.75E+06	1.48E+06	1.14E+06	2.08E+05	1.28E+06	2.61E+06
G3V1Q4	9.78E+03	2.75E+05	5.95E+05	4.08E+04	7.02E+04	4.81E+04	7.17E+05	7.92E+03	2.53E+04	2.94E+04
G3V325	6.38E+04	8.85E+06	5.92E+06	6.11E+06	3.60E+06	3.05E+06	2.57E+06	8.42E+05	2.02E+06	2.55E+06
G3V3H3		6.79E+06	5.68E+06	9.13E+05	2.35E+06	2.12E+06	1.19E+06		1.13E+06	1.72E+06
G3XAL9	3.04E+05	7.15E+05	8.23E+05			2.15E+05				
G5E9D5	6.59E+04	6.43E+05	1.14E+06			6.41E+05	5.46E+05			
G5E9F5				3.28E+05		8.86E+04				
H0YL72	1.70E+05	5.17E+06	2.07E+06	3.69E+06	1.55E+06	5.43E+05	1.53E+06	8.11E+04	1.07E+06	1.51E+06
H3BVI4	2.01E+04	2.89E+05	2.27E+05		1.77E+05	1.55E+05		1.79E+05	2.84E+05	1.05E+05
H7BYP4	7.31E+05	6.09E+05	4.29E+05	1.96E+06	1.41E+06	2.72E+05	1.52E+06	1.26E+06	8.74E+05	7.68E+05
H7C1J4		1.56E+05	5.75E+04	4.74E+04	6.96E+04	2.75E+04	2.97E+04		1.95E+04	4.58E+04
J3KMZ8		2.08E+06	6.48E+05		8.07E+05	5.26E+05				
J3KN16		8.70E+06	8.74E+06		7.06E+05	3.16E+06	2.05E+06	3.00E+05	9.18E+04	3.01E+05
J3KP27	2.48E+05							3.35E+05		2.62E+05
J3KQ48	7.45E+03	5.78E+05	1.86E+05	6.07E+04	1.52E+05	7.66E+04	5.82E+05			
J3KTL2	3.19E+06	3.63E+06	8.47E+06	1.53E+07	3.77E+06	1.96E+06	1.49E+06	1.52E+06	1.78E+06	2.26E+06
K7EK35	1.42E+04	2.07E+06	1.88E+06	4.77E+05	7.95E+05	1.07E+06	7.89E+05		2.49E+05	2.59E+05
M0R026		3.58E+05	3.64E+05							
M0R210	3.65E+06	4.09E+07	3.42E+07	2.97E+07	1.95E+07	2.52E+07	2.79E+07	3.59E+06	1.07E+07	1.87E+07
M0R2B7	6.11E+04	1.28E+06	1.01E+06	2.99E+06	7.67E+05	1.85E+05	1.26E+05	2.52E+05	2.64E+05	
O00154		2.64E+06	2.19E+06	2.16E+06		1.61E+06	4.17E+05			5.84E+05
O00303	1.13E+05	6.72E+06	4.52E+06	1.91E+06	2.13E+06	4.58E+06	2.94E+06		1.07E+06	2.09E+06
O00330		2.46E+06	1.78E+06	3.14E+04	1.04E+06	3.58E+05	2.81E+05	6.71E+04	1.58E+05	1.25E+05
O00410	5.51E+05	1.05E+08	7.01E+07	1.95E+07	2.54E+07	4.80E+07	4.01E+07	6.81E+06	7.64E+06	2.53E+07
O00411	1.12E+05	1.06E+06	6.32E+05		5.19E+05	1.06E+06	9.90E+05		1.42E+06	1.36E+06
O00422	8.13E+04	1.97E+06	1.16E+06	7.29E+05	1.24E+06	8.21E+05	1.01E+06	1.70E+05	9.92E+05	

O00425	3.33E+04	6.93E+06	4.52E+06	1.16E+06	1.26E+06	8.73E+05	4.23E+05		4.41E+05	1.60E+05
O00429		3.98E+06	4.07E+06	5.91E+05	2.29E+05	1.87E+06	1.00E+06		4.04E+05	3.56E+05
O00461						9.98E+05	1.06E+06		8.94E+04	1.10E+05
O00483	1.12E+05	4.67E+06	2.77E+06	3.06E+06	1.11E+06	2.60E+06	1.76E+06	1.79E+05	1.48E+05	1.88E+06
O00505	2.78E+04	5.16E+06	1.85E+06	4.69E+05	2.18E+06	2.50E+06	7.23E+05		1.73E+05	4.24E+05
O00567	2.59E+06	2.57E+07	1.87E+07	8.06E+06	5.49E+06	1.14E+07	5.18E+06	5.72E+05	2.90E+06	5.06E+06
O00571	1.30E+06	3.00E+07	2.34E+07	1.09E+07	7.65E+06	1.91E+07	1.78E+07	8.75E+05	3.27E+06	8.13E+06
O00767	5.80E+04	2.04E+06	1.44E+06	1.84E+06	4.66E+05	1.23E+06	1.14E+06	1.89E+05	6.04E+05	8.48E+05
O14561		2.07E+06	1.15E+06	2.26E+06	1.57E+06	5.03E+05		1.56E+05	1.47E+05	5.70E+05
O14579		1.06E+06	6.89E+05			1.82E+05				
O14617										
O14777		3.63E+05	4.49E+05			1.98E+05	8.31E+04		2.47E+04	1.47E+05
O14925	9.17E+04	2.92E+06	7.96E+05	2.14E+06	1.31E+06	7.11E+05	9.72E+05		2.29E+05	6.81E+05
O14933		2.25E+05	1.68E+05							
O14950	4.64E+04	3.20E+06	1.30E+06	3.76E+06	1.97E+06	9.08E+05		1.35E+05	9.26E+05	1.42E+06
O14975	6.77E+03	7.09E+05	3.53E+05		1.92E+05	3.06E+05		5.24E+03		
O15031	3.72E+04	6.13E+05	1.13E+06	3.18E+05	1.65E+06	8.02E+05	5.10E+05			
O15067	7.13E+04	2.28E+07	1.40E+07	3.06E+06	7.19E+06	5.72E+06	7.75E+06	7.04E+05	3.60E+06	7.54E+06
O15144		2.62E+06	1.25E+06	5.37E+06	1.24E+06	8.48E+05	1.59E+06	9.29E+05	6.43E+05	
O15145		6.02E+05	3.88E+05	1.20E+05	1.01E+05	3.22E+05	2.84E+05		1.17E+05	6.00E+04
O15160	4.55E+04	1.39E+06	1.45E+06	5.77E+05	6.66E+05	1.24E+06	6.91E+05	9.76E+04	2.58E+05	
O15164		1.67E+05	8.33E+04							
O15226	1.17E+04	6.24E+04	2.35E+04	2.56E+04						
O15260	3.06E+05	7.18E+06	5.20E+06	3.94E+06	2.46E+06	3.52E+06	3.39E+06	1.72E+05	8.83E+05	1.82E+06
O15371	2.28E+05	1.32E+07	8.94E+06	4.99E+06	6.30E+06	6.48E+06	8.13E+06	8.97E+05	3.63E+06	4.80E+06
O15431	2.75E+04					5.29E+05				
O15439		4.40E+05	1.99E+05							
O15446		6.15E+05	2.66E+05			2.42E+05	2.14E+05		5.37E+04	
O43143	4.00E+06	5.76E+07	3.23E+07	1.50E+07	1.96E+07	2.49E+07	2.49E+07	2.19E+06	1.16E+07	2.03E+07
O43156						1.55E+04	1.16E+04			

O43166				3.26E+05	1.27E+05				4.70E+04	4.72E+04
O43175	3.15E+05	1.03E+07	5.79E+06	2.70E+05	5.29E+06	2.10E+06	2.06E+06		2.97E+06	2.65E+06
O43242	5.24E+06	1.49E+07	1.42E+07	6.07E+06	3.74E+06	6.87E+06	8.75E+06	6.41E+05	1.48E+06	5.11E+06
O43252		1.39E+06	5.98E+05		3.64E+05	2.36E+05	2.27E+05			
O43264	5.46E+04	9.20E+05	2.21E+06	3.13E+05		2.62E+05	3.98E+05			
O43290		4.06E+06	2.35E+06	4.72E+05	2.46E+06	1.28E+06	3.01E+05		3.06E+05	3.49E+05
O43395	4.29E+05	3.09E+06	3.62E+06	1.62E+05	2.72E+06	1.42E+06	3.08E+06	1.57E+05	1.80E+06	2.88E+06
O43399		2.68E+06	8.61E+05	4.56E+06	1.78E+06	1.20E+06		1.15E+06	8.05E+05	5.13E+05
O43592	3.03E+05	5.21E+06	6.57E+06	3.31E+05	2.76E+06	1.84E+06	3.68E+06	6.62E+05	3.83E+05	8.77E+05
O43617		1.77E+06	1.65E+06	3.65E+05	7.77E+05		7.84E+05	6.28E+04	2.96E+05	3.44E+05
O43674		7.51E+05	4.59E+05	6.11E+05					5.83E+05	4.28E+05
O43678		1.87E+05	6.24E+05		9.57E+05		4.80E+05		3.04E+05	2.14E+05
O43684	1.07E+06	9.61E+06	6.12E+06	4.95E+06	8.78E+06	4.54E+06	4.10E+06	4.17E+05	2.19E+06	3.23E+06
O43707	8.24E+05	1.15E+07	9.94E+06	3.59E+06	3.84E+06	2.06E+06	4.52E+06	2.43E+05	1.15E+06	2.63E+06
O43776	1.53E+05	8.30E+06	5.67E+06	3.60E+06	4.91E+06	4.44E+06	2.32E+06	3.58E+05	3.47E+06	4.65E+06
O43815		1.52E+05	6.39E+04			2.25E+04	1.74E+04			1.70E+04
O43818		4.33E+05	1.90E+05	3.11E+05	1.77E+05		3.68E+05	7.91E+04		
O43837	9.13E+04	2.73E+06	1.96E+06	2.22E+06	6.46E+05	5.94E+05	8.90E+05	4.87E+04	1.15E+05	1.87E+06
O60216		7.31E+05	5.01E+05			9.25E+04	2.14E+05			
O60220		9.22E+05	6.77E+05	9.84E+05	6.38E+05	3.53E+05			3.23E+05	
O60264	1.15E+06	1.93E+07	1.30E+07	1.33E+06	2.36E+06	1.15E+07	8.99E+06	7.49E+05	9.82E+05	3.49E+06
O60287	2.77E+04			7.15E+05		6.99E+05	8.21E+05			6.03E+05
O60343	3.34E+04	4.75E+05	7.95E+05	3.50E+04	3.15E+05	5.61E+05	5.40E+05	1.89E+04	1.53E+05	3.55E+05
O60488		1.32E+04	9.63E+03							
O60506	1.85E+05	8.33E+06	5.20E+06	3.05E+06	1.28E+06	4.85E+06	7.11E+05	2.79E+05	6.31E+05	2.47E+06
O60563		7.64E+04	3.45E+04	4.56E+04	2.31E+04	2.48E+04	1.22E+04		1.21E+04	1.50E+04
O60678	3.29E+04	3.08E+06	3.72E+06	1.42E+06	1.33E+06	1.66E+06	1.47E+06		1.48E+06	2.96E+06
O60684		5.61E+05	1.87E+06			5.33E+05	6.09E+05			
O60701	5.01E+04	8.12E+05	7.58E+05	5.58E+05	4.56E+05	3.02E+05	3.30E+05			2.00E+05
O60732	3.36E+04	1.30E+06	1.67E+06			1.33E+06				

O60749		2.04E+06	1.08E+06	4.55E+05	9.07E+05	1.42E+06	9.48E+05		2.93E+05	4.18E+05
O60763		2.24E+06	2.40E+06		2.54E+05	5.72E+05	1.23E+06			1.52E+05
O60783		8.42E+05	1.86E+06			8.61E+04				1.04E+05
O60814				2.74E+06	4.90E+05			2.46E+05	1.71E+05	3.55E+04
O60832	5.80E+04	6.06E+06	1.46E+06	5.73E+05	9.57E+05	6.92E+05	3.52E+05	4.99E+04	2.00E+05	6.27E+04
O60841	1.11E+06	1.24E+07	5.55E+06	2.00E+06	2.39E+06	2.24E+06	2.16E+06	2.19E+05	1.64E+06	3.32E+06
O60884	6.46E+04	7.69E+06	6.86E+06	2.17E+06	1.77E+06	2.78E+06	1.72E+06		9.84E+05	1.73E+06
O60906		5.18E+03	7.88E+03							
O60930		1.46E+04	1.10E+04							
O60942		5.29E+05	3.08E+05							
O75083		1.07E+05	8.36E+04				1.96E+04	6.75E+03	2.27E+04	2.79E+04
O75131		1.86E+06	1.05E+06	1.98E+05	5.61E+05	1.07E+06	1.27E+06		1.01E+06	3.11E+05
O75152	7.82E+03	4.38E+05	4.53E+05		7.99E+04	1.36E+05	4.87E+04	8.27E+03	5.32E+04	3.42E+04
O75179		1.92E+06	1.26E+06	1.48E+06	9.15E+05	1.51E+06	2.26E+06			
O75251	4.79E+04	1.09E+06	7.28E+05	6.28E+05	1.12E+06	2.68E+05	7.89E+05		7.11E+05	6.73E+05
O75330		1.38E+06	4.23E+05							
O75369	1.53E+05	6.12E+06	5.01E+06	3.67E+05	1.13E+06	7.85E+05	3.37E+05	1.77E+05	2.71E+05	6.98E+04
O75381		4.52E+05	2.34E+05	7.49E+04	1.01E+05	5.66E+04		4.60E+04	5.77E+04	
O75387		7.94E+04	7.98E+04	4.33E+04				4.87E+04		
O75390	1.24E+04	2.02E+06	2.14E+06	4.98E+06	2.23E+06	8.89E+05	1.27E+06	2.10E+05	6.64E+05	1.25E+06
O75400	2.69E+05	1.36E+07	6.23E+06	3.72E+05	3.91E+06	3.96E+06	4.34E+06	2.09E+04	1.37E+06	1.82E+06
O75436	5.61E+05	3.68E+06	2.11E+06	6.28E+06	8.45E+06	3.36E+06	1.46E+06	9.59E+07	2.50E+06	4.21E+06
O75449		1.00E+05	6.37E+04							
O75475	1.26E+05	5.36E+06	3.80E+06	2.03E+06	4.59E+06	1.06E+06	7.45E+05	7.63E+05	2.12E+06	2.61E+06
O75607	3.91E+05	2.05E+06	1.29E+06	2.40E+06	9.68E+05	8.15E+05	1.39E+06	7.28E+04	1.98E+05	3.13E+05
O75608										
O75616		7.48E+05	6.13E+05	4.12E+05	4.62E+05	8.08E+05	3.70E+05		1.35E+05	2.79E+05
O75643	6.14E+05	4.93E+07	2.92E+07	5.98E+06	1.19E+07	1.17E+07	1.76E+07	1.49E+06	7.63E+06	7.74E+06
O75683	2.19E+07	1.54E+07	2.11E+07	5.70E+07	1.24E+07	1.14E+07	9.96E+06	1.25E+07	9.27E+06	1.16E+07
O75691	7.04E+04	1.65E+06	6.43E+05	9.24E+04		2.01E+05	2.26E+05		4.08E+04	

O75694	1.32E+05	7.39E+06	3.88E+06		4.85E+05	2.02E+06	1.47E+06	2.88E+05	6.31E+05	8.79E+05
O75717	4.52E+05	9.96E+06	6.13E+06	5.40E+06	3.48E+06	4.83E+06	6.91E+06	4.21E+05	1.70E+06	3.23E+06
O75844	1.33E+05	5.42E+06	3.73E+06	9.08E+06	6.82E+06	4.07E+06	4.50E+06	1.76E+06	4.37E+06	4.95E+06
O75874	1.52E+04	3.03E+06	1.22E+06		5.23E+05	1.16E+06	1.12E+05		1.63E+05	5.53E+05
O75915		4.86E+05	3.85E+05	4.26E+05	2.95E+05	3.21E+05	2.89E+05		1.56E+05	2.22E+05
O75940	1.23E+06	6.50E+05		5.63E+05			4.28E+06	6.07E+05	1.29E+05	2.16E+05
O76003	1.00E+05	1.13E+06	1.52E+06	1.45E+06	1.29E+06	1.35E+06	1.10E+06		7.27E+05	1.29E+06
O76021	2.81E+06	2.13E+07	1.50E+07	1.13E+07	5.55E+06	7.89E+06	7.01E+06	2.70E+06	1.64E+06	1.88E+06
O76031	5.18E+05	4.52E+06	4.62E+06	1.70E+06	1.22E+06	2.06E+06	8.46E+05		4.35E+05	9.79E+05
O76041	5.23E+04	2.50E+06	1.56E+06	3.94E+05	7.89E+05	6.14E+05	3.46E+05	1.23E+05	7.96E+05	4.79E+05
O94776	1.40E+05	9.05E+06	5.42E+06	1.66E+06	2.33E+06	3.35E+06	2.09E+06		7.54E+05	1.69E+06
O94888		2.35E+06	1.71E+06	6.14E+05	1.50E+06	1.23E+06	8.31E+05	2.86E+04	1.04E+05	5.79E+05
O94889		9.43E+05	1.25E+05		1.58E+05					
O94905		2.10E+06	5.60E+05	8.26E+05	2.33E+06	6.73E+05	8.80E+05		5.98E+05	
O94906	1.73E+05	5.49E+06	2.04E+06	4.64E+05	3.14E+05	2.39E+06	5.51E+06	6.54E+04	7.52E+05	2.77E+06
O94925		4.23E+06	2.23E+06	8.60E+05		7.35E+05	1.07E+06		8.74E+05	1.05E+06
O95104	2.26E+04	4.05E+05	5.20E+05		8.83E+04	1.22E+05	6.30E+04			6.91E+04
O95168		2.60E+06	1.21E+06	1.64E+06	6.17E+05	1.14E+06		1.77E+05	4.70E+05	5.80E+05
O95197	4.03E+04	1.77E+06	1.15E+06	1.23E+06	1.38E+06	1.00E+06	1.04E+06	2.78E+05	6.29E+05	1.20E+06
O95232	1.87E+05	3.04E+06	1.94E+06	8.73E+05	3.28E+06	1.30E+06	3.28E+05		5.70E+05	1.38E+06
O95239		1.31E+06	8.99E+05	2.93E+05	8.89E+05	1.09E+06	1.45E+05			
O95251		1.11E+05	1.04E+05							
O95299		2.30E+06	6.83E+05	6.69E+05	7.11E+05	7.35E+05	2.95E+05		2.50E+05	5.30E+05
O95347	5.95E+05	8.00E+06	5.11E+06	1.63E+06	2.43E+06	3.53E+06	4.21E+06		7.42E+05	1.49E+06
O95382				4.24E+05	2.09E+05			6.10E+04	1.72E+05	
O95394		4.35E+05	1.64E+05	1.23E+06	1.21E+06					
O95456		6.17E+05	6.86E+05		4.42E+05	1.62E+04	1.14E+04			
O95478	1.00E+05	6.84E+05	6.79E+05	4.57E+05	1.89E+04	5.81E+05	3.53E+04	7.79E+03	1.35E+04	1.28E+04
O95486		3.82E+05	3.30E+05			1.14E+05				
O95487		2.43E+05	2.08E+05	1.48E+04	1.90E+04	1.66E+05				

O95573	3.86E+04	6.70E+06	4.28E+06	1.22E+06	2.78E+06	1.37E+06	1.74E+06	5.10E+05	5.52E+05	1.85E+06
O95639		5.03E+05	2.25E+05							
O95674	1.20E+04	2.28E+05	4.90E+05	5.70E+04	1.24E+05	1.07E+05		1.18E+04		
O95721	5.01E+04	1.54E+06	1.01E+06	8.72E+05	6.25E+05	3.94E+05	3.69E+05	2.42E+03	1.01E+05	2.39E+05
O95747	1.90E+04	3.43E+06	3.11E+06		6.36E+05	8.70E+05	1.54E+06	7.58E+05	9.36E+05	1.40E+06
O95758	1.85E+04	6.44E+05	6.66E+05						1.02E+05	4.37E+04
O95782	3.21E+04	2.01E+06	1.04E+06	1.94E+05	5.92E+05	7.50E+05	1.16E+06	6.49E+03		1.33E+06
O95793	1.04E+04	1.46E+05	1.50E+05	4.48E+04			1.85E+04			
O95816	3.39E+05	6.34E+06	3.42E+06	2.45E+06	2.41E+06	3.76E+06	2.02E+06		1.36E+06	4.27E+06
O96005	2.70E+05	4.20E+06	3.55E+06	2.64E+06	2.10E+06	2.23E+06	3.90E+06		5.06E+05	1.22E+06
O96008	3.70E+04	1.47E+07	9.56E+06	8.23E+06	6.65E+06	7.79E+06	4.59E+06	2.22E+06	1.98E+06	3.66E+06
O96019	6.94E+04	6.73E+05	5.24E+05	2.31E+05		1.81E+05	3.13E+05	9.18E+04	8.01E+04	1.64E+05
O96028		6.67E+03	8.31E+03			6.67E+03				
P00390	1.77E+05	4.03E+06	2.35E+06	2.73E+06	3.45E+06	9.27E+05	1.35E+06	5.46E+05	1.85E+06	2.95E+06
P00403	2.84E+05	1.46E+07	1.10E+07	1.08E+07	4.83E+06	4.86E+06	2.38E+06	1.64E+06	3.02E+06	3.39E+06
P00414		5.40E+05	3.00E+05	1.13E+05	1.07E+05	1.16E+05	9.82E+04	2.90E+04	4.71E+04	6.13E+04
P00492		1.15E+07	8.51E+06	5.17E+06	1.83E+07	5.16E+06	5.58E+06	1.22E+06	5.97E+06	4.80E+06
P00558	1.00E+06	4.46E+07	2.72E+07	1.97E+07	1.26E+07	1.20E+07	9.39E+06	1.95E+06	1.08E+07	6.61E+06
P00568		1.22E+06	5.50E+05	1.23E+05	4.08E+05	2.45E+05	6.58E+05		3.13E+05	2.64E+05
P00813	2.28E+04	7.99E+05	7.67E+05	6.93E+05	1.01E+06	1.41E+06		6.15E+05	6.68E+05	
P00846	1.17E+05	1.57E+06	1.24E+06		1.68E+06	1.82E+06	1.46E+06	5.16E+05	4.59E+05	8.07E+05
P02649	1.43E+04	1.07E+07	7.25E+06	4.83E+06	8.19E+06	2.42E+06	6.70E+06	1.87E+06	4.00E+06	7.27E+06
P02768	8.52E+05	4.64E+05	3.34E+05	9.44E+05				2.97E+05	4.96E+05	
P03891		8.27E+05	6.84E+05	3.04E+05	7.02E+05	5.07E+05				
P03928		2.87E+06	9.06E+05		7.50E+05	1.47E+05	2.55E+05	8.46E+04	2.12E+05	3.73E+05
P04075	6.44E+05	1.23E+07	7.50E+06	1.25E+07	6.23E+06	2.79E+06	5.09E+06	3.98E+05	2.69E+06	1.93E+06
P04083	1.78E+05						2.93E+05	1.89E+05	2.31E+05	1.00E+06
P04181	6.19E+04	4.01E+06	2.69E+06	1.94E+06	4.21E+05	8.94E+05	2.73E+06		6.90E+05	7.09E+05
P04183						2.06E+05	1.92E+05			
P04350	9.76E+04	4.04E+06	2.42E+06	2.36E+06	1.19E+06	2.83E+06	5.54E+05		2.66E+05	4.31E+05

P04406	4.58E+06	8.08E+07	6.15E+07	3.84E+07	3.85E+07	2.88E+07	5.80E+07	1.81E+07	2.15E+07	4.46E+07
P04632					1.52E+05	1.47E+05	1.42E+05			
P04792	1.43E+05	4.49E+06	4.71E+06	3.01E+06	5.39E+05	3.94E+06	6.65E+06	6.28E+04	1.15E+06	2.94E+06
P04818	4.26E+04	6.71E+05	5.90E+05			5.96E+05	2.65E+05		1.29E+05	2.47E+05
P04843	1.30E+06	4.30E+07	2.89E+07	3.46E+07	3.17E+07	2.20E+07	2.85E+07	1.16E+07	1.66E+07	2.04E+07
P04899					4.28E+05					3.28E+05
P05091	4.05E+04	1.36E+06	1.19E+06	2.74E+05	1.91E+06	9.12E+04	1.14E+06	1.24E+05	7.82E+05	2.12E+06
P05109	4.37E+05	1.64E+05					1.32E+07	1.31E+05		
P05141	1.11E+06	3.97E+07	2.66E+07	1.55E+07	1.50E+07	1.83E+07	1.41E+07	2.57E+05	7.59E+06	1.27E+07
P05165	6.48E+05	3.16E+06	1.53E+06	4.43E+05	4.10E+05	1.06E+06	3.84E+06	8.91E+04	4.71E+05	1.29E+06
P05166	7.34E+06	9.74E+06	9.10E+06	1.14E+06	1.87E+06	5.49E+06	3.40E+06	6.72E+05	5.11E+05	1.90E+06
P05204				3.46E+05	5.61E+04	9.07E+03		8.43E+04		
P05362	2.09E+05	4.03E+06	2.50E+06	2.23E+06	1.78E+06	1.08E+06	1.63E+06	1.28E+05	9.84E+05	1.38E+06
P05386		5.19E+06	2.95E+06	3.54E+06	2.40E+06	2.67E+06	1.10E+06		5.81E+05	1.65E+06
P05387	2.64E+05	5.03E+06	4.12E+06	8.97E+06	6.37E+06	5.71E+06	3.90E+06	1.08E+06	1.96E+06	4.01E+06
P06493	2.28E+05	9.16E+06	7.33E+06	8.03E+06	6.98E+06	5.59E+06	5.57E+06	3.62E+05	1.36E+06	4.43E+06
P06702	3.14E+05						9.80E+06	2.45E+05		
P06733	1.51E+06	3.44E+07	2.60E+07	1.87E+07	8.22E+06	4.11E+07	1.14E+07	5.13E+06	4.85E+06	7.82E+06
P07225	1.25E+04	2.16E+05	4.62E+05			7.91E+04		5.83E+04	8.76E+04	
P07237	2.00E+05	2.17E+06	1.27E+06	7.98E+06	5.92E+06	2.16E+06	5.29E+06	1.32E+06	3.81E+06	5.34E+06
P07384	2.94E+04	2.78E+06	2.54E+06		7.85E+05	1.68E+06	3.80E+06		2.27E+05	3.60E+05
P07437		7.74E+06	3.60E+06		1.82E+06	1.17E+06	9.42E+05			
P07476							3.28E+05			
P07814	1.27E+06	5.24E+07	4.83E+07	1.57E+07	1.17E+07	1.61E+07	1.87E+07	1.01E+06	5.89E+06	6.72E+06
P07900	6.23E+06	4.79E+07	3.08E+07	1.54E+07	1.74E+07	2.04E+07	2.00E+07	1.82E+06	7.56E+06	1.71E+07
P07919		5.55E+05	4.10E+05	1.12E+06	1.03E+06		4.60E+05	4.56E+05	4.86E+05	
P07948		1.61E+06	4.94E+05	2.21E+06	7.63E+05	5.91E+05	5.97E+05		1.47E+05	3.29E+05
P08237	3.86E+04	1.12E+06	1.87E+06			8.64E+05			1.29E+05	3.46E+05
P08240		2.52E+06	2.68E+06	1.20E+06	1.51E+06	1.16E+06	4.97E+05		4.86E+05	6.75E+04
P08243	1.01E+06	3.83E+06	3.18E+06	3.57E+06	4.01E+06	1.55E+06	2.43E+06	2.44E+05	2.40E+06	2.31E+05

P08559	3.98E+04	5.55E+06	4.70E+06	3.38E+06	2.29E+06	1.44E+06	2.53E+06		8.30E+05	8.78E+05
P08579									2.22E+05	
P08648	7.92E+04	3.94E+06	4.53E+06	6.27E+05	1.31E+06	6.34E+05	2.68E+06		2.97E+05	9.28E+05
P08670	4.57E+06	2.88E+07	2.47E+07	5.68E+06	7.15E+06	8.31E+06	1.61E+07	1.06E+06	2.26E+06	5.11E+06
P08754		1.17E+06	2.12E+06	2.67E+06	1.08E+06	6.34E+05	7.26E+05		3.79E+05	5.38E+05
P09001	1.44E+04	1.22E+06	7.17E+05	4.67E+05	8.67E+05	2.98E+05	2.02E+05	2.88E+04	2.64E+05	2.93E+05
P09234		8.73E+05	4.88E+05	6.38E+05	2.97E+05	5.00E+05	2.73E+05		1.54E+05	2.10E+05
P09382		7.77E+05	1.49E+06	6.28E+05	3.87E+05		3.45E+05		6.88E+05	2.46E+05
P09601							8.46E+04			4.52E+04
P09622	5.31E+04	1.47E+07	9.73E+06	1.06E+07	1.63E+07	3.11E+06	6.66E+06	1.12E+06	6.32E+06	4.68E+06
P10155	6.60E+04	4.12E+06	2.74E+06	1.69E+06	1.57E+06	2.40E+06	1.31E+06	5.51E+04	9.26E+05	9.81E+05
P10586	9.60E+05	6.16E+06	1.36E+07	1.14E+06	1.60E+06	8.69E+06	8.71E+06	5.29E+05	1.32E+06	2.98E+06
P11169	5.78E+04	6.05E+06	7.96E+06	3.57E+06	1.48E+06	1.98E+06	2.93E+06		1.15E+06	2.46E+06
P11172		6.64E+06	5.87E+06		1.67E+06	3.09E+06	2.92E+06	1.35E+05	1.50E+06	1.94E+06
P11279		2.26E+06	1.48E+06	8.43E+05	1.11E+06	1.59E+06	1.07E+06	2.44E+05	2.11E+05	1.35E+05
P11388	9.42E+05	2.38E+07	1.15E+07	1.02E+07	5.70E+06	1.12E+07	2.40E+06	7.64E+05	4.26E+06	4.67E+06
P11413	2.30E+04	3.74E+06	7.24E+05	8.99E+05	1.12E+06		8.69E+05		5.07E+05	1.79E+06
P12235		8.58E+05	8.30E+05	1.69E+06	2.64E+05	7.67E+05	4.56E+05	9.28E+04	3.26E+05	
P12270		2.09E+06	1.20E+06	1.07E+06	1.38E+06	1.43E+06	7.33E+05	5.68E+04	7.44E+05	1.48E+06
P12277	2.77E+05	6.36E+06	4.29E+06	4.29E+06	3.07E+06	2.27E+06	3.55E+06	3.57E+05	1.27E+06	1.00E+06
P13073		4.93E+06	2.68E+06	1.09E+07	5.91E+06	4.86E+06	4.00E+06	2.65E+06	4.04E+06	3.74E+06
P13224	9.84E+04	3.32E+06	5.31E+06	1.40E+06	5.22E+05	6.39E+06	2.98E+06		6.97E+05	4.07E+06
P13489	2.02E+04	5.84E+05	8.49E+05		4.34E+05		3.72E+05		1.90E+05	
P13674		9.95E+05	1.76E+06	8.58E+05	4.70E+05	3.89E+04			2.37E+04	3.57E+04
P13796	6.28E+05	1.41E+07	6.19E+06	1.14E+07	5.42E+06	2.04E+06	4.50E+06	6.40E+05	5.39E+06	4.93E+06
P13861	3.81E+04	4.34E+06	3.32E+06	1.73E+06	2.25E+06	6.55E+05	7.50E+05	3.48E+05	2.31E+05	2.22E+06
P13995	3.59E+04	1.55E+06	1.81E+06	1.42E+06	1.48E+06	9.19E+05	1.07E+06	3.07E+03	1.07E+06	5.25E+05
P14174	6.76E+04	1.64E+06	7.39E+05	4.74E+06	2.79E+06	2.30E+06	3.35E+06	1.24E+06	1.14E+06	1.22E+06
P14324	4.48E+04	6.45E+06	5.93E+06	3.75E+06	4.64E+06	1.19E+06	3.06E+06		1.69E+06	2.99E+06
P14678	3.02E+05	5.69E+05	6.58E+05		3.32E+05	2.75E+05	4.97E+05	6.90E+05	8.70E+05	4.49E+05

P14735		9.91E+04	1.23E+05			4.04E+04	2.45E+04		5.78E+03	2.50E+04
P14854				1.39E+06				2.84E+05		
P14868	9.43E+05	5.22E+07	3.46E+07	1.46E+07	2.42E+07	1.98E+07	1.63E+07	1.40E+06	6.99E+06	1.33E+07
P14927				4.80E+05				5.26E+05	3.07E+05	
P15104	2.79E+04	9.24E+05	2.39E+05		3.78E+05		4.98E+05	7.78E+03	4.06E+04	6.73E+04
P15153					1.97E+05		2.33E+05		1.28E+05	1.55E+05
P15170	1.87E+05	1.14E+07	8.53E+06	2.45E+06	6.17E+06	5.38E+06	4.51E+06	2.00E+05	1.55E+06	4.77E+06
P15924	8.89E+05	4.82E+06	6.95E+06	3.14E+06	8.79E+05	4.50E+06	1.09E+07	7.73E+05	1.36E+06	3.05E+06
P15954				3.07E+06		1.02E+06	1.18E+06	5.87E+05	5.62E+05	6.02E+05
P16157		1.21E+06	1.44E+06	1.52E+05	3.39E+05	3.16E+05	2.78E+05		6.35E+04	1.74E+05
P16402	3.73E+05	9.67E+05	6.89E+05	1.67E+06	1.18E+06		1.03E+06	7.06E+05	5.66E+05	1.02E+06
P16435				6.14E+05	3.81E+05	1.20E+05	2.96E+05	2.66E+05		9.32E+04
P16499		6.81E+05	1.44E+06	1.21E+06	6.41E+05		6.93E+05		1.25E+05	7.74E+05
P16615	4.23E+05	2.86E+07	2.14E+07	2.00E+07	1.27E+07	1.51E+07	1.27E+07	1.26E+06	5.69E+06	8.57E+06
P17096	3.45E+05	3.96E+06	3.16E+06	1.92E+07	8.56E+06	1.95E+06	2.50E+06	6.08E+06	2.82E+06	1.06E+06
P17482		6.69E+04	2.66E+04	1.65E+04	1.54E+04	9.03E+03	3.34E+03			
P17612		1.60E+06	9.15E+05	1.20E+06	2.15E+05	8.45E+05	2.36E+05			
P17655		6.58E+05	1.03E+05		9.01E+04					
P17812	6.92E+05	2.22E+07	1.83E+07	1.30E+07	1.06E+07	1.58E+07	1.52E+07	3.00E+05	4.86E+06	9.71E+06
P17900							6.20E+05			
P18085	5.71E+05	1.00E+07	9.59E+06	3.62E+06	1.48E+06	5.12E+06	4.40E+06	3.66E+05	1.50E+06	6.12E+06
P18583	7.33E+05	9.74E+05	1.22E+06		7.38E+05	8.43E+05	6.09E+05			2.23E+05
P18887		5.97E+05	4.94E+05	1.46E+05	1.67E+05		1.01E+05	2.80E+04	8.03E+04	5.80E+04
P19174	5.27E+04	6.77E+05	4.70E+05		1.56E+04		2.08E+06		8.13E+04	2.68E+05
P19256		9.81E+05	8.71E+05	3.82E+05		8.10E+05			2.90E+05	
P19338	2.57E+06	4.70E+07	3.19E+07	5.82E+07	4.96E+07	1.41E+07	3.65E+07	1.87E+07	2.24E+07	2.59E+07
P19388	1.71E+04	7.91E+05	9.69E+05	2.58E+05	2.11E+05	4.25E+05	1.55E+05		1.04E+05	1.25E+05
P19623	2.56E+06	8.76E+07	5.57E+07	8.04E+07	4.86E+07	4.84E+07	4.63E+07	3.74E+06	5.98E+07	7.12E+07
P19784		3.64E+06	2.02E+06	1.04E+06	1.02E+06	2.27E+06	1.32E+06		2.82E+05	1.34E+06
P20042	1.94E+04	5.98E+06	5.74E+06	1.65E+06	3.30E+06	3.03E+06	3.71E+06		1.08E+06	7.61E+05

P20073	7.59E+04	6.64E+06	2.69E+06	3.10E+06	1.74E+06	1.21E+06	7.65E+05	6.03E+04	2.45E+05	1.04E+06
P20339	3.91E+04	2.87E+06	1.21E+06		4.37E+05	1.10E+06	5.27E+05		2.07E+05	3.94E+05
P20645		5.45E+05	2.90E+06	1.14E+06		5.49E+05	4.87E+05			1.95E+05
P20930							8.08E+05			
P21266	3.85E+04	2.04E+06	2.90E+05		1.35E+06			1.01E+05	9.89E+04	
P21283		2.95E+06	1.06E+06		2.54E+05	1.40E+06	6.19E+05		6.82E+04	6.60E+05
P21333	3.72E+04	1.53E+06	1.14E+06		2.53E+04	1.77E+05	6.28E+05		8.00E+03	2.08E+04
P21399	4.09E+05	1.73E+06	1.85E+06	5.11E+05	3.80E+04	2.79E+05	4.47E+05	3.55E+04	1.09E+05	3.62E+04
P21796	3.87E+05	1.44E+07	1.18E+07	2.67E+07	1.61E+07	9.15E+06	8.98E+06	3.70E+06	4.07E+06	6.86E+06
P21912		6.12E+05	2.77E+05	1.79E+06	9.53E+05	3.62E+05				
P22033	7.92E+04	1.75E+06	1.48E+06		5.74E+05	5.64E+05	1.88E+06		3.15E+05	5.14E+05
P22059	8.86E+04	4.27E+06	2.57E+06	2.13E+05	1.26E+06	2.18E+06	2.89E+06	1.14E+05	7.35E+05	1.46E+06
P22061	2.38E+06	1.85E+07	1.28E+07	1.95E+07	1.49E+07	7.52E+06	5.58E+06	5.56E+06	7.53E+06	6.39E+06
P22087	9.35E+05	2.02E+07	1.45E+07	7.23E+06	8.51E+06	8.90E+06	6.54E+06	1.13E+06	4.72E+06	5.65E+06
P22314		9.64E+05	5.51E+05	2.68E+05	9.04E+05	2.17E+05	7.99E+05		3.86E+05	1.34E+05
P22528	1.31E+05			1.66E+04			6.56E+05	1.97E+04		
P22532	2.54E+04						2.44E+05	1.44E+04		
P22626	2.94E+06	1.90E+07	1.63E+07	1.18E+08	4.47E+07	1.55E+07	2.37E+07	3.02E+07	2.14E+07	3.27E+07
P22735	3.00E+04	1.61E+06	4.58E+05	4.97E+05	4.10E+05		7.64E+05	5.26E+04	3.35E+05	
P23258						4.76E+05		3.77E+05		
P23284	6.54E+05	3.57E+06	2.18E+06	2.73E+07	8.20E+06	4.96E+06	2.24E+06	3.65E+06	3.84E+06	4.40E+06
P23528	6.30E+06	7.19E+07	4.73E+07	4.23E+07	4.75E+07	2.22E+07	2.58E+07	6.51E+06	1.65E+07	2.87E+07
P23786				2.02E+05						
P23919	5.92E+04	5.38E+06	3.60E+06	2.41E+06	3.57E+06	1.31E+06	4.08E+05	3.85E+05	2.05E+06	1.36E+06
P24534	1.04E+06	1.71E+07	1.30E+07	6.83E+06	8.57E+06	6.61E+06	4.67E+06	4.16E+06	2.62E+06	6.74E+06
P24928		9.53E+05	3.34E+05		1.01E+05	4.21E+03		8.83E+03		
P25054		9.75E+03	7.02E+03							
P25325		5.69E+06	1.34E+06	2.56E+05	1.61E+06	1.22E+06	6.72E+05		4.51E+05	7.24E+05
P25786	4.53E+04	1.14E+06	1.03E+06	3.14E+05	2.28E+05	1.89E+05	5.00E+05	7.32E+04	9.61E+05	
P26358	5.20E+04	8.28E+06	4.16E+06	5.20E+05	6.57E+04	5.39E+06	4.90E+06		1.57E+06	1.40E+06

P26368	5.62E+05	1.03E+07	3.29E+06	2.38E+06	5.82E+06	2.78E+06	1.76E+06	2.75E+05	1.59E+06	2.29E+06
P26583								5.72E+04	6.28E+04	8.94E+04
P26641	1.59E+06	6.34E+07	3.50E+07	2.30E+07	3.51E+07	3.88E+07	2.54E+07	2.42E+06	1.31E+07	1.97E+07
P26885				9.08E+05	5.36E+05					3.20E+05
P27144		2.79E+06	6.57E+05	1.58E+06	1.80E+06	1.74E+06	1.50E+06		5.74E+05	5.68E+05
P27635										
P27694		6.52E+04	5.69E+04		2.83E+04	1.72E+04	1.26E+04		9.25E+03	6.46E+03
P27708	2.11E+05	9.74E+06	8.74E+06	1.18E+06	3.53E+05	6.88E+06	4.43E+06	1.08E+05	3.81E+05	8.00E+05
P27816	4.56E+04	4.88E+06	1.75E+06	1.53E+06	3.43E+06	1.57E+06	4.23E+05	1.18E+04	2.03E+05	8.14E+05
P27824	7.71E+04	2.33E+07	1.72E+07	4.48E+07	3.52E+07	1.91E+07	2.21E+07	9.39E+06	1.18E+07	2.10E+07
P28074	2.03E+04	1.36E+06	3.77E+05	1.22E+05	2.25E+05	1.93E+05	1.15E+05		1.29E+05	1.02E+05
P29144	2.24E+04	2.15E+07	1.33E+07	2.92E+06	1.40E+07	8.23E+06	1.35E+07	1.45E+06	2.15E+06	9.49E+06
P29353		6.10E+04	2.26E+04	3.60E+04	5.14E+04	1.19E+04	9.68E+03		1.72E+04	1.11E+04
P29692	1.22E+05	7.03E+06	2.15E+06	2.57E+06	2.07E+06	1.97E+06	1.76E+06		3.41E+05	6.95E+05
P29803		3.92E+06	1.74E+06		1.30E+06	5.69E+05	9.19E+05		3.10E+05	1.23E+06
P30084	1.51E+04	3.06E+06	2.63E+06	1.79E+06	1.92E+06	1.81E+06	1.33E+06		1.06E+06	5.29E+05
P30085	1.75E+05	6.04E+06	2.75E+06	8.59E+05	2.33E+06	2.67E+06	2.96E+06	3.73E+04	1.15E+06	6.41E+05
P30086	3.17E+04			2.82E+05					6.19E+04	
P30153	2.08E+05	3.61E+07	2.52E+07	1.02E+07	2.11E+07	1.37E+07	1.21E+07	6.20E+05	1.20E+07	1.34E+07
P30154		4.92E+06	1.49E+06	1.22E+05		1.95E+06	8.74E+05		1.38E+05	1.02E+06
P30405	7.28E+04			1.93E+06	7.23E+04		2.01E+04	1.18E+05	9.86E+04	9.99E+03
P30520		5.69E+05	1.70E+05		4.05E+05	1.89E+05	1.10E+05		1.81E+05	1.63E+05
P30536	3.13E+04	2.75E+05	3.21E+05	7.84E+04	2.12E+05	4.68E+04	9.61E+04	2.81E+04	6.40E+04	
P30626					1.23E+06	5.77E+05		6.64E+05	8.69E+05	1.45E+05
P30740		3.65E+06	2.69E+06	1.70E+06	1.22E+06	1.39E+06	1.05E+06		8.34E+05	7.21E+05
P30837		3.82E+05	1.57E+05							
P31040	1.64E+04	5.82E+06	4.00E+06	7.74E+06	6.01E+06	1.32E+06	1.97E+06	1.97E+05	1.22E+06	2.55E+06
P31151	1.88E+05						1.47E+06			
P31153	8.57E+04	4.15E+06	2.70E+06	2.64E+06	1.44E+06	3.44E+06	2.55E+06	1.52E+05	2.17E+05	2.78E+06
P31323	1.30E+05	6.13E+06	3.74E+06	5.00E+05	1.61E+06	2.01E+06	4.04E+05	5.42E+04	1.87E+05	4.92E+05

P31689	4.41E+04	5.59E+06	4.46E+06	1.42E+06	6.73E+05	4.90E+06	1.69E+06			4.53E+06
P31930	2.09E+04	1.91E+07	1.23E+07	1.23E+07	1.18E+07	4.55E+06	5.93E+06	2.07E+06	3.59E+06	5.73E+06
P31942	1.73E+05	3.06E+06	3.20E+06	3.56E+06	2.12E+06	4.46E+05	2.68E+06	7.39E+05	2.39E+06	1.08E+06
P31944	4.55E+05	5.59E+05	6.43E+05	1.14E+05	9.31E+04		1.82E+06		5.47E+04	6.80E+04
P31946	2.29E+05	9.48E+06	6.18E+06	1.59E+06	1.02E+06	2.58E+06	2.18E+06	9.13E+04	5.81E+05	1.76E+06
P31947	7.58E+04	5.28E+05	5.32E+05			2.08E+05	1.42E+06			
P31948	4.09E+05	4.95E+07	2.75E+07	1.42E+07	1.06E+07	9.18E+06	5.22E+06	8.24E+05	7.53E+06	9.56E+06
P31949	8.07E+04	9.62E+05	1.41E+06	1.38E+06	2.61E+06	3.28E+05	9.14E+05			
P32019		3.15E+05	2.89E+04							
P33176	8.37E+04	1.14E+07	5.65E+06	2.38E+06	2.74E+06	3.42E+06	1.90E+06	3.70E+03	1.84E+06	2.85E+06
P33240		1.97E+06	2.37E+05		1.44E+05	4.30E+05	8.45E+05			4.56E+05
P33778				3.98E+05				6.11E+04		
P34931	5.57E+04	1.99E+06	1.69E+06	3.22E+05	1.23E+06	6.67E+05	5.93E+05		3.61E+05	4.62E+05
P34932	1.82E+05	5.08E+06	2.45E+06	1.43E+06	3.50E+06	3.92E+05	2.14E+06		1.13E+06	1.38E+06
P35219		1.33E+06	4.46E+05							7.25E+05
P35221							8.60E+04			
P35232	2.45E+06	6.95E+07	4.72E+07	3.49E+07	3.07E+07	3.07E+07	2.17E+07	8.26E+06	9.43E+06	1.29E+07
P35237	6.47E+05	8.83E+06	6.20E+06	1.04E+07	9.37E+06	4.68E+06	2.39E+06	3.76E+05	1.89E+06	2.33E+06
P35250	9.52E+04	5.35E+06	4.94E+06	4.53E+05	1.30E+06	2.72E+06	2.97E+06	5.97E+04	2.55E+05	7.99E+05
P35606		5.12E+05	1.55E+06	3.63E+05	3.58E+05		4.71E+05			1.97E+05
P35658	1.43E+05	4.76E+06	2.44E+06	6.42E+05	8.92E+05	1.71E+06	1.43E+06		1.90E+05	1.86E+06
P35813		2.91E+06	2.09E+06		6.71E+05	7.43E+05	6.11E+05		2.93E+05	2.34E+05
P35914	3.06E+04	2.23E+05	7.15E+05	2.76E+05	5.24E+05			3.87E+04	1.81E+05	
P35998	1.22E+05	2.33E+07	2.21E+07	7.50E+06	7.73E+06	1.10E+07	1.12E+07		2.31E+06	6.37E+06
P36268							7.81E+05			
P36507	1.54E+04	7.37E+05	7.67E+05	1.93E+05	1.41E+05	7.01E+04	9.86E+04		5.06E+04	
P36551	2.01E+06	1.81E+07	6.93E+06	5.63E+06	6.76E+06	3.51E+06	5.19E+06	1.42E+06	4.76E+06	3.46E+06
P36578	4.65E+06	7.56E+07	6.31E+07	3.64E+07	3.23E+07	4.02E+07	3.54E+07	4.17E+06	1.12E+07	2.80E+07
P36873	5.13E+04	3.10E+06	2.27E+06	1.45E+04	1.58E+06	1.46E+06	1.29E+06		6.42E+05	1.74E+06
P36957	1.40E+05	1.10E+07	7.99E+06	5.07E+04	4.87E+06	4.39E+06	3.53E+06	6.64E+04	2.70E+06	6.03E+06

P37235		8.74E+05	2.60E+05							
P37268		8.41E+06	5.07E+06	4.75E+06	3.47E+06	3.71E+06	2.84E+06		1.02E+06	3.68E+06
P38117	3.11E+04	8.44E+06	4.73E+06	1.39E+07	1.30E+07	4.96E+06	2.67E+06	9.57E+05	5.90E+06	3.62E+06
P38570		2.58E+06	1.05E+06	8.89E+05	1.11E+06	7.75E+05	6.47E+05		1.67E+06	1.35E+06
P38606	5.77E+05	5.58E+07	4.10E+07	6.96E+06	1.55E+07	2.71E+07	2.08E+07	1.58E+06	5.56E+06	1.46E+07
P38919	1.29E+06	2.57E+07	1.76E+07	1.48E+07	1.16E+07	1.40E+07	1.13E+07	4.61E+06	4.94E+06	8.49E+06
P39019	8.91E+04	3.23E+06	3.38E+06	8.80E+06	3.92E+06	6.07E+06	3.80E+06	3.45E+06	2.20E+06	4.15E+06
P39023	1.31E+06	3.64E+07	3.29E+07	1.61E+07	1.24E+07	1.54E+07	1.79E+07	9.01E+05	4.55E+06	8.49E+06
P40222		1.36E+07	7.69E+06		6.01E+06	6.55E+06	4.64E+06	1.37E+06	2.85E+06	8.15E+06
P40227	8.64E+05	8.49E+07	5.96E+07	2.83E+07	3.24E+07	3.74E+07	2.62E+07	4.59E+06	1.20E+07	2.51E+07
P40425						3.69E+04	2.01E+04		7.48E+04	1.90E+04
P40429	4.67E+06	2.59E+07	2.24E+07	1.56E+07	7.70E+06	1.66E+07	2.22E+07	2.08E+06	3.52E+06	1.06E+07
P40616	1.60E+05	4.22E+06	3.96E+06	2.75E+06	3.88E+06	2.62E+06	9.20E+05		1.93E+06	2.97E+06
P40855		2.61E+05	7.46E+04		3.35E+05	1.81E+05			1.08E+05	1.49E+05
P40926	3.16E+05	4.99E+07	3.19E+07	7.23E+07	6.65E+07	2.05E+07	1.39E+07	4.25E+06	2.38E+07	2.30E+07
P40937		2.68E+06	1.64E+06		4.96E+05	1.62E+06	4.82E+05			3.55E+05
P41240		7.87E+05	3.43E+05	4.51E+05	1.61E+05	3.75E+05	5.14E+05			
P41440	1.76E+05	6.84E+05	2.61E+06			8.69E+05	1.50E+06	1.42E+05		
P42126		1.35E+06	1.45E+06	2.37E+06	1.86E+06	3.04E+05		2.31E+05	1.12E+06	8.72E+05
P42166	8.07E+03	9.28E+05	1.04E+06		4.52E+05	4.03E+05	1.05E+05			1.51E+06
P42167	5.58E+04	2.29E+06	1.81E+06	2.46E+06	3.79E+06	1.40E+06	1.74E+06	1.79E+06	2.11E+06	1.13E+06
P42224		3.74E+06	8.70E+05	3.33E+05	5.12E+05	1.26E+06	2.53E+06		1.87E+05	3.61E+05
P42285	7.10E+04	5.23E+06	3.26E+06		2.83E+05	1.30E+06	2.60E+06	4.11E+04	1.13E+05	6.46E+05
P42677	1.53E+05	5.52E+06	6.25E+06	1.81E+06	9.49E+05	1.53E+06	2.77E+06		3.55E+05	8.95E+05
P42704	2.43E+06	2.81E+08	2.04E+08	5.32E+07	8.60E+07	8.14E+07	1.02E+08	1.05E+07	3.33E+07	7.10E+07
P42858	5.37E+04	2.04E+06	1.39E+06	6.52E+06	3.03E+06	1.34E+06	9.03E+05	1.86E+06	1.15E+06	8.32E+05
P43007		4.31E+05	5.44E+05							
P43121		3.07E+06	2.41E+06	1.26E+06	2.03E+06	2.22E+06	1.10E+06		6.72E+05	1.26E+06
P43304	5.59E+06	4.91E+06	1.68E+06	8.83E+05	2.73E+06	3.79E+06	1.78E+06	3.44E+06	8.97E+06	1.27E+07
P43487	1.11E+06	1.06E+08	7.96E+07	2.11E+07	3.82E+07	3.36E+07	2.47E+07	4.43E+06	1.61E+07	2.43E+07

P43490		7.07E+05	1.05E+05	1.39E+06		1.57E+06	8.70E+05		1.53E+05	3.42E+05
P43897	1.27E+05	2.52E+06	2.80E+06	1.72E+06	1.61E+06	7.61E+05	1.42E+06	4.00E+04	5.21E+05	7.23E+05
P45974	1.18E+05	1.67E+07	1.01E+07	7.70E+06	1.13E+07	5.30E+06	4.33E+06	1.54E+05	3.76E+06	6.99E+06
P46013	3.28E+05	3.20E+06	3.19E+06	8.80E+04	1.04E+06	2.06E+06	2.83E+06	3.89E+03	2.86E+05	9.24E+05
P46087	5.26E+05	1.65E+06	3.66E+06	3.73E+05		7.16E+05	1.26E+05	8.59E+04	1.38E+05	
P46109	4.12E+05	2.26E+07	1.48E+07	1.39E+07	1.62E+07	8.31E+06	6.11E+06	6.31E+05	5.87E+06	9.65E+06
P46459		8.09E+05	7.55E+05		2.31E+05	2.50E+05	3.45E+05			2.95E+05
P46778	4.11E+05	1.18E+07	1.47E+07	1.20E+07	6.44E+06	6.65E+06	4.90E+06	2.26E+05	1.54E+06	5.79E+06
P46779	2.52E+06	1.18E+07	1.18E+07	6.77E+06	4.69E+06	4.71E+06	6.32E+06	5.21E+05	1.38E+06	3.04E+06
P46781	5.87E+06	5.40E+07	5.20E+07	3.51E+07	2.18E+07	3.47E+07	3.54E+07	4.86E+06	8.10E+06	2.33E+07
P46783	1.64E+05	6.88E+05	5.29E+05	1.02E+06	5.58E+05	1.03E+06	8.14E+05	4.61E+05	3.36E+05	
P46821		1.40E+06	1.50E+06	1.25E+06	8.52E+05	1.31E+06	1.31E+06		9.22E+05	1.26E+06
P46940	1.93E+05	9.16E+06	9.13E+06	3.33E+06	3.77E+06	4.60E+06	4.06E+06		1.13E+05	1.45E+06
P47897	4.99E+04	6.72E+06	5.74E+06	1.56E+06	1.53E+06	3.87E+06	2.67E+06	6.35E+04	6.66E+05	1.66E+06
P47929	1.55E+05						2.07E+06			
P48047	1.45E+05	1.07E+07	6.98E+06	2.10E+07	1.35E+07	8.51E+06	5.38E+06	8.21E+06	7.19E+06	4.70E+06
P48147	5.24E+03	1.01E+06	2.52E+05	5.54E+04	1.01E+05		1.60E+05	6.49E+03	3.59E+04	1.45E+05
P48426	6.05E+04	7.73E+05	4.48E+05	1.00E+05	2.67E+05	3.25E+05				
P48444	8.87E+04	5.66E+06	4.19E+06	2.34E+06	2.22E+06	2.69E+06	1.21E+06	2.41E+04	1.87E+05	4.79E+05
P48449		1.68E+06	9.87E+05	4.54E+05	4.22E+04	3.12E+05	7.80E+05	5.93E+05		7.51E+05
P48634		1.91E+05	1.33E+05		3.45E+04	1.35E+04	2.42E+04			
P48643	1.21E+06	1.10E+08	7.43E+07	3.10E+07	4.27E+07	4.50E+07	3.41E+07	3.60E+06	2.27E+07	3.20E+07
P48735	2.59E+05	2.06E+07	1.27E+07	4.72E+06	9.87E+06	3.65E+06	5.03E+06	1.16E+06	3.90E+06	4.33E+06
P49207	1.35E+06	1.32E+07	9.43E+06	4.56E+06	4.23E+06	7.84E+06	7.21E+06	6.50E+05	3.03E+06	3.52E+06
P49257				2.02E+05	1.31E+06	2.17E+05	2.58E+05	6.91E+04	8.89E+05	2.35E+05
P49321	4.83E+05	3.31E+07	2.18E+07	1.24E+07	3.87E+07	1.09E+07	1.11E+07	2.84E+06	1.58E+07	1.95E+07
P49368	1.16E+06	1.12E+08	7.80E+07	3.15E+07	4.44E+07	5.28E+07	4.57E+07	8.24E+06	1.98E+07	3.48E+07
P49406		8.22E+05	3.43E+05	5.29E+05		5.91E+05	2.12E+05		2.67E+05	
P49427		4.68E+05	4.04E+05		2.78E+05	2.43E+05	2.63E+05	3.09E+04		1.92E+05
P49593		1.14E+06	1.01E+06	9.43E+04	1.16E+05	1.28E+05	8.56E+05	3.69E+03	3.24E+05	2.03E+06

P49721		1.82E+06	1.16E+06	2.12E+06	1.15E+06	1.43E+06	1.61E+06		2.36E+05	6.13E+05
P49736	4.36E+05	3.89E+07	2.49E+07	1.46E+07	1.47E+07	1.61E+07	1.32E+07	7.89E+05	6.08E+06	9.94E+06
P49748		2.14E+05	3.85E+03	2.08E+05	1.40E+05		2.06E+05		8.41E+03	
P49755	8.04E+03			1.05E+06	3.53E+05	2.94E+05		2.99E+05	4.69E+05	4.59E+05
P49756	1.05E+05	6.17E+06	3.90E+06	7.04E+05	1.14E+06	1.42E+06	1.42E+06	4.24E+04	3.09E+05	9.03E+05
P49790	8.65E+04	3.05E+06	1.00E+06	2.04E+05	1.95E+05		2.81E+05			
P49792	7.24E+04	5.22E+06	3.78E+06	6.91E+05	3.69E+05	1.65E+06	3.23E+06	1.67E+05		
P49915	4.16E+05	3.29E+07	2.34E+07	7.01E+06	1.42E+07	1.27E+07	8.47E+06	1.32E+06	8.31E+06	1.11E+07
P50395	6.16E+04	1.10E+06	5.50E+05	1.04E+06		9.07E+05			2.56E+05	2.02E+05
P50402	2.49E+04	7.29E+05	3.57E+05	8.04E+04	2.53E+05	1.29E+05	7.87E+04	7.44E+03	1.04E+05	2.53E+05
P50453		1.56E+06	9.15E+05	3.04E+05	5.22E+05	1.73E+04	7.85E+03	1.02E+04		1.28E+05
P50552	4.31E+03	2.07E+05	1.62E+05	5.67E+04	5.66E+04	2.67E+04	3.75E+04		3.44E+04	1.97E+04
P50570	1.00E+05	3.82E+06	2.79E+06	4.81E+05	3.70E+05	2.28E+05	1.23E+06		6.22E+05	1.62E+06
P50914	1.11E+06	8.24E+06	9.30E+06	3.90E+06	2.68E+06	6.80E+06	7.19E+06		5.17E+05	5.29E+06
P50995		1.57E+06	7.50E+05	1.65E+05		3.66E+05				
P51003					2.19E+05	4.51E+05	8.71E+05			
P51149	2.66E+05	6.66E+06	4.62E+06	2.51E+07	7.59E+06	6.18E+06	3.68E+06	8.84E+06	4.80E+06	6.60E+06
P51532	3.42E+05	9.29E+06	5.55E+06	5.31E+05	3.37E+05	1.80E+06	2.56E+06		3.47E+05	3.29E+05
P51571		2.83E+06	2.64E+06	1.66E+06	1.12E+06	5.94E+05	1.19E+06		5.64E+05	5.92E+05
P51580		4.63E+05	1.82E+05		4.29E+05					
P51665	2.83E+05	1.10E+07	7.48E+06	3.94E+06	2.43E+06	4.44E+06	3.70E+06	9.77E+05	1.73E+06	3.15E+06
P51858	1.91E+05	2.73E+06	1.59E+06	2.25E+06	3.26E+06	5.69E+05	1.33E+06	1.83E+05	2.06E+06	4.09E+06
P51970								1.38E+05	9.57E+04	
P52272	3.90E+06	1.35E+08	8.48E+07	4.26E+07	5.70E+07	7.43E+07	5.51E+07	8.13E+06	3.03E+07	6.96E+07
P52292	5.20E+05	1.64E+07	2.05E+07	4.87E+06	6.74E+06	1.29E+07	1.03E+07	5.10E+05	2.26E+06	6.31E+06
P52294		5.21E+05	2.40E+05	1.12E+05	1.05E+05		1.75E+05			6.06E+04
P52597	7.13E+05	1.50E+07	1.11E+07	9.00E+06	8.95E+06	4.26E+06	4.97E+06	1.90E+06	5.98E+06	3.87E+06
P52701	3.75E+05	9.62E+06	1.07E+07	1.56E+06	1.88E+06	3.54E+06	4.07E+06	2.57E+05	6.84E+05	2.23E+06
P52732		3.47E+05	2.40E+05			2.89E+05				
P52758				3.53E+05						

P52788	1.80E+05	7.93E+05	9.45E+05	2.25E+06	1.98E+06	6.01E+05	3.77E+05	1.39E+05	1.20E+06	9.36E+05
P52789	5.01E+05	1.44E+07	1.02E+07	3.44E+06	4.48E+06	4.62E+06	2.72E+06	1.54E+05	1.25E+06	3.25E+06
P52907		7.68E+05	3.74E+05		4.68E+05					1.86E+05
P52948	5.37E+04	6.81E+05	8.60E+05	3.19E+04	1.54E+05	2.17E+05	8.59E+03	1.07E+05	1.22E+05	2.22E+05
P53004		6.01E+06	2.97E+06	1.56E+06	4.46E+06	1.69E+06	3.13E+06		1.40E+06	2.62E+06
P53007	2.82E+05	2.16E+07	1.66E+07	1.62E+07	1.48E+07	4.47E+06	4.92E+06	2.51E+06	8.16E+06	6.15E+06
P53365		7.08E+04	6.67E+04			1.72E+04	1.32E+04			8.93E+03
P53367		2.45E+06	1.80E+06	7.26E+05	3.65E+05	1.28E+06	9.53E+05		8.17E+05	1.54E+06
P53396	5.08E+06	3.94E+08	3.04E+08	2.68E+07	6.11E+07	1.42E+08	1.52E+08	6.18E+06	3.10E+07	7.08E+07
P53582	1.73E+04	6.68E+05	2.36E+05	3.52E+05		1.36E+05		1.54E+05	4.90E+04	4.44E+04
P53602		2.21E+06	1.32E+06	9.49E+05	9.57E+05	5.67E+04	5.84E+05	1.82E+05	8.17E+05	9.23E+05
P53621	1.82E+05	9.58E+06	9.81E+06	4.82E+06	3.96E+06	3.49E+06	3.06E+06		6.21E+05	9.06E+05
P53985	3.05E+04	6.96E+06	1.08E+07	5.70E+06	5.66E+06	6.62E+06	7.67E+06		1.56E+06	6.03E+06
P54136	1.43E+05	1.50E+07	1.14E+07	3.38E+06	3.31E+06	7.30E+06	4.85E+06	2.29E+05	1.97E+06	6.01E+06
P54578	2.77E+05	1.49E+07	9.52E+06	4.78E+06	5.39E+06	4.92E+06	6.44E+06	2.29E+05	2.96E+06	3.96E+06
P54619	8.87E+04	3.02E+06	2.10E+06	1.02E+06	3.95E+05	7.16E+05	5.31E+05	4.82E+03	5.33E+05	9.58E+05
P54819	3.64E+04	5.97E+06	3.12E+06	1.35E+07	9.15E+06	2.28E+06	2.38E+06	2.95E+06	4.46E+06	3.32E+06
P54886	3.35E+04	5.06E+06	3.29E+06	2.01E+06	1.26E+06	1.98E+06	1.58E+06		8.28E+04	1.10E+06
P54920		8.75E+05	5.64E+05	2.76E+05		1.98E+05	3.35E+05			1.12E+05
P55060	2.00E+06	8.52E+07	5.61E+07	2.93E+07	2.70E+07	3.84E+07	3.47E+07	3.38E+06	1.21E+07	2.71E+07
P55145				8.69E+05	3.52E+05			1.86E+06		
P55199		9.33E+04	8.58E+04							
P55735		2.64E+06	3.92E+06		4.54E+05	9.03E+05				5.83E+05
P55795		3.86E+06	3.44E+06	6.46E+05	1.19E+06	1.85E+06	4.59E+05		8.74E+05	8.02E+05
P55884	1.68E+05	2.78E+07	2.27E+07	3.61E+06	6.51E+06	1.63E+07	1.87E+07	1.53E+05	3.54E+06	1.07E+07
P55957		3.37E+06	1.82E+06	2.79E+06	2.28E+06	3.55E+05	1.14E+05	2.53E+04	8.89E+05	1.14E+06
P56134	2.46E+04			1.18E+06	6.93E+05	4.40E+05		1.44E+05	2.19E+05	
P56192	7.85E+05	1.44E+07	1.26E+07	5.11E+06	4.97E+06	4.35E+06	5.72E+06	1.83E+05	2.16E+06	2.03E+06
P56385	2.57E+04	9.29E+05	1.12E+06	4.16E+06	4.09E+06	1.68E+06	2.10E+06	3.54E+06	2.76E+06	8.98E+05
P56537	5.61E+05	3.73E+06	5.53E+06	7.95E+05	1.48E+06	3.27E+06	3.46E+06	2.57E+05	2.47E+05	1.14E+06

P56589		1.12E+06	5.13E+05			1.92E+05				
P56747		5.57E+05	1.10E+06	2.58E+05			2.11E+06	4.72E+04		1.01E+06
P57088	3.80E+05	3.16E+06	3.11E+06	4.86E+06	6.43E+05	3.66E+06	5.19E+06	4.14E+05	1.79E+05	5.34E+05
P57740	7.93E+04	2.64E+06	1.29E+06	3.14E+05	9.13E+05	2.98E+06	1.42E+06	1.13E+05	1.87E+05	5.10E+05
P59998	1.70E+05	3.35E+06	2.01E+06	4.33E+06	1.89E+06	1.55E+06	1.10E+06	5.03E+04	4.14E+05	6.26E+05
P60174	7.94E+04	5.34E+04	5.50E+04	4.07E+05	3.84E+04	1.52E+04	5.58E+04	7.94E+03	2.83E+04	5.52E+03
P60228	3.42E+05	1.58E+07	1.10E+07	5.34E+06	5.86E+06	7.87E+06	9.46E+06	3.21E+05	1.77E+06	4.10E+06
P60604	2.54E+04	1.51E+06	5.47E+05	2.13E+05	3.32E+05	2.64E+05	2.32E+05		2.12E+05	3.47E+05
P60842	1.56E+06	3.41E+07	2.78E+07	1.81E+07	1.12E+07	2.49E+07	1.54E+07	2.10E+06	3.95E+06	1.09E+07
P60866	1.63E+05	2.15E+07	1.68E+07	1.79E+07	1.08E+07	1.23E+07	1.33E+07	1.87E+06	5.15E+06	8.38E+06
P60953	5.19E+03	1.65E+05	2.56E+05	1.32E+06	2.00E+05	1.80E+05	3.42E+05	3.35E+05		2.15E+05
P60981	1.03E+05	1.39E+07	4.56E+06	4.52E+06	6.15E+06	2.36E+06	3.42E+06		4.24E+06	5.19E+06
P61009	8.07E+04	1.74E+06	2.99E+06	1.78E+06	5.52E+05	1.36E+06	1.03E+06	2.93E+05		3.44E+05
P61020	6.33E+04	5.39E+05	3.91E+05		2.52E+05					
P61026	1.37E+04	1.47E+06	7.14E+05	3.16E+06	4.92E+05	2.32E+05	3.22E+05	2.80E+05	1.34E+06	3.86E+05
P61077	1.61E+05	7.38E+06	5.40E+06	4.27E+06	6.32E+06	4.84E+06	3.53E+06	6.87E+05	2.10E+06	2.45E+06
P61086		5.22E+06	2.32E+06	2.71E+06	2.30E+06	1.17E+06	7.42E+05		1.04E+06	1.50E+06
P61163		1.96E+06	1.48E+06	1.44E+05	1.42E+06	1.72E+06	1.31E+06		3.72E+05	6.98E+05
P61201		3.55E+06	2.79E+06		4.21E+05	6.90E+05	2.93E+05		3.44E+05	7.36E+05
P61224	1.24E+05	6.59E+06	3.82E+06	1.52E+07	5.31E+06	4.53E+06	2.93E+06	4.02E+06	5.10E+06	4.14E+06
P61254	2.37E+05	7.67E+06	4.85E+06	3.34E+06	1.82E+06	2.63E+06	2.78E+06	3.68E+05	1.03E+06	8.11E+05
P61289	1.05E+05	1.21E+07	9.50E+06	3.92E+06	1.03E+07	7.80E+06	3.93E+06	4.14E+05	4.55E+06	8.61E+06
P61313	3.28E+06	2.29E+07	2.13E+07	8.29E+06	6.31E+06	1.30E+07	1.16E+07	7.32E+05	2.81E+06	8.79E+06
P61353	7.71E+05	1.09E+07	9.15E+06	5.89E+06	5.25E+06	5.46E+06	6.68E+06	6.75E+05	1.81E+06	2.82E+06
P61513	6.58E+04	1.68E+06	1.13E+06	1.04E+06	5.55E+05	6.55E+05	6.66E+05	1.92E+04	1.51E+05	3.16E+05
P61586				4.70E+05	5.24E+03	4.64E+03		1.34E+05		
P61604	2.39E+05	3.00E+07	2.30E+07	4.20E+07	3.45E+07	1.43E+07	1.01E+07	3.84E+06	1.37E+07	1.86E+07
P61978	1.94E+05	2.60E+07	1.22E+07	1.76E+07	1.04E+07	8.97E+06	7.33E+06	1.82E+06	6.77E+06	6.75E+06
P61981	1.57E+05	7.99E+06	4.35E+06	9.78E+05	3.26E+06	2.43E+06	2.53E+06	1.32E+05	5.51E+05	8.97E+05
P62070		3.82E+05	2.75E+05	3.18E+05	9.91E+05	2.45E+05		6.67E+04		

P62072		8.61E+05	5.73E+05	7.36E+05	4.99E+05	2.56E+05	4.19E+05	3.18E+05	3.11E+05	
P62081	4.86E+05	1.31E+07	6.04E+06	4.86E+06	5.26E+06	7.32E+06	3.74E+06	1.29E+05	3.17E+06	4.19E+06
P62136	9.25E+04	1.73E+06	9.52E+05	5.17E+05	6.90E+05	1.33E+06	1.69E+06	1.15E+05	6.59E+05	3.55E+06
P62140		1.68E+06	1.56E+06	1.52E+06	9.10E+05	8.40E+05	6.31E+05		1.73E+05	5.16E+05
P62191	1.75E+05	1.39E+07	1.34E+07	1.30E+06	3.25E+06	5.02E+06	3.79E+06		6.45E+05	3.09E+06
P62195	3.38E+05	2.27E+07	9.23E+06	3.90E+06	5.37E+06	8.75E+06	7.06E+06	3.34E+05	2.91E+06	4.85E+06
P62241	4.20E+06	3.87E+07	4.29E+07	2.84E+07	1.06E+07	2.08E+07	1.84E+07	2.04E+06	4.99E+06	1.01E+07
P62244		8.50E+06	5.34E+06	2.23E+06	1.76E+06	2.41E+06	2.28E+06	2.16E+05		
P62258	6.80E+05	2.48E+07	1.96E+07	1.05E+07	1.31E+07	1.19E+07	1.12E+07	2.60E+05	4.68E+06	8.47E+06
P62266	1.15E+06	1.45E+07	9.92E+06	4.35E+06	4.25E+06	8.92E+06	8.89E+06	4.85E+05	1.84E+06	3.55E+06
P62269	3.29E+05	1.05E+07	8.65E+06	1.21E+07	6.07E+06	1.24E+07	7.90E+06	2.03E+06	2.94E+06	5.14E+06
P62277	8.08E+05	1.10E+07	9.06E+06	5.62E+06	4.50E+06	7.71E+06	5.65E+06	1.14E+06	8.04E+05	4.15E+06
P62280	2.51E+06	4.18E+07	4.30E+07	1.41E+07	1.34E+07	2.22E+07	2.16E+07	1.89E+06	6.69E+06	8.24E+06
P62304		2.78E+06	2.55E+06	1.94E+06	1.51E+06	2.30E+06	1.17E+06		1.11E+06	8.82E+05
P62306	3.51E+04	1.67E+06	1.09E+06	1.43E+06	2.32E+06	8.21E+05	9.73E+05	1.22E+05	2.93E+05	3.06E+05
P62314	7.20E+04	4.67E+06	3.53E+06	1.04E+06	1.65E+06	9.97E+05	1.69E+06		6.54E+05	1.12E+06
P62318	5.21E+05	3.27E+06	2.04E+06	5.56E+06	3.93E+06	5.47E+05	3.28E+06	2.62E+06	2.24E+06	2.65E+06
P62491				2.20E+05	8.32E+04					
P62753	2.87E+06	3.55E+07	2.78E+07	1.51E+07	9.42E+06	2.17E+07	1.69E+07	1.58E+06	4.25E+06	8.82E+06
P62829	2.55E+06	3.69E+07	2.96E+07	1.96E+07	1.28E+07	1.94E+07	1.96E+07	1.96E+06	6.26E+06	1.08E+07
P62851	7.11E+05	3.71E+07	2.27E+07	2.03E+07	3.25E+07	2.09E+07	1.53E+07	5.46E+06	1.49E+07	2.46E+07
P62857	4.64E+05	1.85E+07	1.23E+07	2.33E+07	1.93E+07	1.65E+07	7.48E+06	3.22E+06	1.15E+07	1.07E+07
P62873		1.45E+06	1.99E+06	2.83E+06	9.77E+05	2.30E+05	8.30E+05		1.02E+05	7.51E+05
P62875	3.33E+04	4.64E+05	4.55E+05			3.59E+05				2.59E+05
P62877		9.48E+05	4.68E+05	2.31E+05	1.86E+05	1.03E+05	1.37E+05			
P62879		7.14E+05	2.16E+06	2.21E+06	6.81E+05	2.34E+05	3.71E+05		1.17E+05	5.65E+05
P62891				2.36E+05						
P62906	3.12E+05	1.73E+07	1.17E+07	8.15E+06	1.29E+07	1.25E+07	9.06E+06	1.08E+06	4.79E+06	7.59E+06
P62979		6.81E+05	3.81E+05							
P62987		8.87E+03	1.03E+04	1.21E+04	8.74E+03	4.05E+03				2.37E+03

P62993	4.42E+05	6.38E+06	4.38E+06	6.02E+06	4.24E+06	3.24E+06	1.46E+06	8.21E+05	3.58E+06	3.00E+06
P62995	7.17E+05	4.54E+06	3.11E+06	4.01E+06	1.40E+06	6.30E+05	4.96E+05	3.32E+05	1.74E+06	1.46E+06
P63000		1.02E+06	5.81E+05	5.07E+05	4.96E+05	3.43E+05		1.03E+05	7.50E+04	3.58E+05
P63010	1.19E+05	4.44E+06	2.77E+06		7.86E+05	5.71E+05	2.37E+06		4.16E+05	
P63104	1.21E+05	2.69E+07	1.65E+07	7.85E+06	7.93E+06	1.06E+07	1.02E+07	7.42E+04	3.11E+06	5.54E+06
P63151	3.33E+05	8.98E+06	6.79E+06	6.46E+06	8.74E+06	7.06E+06	5.50E+06	6.56E+04	3.15E+06	6.92E+06
P63167		1.14E+06	2.78E+05			1.19E+06				
P63208	1.40E+05	9.13E+06	4.93E+06	4.23E+06	4.38E+06	1.96E+06	1.10E+06	6.95E+05	1.45E+06	1.67E+06
P63272		2.04E+06	1.12E+06	7.35E+05	1.13E+06	1.60E+06	7.01E+05		1.18E+06	1.14E+06
P67775		5.05E+05	7.83E+05	5.99E+05	3.52E+05	3.19E+05	2.97E+05			
P67809	1.09E+05	9.52E+05	1.42E+06	4.66E+06	4.59E+05	6.12E+05	1.78E+05	6.41E+05	6.82E+03	5.13E+05
P67870	1.21E+05	4.59E+06	4.02E+06		2.58E+06	3.15E+06	4.77E+06	1.87E+05	7.89E+05	2.43E+06
P68036	1.14E+06	7.53E+07	5.14E+07	2.59E+07	4.69E+07	3.51E+07	1.94E+07	3.02E+06	1.86E+07	2.73E+07
P68366	3.43E+05	1.45E+07	8.87E+06	4.44E+06	4.66E+06	1.01E+07	4.66E+06		4.66E+06	6.27E+06
P68371	1.32E+05	8.38E+06	6.05E+06	1.62E+06	1.79E+06	1.78E+06	1.42E+06	1.75E+05	8.27E+05	1.31E+06
P68402	1.29E+04	6.05E+05	3.82E+05	3.86E+05						
P78344	8.60E+04	5.60E+06	4.16E+06	1.06E+05		4.90E+06	3.93E+05		3.99E+04	2.70E+04
P78347	5.53E+05	1.54E+07	1.55E+07	1.31E+06	2.63E+06	6.94E+06	5.29E+06	9.77E+04	1.08E+06	3.68E+06
P78371	1.43E+06	6.93E+07	4.91E+07	2.44E+07	4.68E+07	3.19E+07	2.52E+07	3.04E+06	2.19E+07	3.60E+07
P78417	3.51E+05	1.68E+07	8.47E+06	9.16E+06	1.43E+07	1.03E+06	1.21E+07	4.85E+05	7.38E+06	8.30E+06
P78527	5.87E+06	6.33E+07	7.46E+07	3.69E+07	2.14E+07	3.01E+07	4.30E+07	4.64E+06	7.92E+06	1.99E+07
P80217	3.31E+04	4.34E+05	1.21E+05	2.92E+05	1.56E+05	5.39E+04	7.89E+04	6.99E+03	5.80E+04	7.38E+04
P82663		5.88E+05	5.61E+05	1.78E+04		9.21E+05	5.45E+05			
P82673		2.17E+06	1.25E+06	3.25E+05	7.22E+05	1.20E+06	7.46E+05		1.64E+05	2.35E+05
P82675		1.15E+06	6.24E+05		4.18E+05	1.67E+06	4.03E+05			2.50E+05
P82912		7.95E+05	9.08E+05		3.59E+05	1.48E+05	1.41E+05			
P82914	1.19E+05	2.98E+06	1.55E+06	2.92E+05	5.27E+05	9.37E+05	7.44E+05	4.69E+04	2.86E+05	6.32E+04
P82932		2.98E+06	2.42E+06	1.27E+06	1.62E+06	2.33E+06	1.47E+06	1.72E+05	1.28E+06	1.20E+06
P82933	1.43E+05	3.22E+06	2.69E+06	7.58E+05	1.59E+06	1.96E+06	1.63E+06		2.44E+05	1.37E+06
P83731	2.33E+06	2.78E+07	2.28E+07	1.10E+07	7.71E+06	1.61E+07	1.25E+07	7.74E+05	1.51E+06	3.54E+06

P84098	2.24E+06	2.48E+07	2.20E+07	1.82E+07	1.06E+07	7.54E+06	8.88E+06	3.12E+06	5.48E+06	7.41E+06
P84243		4.51E+06	4.59E+05		1.18E+06	5.46E+06			2.63E+05	6.49E+05
P98179				2.59E+05				7.44E+04		
Q00534		2.02E+06	1.92E+06		2.38E+06	1.32E+06	3.11E+05			5.45E+05
Q00577		1.50E+06	9.50E+05	8.56E+04	7.88E+04	3.67E+05	1.17E+05	4.15E+04	4.04E+04	2.85E+05
Q00796	1.08E+05	2.46E+06	1.17E+06	4.54E+05	9.45E+05	3.56E+05	5.81E+05	6.16E+04	4.14E+05	2.85E+05
Q00839	5.29E+06	1.27E+08	8.40E+07	3.98E+07	5.34E+07	4.39E+07	3.99E+07	6.69E+06	1.73E+07	3.33E+07
Q01081	5.75E+05	1.40E+07	5.38E+06	3.34E+06	6.58E+06	3.20E+06	3.39E+06	5.27E+05	2.25E+06	3.63E+06
Q01082	1.76E+04	5.55E+06	2.90E+06	1.39E+06	2.42E+06	9.27E+05	6.81E+05		1.28E+05	1.45E+05
Q01085	8.06E+04	7.74E+05	4.11E+05	8.06E+05	2.54E+05	2.00E+05	2.50E+05		1.26E+05	2.92E+05
Q01105	7.40E+05	7.81E+06	5.88E+06	1.20E+07	6.09E+06	3.99E+06	3.07E+06	1.75E+06	4.01E+06	2.63E+06
Q01196		1.81E+05	8.15E+04			4.88E+04	3.06E+04			6.51E+03
Q01650	4.34E+06	1.74E+07	2.10E+07	3.45E+07	7.30E+06	1.39E+07	1.18E+07	4.34E+06	3.49E+06	6.86E+06
Q01658		2.28E+06	6.26E+05	8.34E+05			2.61E+05		1.24E+05	1.49E+05
Q01780	4.37E+04	6.73E+06	2.72E+06	9.07E+05	2.43E+06	1.94E+06	2.78E+06		9.22E+05	3.50E+06
Q01968		1.77E+06	1.74E+06	4.82E+05	6.23E+05		5.04E+05			
Q02218		6.07E+06	4.54E+06		1.49E+06	1.56E+06	6.80E+05		5.78E+05	1.85E+06
Q02543	2.06E+06	1.59E+07	2.34E+07	3.30E+06	4.33E+06	8.77E+06	1.22E+07	8.70E+05	1.48E+06	6.05E+06
Q02790	3.09E+04	5.68E+06	1.89E+06	2.75E+06	6.92E+05	7.66E+05	4.26E+05		4.02E+05	4.30E+05
Q02880	9.94E+04	3.10E+06	1.07E+06	1.68E+05	1.99E+05	1.99E+06	1.17E+06		3.08E+05	7.73E+05
Q02978		8.21E+06	5.76E+06	4.03E+06	2.62E+06	2.60E+06	1.97E+06	8.70E+05	1.93E+06	1.25E+06
Q03111	8.48E+03	5.21E+04	5.30E+04				9.33E+03			
Q03252	1.85E+05	8.92E+06	8.12E+06	4.34E+06	8.35E+06	1.66E+06	6.82E+06	8.29E+05	4.93E+06	8.71E+06
Q03701	2.34E+05	4.83E+06	1.52E+06		4.35E+05	1.78E+06	8.28E+05		2.26E+05	2.64E+05
Q04323						4.78E+05	7.85E+05			
Q04637	6.45E+05	3.64E+07	2.58E+07	6.62E+06	4.90E+06	1.53E+07	1.44E+07	6.39E+05	1.19E+06	6.52E+06
Q04760	7.15E+04			6.34E+05		5.04E+05	6.54E+05		4.72E+05	6.60E+05
Q04837	8.66E+03	2.33E+06	1.38E+06	4.83E+06	3.13E+06	2.67E+05	1.03E+05	3.38E+05	4.89E+05	4.28E+05
Q04864		4.35E+04	4.45E+04							
Q04917	2.00E+05	8.59E+06	3.77E+06	1.81E+06	2.41E+06	2.59E+06	1.15E+06	5.57E+04	2.23E+06	1.95E+06

Q06124		5.94E+06	4.19E+06	4.44E+06	4.63E+06	1.15E+06	8.24E+05	9.70E+05	1.93E+06	1.16E+06
Q06187	3.74E+04	3.05E+06	1.77E+06	8.28E+05	6.27E+05	4.89E+05	1.25E+06	1.45E+04	2.09E+05	2.14E+06
Q06830	1.51E+07	6.64E+08	4.16E+08	4.16E+08	4.17E+08	4.51E+08	2.90E+08	3.83E+07	1.64E+08	2.88E+08
Q07812		3.84E+06	1.89E+06	1.85E+05	3.97E+05	2.98E+05	3.15E+05	2.68E+04		3.81E+05
Q07973		1.31E+06	1.05E+06	7.79E+05	3.35E+05	5.79E+05	5.93E+05			
Q08170	1.51E+04	4.07E+05	3.21E+05	9.24E+04	1.33E+05	7.92E+04	1.36E+04		1.28E+04	2.69E+04
Q08211	2.83E+06	1.05E+08	7.12E+07	4.33E+07	2.85E+07	4.49E+07	3.92E+07	5.23E+06	1.11E+07	2.72E+07
Q08257	7.60E+04	1.13E+06	1.34E+05	7.36E+05	8.66E+05	3.00E+04	2.22E+05	2.07E+04	9.22E+04	5.66E+04
Q08378		4.56E+04	3.61E+04				1.53E+04			
Q08722		7.84E+06	7.05E+06	3.45E+06	1.25E+06	6.45E+06	7.41E+06	3.66E+05	5.61E+05	1.98E+06
Q08752	6.72E+04	1.58E+06	1.13E+06	8.52E+05	3.22E+05			4.99E+04	3.25E+05	3.54E+05
Q08945	1.48E+05	8.92E+06	7.37E+06	2.77E+06	4.61E+06	6.79E+06	7.14E+06	6.12E+05	3.33E+06	5.18E+06
Q08AM6		3.63E+05	4.72E+05		1.24E+05	1.46E+05				
Q08J23	1.20E+05	1.65E+07	1.05E+07	4.78E+06	8.41E+06	7.58E+06	9.37E+06	2.52E+05	2.74E+06	4.29E+06
Q09161		9.17E+05	3.08E+05							
Q09666							3.40E+05			
Q0VDF9		1.11E+06	7.89E+05		3.12E+05	2.08E+05	5.87E+05			
Q10567	4.49E+04	4.10E+07	2.49E+07	1.27E+07	1.55E+07	8.35E+06	2.06E+07	1.42E+06	3.34E+06	1.43E+07
Q12769		1.91E+06	8.18E+05	9.42E+04		1.09E+06	5.36E+05			5.43E+04
Q12788	9.47E+04	8.19E+06	1.73E+06		4.38E+05	4.17E+06	2.40E+05			
Q12789	6.78E+04	7.32E+05	5.56E+05		6.93E+04	5.86E+04				
Q12872	7.73E+03	5.70E+05	9.97E+04				9.46E+04			
Q12904		2.72E+05	7.98E+05			3.72E+05	2.58E+05			
Q12907	1.18E+05	9.18E+06	1.09E+06	2.99E+06	1.59E+06		1.54E+06	1.34E+06	7.86E+05	3.01E+05
Q12972		2.13E+05	1.52E+05							
Q12981		4.50E+05	8.90E+05	3.62E+05		7.38E+05	1.77E+06	5.03E+04		1.02E+06
Q12996		1.84E+06	1.00E+06	2.18E+05	4.35E+05	1.64E+06				
Q13042		5.44E+05	2.29E+05				1.39E+05			7.00E+04
Q13043		6.84E+05	5.27E+05	7.29E+04	2.88E+05					
Q13084		1.07E+06	2.23E+05		2.01E+05	1.70E+05	1.86E+04	3.92E+03	1.62E+04	1.60E+06

Q13085	1.14E+05	2.57E+06	2.61E+06	7.92E+05	5.25E+05	2.12E+06	5.54E+05	9.63E+04	4.59E+05	1.33E+06
Q13098		4.10E+06	1.11E+06		9.37E+05	7.21E+05	2.62E+06			7.25E+05
Q13144	2.35E+04	6.49E+06	3.74E+06	1.47E+06	1.37E+06	9.65E+05	2.07E+06	1.49E+05	1.14E+06	1.21E+06
Q13151	1.66E+05	8.01E+06	3.85E+06	1.64E+06	3.09E+06	3.03E+06	2.79E+06	4.55E+05	4.75E+05	7.36E+04
Q13177	6.39E+04	3.81E+06	2.67E+06	1.76E+06		2.40E+06	1.15E+06			
Q13185	6.73E+05	8.03E+06	2.66E+06	9.21E+06	5.40E+06	5.41E+06	1.80E+06	3.07E+05	1.13E+06	2.28E+06
Q13200	2.20E+05	2.33E+07	1.76E+07	1.83E+06	6.33E+06	6.07E+06	1.13E+07		1.05E+06	3.99E+06
Q13206		3.31E+05	3.14E+05	6.02E+04		6.35E+04				
Q13242	2.13E+05	5.19E+06	3.29E+06	6.14E+06	3.43E+06	2.00E+06	9.06E+05	2.50E+05	2.19E+06	2.34E+06
Q13243	7.27E+04	2.06E+06	1.36E+06	1.50E+06	3.26E+06	3.52E+05	4.23E+05	2.19E+05	1.41E+06	1.56E+06
Q13257	2.79E+04	2.14E+06	1.93E+06	6.83E+05	2.40E+05	1.19E+05	2.89E+05	1.02E+05	9.37E+04	4.43E+05
Q13263	6.07E+05	4.55E+06	3.82E+06	2.24E+06	3.60E+06	2.82E+06	2.59E+06	1.11E+04	2.13E+06	1.85E+05
Q13308	4.21E+04	3.10E+06	9.79E+06	6.92E+05	2.19E+06	3.24E+06	3.55E+06		2.28E+06	5.03E+06
Q13347	3.80E+05	7.28E+06	6.50E+06	1.94E+05	5.54E+05	5.00E+06	5.56E+06			9.45E+05
Q13356	2.34E+05	3.87E+06	1.57E+06	6.12E+05	4.42E+05	1.00E+06			6.06E+05	4.09E+05
Q13405		1.88E+05	2.16E+05		1.37E+05					
Q13423	2.61E+04	7.86E+06	5.22E+06	9.26E+06	7.10E+06	4.62E+06	3.47E+06	3.06E+06	2.84E+06	1.86E+06
Q13433		3.80E+04	3.62E+04		1.18E+04	2.34E+04	3.07E+05			3.12E+03
Q13443	1.78E+05	5.61E+05	6.70E+05	4.78E+05			4.41E+05			
Q13451	1.74E+05	1.08E+07	7.90E+06	2.55E+06	5.27E+06	3.66E+06	4.65E+06	5.65E+05	2.48E+06	2.47E+06
Q13492	2.62E+04	9.34E+06	6.10E+06	1.95E+06	4.38E+06	3.26E+06	3.38E+06	6.15E+04	8.55E+05	2.64E+06
Q13547	8.68E+04	2.27E+06	1.03E+06			3.08E+05	3.92E+05		2.35E+05	
Q13564		1.17E+06	3.74E+05		2.08E+05		8.58E+04			5.03E+04
Q13576	2.27E+05	8.73E+06	4.82E+06	4.01E+06	1.39E+06	2.04E+06	1.69E+06	1.98E+05	6.18E+05	6.72E+05
Q13596		3.22E+06	7.49E+05	1.73E+05	5.16E+05	1.19E+05	5.35E+05			1.05E+05
Q13601		1.11E+06	8.08E+05	3.66E+05	5.73E+05					
Q13617		3.37E+06	2.05E+06		6.24E+05	3.07E+05	1.82E+05			6.05E+04
Q13618		1.36E+06	7.35E+05	3.29E+05	3.81E+05	2.78E+05			1.97E+05	1.72E+05
Q13619	2.74E+04	1.21E+06	1.36E+06	2.75E+05		6.05E+05	2.45E+05			
Q13769		2.46E+06	5.62E+05		1.57E+05	2.52E+05			5.59E+05	2.51E+05

Q13823	5.17E+04	1.59E+06	7.61E+05	5.46E+04	1.83E+05	4.59E+05	3.52E+04			6.65E+04
Q13838	1.08E+05	1.81E+07	7.12E+06	3.86E+06	4.68E+06	3.82E+06	2.25E+06	4.75E+04	8.04E+05	2.52E+06
Q13868		2.67E+06	2.25E+06		3.75E+05	1.40E+06	3.51E+05		3.12E+05	3.15E+05
Q13895	3.89E+06	6.90E+05	3.29E+06	4.15E+06		2.24E+06	2.40E+05	3.91E+05		
Q13907	4.67E+03	2.57E+05	3.00E+05	1.21E+05			6.04E+04			
Q14008	5.78E+05	3.50E+07	2.44E+07	8.57E+06	1.36E+07	1.83E+07	1.19E+07	1.19E+06	4.96E+06	1.03E+07
Q14011				1.14E+06	3.80E+05		3.67E+05	6.09E+05		
Q14061	5.47E+04	2.85E+04	3.23E+04	7.67E+04	3.30E+04	8.72E+03	1.33E+04	2.53E+04	6.49E+04	
Q14103	4.53E+05	1.85E+07	1.30E+07	8.72E+06	1.11E+07	7.18E+06	6.34E+06	1.61E+06	4.47E+06	3.50E+06
Q14118		7.26E+05	1.50E+06	2.85E+05	4.00E+05	9.78E+05	1.90E+06	1.32E+05		5.61E+05
Q14126		3.75E+05	8.69E+05			3.91E+05	4.52E+05			
Q14137	5.63E+04	1.80E+06	3.34E+05		5.45E+04	1.18E+06	6.35E+05	8.43E+03	5.01E+05	1.47E+06
Q14145	5.04E+04	1.35E+06	2.21E+06	4.18E+05	5.85E+05	1.63E+06	1.03E+06			9.47E+05
Q14152	5.08E+05	1.82E+07	1.86E+07	4.27E+06	3.87E+06	1.08E+07	9.58E+06	2.57E+05	5.00E+05	4.20E+06
Q14157		2.14E+05	1.96E+05	8.33E+04	5.10E+04	5.62E+04	4.13E+03		2.72E+04	3.22E+04
Q14165		1.92E+05	1.09E+05	1.39E+05	5.30E+04		4.68E+04	5.07E+04	8.94E+04	3.58E+04
Q14166		1.45E+07	1.09E+07	1.62E+06	3.91E+06	7.47E+06	2.29E+06	3.85E+04	2.57E+06	3.55E+06
Q14191		2.54E+05	1.52E+05							
Q14232	2.13E+04	7.37E+06	4.71E+06	2.45E+06	1.54E+06	4.25E+06	3.31E+06	6.86E+04	6.25E+05	9.90E+05
Q14254	8.50E+05	2.76E+06	3.00E+06	1.08E+05	3.81E+05	4.99E+05	2.74E+06		2.73E+04	1.27E+06
Q14318	7.70E+04	6.51E+06	2.85E+06	1.96E+06	3.16E+06	1.68E+06	2.04E+05	1.99E+04	1.06E+06	4.49E+05
Q14376		1.24E+06	1.60E+05							
Q14444	2.54E+05	1.10E+07	7.55E+06	8.08E+05	2.91E+06	7.18E+06	4.16E+06	2.34E+05	6.02E+05	2.80E+06
Q14498	6.22E+05	6.33E+06	1.52E+06	1.43E+06	1.68E+06	8.70E+05	3.44E+06		4.90E+05	2.18E+06
Q14574										
Q14657		1.81E+05	5.22E+04							
Q14676		7.55E+05	2.49E+05				2.30E+05			
Q14687		7.18E+04	2.50E+04		4.90E+04	2.38E+04	1.28E+04		2.62E+04	
Q14690	8.65E+05	3.45E+06	1.64E+06	6.48E+05	1.56E+05	1.70E+06	9.37E+05			
Q14692		2.15E+06	1.51E+06	1.22E+05		4.17E+04				

Q14694	1.26E+04	2.38E+06	1.80E+06	1.57E+05	4.29E+05	8.56E+05	4.37E+05			2.19E+05
Q14697	3.71E+05	1.94E+07	1.38E+07	2.35E+07	2.04E+07	8.16E+06	8.72E+06	3.83E+06	7.47E+06	1.19E+07
Q14739	1.27E+06	1.37E+07	8.74E+06	5.45E+06	4.24E+06	5.00E+06	5.26E+06	1.42E+06	1.45E+06	2.97E+06
Q14966		2.60E+04	1.83E+04			2.07E+04	2.08E+03			
Q14974	7.31E+05	6.54E+07	4.50E+07	1.42E+07	2.49E+07	2.48E+07	1.92E+07	1.99E+06	7.19E+06	1.24E+07
Q14C86	1.17E+04	4.61E+06	3.46E+06	7.18E+05	1.05E+06	1.64E+06	3.14E+06		6.38E+05	1.73E+06
Q14CX7		8.60E+05	3.22E+05			3.26E+05				
Q15014						8.55E+05	7.93E+05			
Q15020	4.07E+04	5.45E+06	2.32E+06	1.73E+05	1.37E+05	1.23E+06	4.63E+05			5.11E+05
Q15021	5.37E+04	3.28E+06	2.30E+06	8.25E+05	9.76E+05	2.02E+06	1.31E+06		3.83E+05	3.77E+05
Q15022		6.63E+05	4.45E+05			2.83E+05				
Q15042		6.11E+05	6.32E+05		2.52E+05	2.90E+05	4.24E+05		1.42E+05	2.16E+05
Q15046	3.24E+04	8.12E+06	7.02E+06	5.59E+06	6.44E+06	6.04E+06	3.57E+06	6.42E+04	2.57E+06	6.10E+06
Q15061	1.07E+05	5.87E+06	4.38E+06	7.27E+05	2.59E+05	2.14E+06	6.15E+05	7.61E+05	2.48E+05	2.11E+05
Q15084	8.12E+04	1.04E+07	8.01E+06	1.76E+07	1.06E+07	7.20E+06	4.23E+06	7.03E+05	6.01E+06	4.60E+06
Q15102	1.36E+05	2.32E+06	2.24E+06	8.85E+05	3.23E+06	1.23E+06	4.89E+05		8.77E+05	1.14E+06
Q15121				1.59E+05	2.86E+05	8.17E+04				
Q15181	1.94E+04	1.55E+07	9.49E+06	3.69E+06	6.18E+06	5.51E+06	5.30E+06	6.31E+04	1.41E+06	4.88E+06
Q15269	4.50E+04	1.95E+06	2.22E+06	4.86E+05	8.52E+04	6.80E+05	1.01E+05	1.70E+04	6.60E+05	1.45E+05
Q15291	1.05E+04	7.13E+05	2.75E+05							
Q15365	7.88E+05	3.49E+07	2.69E+07	1.16E+07	1.61E+07	1.19E+07	1.49E+07	8.45E+05	5.42E+06	1.38E+07
Q15366										
Q15388	5.09E+04	7.94E+06	4.66E+06	1.36E+07	5.60E+06	4.15E+06	5.74E+06	2.18E+06	3.42E+06	5.11E+06
Q15392	8.07E+04	1.55E+06	1.41E+06	6.02E+05	3.72E+05	4.58E+05	5.95E+05	1.79E+04	2.20E+05	1.79E+06
Q15393	5.39E+05	3.08E+07	2.24E+07	8.09E+06	8.49E+06	1.13E+07	9.55E+06	4.65E+05	4.95E+06	9.89E+06
Q15397	2.66E+04	1.67E+06	1.29E+06	6.23E+05	8.18E+05	1.33E+06	6.09E+05	9.86E+04	3.08E+05	4.75E+05
Q15424	3.93E+05	7.80E+06	5.29E+06	2.01E+05	1.46E+06	2.53E+06	1.68E+06	3.37E+05	1.09E+06	1.31E+06
Q15427	2.09E+04	2.27E+06	1.58E+06			9.76E+05	1.83E+05			
Q15437	1.88E+04	1.93E+06	5.57E+05	3.46E+05	1.25E+06	2.45E+05	1.81E+06		2.28E+06	1.50E+06
Q15459	5.57E+04	6.65E+06	4.35E+06	6.46E+04	2.06E+06	2.63E+06	1.66E+06	6.97E+04	1.20E+06	1.75E+06

Q15637		3.12E+06	4.09E+05	1.87E+05	1.90E+06	1.27E+05	1.89E+06		8.85E+04	8.18E+05
Q15651		1.08E+05	1.91E+05	3.44E+05	1.65E+05			5.16E+04	2.53E+04	
Q15691	7.05E+04			3.63E+05	1.02E+06					
Q15738	2.88E+04	4.38E+06	3.38E+06	4.93E+06	4.34E+06	2.04E+06	1.58E+06	4.40E+05	9.57E+05	2.30E+06
Q15762		6.59E+05	3.35E+05		4.41E+05	2.05E+05	5.20E+05	1.72E+05	3.32E+05	2.34E+05
Q15828							4.59E+05			
Q15843		6.10E+05	5.18E+05	6.08E+06	9.19E+05	2.16E+05	2.90E+05	1.02E+06	7.41E+05	5.72E+05
Q15907				3.67E+05				8.92E+05		
Q15910				1.83E+05	3.00E+06	2.32E+06	4.84E+05	4.97E+05	1.53E+06	
Q16186	4.37E+03	4.30E+06	2.95E+06	3.62E+05	5.00E+05	2.17E+06	1.11E+06	7.84E+03	4.05E+05	1.46E+06
Q16531		8.12E+05	8.28E+05	2.17E+06		9.48E+05	8.15E+05	1.43E+05		3.75E+05
Q16555		9.15E+06	5.92E+06	5.18E+05	2.67E+06	3.56E+06	2.52E+06	5.58E+05	7.38E+05	4.24E+06
Q16629	5.80E+06	7.63E+06	8.37E+06	9.27E+06	5.02E+06	2.83E+06	4.07E+06	3.64E+06	3.06E+06	3.92E+06
Q16658	3.31E+05	2.59E+07	1.78E+07	5.57E+06	1.25E+07	7.66E+06	4.90E+06	1.87E+05	6.10E+06	1.31E+07
Q16698	5.50E+04	3.45E+06	2.60E+06	1.32E+06	2.80E+06	1.80E+06	2.70E+06	7.43E+04	2.13E+05	
Q16718	8.01E+03	2.87E+06	1.54E+06	2.74E+06	1.53E+06	1.16E+06	2.99E+04	6.74E+04	6.68E+05	6.99E+05
Q16740		1.38E+06	2.23E+06	1.01E+06	1.20E+06	6.96E+04	3.50E+05	2.89E+04	9.36E+05	1.16E+05
Q16891	1.02E+05	2.14E+07	1.48E+07	4.96E+06	8.06E+06	7.73E+06	8.06E+06	5.13E+05	2.53E+06	5.15E+06
Q29RF7		1.14E+06	7.95E+05	4.91E+04		1.15E+05	2.16E+05			4.82E+04
Q2Q1W2		8.05E+05	3.14E+05							
Q2VPA4		1.79E+06	1.83E+06	2.01E+06	8.95E+05					1.27E+06
Q32MZ4		4.60E+06	1.36E+06		2.58E+06	1.78E+06	1.58E+06		1.25E+05	4.06E+05
Q32Q12		1.68E+06	1.30E+06	4.09E+05	1.20E+06	3.06E+06			4.97E+05	3.62E+05
Q49AN9	4.82E+05	2.72E+06	2.07E+06	1.84E+06	1.28E+06	6.78E+05	2.36E+06	3.18E+05	9.40E+05	9.17E+05
Q4G0F5		1.56E+05	1.12E+05							
Q4R9M9				6.72E+05	3.84E+05					2.10E+05
Q53EL6		2.09E+06	4.60E+05		9.11E+05		2.74E+05			
Q53GS7		1.38E+06	7.50E+05			4.34E+05	1.03E+06			1.37E+06
Q53GS9				4.27E+05	2.57E+05	1.20E+04	5.23E+05	7.80E+03	1.56E+04	1.29E+05
Q53R41		1.96E+05	1.46E+05	1.30E+05		4.17E+04				

Q53S33	1.19E+04			3.06E+05	2.86E+05	6.70E+04		9.12E+04		
Q58FF6	1.76E+05	1.20E+07	5.93E+06	3.77E+06	4.35E+06	5.21E+06	1.78E+06	4.09E+05	1.22E+06	
Q5BJF2	1.42E+05	2.38E+06	1.58E+06	1.24E+06	4.96E+05	1.01E+06	6.63E+05	7.54E+04	3.46E+05	5.38E+05
Q5BKZ1	5.61E+04	9.08E+05	9.63E+05	7.02E+05	2.14E+05	1.06E+06	3.33E+04	2.68E+04		
Q5HYI8		3.47E+05	2.43E+05		6.34E+04					
Q5JP53		5.20E+06	2.63E+06		1.02E+06	1.17E+06	9.42E+05			
Q5JPH6		1.47E+06	5.61E+05	1.85E+05	6.46E+04					7.12E+04
Q5JSL0				1.03E+05					8.51E+04	
Q5JTH9	3.76E+05	8.04E+06	4.05E+06	7.18E+05	9.57E+05	2.33E+06	1.19E+06	1.01E+05	2.52E+05	6.38E+05
Q5JTZ9		9.18E+05	5.39E+05		1.91E+04	3.44E+04	3.15E+04			3.32E+05
Q5JVF3		1.97E+04	1.35E+04	2.54E+04	7.56E+03	9.79E+03				
Q5JY01		1.82E+05	5.03E+05		2.03E+05					
Q5QJE6	2.00E+04	1.85E+06	3.38E+05	2.21E+05	6.87E+04	2.16E+05	9.14E+04			
Q5QNW6		6.99E+05	7.30E+05	5.32E+06	1.86E+06	1.35E+06	8.48E+05	1.16E+06	1.69E+06	6.04E+05
Q5QP56										6.78E+05
Q5QPL9	5.17E+05	1.53E+06	1.10E+06	8.47E+05	8.65E+05	5.67E+05	5.74E+05	5.65E+05	1.37E+06	4.21E+05
Q5RKV6		2.93E+06	1.45E+06	2.36E+05		6.79E+05	7.13E+05		2.63E+05	6.50E+05
Q5SRE5		1.16E+05	1.73E+05	2.97E+04	1.91E+04	3.23E+04	3.02E+04	3.56E+03		
Q5SSJ5	2.19E+05	6.82E+06	3.53E+06	1.72E+06	2.19E+06	4.30E+06	4.36E+06	1.48E+05	4.59E+05	1.57E+06
Q5T3Q7	6.46E+05	5.97E+06	3.49E+06	9.10E+05		2.95E+06	2.94E+05			
Q5T440				2.87E+04	4.49E+04	2.07E+04	8.37E+03	2.89E+04	3.39E+04	2.27E+04
Q5T4U5		2.32E+06	1.75E+06	2.75E+06	2.64E+06	4.03E+05	3.78E+05	4.43E+05	1.23E+06	2.48E+06
Q5T6F2		7.88E+04	6.18E+04				2.05E+05			1.15E+05
Q5T6V5	5.87E+03	1.35E+05	7.43E+04	1.65E+05				5.49E+03	3.41E+04	
Q5T6W2										
Q5T749	8.94E+04			1.05E+04			4.54E+05	2.17E+04		
Q5T750	1.30E+05	6.16E+05	9.31E+05		7.97E+05	6.77E+05	8.63E+05	1.26E+05	1.24E+06	1.05E+06
Q5T8P6		1.23E+06	6.52E+05	2.06E+04	3.61E+04	5.23E+05	2.64E+05		1.55E+04	2.07E+04
Q5T9A4	2.70E+04				2.72E+05	3.69E+05	2.79E+05	3.82E+04	1.87E+05	1.98E+05
Q5TBH6		3.33E+05	2.65E+05							

Q5TCT4	1.34E+04	7.49E+06	4.39E+06	2.70E+06	2.67E+06	2.75E+06	2.75E+06			2.00E+06
Q5TFE4	1.08E+05	4.16E+06	4.90E+06	1.46E+06	2.05E+06	4.16E+06	6.53E+06	3.91E+03	9.61E+05	4.07E+06
Q5U5X0		1.36E+06	5.93E+05	4.27E+05	4.84E+05	3.58E+05	1.32E+06			
Q5UIP0	4.94E+05	3.85E+06	2.80E+06	1.49E+06	3.53E+05	1.59E+06	8.04E+05	5.07E+04	1.55E+06	6.43E+05
Q5VT52		1.32E+06	3.07E+05				2.93E+05			3.40E+05
Q5VUB5		4.94E+04	5.46E+04							
Q5VWZ2		2.06E+06	2.97E+05	3.18E+05	1.51E+06				5.28E+05	3.90E+05
Q5VXN0	1.44E+05	3.53E+06	1.93E+06		1.47E+05	1.73E+06				
Q5W0H4	7.84E+04	4.09E+06	2.93E+06	2.29E+06	2.67E+06	2.65E+06	1.70E+06	2.91E+05	1.37E+06	6.02E+05
Q68DQ2	9.88E+04	1.76E+06	1.12E+06	1.20E+06	7.53E+05	3.24E+05	2.47E+05	2.25E+05	3.47E+05	1.55E+05
Q68DW7		4.06E+05	3.47E+05		1.56E+05					
Q6GTS8							3.66E+05			
Q6IN84		3.63E+04	2.94E+04			2.01E+04	5.22E+03		6.85E+03	1.12E+04
Q6JBY9		4.33E+05	3.22E+05		5.43E+05	1.23E+05	1.64E+05		1.65E+05	3.16E+05
Q6NUQ4		1.93E+06	1.53E+06	1.20E+06	1.16E+06	4.97E+05			1.04E+05	
Q6P1J9		7.59E+05	2.89E+05		1.59E+05	1.31E+05			7.82E+04	
Q6P2E9	6.64E+04	7.79E+06	6.54E+06	8.15E+05	5.33E+05	4.40E+06	1.94E+06	1.52E+05	3.58E+05	7.11E+05
Q6P2Q9	3.07E+05	1.48E+07	9.29E+06	2.89E+06	4.60E+06	9.45E+06	6.65E+06	7.45E+05	2.79E+06	2.04E+06
Q6P9B9		4.58E+05	5.39E+05	1.47E+05			2.14E+05		7.27E+04	9.66E+04
Q6PD62		9.70E+05	1.83E+06	2.38E+05	4.97E+05	7.01E+05	7.61E+05			6.72E+05
Q6PI48		1.47E+06	1.94E+06	9.01E+05	1.21E+06	9.83E+05	2.64E+05			5.71E+05
Q6PKG0		1.46E+07	7.17E+06	3.73E+05	5.38E+06	9.48E+06	5.17E+06	2.22E+05	3.13E+06	6.07E+06
Q6STE5		5.69E+05	2.97E+05		1.24E+05	2.16E+05	1.71E+05	4.78E+04		1.24E+05
Q6UW02		1.79E+05	8.38E+04			1.67E+04			9.56E+03	
Q6UWP7	3.17E+04	1.90E+06	1.63E+06	6.74E+05	3.37E+05	3.50E+05	4.27E+05		8.91E+04	6.16E+05
Q6VN20		2.66E+05	2.23E+05		4.38E+04					
Q6ZU65		5.16E+04	1.79E+04				6.16E+03			
Q6ZVX7							1.29E+05			
Q71DI3		5.74E+06	1.42E+06	1.23E+06	2.14E+06	1.08E+07	1.06E+06		1.37E+06	1.34E+06
Q71RC2		4.07E+05	2.14E+05	3.07E+05	1.76E+05	1.81E+06	5.08E+05			

Q71UI9	3.53E+05	6.88E+06	5.06E+06	5.84E+07	9.27E+06	7.29E+06	5.49E+06	7.39E+06	7.45E+06	7.42E+06
Q7KZ85		6.47E+04	9.54E+04		3.02E+04	1.44E+04	2.28E+04		9.12E+04	3.07E+04
Q7L1W4		6.82E+05	3.10E+05							
Q7L2E3	2.11E+05	7.10E+06	6.31E+06	1.67E+06	2.45E+06	5.08E+06	3.61E+06	2.07E+05	8.85E+05	1.48E+06
Q7L2H7		5.98E+06	3.77E+06	2.40E+06	1.98E+06	2.24E+06	1.17E+06		3.54E+05	1.07E+06
Q7L3T8		5.29E+05	7.16E+05	7.50E+05	5.08E+05	3.49E+05	7.16E+05			
Q7L576		9.89E+04	8.93E+04							
Q7L5D6	1.16E+06	1.95E+06	2.13E+06	2.80E+06		6.68E+05	2.76E+05			2.78E+05
Q7L8J4		1.45E+06	1.72E+06	3.28E+05	5.32E+05	5.68E+05	8.36E+05		1.54E+05	8.45E+05
Q7L9L4	4.22E+04	1.36E+06	1.34E+06	4.48E+05	9.20E+05	1.29E+06	8.51E+05		8.47E+05	1.96E+05
Q7LBC6	2.90E+04	2.86E+06	9.22E+05		4.55E+05	1.75E+05	1.10E+05	2.30E+05		
Q7Z2T5		5.13E+05	1.49E+06	4.73E+05	8.64E+05	1.09E+06	1.51E+06		3.89E+05	8.17E+05
Q7Z2W4	3.33E+05	1.05E+07	5.94E+06	2.19E+06	1.71E+06	3.21E+06	1.66E+06	1.03E+05	7.32E+05	2.71E+06
Q7Z2W9	6.10E+04	1.79E+06	2.06E+06	3.36E+05	4.93E+05	1.41E+05	1.14E+06	8.45E+04	6.72E+04	4.33E+05
Q7Z3K3		1.77E+05	1.54E+05			2.57E+04	1.69E+04			6.98E+03
Q7Z434		5.59E+05	2.01E+06	1.55E+05	5.68E+05	5.98E+05	1.50E+05			1.19E+05
Q7Z460		5.62E+05	4.10E+05		1.53E+05	1.27E+06				
Q7Z4Q2	5.44E+04	9.46E+05	6.78E+05	2.44E+05	1.39E+05	1.75E+05	8.42E+04	9.40E+04	9.52E+04	6.67E+04
Q7Z4S6	5.36E+04	3.97E+05	4.28E+05			2.60E+05				
Q7Z4V5		2.77E+06	1.75E+06	4.34E+05	5.07E+05	7.31E+05	5.24E+05	4.34E+04	4.27E+05	7.01E+05
Q7Z4W1	3.37E+04	6.10E+06	3.88E+06	1.44E+06	5.49E+06	2.06E+06	2.25E+06	2.66E+05	2.87E+06	5.27E+06
Q7Z5P9	7.45E+06	1.77E+07	2.49E+07	3.98E+07	1.09E+07	1.81E+07	7.62E+06	5.84E+06	1.02E+07	1.38E+07
Q7Z6Z7		2.13E+06	7.75E+05	5.78E+05	5.43E+05	7.70E+05	3.86E+05			6.45E+03
Q7Z7K6		2.10E+04	1.28E+04				5.83E+03			
Q86SE5	1.13E+05	8.22E+05	4.94E+05	5.81E+05	4.34E+05	3.77E+05	2.71E+05	1.32E+05		3.22E+05
Q86SX6		8.46E+05	3.35E+05	6.92E+05	4.54E+05	3.11E+05				6.48E+05
Q86U28		7.47E+05	1.40E+06	6.76E+05	4.00E+05	4.06E+05	1.90E+06	1.99E+05		5.61E+05
Q86U90		2.57E+06	2.43E+06		4.30E+05	6.18E+05	1.36E+06		2.30E+05	3.81E+05
Q86UP2		2.14E+05	2.22E+05		1.09E+05	6.44E+04	3.03E+04		7.29E+03	3.41E+04
Q86V81		6.97E+05	3.66E+05	6.86E+06	3.24E+06	6.41E+05	2.34E+06	2.61E+06	2.42E+06	2.70E+06

Q86VM9		8.20E+04	4.83E+04							
Q86VY4		3.74E+05	2.55E+05		1.37E+04					
Q86W42	1.16E+04	1.88E+06	2.48E+05	4.49E+05	3.65E+05	2.05E+05	2.02E+05			1.18E+05
Q86WX3				8.62E+05						
Q86X27		6.92E+05	6.60E+05			7.87E+05	8.92E+05			6.67E+05
Q86X29		1.50E+05	2.65E+05			1.11E+05	2.19E+04		1.16E+04	
Q86X55	3.31E+04	4.67E+06	3.58E+06		9.45E+05	8.03E+05	1.41E+06		1.05E+06	1.57E+06
Q86XC5		1.53E+05	1.01E+05	1.17E+05						
Q86XX4	7.56E+03	2.02E+05	2.17E+05			7.04E+04				
Q86Y82		1.83E+05	2.79E+05	6.51E+04	1.34E+05	5.49E+04	6.56E+04	5.25E+04	4.30E+04	
Q86YN1		6.54E+05	3.82E+05	2.76E+05	1.39E+05	2.21E+05	2.73E+05			
Q86YP4	2.79E+04	2.05E+06	1.38E+06	8.45E+04	1.04E+05	1.79E+06	6.05E+05		2.59E+05	3.76E+05
Q8IUR7		2.59E+05	8.20E+04				7.23E+04			
Q8IV08	6.72E+04	5.02E+06	4.10E+06	8.58E+05	1.65E+06	2.03E+06	3.12E+06	1.01E+04	9.35E+05	2.49E+06
Q8IVM0	1.45E+04	5.24E+05	5.63E+05	2.93E+05	2.36E+05	6.35E+04	1.22E+05		3.03E+05	8.45E+04
Q8IWA0		6.44E+05	2.80E+05			3.70E+05				
Q8IWT6						3.70E+05				
Q8IWX8	1.41E+05	1.06E+07	8.70E+06	6.18E+06	6.85E+06	7.77E+06	5.97E+06	5.91E+05	4.58E+06	5.66E+06
Q8IX12	1.22E+05	6.46E+06	7.55E+06	6.28E+04	8.25E+04	2.48E+06	1.93E+06		1.76E+04	1.25E+06
Q8IXI1		8.64E+05	1.35E+05							
Q8IY81	5.94E+05	1.64E+06	1.53E+06	1.41E+05	2.74E+05	5.38E+05	3.24E+05			
Q8IZ69	4.38E+05	2.49E+06	2.61E+06	3.06E+05	8.63E+05	2.16E+06	3.43E+06	3.67E+05	1.81E+06	1.56E+06
Q8IZ81	4.78E+04	1.78E+06	1.56E+06	8.46E+05	1.18E+06	2.32E+05	1.65E+06	8.76E+04	1.33E+05	8.18E+05
Q8IZL8		1.33E+06	6.72E+05	2.95E+04	2.50E+05	3.30E+05	6.81E+04			1.34E+05
Q8N0U8		4.91E+05	2.52E+05			3.57E+05				
Q8N0Y7		3.99E+05	3.55E+05	4.56E+05			3.12E+05			
Q8N163	4.13E+04	9.53E+06	5.10E+06	6.51E+05	2.93E+06	3.79E+06	2.70E+06	1.35E+05	7.78E+05	2.42E+06
Q8N392		2.08E+05	8.73E+04							
Q8N3D4		3.28E+04	2.04E+04							
Q8N5K1	3.75E+05	5.71E+06	4.55E+06	9.35E+06	1.03E+07	1.88E+06	1.55E+06	2.78E+06	3.78E+06	3.26E+06

Q8N6M0		6.87E+05	3.46E+05		5.15E+05	7.69E+05	4.38E+04	1.22E+04	9.55E+04	4.65E+05
Q8N766		2.38E+06	9.34E+05	7.77E+05	8.48E+05	1.00E+06	5.33E+05		6.64E+05	4.46E+05
Q8N8Q8					4.74E+04			1.23E+04	2.88E+04	
Q8NBI5		4.41E+05	3.83E+05			8.01E+05				
Q8NBX0	8.69E+04	1.92E+06	2.70E+06		1.58E+06	1.25E+06	2.58E+06	8.47E+05	6.97E+05	1.46E+06
Q8ND24	4.94E+04	9.32E+05	3.80E+05	1.15E+05	4.07E+05	1.82E+05			4.87E+04	
Q8NDC0					1.77E+06					
Q8NE01		3.55E+05	4.08E+05		1.96E+04	7.29E+05	3.00E+05		3.90E+03	
Q8NE71	3.06E+05	8.75E+06	4.64E+06	1.25E+06	3.57E+06	2.37E+06	2.40E+06	1.14E+04	1.20E+06	1.13E+06
Q8NEJ9		1.11E+05	8.71E+04	3.33E+05	1.02E+05	1.36E+05				
Q8NEZ5		1.59E+06	1.85E+06		1.33E+06	8.99E+05	2.38E+05		8.26E+05	5.94E+05
Q8NF37		4.07E+05	5.64E+05	1.83E+05	1.52E+05					
Q8NFQ8	6.29E+03	9.83E+05	7.97E+05	1.70E+05	3.29E+05	3.61E+05	1.62E+05		1.81E+05	2.18E+05
Q8NFU5		9.68E+06	5.17E+06	4.46E+06	3.39E+06	2.26E+06	3.63E+06		1.06E+06	3.30E+06
Q8NGR6		1.81E+06	2.38E+06	2.14E+07	4.82E+06	7.55E+06	4.12E+06	7.12E+05	2.45E+06	3.86E+06
Q8NI27	4.63E+04	4.35E+06	2.27E+06	3.15E+05	1.84E+04	1.65E+06	1.27E+06	1.68E+05	8.04E+05	2.90E+04
Q8NI51							3.42E+04	2.20E+04	3.21E+04	
Q8TAA5	1.24E+04	9.32E+05	1.83E+05	1.52E+05	2.31E+05	1.95E+05	1.42E+05			6.82E+04
Q8TAQ2	6.46E+03	8.74E+04	8.25E+03		9.20E+04	5.95E+03	5.29E+03	6.07E+03		
Q8TB61		1.17E+05	1.35E+05							
Q8TBQ9				5.46E+05	2.59E+05	1.90E+05		9.39E+04		
Q8TC07	5.62E+04	6.56E+05	4.73E+05		1.60E+05	3.10E+05	4.29E+05		9.00E+04	
Q8TDD1	4.30E+05	2.39E+06	1.99E+06	5.44E+05	7.76E+05	9.45E+05	1.11E+06	2.00E+05		
Q8TDN6	6.64E+05	3.65E+06	2.10E+06	4.01E+05	2.65E+05	2.53E+06	1.08E+06	1.30E+05	2.72E+05	1.68E+05
Q8TDW0		3.84E+05	5.78E+05		1.53E+05	8.48E+05				
Q8TEM1	3.58E+05	1.52E+06	9.66E+05	5.82E+04	1.95E+05	3.86E+05	2.95E+05		1.13E+05	6.52E+04
Q8TEQ6	8.17E+04	2.81E+06	2.27E+06	3.09E+05	8.59E+05	1.17E+06	1.38E+06		4.03E+05	9.22E+05
Q8TEX9	2.16E+05	2.58E+07	1.98E+07	9.31E+06	7.08E+06	8.79E+06	1.25E+07	7.54E+05	4.15E+06	7.93E+06
Q8WTR4				3.98E+05				1.34E+05	4.78E+05	4.51E+05
Q8WTT2	2.48E+05	2.05E+06	9.54E+05	4.01E+05	3.92E+05	9.29E+05	8.34E+04	1.74E+05	4.05E+05	4.93E+04

Q8WUA4	1.57E+04	1.42E+05	4.86E+04		2.48E+04	2.35E+04	5.95E+03	2.96E+03	7.33E+03	9.26E+03
Q8WUM0	7.68E+03	2.50E+06	1.64E+06		4.29E+04	7.41E+05	8.08E+05			1.94E+05
Q8WUX1	1.09E+05	3.61E+05	1.59E+06	1.14E+05			2.38E+06		5.47E+04	
Q8WVV4	1.81E+04						1.96E+05			
Q8WVY7	1.74E+04	1.51E+06	1.85E+06	1.37E+06	4.75E+05	1.04E+06	6.06E+05		1.67E+05	2.49E+05
Q8WW12		1.02E+05	5.22E+04							
Q8WWM7		3.05E+06	1.62E+06		1.55E+06	1.35E+06	1.21E+06		6.11E+05	2.41E+06
Q8WXX5	1.19E+06	4.82E+06	3.42E+06	3.00E+06	2.56E+06	2.41E+06	3.12E+06	8.24E+05	2.19E+06	3.03E+06
Q8WYP5		4.63E+05	2.61E+05	4.19E+05	2.82E+05	2.65E+05			2.47E+05	
Q8WYQ5		2.63E+05	2.39E+05							
Q8WZ42	4.32E+05			3.28E+06			2.28E+06	5.37E+05		3.22E+06
Q92499	1.75E+05	1.10E+07	9.51E+06	9.58E+05	2.26E+06	5.71E+06	4.91E+06	8.55E+05	1.37E+06	1.19E+06
Q92504		3.61E+05	2.85E+05	6.58E+04	8.07E+04	5.78E+04	1.14E+05		2.83E+04	1.75E+04
Q92526		2.37E+06	2.33E+06	7.54E+05	6.33E+05	2.50E+06	1.62E+06		5.66E+05	7.28E+05
Q92530	6.74E+04	1.98E+06	2.20E+06	2.41E+06	1.42E+06	2.40E+06	1.31E+06		4.01E+05	8.30E+05
Q92542		1.63E+06	3.65E+06	9.62E+05	9.59E+05	1.75E+06	2.23E+06		4.65E+05	9.56E+05
Q92572	7.41E+03	8.91E+05	6.58E+05		2.19E+05	5.33E+04			8.72E+04	4.30E+04
Q92598	7.00E+05	4.83E+07	3.02E+07	1.40E+07	2.15E+07	3.03E+07	1.62E+07	8.57E+05	7.35E+06	1.67E+07
Q92609		1.01E+05	9.74E+04		6.60E+03	1.69E+04	2.07E+04			
Q92616	4.85E+05	4.36E+07	3.30E+07	1.20E+07	1.10E+07	1.84E+07	1.96E+07	7.14E+05	4.93E+06	9.70E+06
Q92620		2.49E+05	2.56E+05							
Q92621	4.61E+05	3.62E+06	2.43E+06	1.62E+06		5.88E+05	1.72E+06	6.92E+05	4.26E+04	
Q92665		2.35E+06	1.19E+06		8.11E+05	1.26E+06	2.58E+05		3.49E+05	2.83E+05
Q92686		1.01E+05	3.11E+04	2.17E+04				8.07E+03		
Q92688	2.18E+05	1.59E+06	1.69E+06	2.00E+06	1.36E+06	1.35E+06	1.06E+06		1.16E+05	2.27E+05
Q92734	1.10E+05	5.54E+05	5.46E+05			7.34E+05	2.95E+05			1.60E+05
Q92766	2.15E+04	1.60E+06	1.55E+06		3.80E+05		1.34E+06		9.67E+04	1.43E+06
Q92769	9.76E+04	1.45E+06	1.12E+06			1.14E+06	7.27E+05		2.13E+05	4.74E+05
Q92797	2.12E+04	5.74E+06	4.54E+06	2.11E+06	7.54E+05	1.65E+06	1.09E+06	1.04E+05	1.09E+06	8.64E+05
Q92833		1.37E+04	1.55E+04							

Q92841	1.32E+06	3.04E+07	2.10E+07	1.50E+07	1.33E+07	1.71E+07	1.31E+07	2.78E+06	1.03E+07	1.58E+07
Q92878	3.35E+04	4.65E+05	2.73E+05			1.08E+05				
Q92888		1.70E+06	9.62E+05	2.84E+05	8.40E+05	4.64E+05	6.15E+05			5.19E+05
Q92900	4.45E+04	1.04E+06	1.24E+06	4.94E+05	3.14E+05	2.59E+05	1.67E+05		8.56E+04	2.75E+05
Q92905		2.61E+06	1.00E+06	4.26E+05	7.48E+05	3.18E+05	9.76E+05		2.65E+05	3.49E+05
Q92917		5.38E+05	1.82E+05			4.99E+04	4.80E+04		7.73E+03	
Q92922	1.94E+04	1.48E+06	4.77E+05	1.02E+05	1.02E+05	1.83E+05	4.70E+04	1.20E+04	1.19E+05	3.51E+04
Q92945	8.00E+05	7.54E+07	5.08E+07	1.56E+07	3.60E+07	2.98E+07	2.94E+07	3.18E+06	1.19E+07	2.78E+07
Q92947	3.42E+04	1.92E+06	7.57E+05	6.76E+05	9.60E+05	7.80E+05	4.04E+05		3.63E+05	4.30E+05
Q92973	2.83E+05	1.69E+07	8.86E+06	2.41E+06	1.92E+06	5.29E+06	4.74E+06	2.50E+05	9.74E+05	2.55E+06
Q92990		7.63E+05	4.21E+05	1.07E+05	1.01E+05	3.51E+05				1.06E+05
Q93050	3.43E+04	1.17E+06	1.66E+06	9.90E+05		1.33E+06	1.03E+05	2.08E+05		7.89E+05
Q93074		3.14E+04	4.08E+04							
Q93077		2.07E+06	1.46E+06	1.04E+07	2.52E+06	9.73E+05	1.69E+06	3.25E+05	4.00E+05	4.19E+05
Q969E2		5.49E+05	4.17E+05		2.15E+05	3.06E+05		6.34E+04	1.45E+05	2.12E+05
Q969T9		1.07E+06	1.10E+06	7.92E+05	1.01E+06		3.44E+05	3.39E+05	2.97E+05	4.05E+05
Q969U7		1.82E+06	1.03E+06		3.49E+05	1.19E+05			6.57E+05	3.83E+05
Q969V3	2.44E+04	1.81E+06	6.48E+05	3.27E+05	7.57E+04	3.67E+05		6.18E+04		
Q969Z0		6.84E+06	5.55E+06	1.93E+06	1.07E+06	1.56E+06	3.05E+06	3.22E+04	4.36E+05	8.24E+05
Q96A33	1.08E+04	2.35E+06	1.25E+06	1.29E+06	1.24E+06	2.88E+05	1.01E+06	1.24E+05	3.78E+05	1.83E+06
Q96A35		3.80E+05	2.42E+05							
Q96AB3	1.13E+05	1.86E+06	5.55E+05		1.81E+05					
Q96AE4	4.15E+04	2.62E+05	1.77E+06	1.26E+06	2.55E+06	1.68E+04	1.81E+06	4.91E+05	1.07E+06	1.82E+06
Q96AG4	1.76E+05	2.60E+06	1.93E+06	8.32E+06	4.81E+06	2.03E+06	4.33E+06	2.12E+06	2.36E+06	6.09E+06
Q96AP7		2.00E+06	2.15E+06	5.42E+05	4.69E+05	1.29E+06	2.62E+05		2.94E+05	9.10E+05
Q96CP2		1.48E+05	1.31E+05		6.28E+04				5.66E+04	4.51E+04
Q96CS3		4.09E+05	2.17E+05	4.55E+05	5.98E+05	3.00E+05	2.67E+05		1.09E+05	
Q96CW1	1.41E+04	1.99E+06	1.37E+06	1.03E+06	4.48E+05	8.89E+05	7.55E+05			3.03E+05
Q96DG6	5.29E+05	1.62E+07	3.97E+06	4.72E+06	5.19E+06	1.67E+06	4.07E+06	1.66E+05	1.29E+06	7.62E+05
Q96DI7	4.73E+04	9.51E+05	4.98E+05		2.17E+05	4.65E+05	3.81E+05		2.09E+05	

Q96DV4		1.87E+06	1.43E+06		6.14E+05	7.10E+05	4.95E+05		3.22E+05	4.10E+05
Q96EP5		4.97E+06	2.63E+06	1.48E+06	4.90E+06	1.25E+06	1.32E+06		1.35E+06	2.99E+06
Q96EY1						2.20E+05				
Q96EY7	2.48E+04	4.26E+06	3.93E+06	1.69E+05	7.57E+05	1.26E+06	5.16E+05		1.02E+06	1.27E+05
Q96F86	8.87E+04	9.97E+05	6.92E+05	1.24E+05	2.51E+04	3.40E+05	8.95E+04		2.96E+04	8.04E+05
Q96FJ2		1.73E+06	7.30E+05		6.49E+05	3.93E+05	5.76E+05		1.44E+05	
Q96FN5	1.49E+06	6.27E+05	1.02E+06	1.71E+06	5.84E+05	8.68E+05		3.60E+05		
Q96FV9	2.83E+05	6.41E+06	4.89E+06	5.48E+05	1.72E+06	8.86E+05	2.57E+05		1.23E+05	7.87E+05
Q96G03	2.10E+04	2.02E+06	2.37E+06		4.28E+05	7.51E+05	1.21E+06		3.58E+05	4.19E+05
Q96GQ7	4.92E+04	1.26E+06	3.27E+05	1.82E+05	1.02E+05	5.55E+04	2.48E+05	8.77E+04		
Q96HP4	9.88E+03	2.18E+05	7.89E+04	7.64E+04	1.75E+05					
Q96HR9		1.28E+06	9.50E+05	1.36E+06	5.14E+05	3.96E+05	1.58E+05	3.78E+05	8.61E+05	4.57E+05
Q96I25		5.99E+06	5.54E+06	1.14E+06	3.34E+06	4.25E+06	5.13E+06		1.87E+06	2.90E+06
Q96I99	8.51E+03	4.22E+06	1.40E+06	1.70E+06	2.18E+06	8.39E+05	4.26E+04		1.07E+06	1.80E+06
Q96J01	1.59E+05	2.10E+06	1.67E+06	1.07E+06	2.66E+05	2.97E+05	1.41E+06		1.55E+06	2.83E+06
Q96JB3	1.44E+05	2.09E+06	1.03E+06		2.58E+05	5.98E+05	6.33E+05			6.47E+05
Q96JB5		2.01E+06	6.90E+05	5.42E+05	6.76E+05	1.67E+04	1.25E+05		3.77E+05	1.25E+05
Q96JC9		7.22E+04	4.30E+04				1.23E+04			1.08E+04
Q96JH7		1.60E+05	9.81E+04	8.77E+04				4.07E+04		
Q96K76		9.44E+05	2.18E+05							
Q96KP1		3.39E+05	2.24E+05	2.44E+05	2.28E+05					
Q96KR1	1.25E+05	3.26E+06	6.36E+05	3.27E+06		4.82E+05	2.25E+06			3.93E+05
Q96L12	2.95E+05					4.44E+05				
Q96L93	3.55E+05			2.10E+06		4.26E+05		1.55E+06	1.13E+06	
Q96N66	2.03E+04	2.30E+06	5.32E+05	1.99E+05	2.06E+05	3.29E+05	4.66E+05		1.28E+05	2.38E+05
Q96P70	2.09E+04	2.50E+06	2.50E+06	1.40E+05	1.54E+05	6.82E+05	1.75E+05		8.51E+04	9.68E+04
Q96PE2	2.49E+05	7.32E+05	2.22E+06	1.81E+06	3.74E+06		8.19E+05		1.11E+06	1.59E+06
Q96Q05		1.95E+04	1.11E+04							
Q96QK1		1.15E+07	5.88E+06	5.31E+05	2.35E+06	3.88E+06	3.01E+06		7.60E+05	2.14E+06
Q96R06		5.21E+04	4.32E+04			2.82E+04	1.93E+04			

Q96RS6	3.86E+05	6.59E+06	3.33E+06	3.47E+06	2.57E+06	5.50E+05	3.54E+06	3.18E+05	3.34E+06	8.31E+05
Q96T23	1.02E+04	8.88E+05	3.86E+05	5.30E+04	2.24E+05	1.83E+05	9.93E+04		1.60E+05	7.72E+04
Q96T76		2.37E+05	2.31E+05			1.86E+05	1.39E+05			
Q99442		2.31E+05	1.90E+05	4.46E+05	3.10E+05	3.89E+04	2.95E+04	1.03E+04	2.78E+05	3.20E+04
Q99459	4.05E+04	4.15E+06	3.22E+06	7.15E+05	1.21E+06	1.34E+06	1.51E+06		3.27E+05	1.56E+06
Q99460	4.83E+04	3.72E+06	2.53E+06	2.31E+05	1.42E+06	1.38E+06	1.40E+06			
Q99471	3.49E+04	4.06E+06	1.29E+06		2.83E+06	1.75E+06	1.80E+05	1.59E+05	6.11E+05	1.14E+06
Q99523	8.02E+04	2.89E+05	2.80E+05			2.06E+06			1.56E+05	
Q99536		1.46E+05	8.01E+04							
Q99575		1.46E+05	5.34E+04	4.76E+03	8.75E+03	9.54E+03				
Q99590	9.33E+03	1.77E+06	2.33E+05	1.74E+04	5.61E+05	1.34E+05	2.71E+05	2.89E+03	9.64E+04	1.64E+05
Q99613	1.25E+05	1.35E+07	8.29E+06	3.91E+06	2.84E+06	7.04E+06	5.24E+06	3.20E+05	4.37E+05	3.80E+06
Q99661	7.86E+03	6.38E+06	6.54E+06	1.06E+06	5.36E+06	5.43E+06	2.78E+06		2.03E+06	2.80E+06
Q99714	6.19E+06	3.27E+07	1.29E+07	1.70E+07	1.59E+07	1.07E+07	1.69E+07	2.72E+06	4.18E+06	6.35E+06
Q99735				1.87E+06	3.83E+05			1.71E+05		1.38E+06
Q99808	2.42E+04	1.11E+06	9.44E+05	1.20E+06		1.92E+06	1.68E+06		5.91E+05	3.90E+05
Q99848	2.17E+05	3.91E+06	2.02E+06	2.32E+06	1.11E+06	3.11E+06	1.32E+06	2.97E+05	3.64E+05	5.52E+05
Q99880				1.83E+06	4.10E+05	1.23E+05	2.16E+05	3.12E+05	2.81E+05	1.68E+05
Q99943		1.54E+06	1.34E+06	7.23E+05	3.85E+05	1.58E+06	2.50E+05	1.73E+05	2.20E+05	4.39E+05
Q99986	2.52E+05	1.31E+07	9.26E+06	1.18E+06	3.04E+06	4.62E+06	4.38E+06	8.40E+05	2.18E+06	2.25E+06
Q9BPX3		3.77E+06	3.15E+06	7.03E+05	6.58E+05	2.42E+06	1.67E+06		4.37E+05	1.13E+06
Q9BQ39	4.00E+04	1.57E+06	4.72E+05	3.31E+05	4.38E+05	6.51E+05		5.25E+04	1.75E+05	2.50E+05
Q9BQ67		5.87E+06	2.71E+06	1.39E+06	1.76E+06	1.95E+06	4.19E+06		2.18E+05	9.70E+05
Q9BQA1	3.64E+05	9.32E+06	2.01E+07	3.98E+05	3.49E+06	4.45E+06	6.57E+06	3.60E+05	1.84E+06	3.25E+06
Q9BQG0	1.14E+06	1.52E+07	8.58E+06	7.48E+06	4.02E+06	5.14E+06	4.67E+06	3.42E+05	1.66E+06	1.82E+06
Q9BQG2								3.23E+04		
Q9BR76	3.24E+05	1.66E+06	1.99E+06		1.40E+05	4.35E+05	1.58E+05	2.74E+04	4.78E+05	3.23E+05
Q9BRP1		7.28E+06	4.96E+06	3.67E+06	2.49E+06	3.92E+06	3.82E+06	3.61E+05	1.46E+06	2.89E+06
Q9BRP4		1.07E+05	8.87E+04	4.05E+04						
Q9BSL1	2.71E+04	9.84E+06	5.01E+06	8.22E+05	8.64E+06	3.03E+06	9.29E+05	1.01E+04	4.54E+06	4.65E+06

Q9BT78		7.08E+06	3.16E+06		1.34E+06	1.46E+06	2.14E+06	4.53E+04	2.07E+05	1.39E+06
Q9BTE3		6.67E+05	5.14E+05	1.39E+05	4.14E+05	3.84E+05	4.25E+05		2.25E+05	5.20E+05
Q9BTE7							6.52E+05		7.31E+05	6.12E+05
Q9BTZ2				2.82E+05	3.31E+05		4.06E+05	8.68E+05	2.34E+05	2.97E+05
Q9BU61		5.52E+05	1.16E+06		7.61E+05	5.94E+05	4.61E+05	1.33E+05	9.19E+05	3.20E+05
Q9BUB7		7.88E+05	4.26E+05	8.79E+05	4.40E+05	4.92E+05	5.36E+04			
Q9BUF5		2.04E+06	2.07E+06	1.48E+06	2.00E+06	1.15E+06	1.75E+06			
Q9BUL9		1.41E+05	1.11E+05	1.38E+05	1.02E+05	3.30E+04				
Q9BUN8		8.32E+05	4.05E+05	4.64E+05	5.41E+05	7.24E+05	2.39E+05			
Q9BUQ8		7.03E+05	3.50E+05	2.30E+05		4.40E+05		5.77E+04	1.02E+05	7.44E+04
Q9BV19		3.12E+05	4.61E+05							
Q9BV44		2.11E+06	9.75E+05		2.70E+05	1.86E+05			8.81E+04	
Q9BVA1		1.25E+06	8.57E+05	3.93E+05	2.29E+05	2.97E+05	9.54E+05	1.64E+05		3.37E+05
Q9BVC6		3.80E+05	2.60E+05	9.69E+05	6.75E+05	3.33E+05		2.70E+05	3.29E+05	2.43E+05
Q9BVI4		4.33E+05	3.47E+05		1.66E+05					
Q9BVK6	2.47E+04			6.64E+05	4.18E+05					3.24E+05
Q9BVM2		4.36E+05	1.74E+05		1.39E+05		1.37E+05		7.25E+04	
Q9BVP2	1.92E+06	1.12E+07	1.16E+07	1.14E+07	3.92E+06	8.04E+06	7.50E+06	1.93E+06	1.69E+06	3.37E+06
Q9BW27		7.56E+05	8.22E+05	2.66E+05		3.24E+05	2.60E+05	3.70E+05		
Q9BW92		8.33E+05	5.81E+05		5.75E+05	2.61E+05				2.12E+05
Q9BWE0		6.30E+06	2.90E+06	1.91E+06	1.98E+06	7.07E+05	1.06E+06	2.66E+05	4.19E+05	5.58E+05
Q9BWF3	1.23E+05	2.45E+06	1.76E+06	1.77E+06	6.61E+05	9.22E+05	4.25E+05	3.06E+05	4.81E+05	9.92E+05
Q9BXJ9	4.33E+05	1.69E+07	1.25E+07	3.89E+06	7.88E+06	8.26E+06	9.43E+06	3.19E+05	1.52E+06	3.96E+06
Q9BXL5		4.87E+06	9.74E+05	2.91E+05	6.92E+05	1.08E+05			3.11E+05	3.60E+05
Q9BXP5	3.40E+04	5.99E+06	3.44E+06	9.17E+05	1.19E+06	2.97E+06	2.38E+06		8.39E+05	7.16E+05
Q9BXW9		6.71E+04	9.36E+04							
Q9BYC9	1.66E+05	1.39E+06	8.41E+05	1.67E+05	9.86E+05	1.08E+06	1.06E+06	3.59E+05	1.27E+06	4.81E+05
Q9BYD3		1.15E+06	6.06E+05			7.68E+05				
Q9BYT8		1.78E+05	5.25E+05	1.85E+05						
Q9BZD4		5.78E+05	3.89E+05			1.29E+05			8.67E+04	

Q9BZE4	2.53E+06	1.12E+07	3.40E+06	2.45E+06	1.20E+06	4.74E+06	3.43E+06	1.19E+06	1.77E+06	4.30E+06
Q9C0C4		8.46E+05	2.01E+06		7.82E+05	2.21E+05	1.97E+06		1.45E+05	4.79E+05
Q9GZL7	2.16E+04	2.28E+06	1.66E+06	9.31E+04	1.79E+05	7.77E+05	4.61E+05	5.93E+04	9.27E+04	1.39E+05
Q9GZR7	3.24E+04	1.21E+05	1.13E+05							3.96E+04
Q9GZT3		5.33E+06	3.86E+06	1.51E+06	8.14E+05	6.62E+05	1.48E+06		2.32E+05	2.58E+06
Q9H000		5.00E+04	2.28E+04		2.03E+04	2.33E+04	1.06E+04			7.26E+03
Q9H0A0	1.18E+06	6.82E+06	9.03E+06	5.59E+06	5.80E+05	5.10E+06	3.30E+06	8.27E+05	8.87E+05	1.98E+06
Q9H0D6	1.70E+05	5.71E+06	2.10E+06	1.04E+06	3.28E+06	2.53E+06	2.08E+06		6.18E+05	8.92E+05
Q9H0F6		3.46E+04	3.17E+04	2.72E+04	1.80E+04	2.00E+04	9.37E+03		4.92E+03	6.56E+03
Q9H0S4	2.91E+05	1.86E+06	3.80E+06	1.43E+06	2.69E+06	2.92E+06	3.36E+06	1.59E+05	9.98E+05	1.00E+06
Q9H0U3		6.11E+05	1.13E+06	1.33E+06	4.96E+05	6.58E+05	1.02E+06		3.85E+05	6.50E+05
Q9H0U4	2.10E+04	2.26E+06	1.73E+06	2.23E+06	9.83E+05	1.94E+06	1.69E+06	1.13E+05	4.79E+05	2.70E+05
Q9H0U6		6.25E+05	4.36E+05		1.35E+05	2.31E+05			2.37E+05	1.86E+05
Q9H1A4	1.73E+04	2.57E+06	1.85E+06	4.02E+05	2.05E+05	6.81E+05	2.50E+05		2.36E+04	5.31E+04
Q9H1E3				8.04E+04					3.42E+04	
Q9H2G2	1.48E+04	8.93E+05	7.89E+05	1.08E+05	1.90E+05	1.10E+05	2.77E+05			5.72E+04
Q9H2M9		9.58E+05	8.31E+05		1.82E+05	3.71E+05	8.06E+04			
Q9H2W6				4.72E+04	4.76E+04		4.92E+04	1.02E+04	1.51E+04	1.70E+04
Q9H3K2				4.67E+05	3.03E+05				1.72E+05	1.64E+05
Q9H3K6	1.70E+05	3.82E+06	2.00E+06	2.16E+06	4.14E+06	3.92E+06	1.74E+06	2.05E+06	1.81E+06	1.41E+06
Q9H4L5		4.19E+04	5.14E+04			2.04E+04	1.34E+04			
Q9H501						1.24E+04				
Q9H5V7		5.51E+04	5.91E+04	3.96E+04				6.05E+03		
Q9H6R4	3.21E+04	5.09E+05	3.57E+05	3.64E+05	2.51E+05	2.98E+05	5.07E+05	1.50E+05	1.66E+05	4.11E+05
Q9H773	3.66E+04	6.46E+05	2.70E+05	2.41E+06	1.32E+06	1.57E+06	1.20E+06	1.90E+05	8.88E+05	1.97E+06
Q9H7N4	2.50E+05	1.67E+06	1.12E+06	3.99E+05	3.39E+05	1.32E+06	7.48E+04			2.39E+05
Q9H857		1.75E+06	2.37E+05			3.19E+05	4.84E+05			
Q9H8G2		7.60E+05	2.14E+06		5.83E+05	7.69E+05	8.88E+05		2.72E+05	7.51E+05
Q9H8H0	3.96E+04	2.51E+06	8.32E+05	4.53E+05		4.70E+05	5.09E+05			
Q9H967		6.87E+05	4.15E+05	2.27E+05	2.64E+05				2.68E+05	

Q9H9A6						3.18E+05	1.91E+05			
Q9H9H4		7.35E+05	3.09E+05		3.07E+05	4.16E+05				3.92E+05
Q9H9Q2		7.76E+05	1.78E+05		1.12E+05		1.14E+05	8.56E+04	1.86E+05	1.04E+05
Q9HAV4	2.15E+05	1.04E+07	9.73E+06	1.41E+06	2.08E+06	7.57E+06	3.33E+06	2.16E+05	1.33E+06	3.37E+06
Q9HAV7	1.14E+05	7.69E+06	4.70E+06	6.45E+06	5.65E+06	1.67E+06	1.91E+06	1.52E+06	2.42E+06	2.07E+06
Q9HC35		1.68E+06	1.27E+06		1.47E+06	6.78E+05	5.71E+05	5.16E+05	1.46E+06	8.38E+05
Q9HCC0	1.81E+06	6.04E+06	4.90E+06		2.21E+06	1.63E+06	2.45E+06	4.76E+04	3.68E+05	1.23E+06
Q9HCD5		1.68E+06	6.38E+05		1.37E+05	5.97E+05	5.68E+05			
Q9HD20		1.04E+06	8.84E+05			2.57E+05				
Q9HD33	8.76E+04	2.02E+06	1.25E+06	5.70E+05		3.76E+05	3.68E+05		1.57E+06	
Q9NPA8		7.84E+05	2.43E+05	3.12E+06	7.98E+05	9.86E+05		7.60E+05	6.21E+05	4.28E+05
Q9NPD3	3.24E+04	2.44E+06	1.71E+06	4.65E+05	5.48E+05	1.02E+06	8.33E+05	3.97E+04	3.01E+05	6.25E+05
Q9NPY3		7.30E+05	5.58E+05		2.31E+05	4.03E+05	1.71E+04		2.36E+05	3.60E+05
Q9NQG5	5.95E+04	7.47E+06	2.44E+06	7.33E+05	1.23E+06	2.30E+06	1.22E+06		5.11E+05	4.33E+05
Q9NQT5	5.43E+04	3.29E+06	1.95E+06	2.48E+06	2.01E+06	8.53E+05	8.18E+05	1.05E+05		
Q9NQW6	5.14E+03	7.74E+05	9.09E+05	2.40E+05	1.81E+05	3.41E+05	1.66E+05			1.64E+05
Q9NQX3	6.00E+03	3.75E+06	2.26E+06		1.68E+05	1.12E+06	2.19E+06			3.31E+05
Q9NR28				3.25E+05						
Q9NR30	2.85E+06	6.43E+07	4.50E+07	2.44E+07	1.91E+07	2.73E+07	3.26E+07	3.51E+06	7.74E+06	1.68E+07
Q9NR31		7.68E+05	4.72E+05	4.17E+05		4.89E+05	2.63E+05	1.45E+05	1.55E+05	
Q9NR48	7.23E+04	6.52E+05	3.11E+05	3.05E+05	1.50E+05		1.96E+05	5.76E+04	1.07E+05	1.58E+05
Q9NRG9	3.71E+04	2.35E+06	1.70E+06	4.06E+05	9.56E+05	1.59E+06	1.73E+06		3.95E+05	1.12E+06
Q9NRK6	1.80E+04	1.74E+06	4.99E+05	4.26E+05		2.59E+05	2.48E+05		1.34E+05	
Q9NRL2	1.70E+04	3.00E+06	2.83E+06	8.84E+05	8.05E+05	9.22E+05	2.48E+05		2.49E+05	4.06E+05
Q9NRN7	4.05E+03	1.68E+05	1.84E+05	3.89E+04	6.12E+04	4.63E+04	1.33E+05		1.68E+04	
Q9NRP0		1.36E+06	8.78E+05	4.60E+05	8.86E+05	6.88E+05	2.12E+05		4.35E+05	5.08E+05
Q9NRW3		1.12E+06	6.01E+05	2.46E+04	3.19E+04	4.87E+05	2.10E+04		1.10E+04	6.32E+04
Q9NRX1	1.34E+05	2.20E+06	1.40E+06	6.95E+05	3.72E+05	1.36E+06	3.82E+05	2.60E+05	2.44E+05	6.17E+05
Q9NRZ7	2.50E+04	1.21E+06	7.24E+05		9.80E+04	6.70E+05	5.13E+05	1.35E+05		
Q9NSE4		5.81E+06	4.00E+06	1.84E+06	2.45E+06	2.33E+06	1.15E+06	1.62E+05	1.01E+06	1.01E+06

Q9NUL7		5.03E+04	5.69E+04		7.67E+03	3.36E+04	1.21E+04			7.76E+03
Q9NUP9				1.75E+05	1.54E+05			3.62E+04	7.22E+04	
Q9NUQ3	3.37E+04			4.74E+05		1.77E+05	1.79E+05	1.98E+05	1.15E+05	
Q9NUQ9	1.28E+05	5.28E+06	2.72E+06	5.18E+05	2.51E+06	2.47E+06	1.42E+06		5.98E+05	1.24E+06
Q9NV35		5.20E+04	1.11E+05							
Q9NVH1		3.31E+05	4.78E+05			4.54E+05				
Q9NVI1		6.37E+05	3.02E+05	1.67E+05		2.77E+05				6.42E+05
Q9NVP1	7.00E+05	4.20E+06	4.99E+06	1.58E+06	4.65E+05	4.19E+06	1.26E+06		2.94E+05	7.03E+05
Q9NVS9	1.07E+05	3.90E+06	2.16E+06	4.25E+05	1.35E+06	7.64E+05			6.20E+05	1.53E+06
Q9NVT9		2.31E+06	2.51E+06	5.49E+05	3.15E+05	1.81E+06		3.01E+06	1.42E+05	2.63E+05
Q9NVV4		3.27E+05	2.37E+05							
Q9NVX2		4.91E+05	7.49E+05	4.04E+05	2.56E+05	2.94E+05	2.08E+05			
Q9NW08		1.04E+05	7.46E+04			1.49E+04	1.58E+04			
Q9NW13	6.04E+04	2.87E+06	8.82E+05	3.02E+05	4.02E+05	9.23E+05	3.24E+05		7.23E+03	1.47E+04
Q9NWU2		1.32E+06	2.48E+05	4.48E+04		4.29E+05	2.15E+04		3.58E+04	2.97E+04
Q9NWU5	4.59E+04	1.31E+06	4.74E+05	6.39E+05	2.09E+04	4.32E+05	9.65E+03		1.26E+05	2.54E+05
Q9NX62				4.31E+04						
Q9NXF1	7.09E+04	7.04E+05	2.29E+05		3.35E+05	2.35E+05	1.52E+05			
Q9NXG2		3.52E+05	6.71E+05	5.40E+04	5.56E+05	6.50E+05	2.50E+05			1.11E+05
Q9NXH9		8.27E+05	4.45E+05		1.85E+05	1.26E+05	2.33E+05			2.34E+05
Q9NXV6		4.67E+05	2.45E+05	1.64E+05	1.12E+04	1.06E+05	1.84E+05	6.01E+04		
Q9NYB0		2.45E+05	2.32E+05		2.33E+05	2.12E+05	4.75E+05		3.64E+05	3.62E+05
Q9NYP7		1.14E+06	7.68E+05	3.78E+05	4.80E+05	3.77E+05				
Q9NYU2				4.16E+05	6.93E+05	2.41E+05	2.20E+05		3.27E+05	1.36E+05
Q9NZ01	1.29E+05	7.74E+06	4.49E+06	1.22E+06	3.02E+06	1.76E+06	1.80E+06	1.53E+05	8.38E+05	1.60E+06
Q9NZ53						2.00E+05				
Q9NZC9		1.24E+04	1.13E+04							
Q9NZE8	6.25E+04								1.22E+05	
Q9NZL9		1.52E+06	9.43E+05	2.52E+05	6.12E+05	1.06E+06	1.85E+05		2.29E+05	3.11E+05
Q9NZT1	1.05E+04	9.30E+05	9.52E+05		9.84E+04		6.36E+06	9.19E+04		

Q9NZZ3		2.65E+05	1.75E+05		5.58E+05				2.12E+05	1.31E+05
Q9P0J0	2.94E+05	7.49E+05	6.11E+05	1.65E+06	3.70E+05		6.04E+05		5.37E+05	8.69E+05
Q9P0J7		2.36E+05	1.53E+05		1.63E+05					6.81E+05
Q9P0K7					2.63E+05	2.04E+05	2.12E+05			
Q9P0M6		6.70E+05	2.54E+05	2.82E+05		7.50E+04				
Q9P0M9	1.83E+06	3.89E+06	4.30E+06	1.70E+06	2.74E+06	8.49E+05	2.18E+06	9.37E+05	3.65E+06	2.25E+06
Q9P0S9		4.69E+05	1.81E+05	6.75E+04	1.17E+05	1.54E+05	1.76E+05		5.05E+04	1.02E+05
Q9P0U1		7.28E+05	1.85E+05	7.75E+05	7.32E+05	4.02E+05	2.52E+05		1.96E+05	2.96E+05
Q9P1F3		7.22E+05	4.39E+05	9.66E+05	2.26E+05				2.71E+05	2.45E+05
Q9P258	8.22E+05	2.88E+07	1.95E+07	1.66E+07	2.29E+07	1.18E+07	1.30E+07	3.34E+06	1.10E+07	1.52E+07
Q9P2B2	3.64E+05	3.70E+06	5.65E+06	1.99E+06	1.59E+06	3.09E+06	4.95E+06	3.23E+05	2.08E+06	2.40E+06
Q9P2I0		6.71E+05	2.14E+05		1.84E+05	4.50E+05				5.91E+05
Q9P2N5		3.26E+06	6.07E+05	1.18E+05	6.43E+05	2.31E+05	3.09E+05			9.08E+04
Q9P2W9		5.58E+05	2.44E+05	1.04E+05	1.30E+05					
Q9UBB4	3.63E+05	9.08E+06	5.63E+06	1.51E+06	1.46E+06	2.55E+06	6.60E+05	1.63E+05	3.66E+05	2.07E+06
Q9UBB6		5.30E+05	3.19E+05	9.63E+04		1.30E+05				
Q9UBE0	3.45E+04	5.67E+06	4.22E+06		2.07E+06	1.14E+06	1.47E+06		6.55E+05	4.73E+05
Q9UBL3		9.61E+05	1.28E+05		6.41E+05	1.93E+05	3.08E+05			2.55E+05
Q9UBQ5		1.71E+06	6.96E+05		2.51E+05	3.54E+05	1.32E+05			4.54E+05
Q9UBT2	1.25E+05	1.10E+07	8.26E+06	2.51E+06	4.06E+06	3.84E+06	5.42E+06	5.05E+05	1.48E+06	2.56E+06
Q9UDW1		8.89E+05	9.96E+05	1.30E+06	3.51E+05	6.38E+05		1.18E+06	3.62E+05	1.22E+06
Q9UFN0				1.60E+05	1.05E+06					
Q9UG63	1.22E+05	5.60E+06	2.10E+06		6.33E+05	2.30E+06	2.70E+06			1.88E+05
Q9UGP8	8.21E+04	6.93E+06	2.82E+06	1.63E+06	1.19E+06	1.94E+06	7.29E+05	2.04E+05	1.65E+06	
Q9UH62		4.83E+05	1.36E+06		1.44E+05	4.43E+05	1.30E+06		2.67E+05	4.09E+05
Q9UHB9	1.16E+05	7.48E+06	5.58E+06	1.19E+06	3.83E+06	3.83E+06	2.58E+06	1.71E+05	1.49E+06	1.95E+06
Q9UHD1		2.08E+06	1.83E+06	5.98E+04	3.95E+05	6.92E+05	5.31E+05		1.97E+05	9.16E+04
Q9UHQ9		4.85E+05	3.58E+05	9.61E+05		4.85E+05	7.70E+05		1.60E+06	2.22E+06
Q9UHV9	6.29E+03	8.09E+06	2.83E+06	2.52E+06	5.02E+06	2.67E+06	2.13E+06		2.99E+06	3.15E+06
Q9UI12		8.04E+05	6.75E+05			2.41E+05	2.26E+05			

Q9UI26		5.75E+05	8.00E+05	5.82E+04	1.07E+05	2.39E+05	2.96E+04		1.67E+04	1.25E+05
Q9UIA9	1.18E+05	3.13E+06	2.11E+06	9.06E+05	6.48E+05	3.24E+05	4.59E+05		1.31E+05	
Q9UIG0	1.12E+05	4.48E+06	2.74E+06		5.40E+05	2.24E+06	8.64E+05	7.69E+03	1.56E+05	3.42E+05
Q9UII2	2.15E+04	1.65E+06	1.76E+06	4.11E+06	1.89E+06	2.62E+05	1.66E+05	1.84E+06	1.80E+06	2.36E+06
Q9UIW2		9.85E+05	7.78E+05	1.24E+05	4.51E+05	7.57E+05	8.04E+05		6.03E+04	1.73E+05
Q9UJC3	5.20E+04	1.81E+05	2.97E+05	1.40E+05	1.29E+05	1.74E+05	1.12E+05	2.96E+04	1.55E+05	1.38E+05
Q9UJX2	3.87E+06	8.01E+06	4.98E+06	2.49E+06	1.27E+06	2.54E+06	3.56E+06	2.15E+05	8.19E+05	1.50E+06
Q9UJX3		3.46E+05	3.51E+05	5.27E+05		3.53E+05	2.19E+05	3.50E+05		
Q9UJX5		8.09E+05	9.60E+05				1.29E+06			
Q9UK61		2.54E+05	1.11E+05			4.07E+04				
Q9UKD2	4.07E+05	9.48E+06	6.65E+06	2.87E+06	1.78E+06	4.44E+06	4.48E+06	9.34E+05	1.80E+06	2.53E+06
Q9UKF6	3.49E+04	1.06E+06	1.12E+06		4.79E+05	1.87E+06	1.46E+06	3.67E+05	1.61E+05	3.06E+05
Q9UKL0	7.63E+04	2.01E+06	2.84E+05		5.90E+05				1.38E+05	3.51E+05
Q9UL25		1.90E+06	9.75E+05	7.62E+05	6.87E+05	5.67E+05	3.86E+05	5.23E+04	2.42E+05	
Q9ULV4	1.82E+05	5.85E+06	2.88E+06	1.47E+06	1.41E+06	2.13E+06	1.56E+06	2.19E+04	1.47E+06	1.70E+06
Q9ULW0	1.39E+05	1.98E+06	1.28E+06		1.23E+05	3.33E+05	2.81E+05		3.93E+05	
Q9UMS0				7.02E+05	2.21E+05				4.37E+05	
Q9UMS4	3.53E+05	6.93E+06	4.42E+06	1.84E+06	2.22E+06	1.84E+06	1.75E+06	3.42E+05	1.23E+06	1.15E+06
Q9UN86	1.30E+04	2.37E+05	2.09E+05	8.69E+04	6.12E+04	1.21E+05	6.65E+04			
Q9UNE7		2.88E+05	1.44E+05	1.32E+05	1.36E+05	1.42E+05	9.87E+04	2.54E+04	4.60E+04	
Q9UNH7	3.90E+04	4.60E+06	3.38E+06	1.31E+06	1.81E+06	2.75E+06	1.52E+06	1.03E+05	1.02E+06	2.68E+06
Q9UNM6	1.69E+05	2.30E+07	1.67E+07	7.28E+06	9.74E+06	1.24E+07	6.12E+06	1.89E+06	6.74E+06	1.04E+07
Q9UNN5	7.41E+03	6.21E+06	4.59E+06	9.80E+05	2.33E+06	2.14E+06	7.15E+05		8.94E+05	2.28E+06
Q9UNQ2	1.24E+05	2.17E+06	1.03E+06	3.99E+05	3.55E+05	7.63E+05	2.02E+05		2.00E+05	2.64E+05
Q9UNS2		3.08E+06	2.95E+06	6.32E+05	1.88E+06	7.30E+05	1.27E+06		3.75E+05	5.68E+05
Q9UNX4	6.03E+04	4.53E+06	1.57E+06	1.71E+05		1.72E+06				6.74E+05
Q9UPN6		5.22E+05	3.59E+05				2.65E+05			
Q9UPN7		1.98E+05	1.43E+05			7.62E+04	1.34E+05			
Q9UPN9		4.88E+05	2.88E+05			2.57E+05				9.76E+04
Q9UQ80	5.68E+05	7.76E+06	7.66E+06	1.03E+07	5.95E+06	5.33E+06	5.85E+06	5.31E+05	3.02E+06	3.66E+06

Q9UQE7	2.87E+04	5.16E+06	3.09E+06		3.08E+05	9.36E+05	1.97E+06	1.24E+05	2.80E+05	2.10E+05
Q9Y262	3.20E+05	6.77E+06	8.70E+06	2.74E+06	2.16E+06	4.78E+06	4.70E+06	1.65E+05	6.57E+05	2.85E+06
Q9Y277	1.26E+05	2.22E+07	1.27E+07	1.25E+07	1.68E+07	1.33E+07	8.60E+06	2.30E+06	4.92E+06	4.31E+06
Q9Y294	4.75E+05			7.55E+05	3.82E+05		8.59E+04	1.35E+05		6.74E+04
Q9Y2G3		4.66E+05	2.28E+05				2.79E+05			
Q9Y2K7		7.57E+04	5.78E+04				1.01E+04			
Q9Y2L1	9.79E+04	7.25E+06	3.98E+06	2.31E+06	7.81E+05	1.42E+06	3.33E+06	1.40E+05	1.25E+05	8.21E+05
Q9Y2Q9	2.72E+04	1.36E+06	1.04E+06			2.62E+05		2.00E+05		7.16E+05
Q9Y2R4		1.43E+06	5.09E+05	7.15E+05		1.86E+05	2.15E+05	4.81E+04	1.28E+05	
Q9Y2R9		8.19E+05	5.86E+05	3.60E+05	3.27E+05	1.09E+06	3.29E+05	1.07E+05	1.48E+05	2.75E+05
Q9Y2S7	5.75E+05	6.26E+06	3.37E+06	2.18E+06	8.64E+05	2.52E+06	2.88E+06		8.68E+05	6.86E+05
Q9Y2T2		9.54E+05	1.07E+06		2.22E+05	4.30E+05	3.63E+05		1.33E+05	2.69E+05
Q9Y2X3	1.36E+06	1.90E+07	1.45E+07	1.71E+06	2.22E+06	7.26E+06	2.70E+06		8.94E+05	1.71E+06
Q9Y2Z0		4.08E+06	2.90E+06	2.88E+06	1.27E+06	1.24E+06	3.35E+06		5.50E+05	1.52E+06
Q9Y371		5.11E+06	2.99E+06	1.31E+06	3.71E+06	2.87E+06	2.50E+06	3.96E+04	1.24E+06	2.29E+06
Q9Y383	4.16E+05	4.65E+06	3.12E+06	1.70E+06	5.07E+06	1.48E+06	1.47E+06	5.80E+05	2.00E+06	2.60E+06
Q9Y394				6.21E+05		2.17E+05	4.13E+05	2.47E+05		
Q9Y3A5	4.92E+05	2.18E+07	1.56E+07	5.74E+06	1.53E+07	1.00E+07	6.48E+06	2.81E+06	8.78E+06	1.15E+07
Q9Y3B7		6.20E+06	4.69E+06	1.45E+06	3.54E+06	3.46E+06	3.76E+06	1.00E+05	1.27E+06	2.20E+06
Q9Y3C1	1.05E+04	1.85E+06	1.14E+06	1.46E+06	1.65E+06	1.35E+06	4.77E+05	3.72E+04	6.05E+05	2.08E+06
Q9Y3C6		3.57E+06	1.80E+06	6.79E+05	8.04E+05	9.94E+05	1.09E+06		3.98E+05	8.50E+05
Q9Y3I0	1.66E+05	1.85E+07	1.19E+07	4.92E+06	6.30E+06	9.05E+06	1.01E+07	4.18E+05	2.47E+06	4.30E+06
Q9Y3L3		6.47E+05	3.14E+05			3.02E+05	3.78E+05		6.48E+04	1.53E+05
Q9Y3T9	3.47E+05	2.02E+06	2.67E+06	5.60E+05	4.49E+05	8.40E+05	6.35E+05	3.79E+04	9.61E+04	1.51E+05
Q9Y450	5.92E+05	5.32E+06	4.11E+06	2.79E+06	2.53E+06	2.75E+06	1.80E+06	8.47E+05	1.39E+06	8.71E+05
Q9Y490	5.20E+05	3.83E+07	2.73E+07	3.79E+06	6.40E+06	1.00E+07	1.01E+07	3.35E+05	2.42E+06	6.29E+06
Q9Y4C8	2.72E+05	2.75E+06	4.35E+06				9.65E+05		3.37E+05	
Q9Y4E8	1.60E+05	1.01E+06	5.21E+05	1.85E+05	2.90E+05	9.37E+05	2.77E+05		2.09E+05	2.35E+04
Q9Y4L1	3.95E+05	1.06E+07	8.11E+06	1.16E+07	7.39E+06	5.97E+06	2.83E+06	2.08E+06	7.70E+06	9.24E+06
Q9Y4P1	1.92E+05	7.22E+05	5.59E+05		1.81E+05	2.53E+05				

Q9Y4P3		7.90E+05	1.26E+05							
Q9Y4R8		7.68E+05	1.22E+05			4.49E+04	6.84E+04			
Q9Y4W2		8.54E+05	4.27E+05	2.93E+05		4.21E+05				
Q9Y512		2.47E+06	2.93E+05		8.30E+05	5.76E+05	2.39E+05			
Q9Y520	3.68E+04	1.58E+06	6.65E+05	1.42E+05	1.06E+05	6.31E+05	2.39E+05		4.65E+03	2.87E+05
Q9Y570	1.51E+04	2.25E+06	1.65E+06	2.33E+06	8.23E+05	1.81E+06	1.70E+06	5.98E+05	8.33E+05	6.62E+05
Q9Y5A9	5.79E+04	1.21E+06	8.71E+05	5.57E+05	1.04E+06	9.49E+04	4.81E+05		3.40E+05	3.02E+05
Q9Y5E4		4.27E+05	3.08E+05							
Q9Y5J1	1.00E+05	2.83E+06	1.59E+06	8.12E+04	7.38E+04	1.12E+06	6.88E+05	2.07E+04	9.48E+04	3.96E+04
Q9Y5J7		1.58E+06	1.15E+06		1.11E+06	8.20E+05	9.42E+05	7.07E+05	4.53E+05	8.01E+05
Q9Y5L0	5.15E+04	3.83E+06	1.31E+06	2.11E+05	2.66E+05	1.66E+06	1.45E+06		6.04E+04	8.21E+04
Q9Y5L4		2.00E+05	9.32E+04	1.94E+06	1.67E+05			4.37E+05		6.15E+05
Q9Y5M8	7.83E+04	7.70E+06	3.30E+06	2.40E+06	1.78E+06	3.59E+06	2.81E+06	6.42E+04	1.02E+06	1.32E+06
Q9Y5P6		1.28E+05	1.25E+05				1.77E+04			
Q9Y5Q8	5.77E+04	2.44E+06	2.50E+06	5.36E+05	1.58E+05	1.07E+05	4.96E+05	1.06E+05		4.37E+05
Q9Y5Q9		5.58E+05	1.22E+06		1.06E+06	1.36E+05	3.02E+05			
Q9Y5X1		3.97E+06	9.62E+05		7.81E+05		5.90E+05			6.13E+05
Q9Y5X3	6.04E+03	1.43E+05	8.78E+04	4.40E+04	2.85E+05		4.87E+04		5.70E+04	1.29E+05
Q9Y613		4.64E+05	5.19E+05	1.57E+04		3.11E+03				4.19E+05
Q9Y673	3.99E+04	2.60E+06	2.08E+06	1.34E+06	2.70E+06	3.21E+06	3.06E+06		7.65E+05	1.67E+06
Q9Y676		8.89E+05	3.04E+05	2.04E+05	1.90E+05		2.59E+05		8.36E+04	1.78E+05
Q9Y678	3.60E+05	8.61E+05	8.86E+05	3.89E+05	7.15E+05	2.01E+05	4.24E+05		1.02E+05	1.99E+05
Q9Y696		1.53E+05	1.94E+05				4.84E+04			
Q9Y697		2.52E+05	1.20E+05	9.49E+04	7.54E+04	3.41E+04		5.61E+03	5.15E+03	
Q9Y6C9		4.87E+06	3.14E+06	3.90E+06	2.48E+06	3.46E+06	5.44E+06	3.40E+05	9.85E+05	1.90E+06
Q9Y6E0		6.57E+05	1.39E+05		1.34E+05	2.16E+05				1.44E+05
Q9Y6G9	5.58E+04	2.59E+06	1.91E+06		1.43E+06	1.38E+06	1.42E+06	3.46E+04	3.45E+05	6.71E+05
Q9Y6K0	3.62E+04			3.97E+05		4.10E+05	3.40E+05	6.65E+04	1.05E+06	
Q9Y6M0		6.42E+05	8.10E+05	3.11E+05	2.43E+05	3.11E+05	3.39E+05			2.69E+05
Q9Y6M1		1.08E+06	2.63E+05	9.68E+04	1.90E+05	6.55E+05	1.91E+06			3.51E+05

Q9Y6M5	1.03E+06	1.91E+06	4.01E+06	3.42E+06	9.98E+05	3.72E+06	3.47E+06		1.07E+05	1.55E+05
Q9Y6V7	3.72E+04	1.33E+05	1.19E+05	3.82E+05		3.16E+05	4.97E+04	5.83E+04		
S4R369	1.43E+04	1.42E+06	9.26E+05	3.39E+05	1.40E+06	4.78E+05	7.01E+05	1.11E+05	4.78E+05	4.82E+05
X6RDA4		6.46E+05	2.16E+05		3.39E+05					
X6RGB1		1.26E+06	7.13E+05			4.70E+05			3.72E+05	

Appendix D: Significant hits of KOTMEM30A in surface biotinylation screen

Hits with p-value ≤ 0.012 for $\log_{10}$(fold-change) [log(FC)] of KO to control lines were calculated and collated. Appendix table depicts significant hits that are within all KOTMEM30A lines. Entries highlighted represent hits that are only present in KOTMEM30A lines. Entries are organised with highlighted terms first, then sorted by increasing standard deviation.

Gene Symbol	KO3 TMEM30A log(FC)	KO5 TMEM30A log(FC)	KO TMEM30A 7.9 log(FC)	Mean log(FC)	Standard Deviation
TMEM30A	-19.56	-19.61	-19.58	-19.58	0.02
DLAT	-20.07	-20.12	-20.09	-20.09	0.02
RBM19	-21.47	-21.53	-21.49	-21.50	0.02
CLIC4	-17.34	-17.40	-17.36	-17.37	0.02
FLOT2	-20.86	-20.92	-20.88	-20.89	0.02
ANAPC4	-19.66	-19.72	-19.68	-19.69	0.02
PTBP3	-19.20	-19.26	-19.22	-19.23	0.02
GMPPB	-16.91	-16.96	-16.92	-16.93	0.02
DDX24	-16.32	-16.38	-16.34	-16.35	0.02
CIAPIN1	-17.20	-17.26	-17.22	-17.23	0.02
CNOT9	-19.33	-19.39	-19.35	-19.35	0.02
PLCG1	-18.92	-18.98	-18.94	-18.95	0.02
UBAP2	-16.05	-16.11	-16.07	-16.07	0.02
WDR1	-16.49	-16.55	-16.51	-16.51	0.02
SCAF8	-18.68	-18.74	-18.70	-18.71	0.02
KDM2A	-15.97	-16.03	-15.99	-16.00	0.02
COPS8	-20.66	-20.72	-20.69	-20.69	0.03
ZC3H18	-15.90	-15.96	-15.92	-15.93	0.03
FAM192A	-18.72	-18.78	-18.74	-18.75	0.03
MDC1	-18.73	-18.79	-18.76	-18.76	0.03
PCNP	-16.11	-16.17	-16.14	-16.14	0.03
ATP11B	-18.28	-18.35	-18.31	-18.31	0.03
USP47	-18.82	-18.89	-18.85	-18.85	0.03
CA8	-19.57	-19.63	-19.59	-19.60	0.03
CDC16	-18.41	-18.48	-18.44	-18.44	0.03
RPRD2	-19.33	-19.39	-19.35	-19.36	0.03
ARMC8	-17.12	-17.18	-17.15	-17.15	0.03
ARHGEF2	-17.75	-17.82	-17.78	-17.78	0.03
RPS28	1.69	1.35	1.16	1.40	0.22
RPN1	1.01	0.82	0.30	0.71	0.30
PFDN4	21.59	22.53	21.84	21.99	0.40
NNT	1.57	1.13	0.54	1.08	0.42
ATP5O	2.34	1.63	1.00	1.66	0.55
IPO5	-1.13	-0.80	0.17	-0.58	0.55
SERPINB6	1.58	1.35	0.28	1.07	0.57

UGGT1	20.71	21.39	19.90	20.67	0.61
ATP5J2	22.18	21.33	20.69	21.40	0.61
TMEM109	2.67	2.09	1.10	1.95	0.65
YWHAB	-1.40	-2.24	-0.65	-1.43	0.65
TMEM167A	21.10	19.97	19.56	20.21	0.65
DNM2	-2.01	-2.56	-3.60	-2.72	0.66
PEA15	19.33	20.11	18.34	19.26	0.72
AP1S1	19.93	19.69	21.35	20.32	0.73
PCMT1	1.44	0.93	-0.32	0.69	0.74
H4C1	3.55	1.66	2.34	2.52	0.78
TMED10	22.03	20.38	20.15	20.85	0.84
P4HB	3.45	2.94	1.42	2.60	0.86
VRK1	-2.49	-0.96	-0.28	-1.24	0.92
RAB7A	3.28	1.46	1.18	1.97	0.93
HTT	3.03	1.85	0.68	1.85	0.96
POR	21.27	20.52	18.90	20.23	0.99
RANBP2	-1.77	-2.90	-0.45	-1.71	1.00
DLD	0.86	1.43	-0.95	0.45	1.01
HNRNPA1	3.81	2.60	1.31	2.57	1.02
PURA	-2.76	-2.94	-0.68	-2.13	1.02
BOLA3	20.21	20.05	17.77	19.34	1.11
PPIB	4.68	2.80	2.02	3.17	1.12
ADRM1	-2.27	-1.86	0.30	-1.28	1.13
SDHA	1.73	1.30	-0.87	0.72	1.14
CS	2.47	1.24	-0.53	1.06	1.23
CISD2	1.98	2.07	-0.62	1.14	1.25
HNRNPA2B1	4.03	2.51	0.81	2.45	1.32
ALYREF	4.79	3.65	1.35	3.26	1.43
NCAPH	-3.63	-4.10	-0.79	-2.84	1.46
EZH2	19.53	23.50	23.17	22.07	1.80
SSBP1	2.47	1.78	-1.78	0.82	1.86
HMGN2	20.44	17.76	15.17	17.79	2.15
GATAD2A	-3.83	-3.45	1.10	-2.06	2.24
SMARCA5	-5.27	-2.62	0.52	-2.46	2.37
UTP4	-19.23	-19.29	-6.58	-15.03	5.98
AARS2	-19.39	-4.23	-3.34	-8.99	7.37
NOP9	-19.85	-4.46	-2.88	-9.06	7.65
ATP5SL	-18.44	-18.50	-1.28	-12.74	8.11
PDS5A	-3.23	-19.88	-2.02	-8.38	8.15
RAD21	-19.16	-19.22	-1.69	-13.36	8.25
CERT1	-18.28	-18.34	-0.76	-12.46	8.27

PPM1N	-19.67	-19.73	-2.05	-13.82	8.32
CORO1B	-20.42	-20.47	-2.70	-14.53	8.36
OBSL1	-19.03	-19.09	-1.12	-13.08	8.46
NUF2	-18.81	-18.87	-0.86	-12.85	8.48
FLNA	-20.24	-20.30	-2.17	-14.24	8.53
ANAPC15	-17.18	-17.24	1.17	-11.08	8.66
TPX2	-20.43	-20.49	-1.89	-14.27	8.75
NUP133	-20.91	-4.86	-0.45	-8.74	8.79
HDAC1	-20.45	-20.51	-1.71	-14.22	8.85
MRPS28	-20.10	-20.15	-1.28	-13.84	8.88
VPS29	-19.66	-19.72	-0.66	-13.35	8.97
ACTN2	-20.41	-20.47	-1.37	-14.08	8.99
SMC3	-21.89	-2.85	-1.12	-8.62	9.41
COPS2	-21.53	-1.91	-1.15	-8.20	9.43
CHMP5	-17.67	2.36	-17.70	-11.00	9.45
SKIV2L2	-21.92	-3.28	-0.71	-8.64	9.45
TYMS	-19.10	-19.16	0.95	-12.44	9.47
SMARCA4	-4.14	-22.74	-1.22	-9.37	9.53
TFG	-18.68	-18.74	1.55	-11.96	9.55
TRIP12	-19.14	-19.20	1.27	-12.35	9.63
ENO2	-20.65	-3.06	1.88	-7.27	9.67
RALGPS2	-19.30	-19.35	1.26	-12.46	9.70
MAIP1	-18.89	-18.95	1.96	-11.96	9.85
HDAC2	-20.11	-20.17	0.85	-13.14	9.90
UQCRH	2.28	2.10	-18.84	-4.82	9.91
VAMP8	4.03	2.47	-18.17	-3.89	10.12
SAFB	-22.48	-1.51	-0.48	-8.16	10.14
SORT1	-17.59	-17.65	4.32	-10.30	10.34
C1orf50	-18.45	-18.50	-18.46	-18.47	0.02
DHX38	-17.89	-17.95	-17.91	-17.92	0.02
NT5C2	-18.50	-18.56	-18.52	-18.53	0.02
UNC45A	-18.61	-18.67	-18.63	-18.64	0.02
SLC35B2	-16.89	-16.95	-16.91	-16.92	0.02
ILVBL	-18.40	-18.46	-18.42	-18.42	0.02
DGCR8	-17.89	-17.94	-17.91	-17.91	0.02
KRTCAP2	-19.29	-19.35	-19.31	-19.31	0.02
PPP4R3A	-17.83	-17.88	-17.85	-17.85	0.02
FTSJ3	-19.85	-19.91	-19.88	-19.88	0.02
SLC12A2	-18.73	-18.79	-18.75	-18.76	0.02
BRE	-19.02	-19.08	-19.05	-19.05	0.02
SLC1A4	-18.80	-18.85	-18.82	-18.82	0.02

TRMT112	-18.27	-18.32	-18.29	-18.29	0.02
KAT7	-16.66	-16.72	-16.68	-16.69	0.02
EEF2K	-19.00	-19.05	-19.02	-19.02	0.02
IMPA1	-19.09	-19.15	-19.11	-19.12	0.02
ELL	-16.40	-16.46	-16.42	-16.43	0.02
GNPAT	-18.13	-18.19	-18.16	-18.16	0.02
CYFIP1	-16.48	-16.53	-16.50	-16.50	0.02
ABHD14A-ACY1	-17.99	-18.04	-18.01	-18.01	0.02
PCCB	-20.92	-20.98	-20.95	-20.95	0.02
PCDHB5	-18.42	-18.48	-18.45	-18.45	0.02
MTPAP	-18.04	-18.10	-18.06	-18.07	0.02
UBE2L6	-17.53	-17.59	-17.55	-17.55	0.02
RPS27A	-18.93	-18.99	-18.95	-18.96	0.02
TACC3	-18.88	-18.94	-18.90	-18.91	0.02
INTS14	-17.69	-17.75	-17.72	-17.72	0.02
PPP1R8	-17.41	-17.47	-17.44	-17.44	0.02
VPS26B	-16.97	-17.03	-16.99	-16.99	0.02
PRKRA	-17.91	-17.97	-17.94	-17.94	0.02
RNGTT	-18.59	-18.65	-18.61	-18.62	0.02
TRIM71	-18.94	-19.00	-18.97	-18.97	0.02
ABCD3	-18.62	-18.68	-18.65	-18.65	0.02
MRPL24	-18.17	-18.23	-18.19	-18.20	0.03
LRRC8D	-18.80	-18.86	-18.82	-18.83	0.03
MED16	-18.76	-18.82	-18.78	-18.79	0.03
PIGT	-17.37	-17.43	-17.39	-17.40	0.03
KATNA1	-16.24	-16.31	-16.27	-16.27	0.03
A0A590UJK7	-16.70	-16.76	-16.72	-16.73	0.03
NCBP1	-19.03	-19.10	-19.06	-19.06	0.03
WRN	-17.54	-17.60	-17.56	-17.57	0.03
HPCAL1	-18.88	-18.94	-18.91	-18.91	0.03
RBBP5	-18.71	-18.78	-18.74	-18.74	0.03
VAT1	-16.68	-16.75	-16.71	-16.71	0.03
TRIM24	-16.81	-16.87	-16.83	-16.84	0.03
CPSF4	-18.34	-18.40	-18.36	-18.37	0.03
ARMT1	-19.76	-19.82	-19.79	-19.79	0.03
HMMR	-19.57	-19.63	-19.59	-19.60	0.03
ARHGAP18	-17.00	-17.06	-17.03	-17.03	0.03
ABCC4	-18.15	-18.21	-18.17	-18.18	0.03
PPP4R1	-17.64	-17.71	-17.67	-17.67	0.03
ALDH1B1	-17.87	-17.94	-17.90	-17.90	0.03
CDC23	-21.07	-21.13	-21.10	-21.10	0.03

LYPLA1	-18.07	-18.14	-18.10	-18.10	0.03
TUBB4B	-1.19	-1.09	-1.06	-1.11	0.06
IGF2BP3	-1.26	-1.20	-1.71	-1.39	0.23
ZMPSTE24	2.08	1.60	0.87	1.52	0.50
CANX	2.21	1.80	0.95	1.66	0.52
TLN1	-2.23	-1.45	-0.72	-1.47	0.62
BIN2	22.36	20.73	21.97	21.69	0.69
ANAPC1	-1.44	-2.54	-0.68	-1.55	0.76
LRRC59	3.02	2.15	0.86	2.01	0.89
NCL	1.66	1.36	-0.63	0.80	1.02
LMAN1	19.67	22.31	19.75	20.57	1.23
H2AC11	5.24	3.51	2.25	3.67	1.23
H2AFV	4.44	1.67	1.35	2.49	1.39
SCAF1	-1.87	-2.67	0.96	-1.19	1.55
HIST1H2BL	22.85	20.63	18.93	20.80	1.61
NOP58	-4.38	-3.16	-0.35	-2.63	1.69
USP39	20.75	19.96	15.57	18.76	2.28
GTF3C1	-19.07	-7.56	-19.09	-15.24	5.43
NUP210	-19.66	-19.72	-3.93	-14.44	7.43
DCTN1	-17.89	-17.95	-1.27	-12.37	7.85
ATG4B	-18.71	-18.77	-1.82	-13.10	7.97
RAD50	-18.26	-18.32	-1.10	-12.56	8.10
BMS1	-2.84	-20.79	-4.41	-9.35	8.12
EDC3	-3.34	-19.52	-0.54	-7.80	8.36
COPE	-19.67	-19.73	-1.22	-13.54	8.71
ATP13A1	-19.81	-19.87	-0.87	-13.51	8.94
KIF11	-18.10	-18.16	1.02	-11.74	9.03
VKORC1L1	-18.40	-18.46	1.02	-11.94	9.17
MCCC2	-21.74	-2.20	-21.76	-15.23	9.22
CYB5R1	2.26	-18.68	1.25	-5.06	9.64
EIF4G2	-6.84	-22.19	1.05	-9.32	9.65
MRPL4	-19.65	-19.71	0.88	-12.83	9.69
SLC43A3	-18.59	-18.65	2.00	-11.75	9.72

Appendix E: Significant hits of KOARL5A in surface biotinylation screen

Hits with p-value ≤ 0.012 for $\log_{10}$(fold-change) [log(FC)] of KO to control lines were calculated and collated. Appendix table depicts significant hits that are within all KOARL5A lines. Entries highlighted represent hits that are only present in KOARL5A lines. Entries are organised with highlighted terms first, then sorted by increasing standard deviation.

Gene Symbol	KO2 ARL5A log(FC)	KO5 ARL5A log(FC)	KOARL5A 91.1 log(FC)	KOARL5A 94.4 log(FC)	Mean log(FC)	Standard Deviation
APOE	0.76	1.40	0.96	1.18	1.08	0.24
UROS	21.77	23.55	22.49	22.32	22.53	0.64
COX7C	22.33	23.81	22.21	21.66	22.50	0.80
ATAD3B	20.10	18.10	20.39	19.84	19.61	0.89
CC2D2B	-20.05	-17.66	-19.10	-19.75	-19.14	0.92
NUDT4	-18.28	-15.87	-17.32	-17.97	-17.36	0.93
LRRC8C	-18.63	-16.22	-17.68	-18.33	-17.71	0.93
TMEM263	-18.73	-16.32	-17.79	-18.43	-17.82	0.93
LPCAT1	-18.66	-16.24	-17.71	-18.36	-17.74	0.93
DNAJC11	-18.40	-15.98	-17.44	-18.09	-17.48	0.93
VAC14	-18.46	-16.03	-17.51	-18.16	-17.54	0.93
DNAAF5	-18.47	-16.05	-17.52	-18.17	-17.55	0.94
ARHGAP32	-17.95	-15.52	-16.99	-17.65	-17.03	0.94
GET4	-19.53	-17.11	-18.59	-19.24	-18.62	0.94
MAGEC1	-20.24	-17.82	-19.29	-19.95	-19.32	0.94
SRSF7	-20.82	-18.39	-19.87	-20.53	-19.90	0.94
TRIM25	-18.76	-16.32	-17.82	-18.46	-17.84	0.94
ZNF326	-19.55	-17.11	-18.61	-19.25	-18.63	0.94
KIF21A	-18.27	-15.82	-17.31	-17.96	-17.34	0.94
NSA2	-18.96	-16.51	-18.02	-18.66	-18.04	0.94
CPNE1	-17.54	-15.09	-16.59	-17.24	-16.62	0.95
MRPL49	-17.45	-14.99	-16.50	-17.15	-16.52	0.95
DDX10	-18.13	-15.66	-17.17	-17.82	-17.20	0.95
UQCC1	-18.64	-16.18	-17.69	-18.34	-17.71	0.95
FRAS1	-17.45	-14.99	-16.50	-17.15	-16.52	0.95
SEC24A	-18.27	-15.80	-17.32	-17.97	-17.34	0.95
STAG1	-18.35	-15.88	-17.40	-18.05	-17.42	0.95
ND2	-19.35	-16.88	-18.40	-19.05	-18.42	0.95
MRPL58	-20.16	-17.69	-19.22	-19.87	-19.23	0.95
NOC4L	-18.40	-15.92	-17.45	-18.10	-17.47	0.96
SEC24B	-17.62	-15.14	-16.66	-17.32	-16.68	0.96
RANBP10	-17.73	-15.25	-16.78	-17.43	-16.80	0.96
STK4	-19.03	-16.55	-18.08	-18.73	-18.10	0.96
HEATR1	-21.76	-19.28	-20.81	-21.46	-20.83	0.96
MAPK14	-20.02	-17.54	-19.07	-19.72	-19.09	0.96

PAAF1	-16.41	-13.93	-15.46	-16.11	-15.48	0.96
NELFCD	-18.08	-15.59	-17.13	-17.78	-17.14	0.96
RPP25	-16.78	-14.29	-15.83	-16.48	-15.85	0.96
CLASP1	-18.71	-16.23	-17.76	-18.41	-17.78	0.96
KRR1	-19.69	-17.21	-18.74	-19.39	-18.76	0.96
NGDN	-16.43	-13.94	-15.48	-16.13	-15.49	0.96
FASTKD1	-17.21	-14.72	-16.26	-16.91	-16.27	0.96
RABL3	-17.99	-15.50	-17.04	-17.69	-17.06	0.96
RAB5B	-18.43	-15.94	-17.49	-18.14	-17.50	0.96
TSPYL5	-18.08	-15.59	-17.13	-17.78	-17.15	0.96
ELOVL5	-19.68	-17.19	-18.74	-19.39	-18.75	0.96
EXOC2	-17.92	-15.43	-16.97	-17.62	-16.98	0.96
SUZ12	-18.90	-16.40	-17.95	-18.60	-17.96	0.96
C9JAW5	-19.13	-16.63	-18.18	-18.83	-18.19	0.96
GLYR1	-18.66	-16.16	-17.71	-18.36	-17.73	0.96
NDUFA12	-18.86	-16.36	-17.91	-18.56	-17.92	0.96
PAFAH1B2	-18.69	-16.19	-17.74	-18.39	-17.75	0.97
MINOS1	-17.62	-15.12	-16.68	-17.33	-16.69	0.97
RPF2	-21.10	-18.59	-20.15	-20.80	-20.16	0.97
NCDN	-18.50	-16.00	-17.56	-18.21	-17.57	0.97
CMTR2	-17.37	-14.86	-16.43	-17.08	-16.44	0.97
FAM208A	-17.21	-14.69	-16.26	-16.91	-16.27	0.97
CSTF3	-20.24	-17.73	-19.29	-19.94	-19.30	0.97
PIP4K2A	-18.87	-16.35	-17.92	-18.57	-17.92	0.97
RAD18	-19.28	-16.76	-18.33	-18.98	-18.34	0.97
LAS1L	-19.07	-16.55	-18.12	-18.77	-18.13	0.98
SSR3	-18.88	-16.35	-17.93	-18.58	-17.93	0.98
SLC27A2	-18.78	-16.25	-17.83	-18.48	-17.84	0.98
DHX29	-20.20	-17.67	-19.25	-19.90	-19.25	0.98
ANXA11	-19.92	-17.40	-18.98	-19.62	-18.98	0.98
SDHB	-18.52	-15.99	-17.58	-18.23	-17.58	0.98
VTA1	-18.78	-16.24	-17.83	-18.48	-17.83	0.98
STX18	-18.36	-15.83	-17.42	-18.07	-17.42	0.98
PGM3	-17.89	-15.36	-16.96	-17.60	-16.95	0.98
TPMT	-18.01	-15.48	-17.08	-17.72	-17.07	0.98
PEX3	-19.41	-16.88	-18.46	-19.11	-18.46	0.98
WDR75	-18.57	-16.03	-17.63	-18.27	-17.63	0.98
PDE12	-17.76	-15.21	-16.82	-17.46	-16.81	0.98
DDI2	-18.47	-15.92	-17.52	-18.17	-17.52	0.99
H2AFY2	-18.54	-15.99	-17.60	-18.24	-17.59	0.99
NAA25	-18.90	-16.34	-17.95	-18.60	-17.95	0.99

RNF214	-18.94	-16.38	-17.98	-18.64	-17.98	0.99
PSPC1	-18.40	-15.84	-17.46	-18.11	-17.45	0.99
UTP11	-18.58	-16.02	-17.64	-18.29	-17.63	0.99
DPF2	-20.06	-17.48	-19.11	-19.76	-19.10	0.99
KDM1A	-20.02	-17.42	-19.07	-19.71	-19.05	1.00
ISOC2	-19.67	-17.07	-18.72	-19.37	-18.71	1.01
DYNLL1	-19.03	-16.43	-18.08	-18.73	-18.07	1.01
ANXA1	18.97	18.07	18.82	22.11	19.49	1.55
DHRS4	20.79	24.38	20.94	20.64	21.69	1.56
SLC25A17	21.38	25.13	20.73	21.60	22.21	1.72
SP140L	21.75	23.65	20.23	17.61	20.81	2.21
PRKAR2B	-2.94	-19.53	-4.24	-2.24	-7.24	7.13
KIF4A	-1.75	-17.41	-18.95	-19.60	-14.42	7.36
SF3B4	-2.37	-18.19	-19.73	-20.38	-15.17	7.43
RTRAF	-1.47	-19.76	-3.73	-1.33	-6.57	7.67
TUBA1C	-1.56	-18.31	-19.86	-20.51	-15.06	7.83
CUL2	-2.71	-18.69	-20.24	-3.99	-11.41	8.09
XPO7	-1.69	-18.58	-5.42	-20.77	-11.61	8.20
THOC1	-22.18	-19.68	-21.23	-1.94	-16.25	8.31
NOP56	-1.74	-21.56	-3.84	-1.52	-7.16	8.36
KCMF1	-17.38	-14.89	-16.43	3.29	-11.35	8.50
ANKRD17	1.69	-17.92	-19.47	-20.12	-13.96	9.07
ZMPSTE24	1.16	2.22	2.06	1.60	1.76	0.42
BIN2	21.65	21.25	22.41	22.13	21.86	0.44
CANX	1.30	2.56	1.34	1.53	1.68	0.51
LRRC59	2.17	3.57	2.19	2.98	2.73	0.59
NCL	1.06	2.48	1.24	0.82	1.40	0.64
UNC45A	-18.49	-16.10	-17.54	-18.19	-17.58	0.92
NT5C2	-18.38	-15.99	-17.43	-18.08	-17.47	0.92
C1orf50	-18.33	-15.91	-17.37	-18.02	-17.41	0.93
SLC1A4	-18.68	-16.26	-17.73	-18.38	-17.76	0.93
SLC12A2	-18.62	-16.19	-17.67	-18.31	-17.70	0.93
KRTCAP2	-19.17	-16.73	-18.23	-18.88	-18.25	0.94
BRE	-18.91	-16.46	-17.96	-18.61	-17.98	0.95
ILVBL	-18.28	-15.83	-17.33	-17.98	-17.35	0.95
EEF2K	-18.88	-16.42	-17.93	-18.58	-17.96	0.95
DHX38	-17.77	-15.31	-16.82	-17.47	-16.84	0.95
FTSJ3	-19.74	-17.28	-18.79	-19.44	-18.81	0.95
SLC43A3	-18.48	-16.01	-17.53	-18.18	-17.55	0.95
SLC35B2	-16.78	-14.31	-15.83	-16.48	-15.85	0.95
ATP13A1	-19.70	-17.23	-18.75	-19.40	-18.77	0.95

IMPA1	-18.98	-16.51	-18.03	-18.68	-18.05	0.95
DGCR8	-17.77	-15.30	-16.82	-17.47	-16.84	0.95
PPP4R3A	-17.71	-15.24	-16.76	-17.41	-16.78	0.95
TRMT112	-18.15	-15.68	-17.20	-17.85	-17.22	0.95
KAT7	-16.55	-14.07	-15.60	-16.25	-15.62	0.96
ELL	-16.29	-13.81	-15.34	-15.99	-15.36	0.96
DCTN1	-17.77	-15.30	-16.82	-17.47	-16.84	0.96
CYFIP1	-16.36	-13.88	-15.41	-16.06	-15.43	0.96
GNPAT	-18.02	-15.54	-17.07	-17.72	-17.09	0.96
ABHD14A-ACY1	-17.87	-15.39	-16.92	-17.57	-16.94	0.96
GTF3C1	-18.96	-16.47	-18.01	-18.66	-18.02	0.96
UBE2L6	-17.41	-14.93	-16.46	-17.11	-16.48	0.96
PCCB	-20.81	-18.32	-19.86	-20.51	-19.88	0.96
PCDHB5	-18.31	-15.82	-17.36	-18.01	-17.38	0.96
MTPAP	-17.93	-15.44	-16.98	-17.63	-16.99	0.96
VPS26B	-16.85	-14.36	-15.90	-16.55	-15.92	0.96
PPP1R8	-17.30	-14.81	-16.35	-17.00	-16.37	0.96
BMS1	-20.62	-18.13	-19.67	-20.32	-19.69	0.96
INTS14	-17.58	-15.09	-16.63	-17.28	-16.65	0.96
KIF11	-17.98	-15.49	-17.03	-17.68	-17.05	0.96
ATG4B	-18.59	-16.10	-17.65	-18.30	-17.66	0.96
PRKRA	-17.80	-15.31	-16.85	-17.50	-16.87	0.96
PIGT	-17.26	-14.76	-16.31	-16.96	-16.32	0.96
KATNA1	-16.13	-13.64	-15.18	-15.83	-15.20	0.96
A0A590UJK7	-16.59	-14.09	-15.64	-16.29	-15.65	0.96
COPE	-19.55	-17.06	-18.60	-19.25	-18.62	0.96
MRPL24	-18.06	-15.56	-17.11	-17.76	-17.12	0.96
WRN	-17.43	-14.93	-16.48	-17.13	-16.49	0.96
VAT1	-16.57	-14.07	-15.62	-16.27	-15.63	0.97
SCAF1	-19.94	-17.44	-18.99	-19.64	-19.00	0.97
TRIM24	-16.70	-14.19	-15.75	-16.39	-15.76	0.97
RNGTT	-18.48	-15.97	-17.53	-18.18	-17.54	0.97
RAD50	-18.15	-15.64	-17.20	-17.85	-17.21	0.97
ARHGAP18	-16.89	-14.38	-15.94	-16.59	-15.95	0.97
RPS27A	-18.82	-16.30	-17.87	-18.52	-17.88	0.97
ABCD3	-18.51	-16.00	-17.56	-18.21	-17.57	0.97
PPP4R1	-17.53	-15.02	-16.59	-17.23	-16.59	0.97
VKORC1L1	-18.28	-15.77	-17.34	-17.99	-17.35	0.97
TACC3	-18.77	-16.25	-17.82	-18.47	-17.83	0.97
MRPL4	-19.54	-17.02	-18.59	-19.24	-18.60	0.97
NUP210	-19.55	-17.03	-18.60	-19.25	-18.61	0.97

ABCC4	-18.04	-15.51	-17.10	-17.74	-17.10	0.98
ALDH1B1	-17.76	-15.24	-16.82	-17.47	-16.82	0.98
CPSF4	-18.23	-15.70	-17.28	-17.93	-17.28	0.98
MED16	-18.64	-16.12	-17.70	-18.35	-17.70	0.98
LRRC8D	-18.69	-16.15	-17.74	-18.39	-17.74	0.98
LYPLA1	-17.97	-15.42	-17.03	-17.67	-17.02	0.98
TRIM71	-18.83	-16.28	-17.88	-18.53	-17.88	0.99
RBBP5	-18.60	-16.05	-17.66	-18.31	-17.66	0.99
CDC23	-20.96	-18.40	-20.02	-20.66	-20.01	0.99
ARMT1	-19.65	-17.08	-18.70	-19.35	-18.69	0.99
NCBP1	-18.92	-16.35	-17.97	-18.62	-17.97	0.99
HMMR	-19.46	-16.88	-18.50	-19.16	-18.50	1.00
HPCAL1	-18.77	-16.19	-17.82	-18.47	-17.81	1.00
TUBB4B	-1.27	-3.69	-1.22	-1.11	-1.83	1.08
H2AFV	1.05	4.00	2.46	1.81	2.33	1.08
LMAN1	20.13	20.73	22.87	20.30	21.01	1.10
H2AC11	1.91	4.79	3.10	1.71	2.88	1.22
HIST1H2BL	19.88	22.90	21.21	19.82	20.95	1.25
USP39	21.15	17.58	17.03	19.44	18.80	1.62
ANAPC1	-2.05	-18.39	-6.30	-4.45	-7.80	6.30
IGF2BP3	-2.68	-19.77	-1.67	-4.01	-7.03	7.40
EIF4G2	-2.79	-19.52	-21.06	-21.71	-16.27	7.83
EDC3	-8.72	-16.85	-18.40	1.41	-10.64	7.87
MCCC2	-1.34	-19.13	-20.67	-21.32	-15.62	8.28
CYB5R1	2.05	-16.02	4.05	3.88	-1.51	8.41
TLN1	-0.58	-22.27	-1.96	-1.00	-6.45	9.15
NOP58	-2.34	-21.21	-22.75	-4.00	-12.57	9.44

Appendix F: MS2 of detected ATP11B peptides

ATP11B peptide: MIITQQMEEIVRPLGPESLLLR [224-245aa]

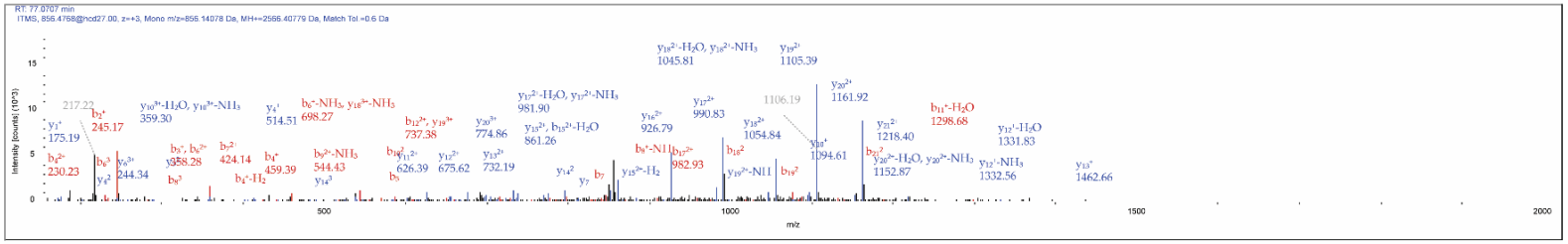

ATP11B peptide: NSDYAIAR [849-856aa]

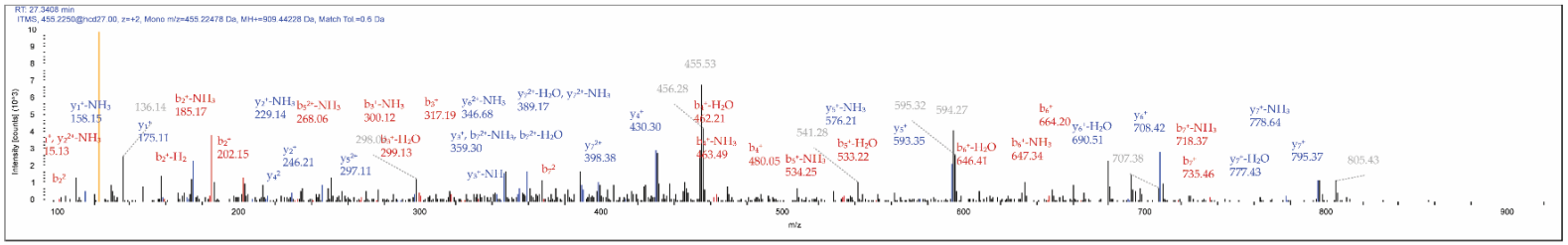

ATP11B peptide: TGTLTENEMQFR [409-420aa]

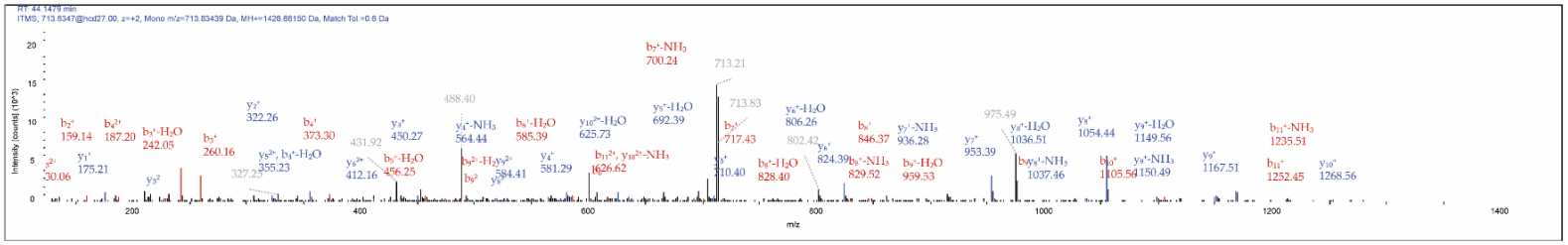

ATP11B peptide: TIYVANR [21-27aa]